# Quantum information and the emergence of spacetime in the AdS/CFT correspondence

Dissertation zur Erlangung des naturwissenschaftlichen Doktorgrades der Julius-Maximilians-Universität Würzburg

Vorgelegt von
Marius Gerbershagen

aus Ulm

Würzburg, 2022

This document is licensed under the Creative Commons Attribution 4.0 International License (CC BY 4.0):
http://creativecommons.org/licenses/by/4.0 This CC license does not apply to third party material (attributed to another source) in this publication.

Eingereicht am: 04.05.2022

bei der Fakultät für Physik und Astronomie

1. Gutachter: Prof. Dr. Johanna Erdmenger

2. Gutachter: Prof. Dr. Thorsten Ohl

3. Gutachter: Prof. Dr. Vijay Balasubramanian

der Dissertation

Vorsitzende(r): Prof. Dr. Raimund Ströhmer

1. Prüfer: Prof. Dr. Johanna Erdmenger

2. Prüfer: Prof. Dr. Thorsten Ohl

3. Prüfer: Prof. Dr. Jens Pflaum

im Promotionkolloquium

Tag des Promotionskolloquiums: 15.07.2022

Doktorurkunde ausgehändigt am: .....

# Abstract

This thesis studies connections between quantum information measures and geometric features of spacetimes within the AdS/CFT correspondence. These studies are motivated by the idea that spacetime can be thought of as an effect emerging from an underlying entanglement structure in the AdS/CFT correspondence.

In particular, I study generalized entanglement measures in two-dimensional conformal field theories and their holographic duals. Unlike the ordinary entanglement entropy of a spatial subregion typically used in the AdS/CFT context, the generalization considered here measures correlations between different fields as well as between spatial degrees of freedom. I present a new gauge invariant definition of the generalized entanglement entropy applicable to both mixed and pure states as well as explicit results for thermal states of the $S_N$-orbifold theory of the D1/D5 system. Along the way, I develop computation techniques for conformal blocks on the torus and apply them to the calculation of the ordinary entanglement entropy for large central charge CFTs at finite size and finite temperature. The generalized Ryu-Takayanagi formula arising from these studies provides further support for the idea that entanglement and geometry are intrinsically linked in AdS/CFT. The results show that the holographic dual to the generalized entanglement entropy given by the length of a geodesic winding around black hole horizons or naked singularities probes subregions of spacetime that are inaccessible to Ryu-Takayanagi surfaces, thereby solving the puzzle of how these features of the spacetime are encoded in the boundary theory.

Furthermore, I investigate quantum circuits embedded in two-dimensional conformal field theories as well as computational complexity measures therein. These investigations are motivated by conjectures relating computational complexity in conformal field theories to geometric features of black hole geometries. In this thesis, I study quantum circuits built up from conformal transformations. I investigate examples of computational complexity measures in these circuits related to geometric actions on coadjoint orbits of the Virasoro group and to the Fubini-Study metric. I then work out relations between these computational complexity measures and the dual gravitational theory. Moreover, I construct a bulk dual to the circuits in consideration and use this construction to study geometric realizations of computational complexity measures from first principles. The results of this part on the one hand rule out some possibilities for dual realizations of computational complexity in two-dimensional CFTs put forward in previous work while on the other hand providing a new robust dual realization of a computational complexity measure based on the Fubini-Study distance.

# Zusammenfassung

Diese Dissertation befasst sich mit Zusammenhängen zwischen Quanteninformationsmaßen und geometrischen Eigenschaften von Raumzeiten im Rahmen der AdS/CFT-Korrespondenz. Diese Untersuchungen sind motiviert durch die Idee, dass die Raumzeit in der AdS/CFT-Korrespondenz als ein Effekt verstanden werden kann, der aus einer zugrundeliegenden Verschränkungsstruktur entsteht.

Insbesondere untersuche ich in dieser Arbeit verallgemeinerte Verschränkungsmaße in zweidimensionalen konformen Feldtheorien und deren holographisch duale Realisierungen. Anders als die normale Verschränkungsentropie einer räumlichen Teilregion, die üblicherweise im AdS/CFT-Kontext betrachtet wird, misst die verallgemeinerte Verschränkungsentropie Korrelationen sowohl zwischen verschiedenen Feldern als auch zwischen räumlichen Freiheitsgraden. Ich stelle eine neue eichinvariante Definition der verallgemeinerten Verschränkungsentropie, die sowohl für reine als auch für gemischte Zustände anwendbar ist, sowie explizite Berechnungen dieser Verschränkungsentropie in der $S_N$-Orbifaltigkeitstheorie des D1/D5-Systems vor. Nebenbei entwickle ich Berechnungsmethoden für konforme Blöcke auf dem Torus und wende diese auf die Berechnung der normalen Verschränkungsentropie für konforme Feldtheorien mit großer zentraler Ladung bei endlicher Systemgröße und endlicher Temperatur an. Die verallgemeinerte Ryu-Takayanagi-Formel, die sich aus diesen Betrachtungen ergibt, unterstützt die Idee, dass Verschränkung und Geometrie in der AdS/CFT-Korrespondenz untrennbar miteinander verbunden sind. Die Ergebnisse zeigen, dass das holographische Dual zur verallgemeinerten Verschränkungsentropie, gegeben durch die Länge einer Geodäte die sich um einen Ereignishorizont eines Schwarzen Lochs oder eine nackte Singularität windet, in Teilregionen der Raumzeit eindringt die für Ryu-Takayanagi-Flächen unerreichbar sind. Damit klären sie auf wie diese Eigenschaften der Raumzeit in der Randtheorie kodiert sind.

Des weiteren untersuche ich Quantenschaltkreise eingebettet in zweidimensionale konforme Feldtheorie und deren Komplexität. Diese Untersuchungen sind motiviert durch Hypothesen, die Komplexitätstheorie mit Eigenschaften von Raumzeiten schwarzer Löcher in Verbindung bringen. In dieser Dissertation analysiere ich Quantenschaltkreise, die aus konformen Transformationen aufgebaut sind. Ich betrachte Komplexitätsmaße in diesen Schaltkreisen zusammenhängend mit geometrischen Wirkungen auf koadjungierten Orbits der Virasoro-Gruppe oder mit der Fubini-Study-Metrik und arbeite Zusammenhänge zwischen diesen Komplexitätsmaßen und Aspekten der dualen Gravitationstheorie heraus. Außerdem konstruiere ich das Dual der betrachteten Schaltkreise in der Gravitationstheorie und untersuche damit geometrische Realisierungen von Komplexitätsmaßen. Die Ergebnisse dieses Teils schließen einerseits einige Möglichkeiten für duale Realisierungen von Komplexitätsmaßen aus, die in vorigen Arbeiten vorgeschlagen wurden, ergeben aber andererseits eine robuste neue duale Realisierung eines Komplexitätsmaßes basierend auf der Fubini-Study-Metrik.

# Publications

The results obtained in this thesis are published in the following research articles and preprints:

1. J. Erdmenger and M. Gerbershagen, *Entwinement as a possible alternative to complexity*, JHEP **03** (2020) 082, arXiv: 1910.05352 [hep-th]

2. J. Erdmenger, M. Gerbershagen, and A.-L. Weigel, *Complexity measures from geometric actions on Virasoro and Kac-Moody orbits*, JHEP **11** (2020) 003, arXiv: 2004.03619 [hep-th]

3. M. Gerbershagen, *Monodromy methods for torus conformal blocks and entanglement entropy at large central charge*, JHEP **08** (2021) 143, arXiv: 2101.11642 [hep-th]

4. M. Gerbershagen, *Illuminating entanglement shadows of BTZ black holes by a generalized entanglement measure*, JHEP **10** (2021) 187, arXiv: 2105.01097 [hep-th]

5. J. Erdmenger, M. Flory, M. Gerbershagen, M. P. Heller, and A.-L. Weigel, *Exact Gravity Duals for Simple Quantum Circuits*, arXiv: 2112.12158 [hep-th]

# Contents


1 Introduction 1

2 Preliminaries 9
2.1 The AdS/CFT correspondence . . . 9
2.1.1 Generalities . . . 9
2.1.2 The AdS/CFT dictionary . . . 12
2.1.3 The D1/D5 system . . . 15
2.1.4 Orbifold conformal field theories . . . 23
2.2 Entanglement in quantum field theory and holography . . . 28
2.2.1 Entanglement entropy . . . 28
2.2.2 The Ryu-Takayanagi formula . . . 31
2.2.3 Entanglement builds geometry . . . 35
2.3 Quantum circuits, black holes and computational complexity . . . 37
2.3.1 The Page curve . . . 37
2.3.2 Firewalls and computational complexity . . . 39
2.3.3 Computational complexity in holography . . . 41
2.3.4 Computational complexity in quantum field theory . . . 46
2.4 Geometric actions on coadjoint orbits . . . 48
2.4.1 Coadjoint orbits in general . . . 48
2.4.2 The Virasoro group . . . 49
2.4.3 Coadjoint orbits of the Virasoro group . . . 52
2.4.4 Geometric actions . . . 54

3 Generalized entanglement measures 57
3.1 Introduction and motivation . . . 57
3.2 Definition of generalized entanglement entropy . . . 61
3.2.1 Hilbert space structure of orbifold conformal field theories . . . 61
3.2.2 $\mathbb{Z}_n$ orbifolds . . . 64
3.2.3 $S_N$ orbifolds and mixed states . . . 70
3.3 Calculation of the generalized entanglement entropy . . . 71
3.4 Monodromy methods for conformal blocks . . . 74
3.4.1 Conformal blocks on the plane . . . 74
3.4.2 Conformal blocks on the torus . . . 77
3.4.3 Partition function on the replica surface . . . 81
3.5 Ordinary entanglement entropy at finite size and finite temperature . . . 85
3.5.1 Limiting cases . . . 86
3.5.2 Holographic CFTs . . . 89
3.5.3 Multiple intervals . . . 91
3.5.4 Vacuum block dominance . . . 92
3.6 Generalized entanglement entropy at finite size and finite temperature . . . 94

3.6.1 Results . . . 95
3.6.2 Bulk geometry reconstruction . . . 98
3.6.3 String theory interpretation of twisted sectors . . . 99
3.6.4 Entanglement entropy for single twisted sectors . . . 99
3.6.5 Probability factors and fluctuation entropy . . . 101
3.6.6 Deformations of the $S_N$ orbifold . . . 102

**4 Quantum circuits of the Virasoro group and computational complexity in AdS/CFT 109**
4.1 Introduction and motivation . . . 109
4.2 Quantum circuits from Virasoro group transformations . . . 111
4.3 Computational complexity and geometric actions on coadjoint orbits . . . 114
4.3.1 Complexity for symmetry groups . . . 114
4.3.2 From complexity to geometric actions . . . 117
4.3.3 Constructing optimal transformations and computing complexity . . . 121
4.3.4 Boundary terms and Berry phases . . . 125
4.3.5 Relation to gravitational actions and Liouville theory . . . 127
4.4 Computational complexity, the Fubini-Study metric and "complexity=volume" . . . 131
4.4.1 Motivation: geodesics in Lie groups and the Euler-Arnold method . . . 132
4.4.2 Complexity from the Fubini-Study metric . . . 135
4.4.3 Complexity=volume for conformal transformations of the vacuum . . . 139
4.4.4 Comparison between the Fubini-Study complexity and complexity=volume 141
4.5 Bulk duals to Virasoro circuits . . . 143
4.5.1 Deriving the boundary metric . . . 143
4.5.2 Mapping to gravity . . . 148
4.5.3 Lessons for holographic complexity . . . 149

**5 Conclusions and Outlook 156**

**A Conventions for elliptic functions 161**

**B Recursion relations for torus conformal blocks 162**

**C The $S_N$ orbifold partition function 164**
C.1 Recursion formula . . . 164
C.2 Large $N$ behavior . . . 165

**D Details of the perturbative calculation of the Fubini-Study complexity and complexity=volume 169**

# 1. Introduction

The unification of gravity with quantum mechanics is one of the primary unsolved problems of modern physics. General relativity, the best classical theory of gravity to date, has passed many remarkable experimental tests such as recently the advent of gravitational wave astronomy through the LIGO/VIRGO experiments [6]. However, it is clear that general relativity cannot be the entire story: on a fundamental level, a classical theory of gravity in an otherwise quantum world is inconsistent with the basic principles underlying general relativity. To be concrete, consider coupling quantum matter to a classical gravity theory. In general relativity, all matter theories couple uniformly to gravity because energy and momentum source the metric via Einstein's equations

$$R_{\mu\nu} + \left(\Lambda - \frac{1}{2}R\right) g_{\mu\nu} = \frac{8\pi G_N}{c^4} T_{\mu\nu}. \tag{1.1}$$

Implementing this coupling by taking $T_{\mu\nu} = \langle \hat{T}_{\mu\nu} \rangle$ to be the expectation value of the energy-momentum tensor in a quantum theory can lead to causality violations when a measurement collapses a superposition such that the energy-momentum tensor expectation value and with it the metric changes instantaneously. Therefore, a theory incorporating quantum effects for both the matter as well as the gravitational sector is necessary for a consistent and complete description of our universe. The fact that a straightforward quantization of general relativity yields a (at least perturbatively) non-renormalizable theory has lead to the development of numerous quantum gravity theories that attempt to address this issue. These include for instance the asymptotic safety program and loop quantum gravity which attempt to circumvent the renormalization problem in a direct fashion (by searching for a non-trivial renormalization group fixed point and by quantizing gravity in a non-perturbative background independent way respectively) or string theory which replaces point particle gravitons with extended objects.

Another field that has expanded rapidly in recent years is quantum computing and quantum information, driven by the goal to develop practically useful quantum computers and to achieve "quantum supremacy", the point at which quantum computers can solve problems faster than currently available classical ones.[1] Remarkably, concepts from quantum information theory such as entanglement measures, quantum error correcting codes or even quantum computational complexity theory have also found their way into quantum gravity research. The aim of this research program, which the present thesis is part of, is to apply quantum information theory to gain insights into open questions from quantum gravity.

Many of these open questions revolve around black hole physics and in particular the thermodynamic behavior of black holes expected to occur once quantum effects are taken into account. Historically, black hole thermodynamics developed out of thought experiments that involve throwing a thermodynamic system into a black hole. Due to the fact that no physical process in general relativity can decrease the area of the event horizon of a black hole [8, 9], Jacob Bekenstein argued that this kind of experiment will violate the second law of thermodynamics unless the black hole carries an entropy proportional to the area of its event horizon [10, 11]. The proportionality

[1] Note that in 2019, a research group at Google claimed to have already achieved quantum supremacy for a specific computation task consisting of sampling probability distributions created by random quantum circuits with their 53 qubit quantum computer based on superconducting qubit technology [7].

constant between the entropy and the horizon area was soon after fixed by Stephen Hawking [12, 13], leading to the Bekenstein-Hawking entropy formula

$$S_{\mathrm{BH}} = \frac{c^3 k_B A_{\mathrm{horizon}}}{4 G_N \hbar}. \tag{1.2}$$

The presence of both $G_N$ and $\hbar$ in equation (1.2) clearly indicates that the black entropy is a quantum gravity effect. One of the reasons why string theory is one of the primary candidates for a theory of quantum gravity is that it reproduces the Bekenstein-Hawking entropy by a counting of microstates in many cases, as was first found for extremal black holes[2] in five dimensions in [14]. Moreover, treating black holes as thermodynamic objects implies that they should emit thermal radiation, the Hawking radiation [12, 13]. While classically the horizon is an impenetrable barrier, in a quantum description radiation must be able to escape the black hole. However, because the spectrum of the Hawking radiation depends only on the few parameters of the black hole visible in classical general relativity from the outside (mass, angular momentum, electric charge), it contains no information about the state of matter that fell into the black hole before evaporation. Therefore, unitarity of quantum mechanics appears to be lost: the collapse and subsequent evaporation process seems to destroy information [15]. This is the famous black hole information paradox.

The Bekenstein-Hawking entropy not only describes the amount of information contained in a black hole but it also bounds the maximum amount of information that it is possible to store in a system of the same size as the black hole in question. If a courageous observer tried to violate this bound by putting to much energy in a certain region of spacetime a black hole would form, hiding the information from his view again [16].[3] The curious scaling of the black hole entropy (1.2) with the area of the event horizon, i.e. the boundary of the black hole subsystem, instead of the volume enclosed by it as is typical for subsystems in statistical physics has lead to the suggestion that quantum gravity theories should obey a so-called holographic principle [19, 20]. The holographic principle states that in a quantum gravity theory, the information about a spatial subsystem obeying the Bekenstein entropy bound is encoded on the subsystem boundary. Thus, according to the principle quantum gravity theories behave like a hologram in the sense that data about a higher dimensional object is stored on a lower dimensional object, in this case the subsystem boundary.

A striking implementation of this idea emerged in the form of the Anti-de Sitter/conformal field theory (AdS/CFT) correspondence [21] shortly after the holographic principle was first proposed. The AdS/CFT correspondence is a conjectural duality between a gravitational theory on a $d+1$-dimensional negatively curved spacetime and a non-gravitational quantum field theory on the $d$-dimensional asymptotic boundary[4] of the $d+1$-dimensional space. The word "duality" in this context means a dynamical equivalence: the outcome of any physical measurement (a correlation function, expectation value, etc.) in the gravitational theory can be equivalently obtained by a measurement in the non-gravitational theory and vice versa. In the most general form of the

[2] Black holes with angular momentum and additional charges such as electric charge only exist if the black hole mass $M$ is large enough, for example for a four-dimensional black hole with angular momentum $J$ and electric charge $Q$, $(G_N M/c)^2 \geq (J/M)^2 + Q^2 G_N / 4\pi\epsilon_0 c^2$. A black hole is called extremal if it has the smallest possible mass compatible with the value of its angular momentum and charges.

[3] The Bekenstein entropy bound as stated above applies only to spherical regions of space; later generalizations known as covariant entropy bounds include more general subsystems formed by converging light rays emanating from a spacelike codimension-two surface [17, 18].

[4] Intuitively, to get to the asymptotic boundary one has to follow a spacelike geodesic for an infinitely long distance. For a negatively curved spacetime, the asymptotic boundary is a timelike $d$-dimensional spacetime which is typically flat. Lightlike geodesics can reach this asymptotic boundary in finite time.

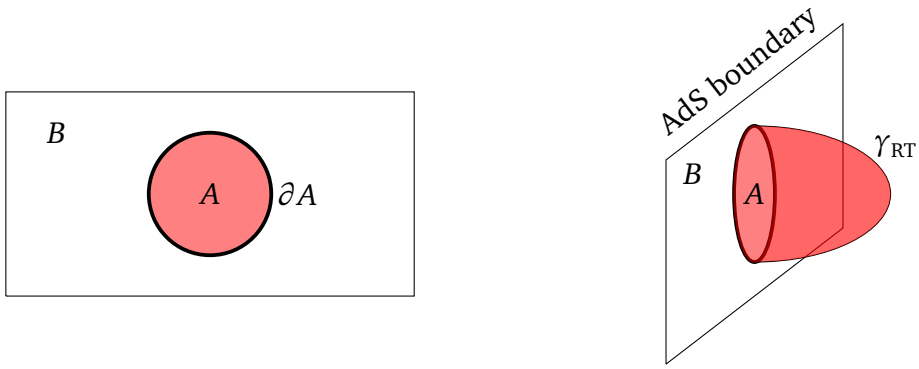


Figure 1.1.: The Ryu-Takayanagi surface $\gamma_{\mathrm{RT}}$ is the codimension-two surface with smallest area intersecting with the asymptotic AdS boundary at the bipartition surface $\partial A$ between the subregion $A$ and its complement $B$ on a constant time slice. The area of $\gamma_{\mathrm{RT}}$ is proportional to the entanglement entropy of $A$.

correspondence the gravitational theory is a string theory incorporating the full range of quantum gravity effects. In appropriate limits the gravitational theory reduces to a classical theory of general relativity with supersymmetric extensions depending on the details of the particular model chosen. The dual quantum field theory is generally invariant under conformal symmetry.[5] Although the AdS/CFT correspondence has not been directly proven, a large amount of evidence for its validity in the form of agreement between various quantities on the two sides of the duality has accumulated since its inception.

A particularly useful aspect of the AdS/CFT correspondence is that it is a strong-weak coupling duality, that is in the limit where the quantum field theory is strongly coupled the gravitational theory is weakly coupled and vice versa. This feature has been exploited in a wealth of applications to investigate properties of strongly coupled quantum field theories that are out of reach of more conventional methods. This includes for instance applications to QCD topics like the quark-gluon plasma or meson spectra (see [22, 23] for reviews), condensed matter systems like superconductors (reviewed for example in [24, 25]) or fluid dynamics under the name of fluid/gravity correspondence (see e.g. [26] for an overview on this topic).

Apart from being a useful tool for studying strongly coupled quantum field theories, the AdS/CFT correspondence also provides valuable insights into quantum gravity and black hole physics. In particular, because the correspondence equates a gravitational theory with a unitary quantum theory it is clear by construction that the gravity theory also respects unitarity and hence the information paradox is resolved for black holes in the AdS space. The precise manner in which the resolution of the paradox happens is, however, still subject to debate. An important development in this regard is the discovery of the so-called Ryu-Takayanagi formula, a duality between the area $A_{\mathrm{RT}}$ of a certain minimal surface $\gamma_{\mathrm{RT}}$ in the asymptotically AdS space (see figure 1.1) and the entanglement entropy $S_A$ of a corresponding subregion $A$ of the quantum field theory [27],

$$S_A = \frac{c^3 k_B A_{\mathrm{RT}}}{4 G_N \hbar}. \tag{1.3}$$

[5] Conformal transformations are an extension of the Poincaré transformations incorporating general angle-preserving maps. In dimensions higher than two, conformal transformations are composed out of translations $x^\mu \to x^\mu + a^\mu$, Lorentz transformations $x^\mu \to \Lambda^\mu_\nu x^\nu$, scale transformations $x^\mu \to \lambda x^\mu$ and inversions $x^\mu \to x^\mu/|x|^2$. In two dimensions, any analytic map $x^\pm \to f_\pm(x^\pm)$ of the lightcone coordinates $x^\pm = t \pm x$ is a conformal transformation.

Intuitively, the entanglement entropy $S_A$ is a measure for the amount of correlations between the subregion $A$ and its complement $B$. In formal terms, it is defined by the von Neumann entropy

$$S_A = -k_B \mathrm{Tr}(\rho_A \log \rho_A) \tag{1.4}$$

of the reduced density matrix $\rho_A = \mathrm{Tr}_B(\rho)$ for the subregion $A$ obtained by taking a partial trace over the degrees of freedom of the complement $B$. If the total state $\rho$ is pure, then the correlations measured by $\rho_A$ can come only from entanglement between $A$ and $B$ and thus $S_A$ is called entanglement entropy. The Ryu-Takayanagi formula (1.3) generalizes the Bekenstein-Hawking entropy formula in the AdS/CFT context. Moreover, it provides a new perspective on the holographic principle. Not only is the physics of the AdS space encoded like a hologram on its asymptotic boundary, but also certain subsystems of both theories obey this property: the physics of low-energy excitations in the boundary subregion $A$ that do not change the location of the Ryu-Takayanagi surface $\gamma_{\mathrm{RT}}$ is encoded in a subregion of the AdS space enclosed by $\gamma_{\mathrm{RT}}$ and $A$, the so-called entanglement wedge [28–30]. A striking example how the Ryu-Takayanagi formula helps in answering quantum gravity related questions can be found in [31–33] where the Ryu-Takayanagi formula (or more precisely a generalization thereof including quantum gravity corrections in higher orders in $G_N$ derived in [34, 35]) is used to propose a precise description how the black hole information paradox is resolved and unitarity is restored in an AdS black hole coupled to a non-gravitating bath.[6] In particular, as the black hole evaporates a growing part of the black hole interior – which classically is hidden behind the event horizon – appears in the entanglement wedge of the bath region that contains the Hawking radiation in these models. This shows that the state on this part of the black hole interior is encoded in the state of the Hawking radiation.

The Ryu-Takayanagi formula equates the entanglement entropy in the non-gravitational quantum theory with a geometric quantity that is related to the metric of the AdS space. Therefore, the holographic encoding of the AdS spacetime geometry in the state of the boundary theory is mediated by the entanglement inherent in this state. This has lead to the proposal that the geometry underlying classical general relativity is an emergent effect in AdS/CFT originating from entanglement in the boundary quantum field theory [37, 38]. This proposal has been subsumed under the catchphrase *entanglement builds geometry*. A simple example showing how entanglement and geometry are connected in AdS/CFT is provided by a non-traversable wormhole[7] between two asymptotic boundaries (denoted $L$ and $R$ for left and right here) in the AdS space. This wormhole has two event horizons. Far away from these horizons outside of the wormhole, the geometry looks like an AdS space. This kind of wormhole in AdS/CFT is dual to a thermofield double state [39]

$$|\psi\rangle_{\mathrm{TFD}} = \frac{1}{\sqrt{Z(\beta)}} \sum_n e^{-\beta E_n/2} |E_n\rangle_L \otimes |E_n\rangle_R. \tag{1.5}$$

Here, $|E_n\rangle$ are energy-eigenstates and $Z(\beta) = \sum_n e^{-\beta E_n}$ denotes the thermal partition function. The temperature $T = 1/\beta$ is equal to the Hawking temperature of the wormhole in the AdS space. $|\psi\rangle_{\mathrm{TFD}}$ is a highly entangled state of two conformal field theories living on disconnected Minkowski spaces denoted by $L$ and $R$. In the dual AdS space, the high degree of entanglement leads to a spacetime connection between the left and right system implemented by the wormhole. On the other hand, at zero temperature $|\psi\rangle_{\mathrm{TFD}} = |0\rangle_L \otimes |0\rangle_R$ is a product state dual to two disconnected empty AdS spacetimes.

[6] Note, however, that this is not the last word on the black hole information paradox as the systems with a non-gravitating bath used in [31–33] lead to massive gravitons [36] and therefore this description is not a realistic model of black holes evaporation in standard gravity theories with vanishing graviton mass.

[7] In this context, non-traversable refers to the fact that any object moving slower than or at the speed of light will eventually hit the singularity after crossing any one of the two event horizons.

A further interesting aspect of the Ryu-Takayanagi formula is that it admits phase transitions. For certain choices of subregion $A$ and quantum state $|\psi\rangle$ of the boundary theory, the location of the minimal surface $\gamma_{\mathrm{RT}}$ changes discontinuously as the state $|\psi\rangle$ or the size of the subregion $A$ is varied. This kind of phase transition in the entanglement entropy has applications for instance in probing confinement/deconfinement transitions of strongly coupled field theories [40, 41] or in condensed matter theory where entanglement entropy can be used as an order parameter indicating which side of a phase transition a topologically ordered system is at (see e.g. [42, 43]). Phase transitions in the entanglement entropy not only provide a useful tool for applications of AdS/CFT to the study of strongly coupled field theories, but they also present a challenge for the interpretation of the entanglement builds geometry proposal. The phase transition behavior of the entanglement entropy prevents the dual Ryu-Takayanagi surfaces from probing the entire AdS geometry and therefore there are certain subregions of the AdS spacetime known as *entanglement shadows* whose geometry is not encoded in entanglement data in the quantum field theory[8] [28, 44–47]. This incompleteness applies most interestingly to geometries in which the AdS space contains a black hole, wormhole or naked singularity. Here, the entanglement shadows lie close to event horizons or naked singularities, regions where strong quantum gravity effects might be expected to occur.

The Ryu-Takayanagi formula provides an interesting connection between the entanglement entropy and a gravitational observable, but the connections between quantum information and gravity in AdS/CFT extend beyond this example. For instance, the holographic mapping between gravity and field theory degrees of freedom in AdS/CFT can be interpreted as a quantum error correcting code (see e.g. [48–50]). The physics of low-energy excitations in the AdS space is encoded in the CFT in much the same way that a small set of logical qubits is encoded in the actual physical qubits of a quantum computer in the form of a quantum error correcting code. An error correcting code allows for reconstructing the logical qubits even in the presence of errors similar to how in AdS/CFT low-energy excitations in the entanglement wedge of a boundary subregion $A$ can be reconstructed even when an observer on the boundary only has access to the subregion $A$. Quantum error correction is central to the development of fault tolerant quantum computers, therefore it is quite striking to see this concept emerging also in AdS/CFT.

Further concepts from quantum information of interest in AdS/CFT are *quantum circuits* and their *computational complexity*. In computer science, computational complexity quantifies the minimal number of computation steps a certain algorithm needs to run on a computer (which may be either a classical or quantum computer with corresponding values of the computational complexity that can differ substantially between classical and quantum computers). This concept has been conjectured to play a role in black hole physics in AdS/CFT [51–54]. In this conjecture, the time-evolution of a black hole in the AdS space together with infalling and outgoing radiation is modeled by a quantum circuit. In principle, the exact decomposition of such a circuit could only be fixed by a complete theory of quantum gravity. However, taking quite generic assumptions on the number of degrees of freedom in the circuit as well as their time-evolution (e.g. using a number of qubits of the order of the black hole entropy and a random Hamiltonian) allows for modeling the black hole system and its radiation in a description that is unitary by construction. This kind of model has been used also beyond AdS/CFT e.g. to estimate the time-evolution of the entropy of Hawking radiation [55, 56] or the time-scales at which information thrown into a black hole leaks out again [57].

The computational complexity conjecture of [51–54] relates statements about the time-evolution of a black hole system to statements about the behavior of computational complexity in the quan-

[8] At least if only the subset of the entanglement data obtainable from the Ryu-Takayanagi formula, i.e. entanglement between complementary spatial subregions, is considered.

tum circuit modeling this black hole system. In a general sense, complexity theory puts restrictions on possible computations. In the quantum computing setup, these restrictions are statements about time-scales needed for quantum systems to evolve between particular input and output states when the time-evolution is generated by a sequence of unitary operators implementing the elementary computation steps. Because the black hole system in [51–54] is modeled by this kind of quantum circuit, restrictions on possible computations from complexity theory are translated into restrictions on physical processes in the black hole system.

The conjectured relation between computational complexity and black hole physics in AdS spaces is particularly interesting due to its connection to the "entanglement builds geometry" idea. In precise terms, [51–54] conjectures a relation between a suitable measure of computational complexity in the boundary quantum theory and a class of geometric objects in an AdS space containing a black hole or wormhole. These geometric objects probe precisely the features of the geometry which cannot be explained by the entanglement entropy in the boundary CFT. For instance, in the case of an AdS wormhole only a small part of the interior region behind the event horizons is penetrated by Ryu-Takayanagi surfaces $\gamma_{\mathrm{RT}}$ [58]. On the other hand, extremal spacelike hypersurfaces of dimension $d$ in a $d+1$-dimensional AdS space reaching through the wormhole from one asymptotic boundary to the other – whose volume was proposed as a candidate for a dual to computational complexity in [51, 52] – penetrate much deeper into the entire interior region. In particular, the time-evolution of this quantity (a linear growth for a time-scale exponential in the black hole entropy [59]) is in close accord with the time-evolution of computational complexity in the quantum circuit picture from [51–54]. In contrast, the time-evolution of the entanglement entropy (a saturation after a short time scale independent of the black hole entropy [58]) is drastically different. Therefore, if the conjecture of [51–54] is true, then knowledge of a suitable measure for the computational complexity of the boundary state can be used to gain information about the dual AdS geometry that is not accessible from entanglement data alone.

## Results and Outline

Let me now summarize the goals pursued in this thesis.

- Development of generalized holographic entanglement entropy formulas.

  The holographic dual of entanglement entropy currently known via the Ryu-Takayanagi formula applies only to spatial entanglement, that is entanglement between all of the degrees in a spatial subregion and its complement. This thesis studies generalized entanglement measures which quantity correlations between different fields of a conformal field theory as well as between spatial degrees of freedom. The gravitational dual to the corresponding entanglement entropy is given by a simple generalization of the Ryu-Takayanagi formula. The generalized Ryu-Takayanagi surfaces encountered in this formula resolve a puzzling feature of the "entanglement builds geometry" idea due to the Ryu-Takayanagi surfaces not probing entanglement shadow subregions in various asymptotically AdS spaces.

- Realization of quantum circuits in AdS/CFT and the study of computational complexity therein.

  This topic is studied in the restricted setup of quantum circuits composed out of consecutive conformal transformations. In particular, the aim here is to develop dualities between computational complexity measures and geometric features of the dual asymptotically AdS geometry. To this end, several proposals for computational complexity applicable to circuits built out of conformal transformations are examined critically. Moreover, gravity duals for

these circuits are developed in order to derive geometric duals to computational complexity measures (or building blocks thereof) from first principles.

The key conclusions of this thesis are:

- There is strong evidence for a duality between generalized entanglement entropy and the area of an extremal surface in the AdS space.

  Equalities between the area of extremal surfaces in spacetimes and entropies in the form of the Bekenstein-Hawking entropy (1.2) and the Ryu-Takayanagi formula (1.3) provide some of the most robust indications of quantum gravity effects found so far. The generalized Ryu-Takayanagi formula investigated in chapter 3 extends these equalities between surface areas and entropies even further in the AdS/CFT setting. The extremal surfaces for this case are codimension-two surfaces extending out to the AdS boundary like the Ryu-Takayanagi surfaces, but differ in their topology by for example winding around black hole horizons. This duality statement clarifies some important questions regarding the encoding of certain subregions of the AdS geometry (the entanglement shadows) in terms of CFT quantities, thereby contributing to a better understanding of the AdS/CFT correspondence. Moreover, the results of chapter 3 provide a stepping stone for future explorations. Just as the Ryu-Takayanagi formula has found applications to topics such as black hole physics or phase transitions in strongly coupled quantum field theories, its generalization will likely do so as well. Extending the somewhat restricted results obtained in this thesis which apply only to three-dimensional AdS spaces dual to two-dimensional conformal field theories and in part only to a specific AdS/CFT model (the D1/D5 system) is an important task in this regard to be tackled in the future.

- Quantum circuits built up from conformal transformations provide a good model to put computational complexity conjectures in AdS/CFT to the test.

  To date, various studies of computational complexity in the AdS/CFT context have been performed motivated by conjectures of [51–54] relating this quantity to features of black holes in AdS spaces. However, this research direction has been somewhat hampered by the fact that most of these studies were only able to perform qualitative comparisons between field theory and gravity features. One reason for this was often due to a lack of a detailed mapping between the implementation of a computation step in the quantum circuit construction in the field theory and of a corresponding implementation in the gravity theory. Here, a simple yet non-trivial model of a quantum circuit is provided in which both the field theory and gravity side is under good control. This allows for studying aspects of computational complexity in a quantitative way from first principles. Although this is still work in progress, at the time of writing a promising realization of a computational complexity measure has been identified whose interpretation on both sides of the duality is clear and which fulfills many of the properties expected from the conjectures of [51–54]. This construction may help in the future in answering the question whether computational complexity theory can provide insights into black hole physics. Moreover, there are surprising connections with the generalized entanglement entropy which deserve to be studied further.

This thesis is structured as follows:

- Chapter 2 reviews prior material needed in the remainder of the thesis. In particular, the AdS/CFT correspondence is reviewed in section 2.1, while section 2.2 gives an overview over the entanglement entropy in quantum field theory, its dual realization in AdS/CFT as well as the entanglement builds geometry proposal. In section 2.3, quantum circuits

for black holes are presented, holographic complexity conjectures are reviewed and an overview over previous work on computational complexity in quantum field theories is given. Finally, section 2.4 introduces coadjoint orbits and geometric actions, concepts from Lie group theory to be used later on in chapter 4.

- Chapter 3 studies generalized entanglement measures in AdS/CFT. After an introduction and motivation in section 3.1, the generalized entanglement measures are defined rigorously in section 3.2, paying particular attention to find a manifestly gauge invariant definition. Following this, section 3.3 gives a brief overview on the calculation methods used to derive explicit results for the generalized entanglement entropy. As a prerequisite for this, calculation methods for conformal blocks on the torus are developed in section 3.4. These methods are applied to the calculation of the ordinary and generalized entanglement entropy at finite size and finite temperature in section 3.5 and section 3.6 respectively.

  The results of this chapter have been published in [1] in collaboration with J. Erdmenger as well as in [3, 4].

- Chapter 4 is concerned with implementing quantum circuits in AdS/CFT and studying computational complexity measures therein. This line of research is motivated in section 4.1 before introducing the concrete class of circuits studied in section 4.2. Then, in section 4.3 and section 4.4, examples for complexity measures in these circuits are studied from geometric actions on coadjoint orbits and the Fubini-Study metric respectively. Finally, section 4.5 develops gravity duals to the field theory circuits in question and studies aspects of computational complexity in these gravity duals from first principles.

  The work presented in this chapter has resulted in the publication of [2, 5] in collaboration with J. Erdmenger, M. Flory, M. Heller and A.-L. Weigel.

- Chapter 5 contains conclusions and an outlook on future directions.

- A number of appendices present less important material on the conventions used for elliptic functions in appendix A, recursion relations for conformal blocks in appendix B, the thermal partition function of the $S_N$ orbifold conformal field theory in appendix C and some details of perturbative calculations of computational complexity measures in appendix D.

## Conventions

Unless indicated otherwise, I will use natural units in the rest of this thesis such that

$$c = \hbar = k_B = 1. \tag{1.6}$$

Newton's constant $G_N$ is left as an independent dimensionfull natural constant. The string length $l_s$ is defined to be

$$l_s = \sqrt{\alpha'}, \tag{1.7}$$

where $\alpha'$ is the universal Regge slope. Metrics in Lorentzian signature will use the mostly plus sign convention. I will always include the time direction when counting the number of dimensions of a Lorentzian manifold. Therefore, a $d$-dimensional theory lives in $d-1$ space dimensions and one time dimension.

# 2. Preliminaries

This chapter reviews prior work which forms the foundation of this thesis for the benefit of readers that are not immersed deeply in research on the Anti-de Sitter/conformal field theory correspondence. I will start in section 2.1 with background material on AdS/CFT. In particular, I will give a general overview on the most important features of the correspondence before describing in detail an example of an AdS/CFT model known as the D1/D5 system which will be used in later chapters. In section 2.2, I will turn to a review of entanglement in the AdS/CFT correspondence. I will show how entanglement can be quantified using the entanglement entropy in quantum mechanics and quantum field theory, explain the gravitational dual to entanglement entropy in AdS/CFT and the role of entanglement in the encoding of geometric features of the AdS space in terms of field theory data. Subsequently, in section 2.3 I will give an overview over the role of quantum circuits and computational complexity in black hole physics in AdS/CFT as well as a short introduction to computational complexity in quantum field theories. Finally, section 2.4 explains coadjoint orbits and geometric actions, concepts from Lie group theory to be used in chapter 4.

## 2.1. The AdS/CFT correspondence

When one speaks of a duality in physics, what is meant is an equivalence between two distinct descriptions of the same physical system. Dualities are not uncommon occurrences, for instance the equivalence of Hamiltonian and Lagrangian descriptions of classical mechanics constitutes one. The duality I am going to discuss in this section has some peculiar features: it equates two theories in different number of dimensions, it provides a duality between a theory with gravity effects and one without and finally – in appropriate limits – it maps a classical to a quantum theory. These features make the AdS/CFT correspondence a particularly interesting physical system to study.

### 2.1.1. Generalities

Let me start by summarizing the most important general features of the AdS/CFT correspondence. The presentation in this section largely follows the reviews in [60, 61].

The AdS/CFT correspondence is the statement that a $d+1$-dimensional gravitational theory on a spacetime with negative curvature is equivalent to a $d$-dimensional non-gravitational quantum field theory. This conjecture was first put forward in [21]. Spacetimes of constant negative curvature are called Anti-de Sitter or AdS spaces and general negatively curved spacetimes are referred to as asymptotically AdS, hence the "AdS" part of AdS/CFT. The "CFT" part stands for conformal field theory and refers to the fact that the non-gravitating quantum field theory generally is invariant under conformal symmetry. By equivalence of the two theories, it is meant that each physical observable in one description has a counterpart in the dual description and all possible measurements of those observables (such as expectation values, correlation functions, etc.) on both sides of the duality agree with each other. Formally, this is expressed as the equivalence of

the generating functionals of correlation functions of both theories [21, 62, 63],

$$Z_{\text{AdS}}[J] = Z_{\text{CFT}}[J], \tag{2.1}$$

where $J$ denotes collectively the source currents for the conformal field theory operators. These currents turn up also on the AdS side, see below for details. Differentiating w.r.t. $J$ gives the correlation functions of the theories which due to (2.1) must agree for the "CFT" and the "AdS" theory.

The details of the theories on the two sides of the correspondence – the Lagrangian and the exact number and types of fields present – depend on the number of spacetime dimensions and the exact model chosen. In the strongest form of the correspondence, the gravitational theory is a string theory on a $d+1$-dimensional spacetime times a number of compact directions. For instance, one of the most well-known AdS/CFT dualities posits a duality between four-dimensional $\mathcal{N} = 4$ super Yang-Mills theory with $SU(N)$ gauge group and type IIB string theory on $\text{AdS}_5 \times S^5$ [21]. Another popular model is a two-dimensional superconformal field theory with $S_N$ gauge group dual to type IIB string theory on $\text{AdS}_3 \times S^3 \times T^4$ [21]. The latter model will be used to a large extent in this thesis and I will introduce it in detail in section 2.1.3.

Often, the full range of quantum gravity effects described by the string theory is either not needed for some applications or too complex to handle and a limit in which this string theory reduces to supergravity, i.e. a supersymmetric extension of general relativity, is taken. In this case, a saddle point approximation of the gravity partition function reduces (2.1) to [62, 63]

$$e^{iS_{\text{grav}}[J]} = Z_{\text{CFT}}[J], \tag{2.2}$$

where $S_{\text{grav}}[J]$ is the (on-shell) supergravity action. This is known as the weak form of the AdS/CFT correspondence [60]. This limit involves both a small string coupling constant $g_s$ such that string theory quantum corrections are suppressed as well as a string length $l_s$ that is small compared to the only dimensionfull scale of the bulk AdS space, the AdS radius $L$.[1] Hence, in the weak limit

$$g_s \to 0 \quad \text{and} \quad l_s/L \to 0. \tag{2.3}$$

The AdS radius is related to the Ricci scalar by $R = -(d+1)d/L^2$. On the field theory side, the weak form of the AdS/CFT correspondence is attained at strong coupling and in the limit of a large number of degrees of freedom, i.e. large rank of the CFT gauge group. For example, for $\mathcal{N} = 4$ SYM with gauge group $SU(N)$ the weak limit is characterized by large 't Hooft coupling $\lambda = g_{\text{YM}}^2 N$ and large $N$ such that [21]

$$\lambda \to \infty \quad \text{and} \quad N/\lambda = g_{\text{YM}}^{-2} \to \infty, \tag{2.4}$$

where $g_{\text{YM}}$ is the Yang-Mills coupling constant. In this AdS/CFT construction, the parameters are related by [21]

$$\lambda/N = g_{\text{YM}}^2 = 2\pi g_s \quad \text{and} \quad 2\lambda = L^4/l_s^4. \tag{2.5}$$

For two-dimensional CFTs which I will focus on, there is a universal relation between the central

[1] The physical interpretation of the string length is that $l_s$ sets the scale for the length of a typical string, i.e. the smaller $l_s$, the more energy it takes to stretch out a string. Oftentimes, the parameters $\alpha' = l_s^2$ (the universal Regge slope) or $T = 1/(2\pi l_s^2)$ (the string tension) are used instead of $l_s$. Note that some references use a different convention for the string length than in this thesis with an additional factor of $2\pi$, $l_s = 2\pi\sqrt{\alpha'}$. The string coupling constant $g_s$ is the analog of the coupling constant in ordinary quantum field theory, i.e. loop contributions to string amplitudes are suppressed by powers of $g_s$.

charge and the AdS radius divided by Newton's constant [64],

$$c = \frac{3L}{2G_N}. \tag{2.6}$$

Equation (2.6) is valid for any two-dimensional CFT with an AdS dual. In this case, the limit of large numbers of degrees of freedom is equivalent to the limit of large central charge $c \to \infty$ and hence implies that the gravity dual is weakly coupled, i.e. Newton's constant is small.

It is in the weak limit that the most evidence has accumulated for the validity of the AdS/CFT correspondence although a proof from first-principles seems to be out of reach at the present moment. This thesis will also focus mostly on the weak form of the AdS/CFT correspondence, although in chapter 3 some calculation will be done in an intermediate limit in which the string coupling constant is still small while the string length is parametrically large compared to the AdS radius, equivalent to the $c \to \infty$ limit at weak coupling in the CFT. This is sometimes termed the strong form of the AdS/CFT correspondence as opposed to the strongest form where both the coupling constant and the string length are allowed to be large [60, 61].

Another distinction that is often made in discussions of the AdS/CFT correspondence (for instance in [61]) is between "top-down" and "bottom-up" AdS/CFT models. The AdS/CFT correspondence has shown to be valid for a large class of quantum field theories. These theories are called holographic conformal field theories. In many cases, it is advantageous to consider not a particular member of this class of CFTs but instead work with a generic holographic CFT without specifying in detail the field content or Lagrangian of the theory. This method is referred to as "bottom-up" in contrast to the "top-down" method where starting from a string-theory construction the CFT in question is derived from first principles. The main advantage of the bottom-up method – apart from being technically simpler in many cases – is that the results obtained with this method apply to all members of the class of holographic CFTs considered instead of just a specific member of the class as in the top-down method. However, the disadvantage of the bottom-up method is of course that some of the details of the correspondence may be missing because the CFT chosen is too generic. Such effects will turn up in chapter 3 where I will make use of both top-down and bottom-up constructions.

Finally, another important point to note about the AdS/CFT correspondence is that it is a concrete manifestation of the holographic principle. This was first pointed out in [62, 65]. As stated in the introduction, the holographic principle posits that the maximum amount of information contained in a subsystem of a quantum gravity theory scales with the area of the subsystem boundary [19, 20]. Thus, one might speculate that there is a lower-dimensional description of the subsystem from a theory living on its boundary. This is of course exactly the situation described by the AdS/CFT correspondence, where the gravitational subsystem consists of the entire asymptotically AdS space dual to a conformal field theory living on its boundary. This has a number of interesting implications. For example, it is immediately obvious that the gravity theory is unitary because it is dual to a conformal field theory that is unitary by construction. Thus, it is clear that the black hole information paradox is solved in this theory of quantum gravity because by construction black hole evaporation is a unitary process.[2] The precise manner in which this happens in the gravity theory is, however, a quite non-trivial problem which is still subject to investigation.

[2]Note that not all black holes in asymptotically AdS spaces evaporate because massless particles emitted by the black hole reach the asymptotic boundary in a finite time where they are reflected and fall back into the black hole. Thus, only small black holes evaporate in asymptotically AdS spaces while large black holes are in thermal equilibrium with their Hawking radiation. However, constructions that couple the AdS space to a bath system in which the black hole evaporates are also available (see for instance [31, 32, 66–68]).

### 2.1.2. The AdS/CFT dictionary

Let me now describe in detail the map between field theory operators and their holographic duals. This map is usually called the *AdS/CFT dictionary*. It contains among many other entries for instance a duality between the metric of the bulk AdS space and the energy-momentum tensor in the boundary CFT or between scalar operators in the bulk and scalar quantum fields on the boundary.[3] This section explains how the map works in detail for correlation functions and expectation values of local operators.[4] The presentation here follows the reviews in [69] and [61].

The main feature of the AdS/CFT dictionary for local operators is an identification of the leading asymptotic term in a near-boundary expansion of a bulk field with the source for the corresponding boundary operator while the vacuum expectation value of this operator is encoded in a subleading term in the expansion [62, 63]. To be precise, let me first note that a general $d+1$-dimensional asymptotically AdS metric may be written in the Fefferman-Graham coordinate system [70],

$$ds^2 = L^2\left[\frac{d\rho^2}{4\rho^2} + \frac{1}{\rho}\kappa_{ij}(x,\rho)dx^i dx^j\right], \tag{2.7}$$

where $i,j \in \{1,...,d\}$ and $\rho$ is the radial coordinate of the AdS space such that the asymptotic boundary is located at $\rho = 0$. The AdS radius $L$ is related to the cosmological constant by $\Lambda = -\frac{d(d-1)}{2L^2}$. Close to the boundary, a field $\mathscr{F}$ of the gravity theory may be expanded as [69]

$$\mathscr{F}(x,\rho) = \rho^m(f_{(0)}(x) + \rho f_{(2)}(x) + ... + \rho^n(f_{(2n)}(x) + \tilde{f}_{(2n)}(x)\log\rho) + ...) \tag{2.8}$$

for some constants $m,n$. The coefficients in the expansion are determined as follows [69]. The leading coefficient $f_{(0)}(x)$ is identified with the source for the dual operator while $f_{(2n)}(x)$ is related to its expectation value. The other coefficients are fixed from the bulk equations of motion. There are two independent coefficients $f_{(0)}(x)$ and $f_{(2n)}(x)$ whose value is not determined from the bulk e.o.m. because these equations are generally second order differential equations whose solution depends on two boundary conditions. The coefficient $\tilde{f}_{(2n)}(x)$ of the logarithmic term is generally related to conformal anomalies and also determined from the bulk equations of motion.

Calculating expectation values and correlation functions from differentiating a generating functional generally requires renormalization in QFT. Thus, it comes as no surprise that a renormalization procedure is also needed for this calculation from the gravity side. This procedure is known as holographic renormalization and works as follows [69, 71–73]. The first step is to insert the solutions to the bulk equations of motion into the bulk action. The on-shell action obtained in this way is divergent with the divergences originating from the region close to the boundary. Thus, the second step is to regularize the on-shell action by restricting the integration range of the radial direction $\rho$ to $\rho \geq \epsilon$. The regularized on-shell action can then be written in an expansion in inverse powers of $\epsilon$,

$$S_{\text{reg}}[f_{(0)}] = \int_{\rho=\epsilon} d^d x[\epsilon^{-\nu}a_{(0)} + \epsilon^{-(\nu+1)}a_{(2)} + ... + a_{(2\nu)}\log\epsilon + O(\epsilon^0)], \tag{2.9}$$

where $\nu$ is a positive number and the coefficients $a_{(2k)}$ are local functions of the source $f_{(0)}$. The

[3] In the following, I will often call the asymptotically AdS space the "bulk" while the manifold on which the CFT lives will be called the "boundary" when it is clear from context that this refers to the AdS boundary.

[4] There is also a multitude of entries in the AdS/CFT dictionary for various non-local observables. These entries are not accessible with the methods described in this section. I will describe one such entry – the entanglement entropy – in detail in section 2.2.2.

third step, renormalizing the bulk action, involves adding covariant counterterms to the regularized bulk action $S_{\text{reg}}$ and taking the $\epsilon \to 0$ limit. These counterterms cancel the contributions to $S_{\text{reg}}$ that diverge as $\epsilon \to 0$. In order to be independent of the coordinate system in use, these counterterms are expressed in terms of the bulk field $\mathscr{F}(x,\epsilon)$ and the induced metric at the cutoff surface $\rho = \epsilon$. Thus the counterterm action $S_{\text{ct}}$ is the unique covariant action that when added to the on-shell bulk action gives a finite total action as $\epsilon \to 0$. On a technical level, it is obtained by inverting the series (2.8) to express $f_{(0)}(x)$ as a function of $\mathscr{F}(x,\epsilon)$ and inserting the result into the coefficients $a_{(2k)}$ from (2.9). Then, the vacuum expectation value of the CFT operator $\mathscr{O}_f$ dual to $\mathscr{F}(x,\epsilon)$ is obtained by taking a variational derivative of the renormalized action

$$S_{\text{ren}} = S_{\text{reg}} - S_{\text{ct}} \tag{2.10}$$

w.r.t. the source $f_{(0)}$,

$$\langle \mathscr{O}_f(x) \rangle = \left. \frac{\delta S_{\text{ren}}}{\delta f_{(0)}(x)} \right|_{f_{(0)}=0} \tag{2.11}$$

To calculate higher-point correlation functions, one simply takes further variational derivatives.

As an example, consider the duality between the bulk metric and the expectation value of the boundary energy-momentum tensor. This duality was derived in detail in [73], whose exposition I will follow here. The Einstein-Hilbert action on a $d+1$-dimensional asymptotically AdS space $\mathscr{M}$ with boundary $\partial\mathscr{M}$, including the Gibbons-Hawking-York boundary term, is given by

$$S_{\text{grav}} = \frac{1}{16\pi G_N} \left[ \int_{\mathscr{M}} d^{d+1}x \sqrt{g}(R[g] - 2\Lambda) - 2 \int_{\partial\mathscr{M}} d^d x \sqrt{\gamma} K \right]. \tag{2.12}$$

As explained above, asymptotically AdS spaces can be written in Fefferman-Graham form (2.7) where $\kappa_{ij}$ can be expanded as

$$\kappa(x,\rho) = \sum_{k=0}^{\lfloor (d-1)/2 \rfloor} \rho^k g^{(2k)}(x) + \rho^{d/2}(g^{(d)}(x) + h^{(d)}(x)\log\rho) + O(\rho^{(d+1)/2}) \tag{2.13}$$

The coefficient of the logarithmic term vanishes for $d$ even. The boundary metric $g^{(0)}(x)$ is obtained from the divergent part of the bulk metric at $\rho = 0$,

$$g^{(0)}_{ij}(x) = \lim_{\rho\to 0}(\rho\, g_{ij}(x,\rho)). \tag{2.14}$$

Inserting this into Einstein's equations and solving order by order gives expressions for the coefficients $g^{(2k)}(x)$ from (2.13) in terms of $g^{(0)}(x)$. This method gives unique solutions for all terms up to order $\rho^{d/2}$. At this order in the $\rho$ expansion, undetermined integration constants appear in the solution of Einstein's equations. These integration constants are related to the vacuum expectation value of the energy-momentum tensor. Let me focus on the case $d = 2$ which will be considered in much of the remainder of this thesis. In this case, the solution for $g^{(2)}$ is given by [73, 74]

$$g^{(2)}_{ij} = \frac{1}{2}(R^{(0)} g^{(0)}_{ij} + t_{ij}) \tag{2.15}$$

where $t_{ij}$ are integration constants which are constrained by Einstein's equation to fulfill

$$\nabla^i t_{ij} = 0 \quad \text{and} \quad g^{ij}_{(0)} t_{ij} = -R^{(0)}. \tag{2.16}$$

Equation (2.16) is equivalent to the conservation equation and Weyl anomaly for the expectation value of the energy-momentum tensor $\langle T_{ij}\rangle = \frac{c}{12} t_{ij}$ in a two-dimensional conformal field theory,

$$\nabla^i T_{ij} = 0 \quad \text{and} \quad \mathrm{Tr}(T) = -\frac{c}{12} R^{(0)}. \tag{2.17}$$

This justifies the identification of $g_{ij}^{(0)}$ with the source for $T_{ij}$. For the higher order terms in the $\rho$ expansion, note that the Fefferman-Graham expansion truncates at the $\rho^2$ term for $d = 2$. The coefficient of this term is given by [73, 74]

$$g_{ij}^{(4)} = \frac{1}{4}(g^{(2)}(g^{(0)})^{-1} g^{(2)})_{ij}. \tag{2.18}$$

In this manner, the bulk metric is determined uniquely[5] from the expectation value of the energy-momentum tensor and the boundary metric. Note that this is special to three-dimensional asymptotically AdS spaces. In general, the $\rho$ expansion in (2.13) does not truncate and therefore the solution for the bulk metric obtained by the procedure described above is only valid in a series expansion near the boundary [69].

The holographic renormalization procedure for energy-momentum tensor correlators works as follows. The regulated Einstein-Hilbert action is obtained by integrating $\rho$ in (2.12) from some small number $\epsilon$ to $\infty$. Inserting the Fefferman-Graham expansion (2.7), the regulated action is given by [69]

$$\begin{aligned} S_{\text{reg}} = \frac{1}{16\pi G_N} \int d^d x \Bigg[ \int_\epsilon^\infty d\rho \, \frac{d}{\rho^{d/2+1}} \sqrt{\det \kappa(x,\rho)} \\ + \frac{1}{\rho^{d/2}} \left( -2d \sqrt{\det \kappa(x,\rho)} + 4\rho \partial_\rho \sqrt{\det \kappa(x,\rho)} \right) \Bigg]. \end{aligned} \tag{2.19}$$

The $\rho$ integral in (2.19) can then be evaluated using (2.13). This allows an expansion of the regulated action in powers of $\epsilon$ as in (2.9). Here, $\nu$ from (2.9) is equal to $d/2$. For the coefficients, one finds for instance for $d = 2$ [73],

$$a_{(0)} = \frac{L}{16\pi G_N} \sqrt{\det g^{(0)}}(-2), \quad a_{(2)} = \frac{L}{16\pi G_N} \sqrt{\det g^{(0)}} g_{(0)}^{ij} g_{ij}^{(2)}. \tag{2.20}$$

To renormalize the regulated action, it is necessary to add covariant counterterms. These are obtained by expressing the boundary metric $g^{(0)}$ in terms of the induced metric $\gamma$ on the cutoff surface $\rho = \epsilon$. Inserting this form of $g^{(0)}$ back into the coefficients (2.20), covariant expressions for counterterms are obtained that when subtracted from the regulated action cancel the divergent parts. In $d = 2$, one finds [73]

$$\sqrt{\det g^{(0)}} = \epsilon \sqrt{\det \gamma} + O(\epsilon^2), \quad g_{(0)}^{ij} g_{ij}^{(2)} = \frac{1}{2\epsilon} R[\gamma] + O(\epsilon^0), \tag{2.21}$$

where $R[\gamma]$ is the Ricci scalar of $\gamma$. Therefore, the counterterm action is given by

$$S_{\text{ct}} = \frac{1}{16\pi G_N} \int d^d x \sqrt{\det \gamma} \left[ -2 + \log \epsilon \, \frac{1}{2} R[\gamma] \right]. \tag{2.22}$$

[5] At least in the coordinate patch covered by the Fefferman-Graham coordinates (2.7) which may not cover the entire spacetime [69].

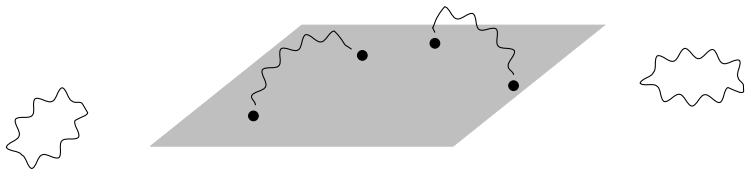

Figure 2.1.: An illustration of a D-brane together with a few open strings attached to it and closed strings in the surrounding spacetime.

The energy-momentum tensor expectation value is obtained by varying the renormalized action (2.10) w.r.t. the boundary metric $g^{(0)}$,

$$\langle T_{ij}\rangle = \frac{4\pi}{\sqrt{\det g^{(0)}}}\frac{\delta S_{\text{ren}}}{\delta g^{ij}_{(0)}}. \tag{2.23}$$

As expected, the result is proportional to the undetermined integration constant $t_{ij}$ in the metric [73],

$$\langle T_{ij}\rangle = \frac{L}{8G_N}t_{ij} = \frac{L}{4G_N}\big(g^{(2)}_{ij} - g^{(0)}_{ij}(g^{kl}_{(0)}g^{(2)}_{kl})\big). \tag{2.24}$$

The prefactor $\frac{L}{8G_N}$ is equal to $\frac{c}{12}$ due to (2.6). Higher point correlation functions of the energy-momentum tensor are determined by simply applying further variational derivatives onto the one-point function. Note that for this procedure one has to take into account that $t_{ij}$ depends non-locally on the boundary metric $g^{(0)}_{ij}$ through (2.16).

### 2.1.3. The D1/D5 system

The D1/D5 system is one of the most well-known examples of a top-down AdS/CFT construction. In this section, I will show how the D1/D5 system is constructed from stacks of D1 and D5 branes and how this constructions leads to the duality between a two-dimensional conformal field theory and string theory on three-dimensional asymptotically AdS spaces. Readers interested in more details are instructed to look into the reviews [60, 75].

#### D-branes from two viewpoints

I begin the exposition with a brief introduction to the basic concepts of string theory, namely strings and D-branes. As the name implies, strings are one-dimensional objects moving in spacetime. They come in two flavors: closed strings form a closed loop in space while open strings do not. The equations of motion of string theory admit two possible boundary conditions at the endpoints of an open string. For Neumann boundary conditions, the string endpoints move freely at the speed of light. On the other hand, for Dirichlet boundary conditions the endpoints are fixed at a particular position in space or time. Hypersurfaces where open strings with Dirichlet boundary conditions end are called D-branes. There are two facets of D-branes which are important for AdS/CFT constructions which I will now explain in turn. More details on the material in this section may be found in most textbooks on string theory, for instance in [76, 77].

The first facet is that the fluctuations of string endpoints on D-branes are described by a quantum field theory that incorporates gauge symmetries characterized by the specific configuration of D-branes in question. Consider for example a $d$-dimensional Minkowski spacetime in which lives a $p+1$-dimensional D-brane[6] extending infinitely along the time direction and $p$ space directions

[6]This is referred to as a D$p$-brane for short.

at coordinates $c^I$ for $I \in \{p+1, ..., d-1\}$. The first excited states of an open string along the $p+1$ directions longitudinal to the brane are massless and of spin one, leading to a $U(1)$ gauge theory with gauge fields $A_a$ for $a \in \{0, ..., p\}$. From the point of view of this gauge theory, the lowest excitations of an open string in the $d-p-1$ directions transversal to the brane are massless scalars $\phi^I$. These scalars parametrize fluctuations of the location of the D$p$-brane. The presence of the D$p$-brane breaks the $SO(1,d-1)$ Lorentz symmetry of the surrounding Minkowski space to $SO(1,p)\times SO(d-p-1)$. The gauge fields transform as a vector under the $SO(1,p)$ part while the scalars transform as a vector under the $SO(d-p-1)$ rotation group. Together, these excitations are described by a low-energy effective action known as the Dirac-Born-Infeld action,[7]

$$S_{\text{DBI}} = -\frac{T_p}{g_s}\int d^{p+1}\xi\sqrt{-\det(g_{ab}+2\pi l_s^2 F_{ab})}, \tag{2.25}$$

where $g_s$ is the string coupling constant, $l_s$ the string length, $T_p = 2\pi/l_s^{p+1}$ the tension of the D$p$-brane and $F_{ab}$ the field strength corresponding to $A_a$. The action (2.25) describes the dynamics of the D$p$-brane to leading order in an expansion for small $g_s$ and to all orders in $l_s$. The coordinates $\xi^a$ are intrinsic to the brane while $X^\mu$ are the coordinates of the surrounding Minkowski space. The metric $g_{ab}$ is obtained by pulling back the target space Minkowski metric $\eta_{\mu\nu}$ onto the brane,

$$g_{ab} = \frac{\partial X^\mu}{\partial \xi^a}\frac{\partial X^\nu}{\partial \xi^b}\eta_{\mu\nu}. \tag{2.26}$$

Now choose w.l.o.g. the static gauge $\xi^a = X^a$ and parametrize the fluctuations of the brane location in the transverse space as

$$X^I = c^I + 2\pi l_s^2 \phi^I(\xi) + ... \tag{2.27}$$

Then, expanding (2.25) in powers of $l_s$ gives to leading order

$$S_{\text{DBI}} = -\frac{T_p}{g_s}\int d^{p+1}\xi\left(1+(2\pi l_s^2)^2\left[\frac{1}{4}F_{ab}F^{ab}+\frac{1}{2}\partial_a\phi^I\partial^a\phi^I\right]\right)+O(l_s^6) \tag{2.28}$$

We recover the well-known action for a $U(1)$ gauge field and free scalars. The coupling constant $g_{\text{YM}}$ for the gauge field action can be immediately read off from (2.28),

$$g_{\text{YM}}^2 = \frac{g_s}{T_p}(2\pi l_s^2)^{-2} = g_s(2\pi)^{p-2}l_s^{p-3}. \tag{2.29}$$

Up to now, only the lowest energy excitations were included in the low-energy effective description. Higher excited states lead to massive fields from the point of view of the $p+1$-dimensional gauge theory. In the following, I will always work in the limit where $g_s$ and $l_s$ are small such that the effect of these excitations can be neglected and (2.28) is a good description of the D-brane physics.

More general gauge theories are possible for constructions involving multiple branes. These constructions include open strings stretching between two different branes. Such configurations lead to gauge theories with larger gauge groups. For instance, $N$ D$p$-branes are described at low energies by a $U(1)^N$ gauge theory with $N^2$ spin one fields and $N^2$ scalars. The gauge symmetry gets enhanced to $U(N)$ when the branes are coincident in space and time. Such a configuration of coincident branes is called a *stack of D-branes*. The low-energy effective action for this system

[7] The form of the DBI action presented here is valid for a Minkowski space background with vanishing Kalb-Ramond field and constant dilaton. See [76] for the general form.

is an immediate generalization of (2.28),

$$S_{\rm DBI} = -\frac{T_p}{g_s}\int d^{p+1}\xi\left(1+(2\pi l_s^2)^2{\rm Tr}\left[\frac{1}{4}F_{ab}F^{ab}+\frac{1}{2}D_a\phi^I D^a\phi^I-\frac{1}{4}\sum_{I,J}[\phi^I,\phi^J]^2\right]\right)+O(l_s^6), \quad (2.30)$$

where $D_a$ denotes the covariant derivative w.r.t. the $U(N)$ gauge connection,

$$D_a\phi^I = \partial_a\phi^I + i[A_a,\phi^I], \quad (2.31)$$

the field strength is defined as

$$F_{ab} = \partial_a A_b - \partial_b A_a + i[A_a, A_b] \quad (2.32)$$

and the trace runs over the indices labeling the $U(N)$ generators $T^j$ in which the fields are expanded,

$$A_a = A_a^j T^j \quad \text{and} \quad \phi^I = \phi^{I,j}T^j. \quad (2.33)$$

The action (2.30) approximates the physics of the D-brane stack well if $g_sN$ and $l_s$ are both small.[8]

The second important facet of D-branes is that the branes themselves are dynamical objects. In particular, they are charged under $p+1$ form gauge potentials.[9] This charge contributes to the energy-momentum tensor. In an appropriate limit, a stack of D-branes is well approximated by supergravity as the low-energy effective description of string theory. Due to the effect of the charge on the energy-momentum tensor, the branes can be treated as heavy extended objects in this limit. In this description, the presence of the D-branes leads to a curved background geometry on which small stringy perturbations live. The metric and dilaton of a stack of $N$ coincident D$p$-branes in type IIA or type IIB supergravity in 10 dimensions is given by [60]

$$\begin{aligned} ds^2 &= \frac{1}{\sqrt{H(r)}}\left(-dt^2+\sum_{a=1}^{p}dx^a dx^a\right)+\sqrt{H(r)}(dr^2+r^2 d\Omega_{8-p}^2), \\ e^{\Phi} &= g_s H(r)^{(3-p)/4}, \end{aligned} \quad (2.34)$$

where

$$r^2 = \sum_{i=p+1}^{9} x^i x^i\,, \quad H(r) = 1+\frac{r_+^{7-p}}{r^{7-p}}\,, \quad r_+^{7-p} = d_p g_s N l_s^{7-p} \quad (2.35)$$

and $d_p = 2^{5-p}\pi^{(5-p)/2}\Gamma((7-p)/2)$. The solution also includes a non-vanishing $p+2$ form field strength $F_{p+2}$ such that the stack of D$p$-branes has charge

$$\int_{S^{8-p}} \star F_{p+2} = N \quad (2.36)$$

where $S^{8-p}$ is an $(8-p)$-dimensional sphere surrounding the branes in the transverse directions. The supergravity solution (2.34) includes an event horizon at $r=0$. The stack of branes thus appears in the supergravity approximation as a charged black hole with an extended non-compact horizon. This object is also termed a *black brane*. The description as a black brane is accurate in

[8] Because there are $N$ branes between which strings can stretch, the string coupling constant effectively becomes $N$ times as large as for a single brane.

[9] These potentials are differential forms of rank $p+1$ leading to field strengths described by differential forms of rank $p+2$. In this language, the gauge field from electromagnetism is a one-form gauge potential which has a rank-two field strength tensor.

| | $\mathbb{R}^{1,1}$ | | $\mathbb{R}^4$ | | | | $T^4$ | | | |
|---|---|---|---|---|---|---|---|---|---|---|
| | 0 | 1 | 2 | 3 | 4 | 5 | 6 | 7 | 8 | 9 |
| D1 | • | • | - | - | - | - | - | - | - | - |
| D5 | • | • | - | - | - | - | • | • | • | • |

Table 2.1.: D-brane configuration for the D1/D5 system. The D-branes extend into the directions indicated by the black dots.

the limit that $g_sN$ is large and $g_s$ small.[10] The latter statement ensures that string loop corrections are suppressed such that quantum corrections to supergravity are negligible. The former statement ensures that the string length $l_s$ is small compared to the curvature scale of the supergravity solution (2.34). The relation between $l_s$ and the curvature scale is determined through the dependence of the supergravity solution on $l_s$ via equation (2.35).

To summarize, there are two descriptions of a stack of coincident D$p$-branes: one description as a $p+1$-dimensional gauge theory and another description as a charged black brane in supergravity. These descriptions are applicable in different parameter regimes: while the gauge theory description requires $g_sN \ll 1$, the supergravity description is valid for $g_sN \gg 1$.

### The D1/D5 system

In this section, the discussion which up to now was quite general specializes to a brane configuration involving both D1 and D5 branes termed the D1/D5 system. This system will be examined again from the two viewpoints introduced in the previous subsection. From this discussion, the AdS/CFT duality will naturally emerge.

The D1/D5 system arises from two stacks of D-branes: $N_1$ D1-branes extending along the time direction $x^0$ and the first spatial direction $x^1$ as well as $N_5$ D5-branes extending along the same directions and four spatial directions $x^6, ..., x^9$ compactified on a four-torus $T^4$ (see table 2.1). This four-torus is taken to be parametrically small, its volume being of the order $l_s^4$,

$$V_{T^4} = l_s^4 v_4, \tag{2.37}$$

where $v_4$ is a dimensionless number of order one.[11] The remaining directions $x^2, ..., x^5$ comprise a Euclidean space $\mathbb{R}^4$.

From the supergravity viewpoint, the D1/D5 system is described by a classical solution of type IIB supergravity in 10 dimensions with action

$$\begin{aligned} S =& \frac{1}{2\tilde{\kappa}_{10}^2} \int d^{10}x \sqrt{-g} \left[ e^{-2\Phi} \left( R + 4(\partial\Phi)^2 - \frac{1}{2}H^2 \right) - \frac{1}{2} \left( F_{(1)}^2 + F_{(3)}^2 + \frac{1}{2}F_{(5)}^2 \right) \right] \\ & - \frac{1}{4\tilde{\kappa}_{10}^2} \int C_{(4)} \wedge H \wedge dC_{(2)}, \end{aligned} \tag{2.38}$$

where $\tilde{\kappa}_{10}^2 = l_s^8/(4\pi)$ is the ten-dimensional gravitational coupling constant and

$$H = dB, \quad F_{(1)} = dC_{(0)}, \quad F_{(3)} = dC_{(2)} - C_{(0)}H, \quad F_{(5)} = dC_{(4)} - H \wedge C_{(2)}. \tag{2.39}$$

[10] Of course, close to the black brane singularity the supergravity description breaks down [60]. Note, however, that in the special case of $p = 3$, the black brane geometry does not contain a singularity despite the existence of a horizon [78].

[11] When speaking of an order one number, it is meant that the number is neither parametrically large nor parametrically small and is kept fixed whenever particular limits are taken in the following.

$F_{(5)}$ has to be self-dual, $F_{(5)} = \star F_{(5)}$. The rank $k$ differential forms $C_{(k)}$ are called Ramond-Ramond gauge fields while the two-form $B$ is known as the Neveu-Schwarz $B$-field. $\Phi$ is the dilaton and $g$ the metric with Ricci scalar $R$ as usual. The D1/D5 system is then described by the following solution to the equations of motion of (2.38) [79] (see also [75]),

$$\begin{aligned} ds^2 &= \frac{-(dx^0)^2 + (dx^1)^2}{\sqrt{f_1 f_5}} + \sqrt{f_1 f_5}\sum_{i=2}^{5}(dx^i)^2 + \sqrt{\frac{f_1}{f_5}}\sum_{a=6}^{9}(dx^a)^2 \\ e^{-2\Phi} &= \frac{f_5}{f_1}, \quad C^{(2)}_{01} = \frac{1}{f_1} - 1, \quad dC^{(2)}_{ij} = -(\star_{\mathbb{R}^4} df_5)_{ij}, \quad C_{(0)} = C_{(4)} = B = 0 \end{aligned} \tag{2.40}$$

where

$$f_{1,5} = 1 + \frac{r_{1,5}^2}{r^2} \quad \text{for} \quad r^2 = \sum_{i=2}^{5}(x^i)^2,\ r_1^2 = N_1 \frac{g_s l_s^2}{v_4},\ r_5^2 = N_5 g_s l_s^2. \tag{2.41}$$

The Hodge star $\star_{\mathbb{R}^4}$ is defined w.r.t. the flat metric $dx_i dx^i$ on $\mathbb{R}^4$. The supergravity approximation is valid when $g_s N_1 \gg 1$, $g_s N_5 \gg 1$ and $g_s < 1$.

From the gauge theory point of view, the D1/D5 system is described by a two-dimensional quantum field theory arising from the combination of the following degrees of freedom [75]. First, there is the two-dimensional $U(N_1)$ gauge theory from the D1-brane stack and the six-dimensional $U(N_5)$ gauge theory from the D5-brane stack. These degrees of freedom come from strings stretching between either two D1 or two D5 branes. The six-dimensional $U(N_5)$ theory is compactified on $T^4$ down to a two-dimensional theory by Kaluza-Klein reduction. Due to the four-torus $T^4$ being very small, of the order of the string length, the masses of massive Kaluza-Klein modes become very large. Therefore, only the massless Kaluza-Klein modes are kept in dimensionally reducing the six-dimensional $U(N_5)$ theory to two dimensions. The Kaluza-Klein reduction changes the coupling constant for the $U(N_5)$ theory by a prefactor of $v_4$. Strings stretching between a D1 and a D5 brane couple the $U(N_1)$ and $U(N_5)$ theories so that in total a $U(N_1) \times U(N_5)$ gauge theory emerges. The detailed field content of the theory as well as its Lagrangian can be found in [75]. This gauge theory perspective on the D1/D5 system is applicable when $g_s N_1 \ll 1$ and $g_s N_5 \ll 1$.

### The AdS/CFT correspondence in the D1/D5 system

The AdS/CFT correspondence emerges in the D1/D5 system upon taking a certain low-energy limit in both viewpoints – the supergravity and the gauge theory perspective – and identifying the two descriptions of the D1/D5 system arising in this limit.

Let me start with the supergravity viewpoint by taking a detailed look at the harmonic functions $f_1$, $f_5$ specifying the supergravity solution (2.40). Far away from the extended horizons of the D-branes at $r \to \infty$ the harmonic functions approach a constant, $f_{1,5} \to 1$, and the geometry reduces to flat Minkowski space. Close to the horizon at $r \to 0$, the harmonic functions scale as $r^{-2}$, $f_{1,5} \to r_{1,5}^2/r^2$. In this region, the supergravity geometry approximates to $\mathrm{AdS}_3 \times S^3 \times T^4$,

$$ds^2 = \frac{r^2}{\sqrt{r_1 r_5}}(-(dx^0)^2 + (dx^1)^2) + \sqrt{r_1 r_5}\frac{dr^2}{r^2} + \sqrt{r_1 r_5}\, d\Omega_3^2 + \sqrt{\frac{f_1}{f_5}}\sum_{a=6}^{9}(dx^a)^2. \tag{2.42}$$

The $S^3$ and the $\mathrm{AdS}_3$ space have the same radius $(r_1 r_5)^{1/4}$. Thus, the geometry interpolates between flat space far away from the D-branes and $\mathrm{AdS}_3 \times S^3 \times T^4$ very close to the branes, where the size of the $T^4$ part is much smaller than that of the $\mathrm{AdS}_3$ and $S^3$ parts.

Now, consider the low-energy excitations in this geometry from the viewpoint of an observer at $r = \infty$. There are two kinds of low-energy excitations. First, there are massless particles with

long wavelengths. These particles effectively move in flat Minkowski space and do not sense the presence of the branes. Second, there are low-energy excitations close to the brane. Arbitrary objects appear to have low-energy for an observer at infinity when they come close to the extended horizon of the D-branes. The energy measured at infinity is redshifted from the energy measured at constant $r$ by

$$E_\infty = \sqrt{-g_{tt}}E_r = (f_1 f_5)^{-1/4}E_r. \tag{2.43}$$

Thus objects with constant $E_r$ appear to have lower and lower energy $E_\infty$ as they approach the horizon. In the low-energy limit, the two kinds of excitations introduced above decouple for the following reasons. The cross section for the absorption process of a long wavelength particle by the branes vanishes in the low-energy limit [60]. Intuitively, the wavelength of the low-energetic particles in consideration is much larger than the size of brane system and hence we cannot resolve the branes with these excitations. Conversely, objects close to the branes need higher and higher energies to escape the gravitational attraction of the branes as they get closer to the horizon. Therefore, these objects are confined to the near-horizon region and cannot couple to the long wavelength excitations far away from the brane.

In fact, by taking a certain combined near-horizon and vanishing string length limit, it is possible to describe arbitrarily high energy excitations in the near-horizon region. This combined limit is obtained in the following way [21]. For small $r$, the energy (2.43) measured from infinity scales as $E_\infty \sim E_r r/l_s$. In the limit $r \to 0$ and $l_s \to 0$, $E_\infty$ should be invariant while still allowing arbitrarily high energy excitations in the near horizon region. Because the energy of excited states in string theory scales with $1/l_s$, the latter requirement is equivalent to keeping $l_s E_r$ invariant. Therefore, the combined near-horizon and small string length limit is given by taking $r \to 0$, $l_s \to 0$ while keeping $U \equiv r/l_s^2$ fixed. This is known as the Maldacena limit. The parameters $v_4 = V_{T^4}/l_s^4$ and $g_6 = g_s/\sqrt{v_4}$ (the six-dimensional string coupling) are also held fixed in this limit. In terms of the new variable $U$, the bulk geometry in the Maldacena limit is given by $\mathrm{AdS}_3 \times S^3 \times T^4$ with metric

$$ds^2 = l_s^2\left(\frac{U^2}{g_6\sqrt{N_1N_5}}(-(dx^0)^2+(dx^1)^2) + g_6\sqrt{N_1N_5}\left(\frac{dU^2}{U^2}+d\Omega_3^2\right)\right) + \sqrt{\frac{N_1}{N_5 v_4}}\sum_{a=6}^{9}(dx^a)^2. \tag{2.44}$$

The $\mathrm{AdS}_3$ and $S^3$ radii are equal and given by $L^2 = \sqrt{N_1N_5}g_6 l_s^2$. In summary, an observer at infinity in the supergravity description of the D1/D5 system that has access only to low energies detects two decoupled systems: massless excitations of a free supergravity theory on Minkowski space from the long wavelength excitations far away from the brane and the full spectrum of string theory (including all of the high energy excitations) from objects confined to the region close to the brane.

From the gauge theory viewpoint, the system is described by open strings stretching between the branes of the system, closed strings in the surrounding Minkowski space and the interactions between them,

$$S = S_{\text{open}} + S_{\text{closed}} + S_{\text{interactions}} \tag{2.45}$$

The AdS/CFT correspondence emerges upon taking a low-energy limit in this description as well. In this limit, the string length $l_s$ goes to zero while the other parameters such as the string coupling constant and the number of D1 and D5-branes are kept fixed. Because the energy of excitations in string theory scales with the inverse of the string length, this is a low-energy limit and the first step to derive the action in this limit is to integrate out the massive excitations in both the open and closed string actions. The low-energy effective action for the closed strings emerging from this procedure is the type IIB supergravity action [60]. Since the backreaction of the brane stack onto the background geometry is small in the gauge theory viewpoint, it is justified to

further expand this action into fluctuations around Minkowski space in a power series in the ten-dimensional gravitational coupling constant $\kappa_{10} = g_s\tilde{\kappa}_{10}$. The lowest order in this series gives an action for the theory of free massless supergravity modes of type IIB while higher orders give the interactions between these modes [60]. However, the interactions between supergravity modes vanish in the low-energy limit because $\kappa_{10} \sim g_s l_s^4 \to 0$. For the open string sector, the low-energy limit takes us to the IR fixed point of the gauge theory description of the D1/D5 system introduced in the previous section. This fixed point will be described in detail below. For now, let me just mention that the theory at the IR fixed point is conformally invariant and that – unlike for the closed string sector – the interactions between the fields of the gauge theory are not suppressed in the limit $l_s \to 0$. The interactions between the open and closed string sector governed by $S_{\text{interactions}}$ are obtained from the DBI action (2.25) expanded around Minkowski space, $g_{\mu\nu} = \eta_{\mu\nu} + \kappa_{10} h_{\mu\nu}$ and similar for the other supergravity fields. These interactions between supergravity modes and gauge theory fields also vanish in the low-energy limit because $S_{\text{interactions}}$ contains only positive powers of $\kappa_{10}$ [60]. Thus, from the gauge theory viewpoint the low-energy limit gives two decoupled theories: free supergravity in Minkowski space from the closed strings and a fully interacting conformal field theory from the open strings on the branes.

Comparison of the two viewpoints shows that in both cases a decoupled free supergravity theory in a flat space background appears. This motivates the conjecture made in [21] that the remaining systems in the two viewpoints on the D-brane stacks, i.e. string theory on $\text{AdS}_3 \times S^3 \times T^4$ on the one hand and the two-dimensional CFT of the D1/D5 system on the other hand, are equivalent. The above arguments do not constitute a proof for this equivalence because the supergravity and gauge theory descriptions of the D-brane stacks are valid in different parameter regimes. While the supergravity regime requires $g_s N_{1,5} \gg 1$, the gauge theory description is applicable for $g_s N_{1,5} \ll 1$. Therefore, the correspondence takes on a few different forms according to how far one trusts the conjecture. The weak form of the AdS/CFT correspondence only states that the equivalence holds in the limit $g_s N_{1,5} \gg 1$ where the supergravity approximation on the gravity side is valid. A stronger form applies if the correspondence holds for $g_s N_{1,5}$ finite but $N_1 N_5 \gg 1$. In this limit $l_s$ may be comparable to $L$ such that corrections due to finite string length need to be included but $g_s$ is still small such that quantum corrections can be neglected. Finally, the strongest form applies if the correspondence holds for all values of $g_s$ and $l_s$. The AdS/CFT correspondence in general has passed a large number of tests in the weak limit including the matching of symmetries, correlation functions and spectra on both sides of the correspondence (see [60, 61] for an overview over some of these tests). For the D1/D5 system in particular there is also a good deal of evidence that the correspondence is correct in its stronger form coming from the study of string theory on $\text{AdS}_3 \times S^3 \times T^4$ in the so-called tensionless limit [80–89]. The tensionless limit is characterized by $l_s = L$, i.e. the gravity theory is in a regime where the typical string is of similar size as the curvature scale of the background AdS geometry. Equivalence between the spectra [80–82] and various correlation functions [83–87] of the tensionless string and the dual conformal field theory has been found, giving very strong evidence that the AdS/CFT correspondence also holds in this limit.

### The D1/D5 conformal field theory

Let me now collect some more details on the quantum field theory emerging in the low-energy limit of the D1/D5 system following the review in [75].

As is clear by this point, this theory is a two-dimensional conformal field theory. Its central charge $c = 6(N_1 N_5 + 1)$ can be identified from the field content of the gauge theory [75]. This is consistent with the gravity derivation of the central charge from the Poisson brackets of the generators of infinitesimal diffeomorphisms dual to conformal transformations on the boundary.

This derivation, which was already performed a long time before the discovery of the AdS/CFT correspondence [64], yields the general relation (2.6) between the central charge of a holographic two-dimensional CFT and Newton's constant in the bulk. For the supergravity solution (2.40) this gives $c = 6N_1N_5 + O\left((N_{1,5})^0\right)$. The $U(N_1) \times U(N_5)$ gauge symmetry reduces to $S_{N_1} \times S_{N_5}$ in the conformal fixed point [90]. Here $S_N$ is the symmetric group, i.e. the group of all permutations of $N$ elements. The CFT obtained in this way is a sigma model with target space $\mathscr{M}$.

To derive this target space $\mathscr{M}$ in detail, it is important to note that the gauge theory description of the D1/D5-system introduced so far has a limited range of validity. A more precise description is possible by viewing the D1-branes as instantons of the $U(N_5)$ gauge theory on the D5-branes [91, 92]. From this perspective, the D1 branes arise as a continuous family of classical solutions to the equations of motion of the $U(N_5)$ gauge theory, known under the name of instantons. In fact, the solutions in question are localized in the $T^4$ directions (they are independent of $x^0$ and $x^1$) and hence they are described by classical solutions of four-dimensional (Euclidean) Yang-Mills theory on the $T^4$. They are characterized by a field strength tensor that fulfills $F = \star_{T^4} F$.[12] The $U(N_1) \times U(N_5)$ gauge theory emerges in the limit where the size of the instantons goes to zero [93].

The space of parameters of the family of instanton solutions is called the instanton moduli space. In [91, 94], it has been argued that this moduli space is given by a smooth deformation of $(\tilde{T}^4)^N/S_N$ where $N = N_1N_5$. The moduli space torus $\tilde{T}^4$ is in general distinct from the compactification torus $T^4$. Small fluctuations in the D1-brane configuration are described by fluctuations of the moduli. Therefore, there is a correspondence between moduli and fields in the low-energy gauge theory description of the D1/D5 system in the same manner as fluctuations in the configuration of a stack of D$p$-branes were identified in the previous section with massless gauge and scalar fields. Hence, the target space $\mathscr{M}$ of the sigma model D1/D5 CFT is identified with the instanton moduli space.[13]

The symmetries of the D1/D5 CFT can be matched with those of the dual gravity theory as follows [75]. First, note that the CFT has $\mathscr{N} = (4,4)$ superconformal symmetry.[14] Type IIB supergravity has 32 supercharges. The presence of the D1 and D5-branes breaks some of those supersymmetries, so that only a quarter of the 32 supercharges remain. However, in the near-horizon limit the symmetry is enhanced again such that in this regime 16 unbroken supercharges exist in agreement with the number of supercharges of the $\mathscr{N} = (4,4)$ superconformal group. The global symmetry group of the theory is given by the supergroup $SU(1,1|2) \times SU(1,1|2)$. Its bosonic part is given by $SO(2,2) \times SO(4)$. The $SO(2,2) \simeq SL(2,\mathbb{R}) \times SL(2,\mathbb{R})$ is the global part of the Virasoro group which manifests as the group of isometries of $\mathrm{AdS}_3$ in the bulk. The $SO(4) \simeq SU(2) \times SU(2)$ is the $R$-symmetry of the superconformal group which manifests as the isometries of $S^3$.[15]

From the instanton description of the D1/D5 system introduced above it is known that the target space $\mathscr{M}$ of the boundary theory is equal to the instanton moduli space, which is given by a deformation of $(\tilde{T}^4)^N/S_N$. The deformation is parametrized by another moduli space, the CFT moduli space, not to be confused with the instanton moduli space. The point in the CFT moduli

[12] This field strength is not to be confused with the supergravity field $F^{(3)}$.

[13] Strictly speaking, the target space includes another decoupled $T^4$ (this is the origin of the $+1$ term in $c = 6(N_1N_5 + 1)$). However, in the AdS/CFT setting this decoupled $T^4$ must be neglected in order to match with the gravity theory: all fields couple to gravity and therefore, there can be no completely decoupled degrees of freedom [75].

[14] For ordinary supersymmetry, the notation $\mathscr{N} = (4,4)$ means that the system possesses four conserved charges (the so-called supercharges) of the supersymmetry for both the holomorphic and antiholomorphic sector of the conformal field theory. For superconformal symmetry, the number of conserved charges is twice that amount.

[15] There is another global $SO(4)$ symmetry from the rotations of the $6,7,8,9$ directions which is broken by the compactification on $T^4$. Nevertheless, the quantum numbers of this $SO(4)$ group are often used to classify states of the D1/D5 CFT [75], although I will not make use of this procedure in this thesis.

space where the CFT target space is exactly $(\tilde{T}^4)^N/S_N$ is referred to as the *orbifold point*. At this point, the CFT is the weakly coupled $S_N$ orbifold theory described in detail in the next section, dual to a string theory on $\mathrm{AdS}_3 \times S^3 \times T^4$ in the strong coupling limit [75]. The orbifold point is far away in moduli space from the *supergravity point* at which the description by the solution (2.40) is applicable [75]. Close to the supergravity point, the CFT is strongly coupled and there is no orbifold structure.

From the CFT viewpoint, the deformation is implemented by an exactly marginal operator (in the renormalization group sense) that generates a renormalization group flow to another conformal fixed point. There are 20 exactly marginal operators in the D1/D5 CFT which I will introduce in detail at the orbifold point in the following section. In the supergravity point, the moduli space manifests as the space of massless scalars in the near-horizon limit. There are also 20 of these scalars arising from supergravity degrees of freedom along the $T^4$ directions [75].[16] In the solution (2.40), the value of all of these moduli is zero. Moving away from this point in moduli space generates non-zero values for these supergravity moduli.

### 2.1.4. Orbifold conformal field theories

This section introduces orbifold conformal field theories with a focus on permutation orbifolds and especially the $S_N$ orbifold theory of the D1/D5 system. Orbifolds are a standard topic in conformal field theory, explained in detail for instance in [95] or [96].

#### Orbifold theories in general

Orbit-manifolds or orbifolds for short are generalizations of manifolds that allow for the existence of a discrete set of singularities [76, 95]. Orbifolds arise from identifying parts of manifolds with each other. Consider a manifold $\mathscr{M}$ with discrete group action $G : \mathscr{M} \to \mathscr{M}$. Identifying points related by the group action, $x \sim gx$ for $g \in G$, gives a quotient space $\mathscr{M}/G$ that is called an orbifold. At the fixed point set $\{x|gx = x\}$ for $g \in G$, $g \neq \mathbb{1}$, a discrete set of singular points appears. The tangent spaces of the fixed points are not ordinary Euclidean spaces but Euclidean spaces with discrete identifications. As an example, consider a disk partitioned into $n$ wedges. Identifying the wedges gives a cone that is everywhere regular except at the tip.

In conformal field theory, an orbifold theory refers to a theory arising from gauging a discrete global symmetry. In some cases orbifold conformal field theories have an interpretation as a sigma model whose target space is an orbifold, although this is not always the case. In general, orbifold CFTs are defined as follows [95]. Consider a CFT $\mathscr{T}$ with a discrete global symmetry group $G$. The orbifold CFT $\mathscr{T}/G$ is obtained by promoting $G$ from a global to a gauge symmetry. This procedure restricts the set of allowed states. While states do not need to be invariant under global symmetries, gauge symmetries are unphysical redundancies in the description and hence only states that are $G$ invariant are in the Hilbert space of the orbifold CFT. These states can be obtained by applying a projector

$$P_G = \frac{1}{|G|} \sum_{g \in G} g \tag{2.46}$$

[16] These are nine scalars from the traceless part of the metric $h_{ab}$, three scalars from the self-dual part of the Neveu-Schwarz $B$-field $B_{ab}$, six scalars from the Ramond-Ramond field $C^{(2)}_{ab}$, one scalar from the six-dimensional dilation $\phi_6$ and finally one scalar from a linear combination of the Ramond-Ramond scalar $C^{(0)}$ and the four-form component $C^{(4)}_{6789}$ [75].

onto a state $|\psi\rangle_{\mathscr{T}}$ of the theory $\mathscr{T}$, [17]

$$|\psi\rangle_{\mathscr{T}/G} = P_G|\psi\rangle_{\mathscr{T}}. \tag{2.47}$$

Here $|G|$ is the cardinality of the group $G$. These states, however, do not comprise the entire Hilbert space of the orbifold theory: the consistency requirement of modular invariance of the torus partition functions demands the introduction of additional Hilbert space sectors. These additional Hilbert space sectors are known as *twisted sectors*. This procedure works as follows [95]. The thermal partition in a system with finite size and finite temperature is calculated from the path integral with periodic boundary conditions in space and time, giving what is known as the torus partition function. Only incorporating the projection onto gauge invariant states but not the twisted sectors, the torus partition function of the orbifold theory is given by

$$Z_{\mathscr{T}/G,\text{naive}} = \frac{1}{|G|}\sum_{g\in G} g\underset{\mathbb{1}}{\square}, \tag{2.48}$$

where the $g\underset{h}{\square}$ denotes the contribution to the partition function from a path integral with $X^i(z+1) = hX^i(z)$ boundary conditions along the spatial direction and $X^i(z+\tau) = gX^i(z)$ boundary conditions along the time direction.[18] The object $g\underset{h}{\square}$ is called a spinstructure. Here, $\tau$ is the modular parameter of the torus ($\tau = i\frac{\beta}{2\pi}$ for vanishing chemical potential with $\beta$ the inverse temperature) and $X^i$ denotes the fields of the theory, $i$ being an index. It can be shown that this naive attempt at defining a partition function is not invariant under modular transformations

$$\tau \to \frac{a\tau+b}{c\tau+d} \quad \text{for} \quad a,b,c,d\in\mathbb{Z} \quad \text{and} \quad ad-bc=1. \tag{2.49}$$

The modular $S$ transformation $\tau \to -1/\tau$ exchanges the space and time directions of the torus and thus acts as $g\underset{h}{\square} \to h\underset{g}{\square}$. The modular $T$ transformation $\tau \to \tau+1$ acts as $g\underset{h}{\square} \to gh\underset{h}{\square}$. Together, these two transformations generate the entire modular group $PSL(2,\mathbb{Z})$ and it is obvious that (2.48) is not invariant under these transformations. A modular invariant partition function can be constructed as

$$Z_{\mathscr{T}/G} = \frac{1}{|G|}\sum_{g,h\in G, gh=hg} g\underset{h}{\square}. \tag{2.50}$$

Note that without the restriction to $gh = hg$ the boundary conditions for $X^i(z+\tau+1)$ are ambiguous if the group $G$ is non-abelian. The sum in equation (2.50) can be reorganized in terms of conjugacy classes $C_a$ and stabilizer subgroups $N_{h_a}$ of $G$, [19]

$$Z_{\mathscr{T}/G} = \sum_a \frac{1}{|N_{h_a}|}\sum_{g\in N_a} g\underset{h_a}{\square}, \tag{2.51}$$

[17] To lighten the notation, the state $|\psi\rangle_{\mathscr{T}/G}$ is not properly normalized. A normalized state with $\langle\psi|_{\mathscr{T}/G}|\psi\rangle_{\mathscr{T}/G} = 1$ is given by $\sqrt{|G|}P_G|\psi\rangle_{\mathscr{T}}$. The projection operator is canonically normalized such that $P_G^2 = P_G$.

[18] Cyclicity of the trace and $P_G^2 = P_G$ yields $Z_{\mathscr{T}/G,\text{naive}} = \text{Tr}[P_G e^{-\beta H}P_G] = \text{Tr}[P_G e^{-\beta H}]$. The projection onto gauge invariant states leads to non-trivial boundary conditions along the time direction due to the application of $P_G$ in $\text{Tr}[P_G e^{-\beta H}]$ being preceded by time evolution with the Hamiltonian $H$ along the Euclidean time direction.

[19] The conjugacy classes of a group $G$ are made up of the sets $\{ghg^{-1}|g\in G\}$ for fixed $h$. A stabilizer subgroup of an element $g\in G$ is the set of elements of $G$ that commutes with $g$. The size of the stabilizer subgroup $N_g$ depends only on the conjugacy class that $g$ is in and is given by $|N_{h_a}| = |G|/|C_a|$ where $h_a$ is an element of $C_a$.

where $h_a$ is a representative of $C_a$ and $N_a$ the corresponding stabilizer subgroup. From this partition function, one sees the emergence of new Hilbert space sectors for each $C_a$, the so-called twisted sectors. States in these twisted sectors describe sectors in which the fields obey twisted boundary conditions, that is the states are given by

$$|\psi\rangle_{\mathscr{T}/G,C_a} = P_G|\psi\rangle_{\mathscr{T},h_a} \tag{2.52}$$

where the fields in $|\psi\rangle_{\mathscr{T},h_a}$ obey boundary conditions that are periodic to the group action by $h_a$, $X^i(z+1) = h_a X^i(z)$. Gauge invariant states in non-trivial twisted sectors are obtained by summing over states $|\psi\rangle_{\mathscr{T},h_a}$ for all elements $h_a$ of $C_a$ and for each $h_a$ symmetrizing with the projector on the stabilizer subgroup $N_{h_a}$,

$$|\psi\rangle_{\mathscr{T}/G,C_a} = \sum_{h_a \in C_a} P_{N_{h_a}}|\psi\rangle_{\mathscr{T},h_a}. \tag{2.53}$$

Using the state-operator correspondence in conformal field theory one may introduce *twist operators*, that is operators which move from one twisted sector to another. The twist operators that generate the ground states of twisted sectors are denoted by $\sigma_{h_a}$,

$$|0\rangle_{\mathscr{T},h_a} = \sigma_{h_a}(0)|0\rangle_{\mathscr{T}} \tag{2.54}$$

where $|0\rangle_{\mathscr{T}}$ is the vacuum state, i.e. the ground state of the untwisted sector corresponding to the conjugacy class that contains only the identity operator. The twist operator $\sigma_{h_a}$ is a primary operator implementing the change of boundary conditions from periodic boundary conditions to the boundary conditions $X^i(z+1) = h_a X^i(z)$ specified by $h_a$.

### Cyclic permutation orbifold theories

A common type of orbifold CFTs are permutation orbifolds, that is orbifolds with symmetry groups $G$ given by permutation groups, i.e. subgroups of the symmetric group. Let me now briefly discuss an example of this: cyclic permutation orbifolds where $G = \mathbb{Z}_n$. In this case, the theory $\mathscr{T}$ is given by $n$ identical copies of a *seed theory* $\mathscr{S}$. The corresponding action is

$$S_{\mathscr{T}} = \sum_{i=1}^{n} S_{\mathscr{S}}, \tag{2.55}$$

where $S_{\mathscr{S}}$ is the action of the seed theory. The orbifold procedure identifies copies related by $\mathbb{Z}_n$ transformations with each other. Because $\mathbb{Z}_n$ is abelian, its conjugacy classes consist only of a single element. Therefore, I will label conjugacy classes of $\mathbb{Z}_n$ by group elements. The stabilizer subgroup for any group element is equal to the entire $\mathbb{Z}_n$ group. The fields of the theory $\mathscr{T}$ are denoted by $X^1, ..., X^n$ where $X^i$ stands collectively for the fields of the $i$-th copy of the seed theory. The $\mathbb{Z}_n$ group acts by permuting fields as $gX^i = X^{g(i)}$ where $g(i)$ is the standard action of a cyclic permutation $g$ on the numbers $i = 1, ..., n$. States of the orbifold theory are given by

$$P_{\mathbb{Z}_n}|X^1, ..., X^n\rangle_h = \frac{1}{n}\left[|X^1, ..., X^n\rangle_h + |X^2, X^3, ..., X^n, X^1\rangle_h + ... + |X^n, X^1, ..., X^{n-1}\rangle_h\right], \tag{2.56}$$

where $h$ labels the twisted sector, i.e. the field eigenvalues $X^i$ of the state $|X^1, ..., X^n\rangle_h$ obey boundary conditions $X^i(z+1) = X^{h(i)}(z)$. The twist operators $\sigma_h$ all have the same conformal weight

$$h = \bar{h} = \frac{c_{\mathscr{S}}}{24}(n - 1/n), \tag{2.57}$$

where $c_{\mathscr{S}}$ denotes the central charge of the seed theory $\mathscr{S}$ which is $n$ times smaller than the central charge $c = nc_{\mathscr{S}}$ of the orbifold theory $\mathscr{T}/\mathbb{Z}_n$. Equation (2.57) may be derived as follows [97]. The ground state of a twisted sector is the vacuum state for a conformal field theory on a Riemann surface related to the complex plane by the uniformization transformation $z \to w = z^{1/n}$. Under this transformation, the expectation value of the energy-momentum tensor transforms as

$$\langle T(z)\rangle = \left(\frac{\partial w}{\partial z}\right)^2 \langle T(w)\rangle + \frac{c}{12}\{w,z\} = \frac{1}{z^2}\frac{c}{24}\left(1-\frac{1}{n^2}\right) \tag{2.58}$$

due to $\langle T(w)\rangle = 0$. Comparing this with the expectation value of $T(z)$ in the twisted sector ground state $\sigma_h(0)|0\rangle$

$$\langle T(z)\rangle = \langle 0|\sigma_h(\infty)T(z)\sigma_h(0)|0\rangle = \frac{h}{z^2} \tag{2.59}$$

obtained from the conformal Ward identity

$$\langle T(z)\sigma_h(z_1)\sigma_h(z_2)\rangle = \sum_{i=1,2}\left(\frac{h}{(z-z_i)^2} + \frac{1}{z-z_i}\partial_{z_i}\right)\langle \sigma_h(z_1)\sigma_h(z_2)\rangle \tag{2.60}$$

leads to (2.57). Because the conformal weights of these twist operators are all the same, I will simply refer to $\sigma_h$ as $\sigma_n$ in the following when the distinction between different twisted sectors is not important.

### The $S_N$ orbifold theory of the D1/D5 system

I will now introduce another example of a permutation orbifold, the D1/D5 CFT at the orbifold point (see [75, 98] for more detailed reviews). Recall that at the orbifold point, the D1/D5 CFT is given by a sigma model with target space $(\tilde{T}^4)^N/S_N$. This theory is composed of $N$ copies of a free $\mathscr{N} = (4,4)$ supersymmetric seed theory identified under the $S_N$ permutation symmetry. The action is given by [75] [20]

$$S = \frac{1}{2\pi}\int d^2z\left[\partial x^i_a(z,\bar{z})\bar{\partial}x^i_a(z,\bar{z}) + \psi^i_a(z,\bar{z})\bar{\partial}\psi^i_a(z,\bar{z}) + \bar{\psi}^i_a(z,\bar{z})\partial\bar{\psi}^i_a(z,\bar{z})\right] \tag{2.61}$$

where $i = 1,\ldots,N$ labels the $N$ copies and $a = 6,\ldots,9$ the $\tilde{T}^4$ directions. The target space of each copy is a $\tilde{T}^4$. The central charge can be read off from the action as $c = 6N$. Twisted sectors of the orbifold theory are labeled by conjugacy classes of the $S_N$-group. These conjugacy classes are in one-to-one correspondence with integer partitions of $N$. I will denote the conjugacy classes as

$$(1)^{n_1}(2)^{n_2}\ldots(N)^{n_N}, \tag{2.62}$$

where the number $n_m$ counts the number of cycles of length $m$ in the conjugacy class[21] or equivalently the number of times $m$ occurs in the integer partition of $N$. Thus,

$$\sum_{i=1}^{N} m\cdot n_m = N. \tag{2.63}$$

[20] I am using complex coordinates $z,\bar{z}$ in Euclidean signature and the standard notation $\partial = \frac{\partial}{\partial z}, \bar{\partial} = \frac{\partial}{\partial \bar{z}}$.

[21] This number is the same in all elements of a conjugacy class of $S_N$ although which copies of the seed theory are permuted in a given cycle of course differs from element to element.

For example, the untwisted sector is denoted by $(1)^N$ while a twisted sector containing a single cyclic permutation of length $k$ is denoted by $(1)^{N-k}(k)$.

The D1/D5 CFT at the orbifold point possesses 20 exactly marginal operators with $h = \bar{h} = 1$ [75]. 16 of those are non-twist operators $\partial x_a^i \bar{\partial} x_b^i$ (summation over $i$ is implied). The remaining four exactly marginal operator are combinations of a two-cycle supersymmetric twist operator $\Sigma_2$ [22] with fermionic field operators,

$$\begin{aligned} &\Sigma_2(z,\bar{z})(\psi_6^i(z)+i\psi_7^i(z))(\bar{\psi}_6^i(\bar{z})+i\bar{\psi}_7^i(\bar{z}))/2, \quad \Sigma_2(z,\bar{z})(\psi_6^i(z)+i\psi_7^i(z))(\bar{\psi}_8^i(\bar{z})-i\bar{\psi}_9^i(\bar{z}))/2, \\ &\Sigma_2(z,\bar{z})(\psi_8^i(z)-i\psi_9^i(z))(\bar{\psi}_6^i(\bar{z})+i\bar{\psi}_7^i(\bar{z}))/2, \quad \Sigma_2(z,\bar{z})(\psi_8^i(z)-i\psi_9^i(z))(\bar{\psi}_8^i(\bar{z})-i\bar{\psi}_9^i(\bar{z}))/2. \end{aligned} \tag{2.64}$$

The conformal dimension of a $k$-cycle supersymmetric twist operator of the D1/D5 CFT is given by $h = \bar{h} = (k-1)/2$ while the fermions have conformal dimension $(h,\bar{h}) = (1/2,0)$ and $(h,\bar{h}) = (0,1/2)$ respectively such that in total $h = \bar{h} = 1$. Note that there exist other marginal operators with $h = \bar{h} = 1$ in the orbifold CFT, however the conformal dimensions of these operators change under deformations away from the orbifold point. Thus these operators are only marginal but not exactly marginal. The dimensions of the exactly marginal operators are determined by the $\mathcal{N} = (4,4)$ supersymmetry and therefore are invariant under deformations that preserve the supersymmetry [75]. The exactly marginal operators parametrize a 20-dimensional moduli space of deformations away from the orbifold point. The action changes under these deformations as

$$S \to S + \lambda \int d^2z\, \Phi(z,\bar{z}), \tag{2.65}$$

where $\Phi$ is an exactly marginal operator and $\lambda$ the corresponding deformation parameter. If $\Phi$ is a non-twist operator, the deformation yields an $S_N$ orbifold of a different seed theory. If $\Phi$ is one of the two-cycle twist operators, the orbifold structure is destroyed in the deformation. The latter case corresponds to moving away from the weak coupling limit in the CFT [75, 99].[23]

Finally, let me briefly mention how the orbifold structure manifests in the dual gravity theory. At the orbifold point, the dual string theory is the tensionless limit where the string length $l_s$ is equal to the AdS radius $L$. A particular striking property of string theory in the tensionless limit is a localization of worldsheet moduli [83, 86, 87]. In general, calculating correlation functions in string theory requires integrating over moduli[24] parametrizing the shape of string worldsheets at fixed genus. However, in the tensionless limit the integral over worldsheet moduli degenerates into a discrete sum, i.e. the moduli localize [83, 86, 87]. As an example consider the thermal partition function of the $S_N$ orbifold CFT. This partition function is dual to the string theory partition function on a background determined by the property that it has the same boundary conditions as the BTZ black hole respectively thermal $AdS_3$ spacetime, i.e. a torus topology on the AdS boundary. In the large $N$ limit, the leading contributions to the dual string theory partition function come from spherical (tree-level) and toroidal (one-loop) worldsheets [87]. Due to the moduli localization property, in the tensionless limit there are only contributions from toroidal worldsheets that cover the boundary of the asymptotically AdS space an integer number of times [87]. This allows identifying contributions to the partition function from particular string worldsheets with

[22] A $k$-cycle twist operator implements a permutation that cyclically permutes $k$ elements. A twist operator is called supersymmetric if it acts on both the fermions and the bosons of the D1/D5 CFT to change the boundary conditions for both of them.

[23] On the supergravity side, the moduli corresponding to the four exactly marginal two-cycle twist operators are the self-dual part of the NS $B$-field and the linear combination of the RR scalar and the four-form [75].

[24] These moduli are not to be confused with those of the moduli space of deformations of the $S_N$ orbifold or the instanton moduli space of the D1/D5 system.

contributions from particular twisted boundary conditions of the orbifold CFT along the space and time directions.

Consider for instance the case $N = 2$. On the CFT side, the partition function is given by four contributions

$$\begin{aligned} Z(\tau) &= \frac{1}{2}\left[{}^{(12)}\underset{(12)}{\square} + {}^{(21)}\underset{(12)}{\square} + {}^{(12)}\underset{(21)}{\square} + {}^{(21)}\underset{(21)}{\square}\right], \\ &= \frac{1}{2}\left[Z_{\mathscr{S}}(\tau)^2 + Z_{\mathscr{S}}(2\tau) + Z_{\mathscr{S}}(\tau/2) + Z_{\mathscr{S}}((\tau+1)/2)\right] \end{aligned} \tag{2.66}$$

where (12) is the identity and (21) the non-identity permutation of the $S_2$ group while $Z_{\mathscr{S}}(\tau)$ denotes the partition function of the seed theory. This can be matched with contributions from string theory worldsheets: for the $g\underset{h}{\square}$ spinstructure, the corresponding string theory contribution comes from worldsheets which wind $n_g$ times around the time circle and $n_h$ times around the space circle of the torus on the boundary of the bulk asymptotically AdS space, where $n_g = 1$ for $g = (12)$ and $n_g = 2$ for $g = (21)$. This is reflected in the arguments to $Z_{\mathscr{S}}$ in (2.66), e.g. ${}^{(21)}\underset{(12)}{\square}$ gives the contribution of a worldsheet winding twice around the time direction and hence corresponds to $Z_{\mathscr{S}}(2\tau)$.

## 2.2. Entanglement in quantum field theory and holography

Entanglement is one of the key features distinguishing classical from quantum theories. Therefore, entanglement also plays an important part in quantum gravity in general as well as the AdS/CFT correspondence in particular. Characterizing the entanglement structure of a quantum state necessitates the introduction of a measure of entanglement between two complementary subsystems. This measure is provided by the entanglement entropy, a quantity measuring the amount of information contained in a subsystem of a quantum theory. It turns out that the gravitational dual to the entanglement entropy in the boundary field theory in AdS/CFT is a simple geometric quantity generalizing the Bekenstein-Hawking entropy. This has striking consequences for the description of the bulk spacetime in AdS/CFT which is in a sense an emergent concept originating from entanglement. The purpose of this section is to review these concepts in detail.

### 2.2.1. Entanglement entropy

The starting point for the review is the entanglement entropy. The standard textbook definition of this quantity is given as follows (see e.g. [100]).[25] Consider a physical system in a pure quantum state $\rho$ and let the Hilbert space of the system factorize into tensor products,

$$\mathscr{H} = \mathscr{H}_A \otimes \mathscr{H}_B, \tag{2.67}$$

associated to the subsystem $A$ and its complement $B$. The state in the subsystem $A$ is obtained by a partial trace over the degrees of freedom in $B$,

$$\rho_A = \mathrm{Tr}_{\mathscr{H}_B}(\rho). \tag{2.68}$$

[25] In chapter 3, I will introduce a generalization of this definition which does not depend on a factorizing Hilbert space.

If $\rho_A$ is pure then there is no entanglement between $A$ and $B$. Otherwise the state is entangled and the closer $\rho_A$ is to a maximally mixed state, the higher the amount of entanglement. Thus, the amount of entanglement between $A$ and $B$ is measured by the von Neumann entropy of $\rho_A$,

$$S_A = -\mathrm{Tr}_{\mathscr{H}_A}(\rho_A \log \rho_A). \tag{2.69}$$

$S_A$ is called entanglement entropy. Note that if the state $\rho$ of the total system is mixed then $S_A$ is a measure for the total amount of correlations – classical and quantum – between $A$ and $B$. Despite this, I will keep referring to $S_A$ as the entanglement entropy even for mixed states $\rho$. This nomenclature has become standard in quantum information theory.

For simple quantum mechanical systems that are defined on a finite-dimensional Hilbert space $S_A$ can be computed by direct application of (2.69). In quantum field theory this is no longer possible. In order to calculate the entanglement entropy in these systems one usually makes use of a one-parameter family generalization of the von Neumann entropy called the *Rényi entropy* [101]

$$S_A^n = \frac{1}{1-n} \log \mathrm{Tr}(\rho_A^n). \tag{2.70}$$

In the limit $n \to 1$ the ordinary von Neumann entropy is recovered,

$$S_A = \lim_{n\to 1} S_A^n. \tag{2.71}$$

The entanglement entropy in quantum field theories is typically computed by calculating the Rényi entropy for integer $n > 1$, analytically continuing to real $n$ and then taking the $n \to 1$ limit.

The Rényi entropy for integer $n > 1$ is obtained in this computation by means of the following path integral method known as the *replica trick* [97], which I present here for simplicity only for the vacuum state of a two-dimensional QFT in Euclidean signature. It is well known that ground state wave functionals $\Psi(\phi_1(x)) = \langle \phi_1(x)|0\rangle$ can be obtained through a Euclidean path integral in the $\tau < 0$ half of the spacetime with boundary conditions at the $\tau = 0$ plane

$$\Psi(\phi_1(x)) = \int_{\tau=-\infty}^{\tau=0;\phi(\tau=0,x)=\phi_1(x)} \mathscr{D}\phi\, e^{-S[\phi]}, \tag{2.72}$$

where $\phi$ is a short hand for the fields of the theory, $S[\phi]$ is the action and $\tau$ the time coordinate in Euclidean signature. Complex conjugation of the wave functional is implemented by integrating from $\tau = 0$ to $\tau = +\infty$ with boundary conditions at $\tau = 0$. Matrix elements $\langle \phi_1|\rho|\phi_1'\rangle$ of the density matrix $\rho = |0\rangle\langle 0|$ are given by

$$\Psi(\phi_1(x))\Psi^*(\phi_1'(x)) = \frac{1}{Z_1}\int_{\tau=-\infty}^{\tau=+\infty} \mathscr{D}\phi\, e^{-S[\phi]} \prod_x \delta(\phi(+0,x) - \phi_1'(x)) \prod_x \delta(\phi(-0,x) - \phi_1(x)), \tag{2.73}$$

where the $\pm 0$ notations means taking the limit $\tau \to 0$ from above respectively below and $Z_1 = \int_{\tau=-\infty}^{\tau=+\infty} \mathscr{D}\phi\, e^{-S[\phi]}$ is the vacuum partition function needed to normalize the trace of $\rho$ to one. To obtain the reduced density matrix $\rho_A$, the subsystem $B$ needs to be traced out which is done by integrating out $\phi_1$ with the condition $\phi_1(x) = \phi_1'(x)$ for $x \in B$,

$$\langle \phi_1|\rho_A|\phi_1'\rangle = \frac{1}{Z_1}\int_{\tau=-\infty}^{\tau=+\infty} \mathscr{D}\phi\, e^{-S[\phi]} \prod_{x\in A} \delta(\phi(+0,x) - \phi_1'(x)) \prod_{x\in A} \delta(\phi(-0,x) - \phi_1(x)). \tag{2.74}$$

One can think of the integration as going over all of the $\mathbb{R}^2$ except for an open cut along $A$, where

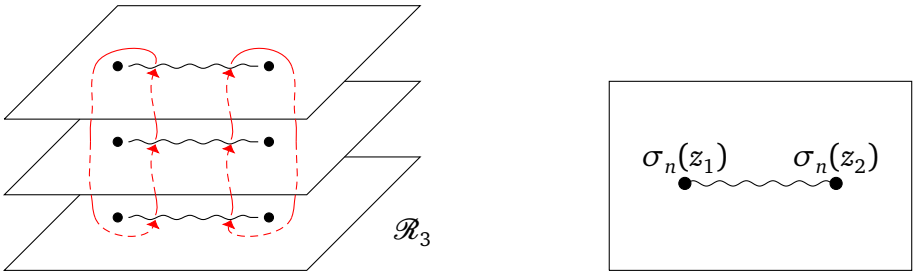


Figure 2.2.: LHS: Illustration of the Riemann surface $\mathscr{R}_n$ for the computation of the $\mathrm{Tr}(\rho_A^n)$ for the case $n=3$. The red arrows illustrate the cyclic gluing procedure between the $n$ sheets. RHS: The partition function $Z_n$ on $\mathscr{R}_n$ is related to the two-point $\langle\sigma_n(z_1)\sigma_n(z_2)\rangle$ on the complex plane. The insertion of the twist operators $\sigma_n$ create a branch cut running along the entangling interval $A=[z_1,z_2]$ that transforms the complex plane into the Riemann surface $\mathscr{R}_n$.

boundary conditions $\phi_1(x)$, $\phi_1'(x)$ are specified. To obtain $\mathrm{Tr}(\rho_A^n)$, take $n$ copies

$$\langle\phi_1|\rho_A|\phi_1'\rangle\langle\phi_2|\rho_A|\phi_2'\rangle...\langle\phi_n|\rho_A|\phi_n'\rangle, \tag{2.75}$$

integrate over the fields $\phi_i'(x)$ and set

$$\phi_i'(x)=\phi_{i+1}(x),\ \phi_n'(x)=\phi_1(x) \tag{2.76}$$

for $x\in A$. Then the integration is no longer over the fields on a single $\mathbb{R}^2$, but over those on an $n$-sheeted Riemann surface $\mathscr{R}_n$:

$$\mathrm{Tr}(\rho_A^n)=\frac{1}{Z_1^n}\int_{(\tau,x)\in\mathscr{R}_n}\mathscr{D}\phi\, e^{-S[\phi]}\equiv\frac{Z_n}{Z_1^n}. \tag{2.77}$$

The different sheets of $\mathscr{R}_n$ are copies of $\mathbb{R}^2$ and cyclically "glued together" along the branch cuts at $A$. In this way, the computation of the entanglement entropy of $A$ can be rewritten as the computation of a partition function on $\mathscr{R}_n$ (see figure 2.2).

For two-dimensional conformal field theories, the partition function $Z_n$ can be further related to a correlation function of twist operators [97]. By construction, the surface $\mathscr{R}_n$ is $\mathbb{Z}_n$ symmetric under cyclic permutations of the $n$ sheets. Recall from section 2.1.4 that inserting a $\mathbb{Z}_n$ twist operator $\sigma_n$ at some point $z_1$ implements twisted boundary conditions such that the fields of the theory are cyclically glued together along a branch cut from $z=z_1$ to $z=\infty$. Thus, going once in a loop around the insertion at $z=z_1$ leads to a different sheet of $\mathscr{R}_n$. The insertion of a second twist operator at a point $z_2$ with boundary conditions inverse to that at $z=z_1$ produces a branch cut running from $z_1$ to $z_2$. Thus, the partition function $Z_n/Z_1^n$ for a single entangling interval $A=[z_1,z_2]$ is equal to a two-point function of twist operators [97],[26]

$$Z_n/Z_1^n=\langle\sigma_n(z_1,\bar{z}_1)\sigma_n(z_2,\bar{z}_2)\rangle=(z_1-z_2)^{-c/6(n-1/n)}(\bar{z}_1-\bar{z}_2)^{-c/6(n-1/n)}. \tag{2.78}$$

[26]Note that the central charge of the theory on the Riemann surface $\mathscr{R}_n$ is still given by $c$ and not $n$ times $c$ as for the permutation orbifolds in section 2.1.4. The theory on $\mathscr{R}_n$ is the same theory as that on the complex plane and not $n$ copies thereof as in section 2.1.4. Thus, the conformal weight of the twist operators are given by $h=\bar{h}=c/24(n-1/n)$, i.e. $c=c_{\mathscr{S}}$ in (2.57).

Thus the entanglement entropy for 2d CFTs is universally given by[27]

$$S_A = \frac{c}{3}\log(|z_2 - z_1|/\epsilon_{\text{UV}}). \tag{2.79}$$

The result depends only on the central charge $c$ due to the universality of two-point functions in two-dimensional conformal field theories. The entanglement entropy for other configurations (subregions $A$ consisting of the union of multiple intervals or systems with both finite size and finite temperature) is no longer universal in general. However, for holographic CFTs with large central charge universal results are again recovered at leading order in $c$ [103]. This large $c$ universality will turn out to be important in chapter 3.

### 2.2.2. The Ryu-Takayanagi formula

I now turn to the holographic dual to the entanglement entropy. It was observed by Ryu and Takayanagi in [27] that there is a surprisingly simple bulk quantity dual to the von Neumann entropy of a reduced density matrix on a boundary subregion $A$. This bulk dual to the entanglement entropy is constructed as follows. Consider all codimension-two surfaces $\mathscr{E}_A$ in the bulk that asymptote to $\partial A$, the boundary of $A$, on the AdS boundary. The entanglement entropy is then obtained from the surface $\gamma_A$ with smallest area [27], $\text{Area}(\gamma_A) = \min_{\mathscr{E}_A} \text{Area}(\mathscr{E}_A)$, subject to the constraint that $\gamma_A$ must be homologous to $A$ [104], [28]

$$S_A = \frac{\text{Area}(\gamma_A)}{4G_N}. \tag{2.80}$$

The minimal surface $\gamma_A$ is called the Ryu-Takayanagi surface. The Ryu-Takayanagi formula (2.80) generalizes the Bekenstein-Hawking entropy formula in asymptotically AdS spaces. For an AdS black hole and a subregion $A$ covering an entire constant time slice on the boundary, equation (2.80) reduces to the Bekenstein-Hawking entropy [27]. Because black holes are dual to thermal states in AdS/CFT, the entanglement entropy reduces to the thermal entropy in this case, making the connection to black hole thermodynamics obvious.

As an example for a Ryu-Takayanagi surface, consider $\text{AdS}_3$ with metric

$$ds^2 = \frac{L^2}{r^2}(dr^2 - dt^2 + dx^2). \tag{2.81}$$

Minimal codimension-two surfaces are geodesics in this case. The length of a geodesic in $\text{AdS}_3$ stretching between two points $x = z_1$ and $x = z_2$ on the boundary is given by

$$S_A = \frac{\text{Area}(\gamma_A)}{4G_N} = \frac{L\log((z_2 - z_1)/\epsilon_{\text{UV}})}{4G_N}, \tag{2.82}$$

where $\epsilon_{\text{UV}}$ is a UV cutoff. Applying (2.6) shows perfect agreement with the field theory result (2.79).

[27] Note the presence of a UV regulator $\epsilon_{\text{UV}}$ in the expression. In general in quantum field theory, the entanglement entropy of a spatial subregion $A$ diverges. For two-dimensional CFTs, the divergence is logarithmic in $\epsilon_{\text{UV}}$ [97, 102] and only the overall prefactor as well as the dependence on $z_1, z_2$ is physically meaningful. The path integral $Z_n/Z_1^n$ computes only the physically meaningful parts of the expression while the UV regulator has to be inserted by hand in the replica trick method.

[28] Intuitively, the homology constraint demands that $\gamma_A$ must be smoothly retractable to the asymptotic AdS boundary. In precise terms, it says that there must exist a non-empty codimension-one spacelike surface in the bulk that is bounded by $\gamma_A$ and the subregion $A$ on the boundary [104, 105].

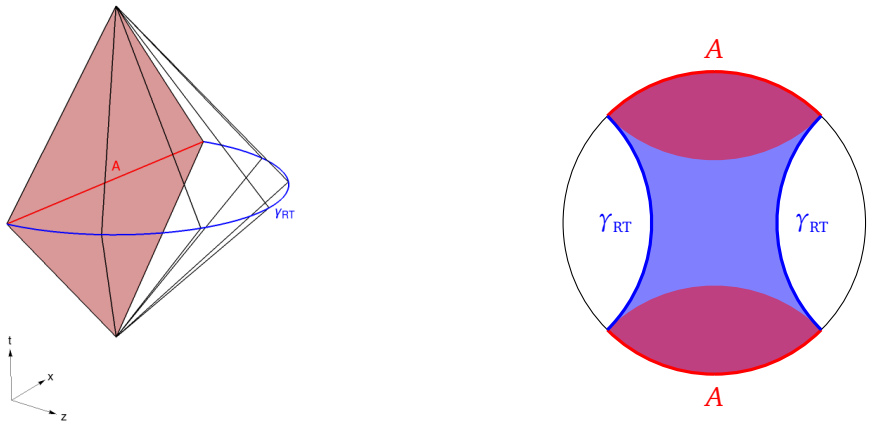


Figure 2.3.: LHS: Causal wedge of an interval $A$ on the boundary of $AdS_3$ in Poincaré patch coordinates. The domain of dependence of $A$ is given by the diamond shaped region in red on the boundary. The RT surface is drawn in blue while black lines represent light rays which bound the causal wedge. RHS: Example of an entanglement wedge that is larger than the causal wedge. Indicated is a time slice of $AdS_3$ in global coordinates with the entanglement wedge in blue overlapping – but not coincident – with the causal wedge in red.

The Ryu-Takayanagi formula (2.80) as stated here only applies to static geometries and does not take into account quantum corrections, i.e. terms subleading in $G_N$ respectively $N$ (the rank of the gauge group, proportional to the central charge in two dimensions). A covariant generalization of the Ryu-Takayanagi formula has been developed in [106] and is known as the Hubeny-Rangamani-Takayanagi (HRT) formula. Quantum corrections have been considered for instance in [34] for the first subleading order in the $G_N$ expansion while in [35] a "quantum extremal surface" formula for the gravitational dual to the entanglement entropy has been developed that is valid to all orders in $G_N$. See [105] for a comprehensive treatment of holographic entanglement entropy and applications thereof.

### Entanglement wedges

Further insight into the nature of the holographic encoding between boundary and bulk degrees of freedom can be gained by exploring which subregions on the boundary contain complete information about subregions in the bulk. This problem is known as subregion-subregion duality [28, 107, 108] and as it turns out, also here the Ryu-Takayanagi formula is of importance.

From causality, it is clear that a causal diamond[29] on the boundary contains complete information about a bulk subregion known as the causal wedge, defined as the intersection between the (bulk) causal future and past of the (boundary) causal diamond [109]. However, it turns out that in AdS/CFT the subregion for which complete information can be gained is the *entanglement wedge* which is in general larger than the causal wedge [28–30, 48, 110–112]. The entanglement wedge is constructed as the causal domain of dependence of a Cauchy slice between a boundary interval $A$ and the corresponding Ryu-Takayanagi surface $\gamma_A$ (see figure 2.3).[30] The

[29] A causal diamond of a subregion $A$ is the causal domain of dependence of $A$, i.e. the region bounded by converging lightrays emerging from the boundary of $A$ to the past and future. In this region, the physics is entirely determined by initial conditions on $A$.

[30] This Cauchy slice is guaranteed to exist and to be non-empty due to the homology constraint on $\gamma_A$.

Ryu-Takayanagi surface $\gamma_A$ induces a splitting of bulk degrees of freedom on a Cauchy slice into the degrees of freedom contained in the entanglement wedge which the holographic mapping encodes in the boundary causal diamond corresponding to $A$ and the degrees of freedom in the complement of the entanglement wedge which are not encoded solely in the causal diamond of $A$.

The precise statement of subregion-subregion duality is as follows [48, 111, 112]. Consider a bulk operator $\phi(x)$ which may be for instance a scalar or tensor field of the gravitational theory. Subregion-subregion duality states that there exists an operator $\mathcal{O}_A$ acting locally in the subregion $A$ and dual to $\phi(x)$ if the point $x$ is inside the entanglement wedge of $A$. The procedure of constructing this boundary operator $\mathcal{O}_A$ is termed bulk reconstruction. Note that one cannot reconstruct arbitrary operators in the entanglement wedge due to backreaction or even black hole formation if too much energy is injected into the bulk by application of the operator. Thus bulk reconstruction in the entanglement wedge is only possible in a so-called code subspace, a Hilbert space consisting of states obtained by the application of operators for which the backreaction of the metric is negligible. Due to a bulk point $x$ being in general inside multiple entanglement wedges, there exist multiple operators $\mathcal{O}_A$ dual to $\phi(x)$ which act locally in different boundary subregions. These operators, although acting differently on the total Hilbert space for different subregions $A$, have the same action in the code subspace.[31]

### Deriving the Ryu-Takayanagi formula from the AdS/CFT conjecture

A derivation of the Ryu-Takayanagi formula from the basic statement of the AdS/CFT correspondence (2.1) is possible by extending the replica trick into the bulk [113].[32] Recall from section 2.2.1 that the entanglement entropy in the boundary theory is calculated from the partition function on a replica surface $\mathcal{R}_n$ given by $n$ copies of Minkowski space glued together along the subregion $A$. The basic idea in the derivation of [113] is to use (2.1) to map this computation into the calculation of the on-shell supergravity action. The bulk action must then be evaluated with boundary conditions such that the bulk manifold $\mathcal{M}_n$ asymptotes to $\mathcal{R}_n$ on the boundary. The presentation in the following uses Euclidean signature such that the partition function is given by minus the exponential of the on-shell action $Z_{\text{CFT}} = e^{-S_{\text{grav}}}$. Moreover, the derivation will only be presented for the static setting, see [114] for the generalization to the covariant HRT prescription.

Let me first assume, following [113], that the $\mathbb{Z}_n$ replica symmetry of the boundary manifold $\mathcal{R}_n$ extends into the bulk, i.e. the solution of the gravitational equations of motion yields a bulk manifold $\mathcal{M}_n$ that is also $\mathbb{Z}_n$ symmetric. Then, one may consider the quotient space $\mathcal{M}_n/\mathbb{Z}_n$ which has singularities along the fixed points of the $\mathbb{Z}_n$ action. Note that $\mathcal{M}_n$ itself is generally free of singularities. Due to the $\mathbb{Z}_n$ symmetry, the gravitational actions for $\mathcal{M}_n$ and $\mathcal{M}_n/\mathbb{Z}_n$ are related,

$$S_{\text{grav}}[\mathcal{M}_n] = nS_{\text{grav}}[\mathcal{M}_n/\mathbb{Z}_n]. \tag{2.83}$$

Another necessary assumption for the derivation of [113] is that the fixed points of the $\mathbb{Z}_n$ action form a codimension-two surface $\mathbf{e}_n$. The quotient space $\mathcal{M}_n/\mathbb{Z}_n$ then equivalently arises from a codimension-two cosmic brane at $\mathbf{e}_n$ in the original bulk manifold $\mathcal{M} = \mathcal{M}_{n=1}$. The cosmic brane is a source of energy and momentum that deforms the bulk geometry from $\mathcal{M}$ to $\mathcal{M}_n/\mathbb{Z}_n$. The

[31] In fact, the bulk reconstruction procedure can be interpreted as a quantum error correcting code protecting against the erasure of subregions $B$ complementary to $A$ [48]. While tracing out $B$ does not allow to reconstruct the entire state, the code subspace states can still be recovered.

[32] See also [105] for a review article explaining this method.

tension of the brane necessary to generate a $\mathbb{Z}_n$ quotient is given by [105]

$$T_n = \frac{1}{4G_N}\left(1-\frac{1}{n}\right). \tag{2.84}$$

The advantage of the cosmic brane formulation is that $n$ appears only as a parameter for the tension of the cosmic brane and hence there are no obstacles for the analytic continuation to $n \in \mathbb{R}$. The analytic continuation is simply achieved by tuning the tension of the cosmic brane. Therefore, the task at hand is to solve solve Einstein's equations in the presence of the cosmic brane and then to evaluate the on-shell action for this solution.

In order to solve Einstein's equations, it is convenient to write the metric in the neighborhood of the surface $\mathbf{e}_n$ in Gaussian coordinates. For the manifold $\mathscr{M}$ this gives

$$ds^2 = dx^2 + dt^2 + (\gamma_{ij}^{(n=1)} + 2K_{ij}^{x,(n=1)}x + 2K_{ij}^{t,(n=1)}t)dy^i dy^i + \ldots, \tag{2.85}$$

where $x, t$ are coordinates transverse to $\mathbf{e}_n$ and $y^i$ are coordinates on $\mathbf{e}_n$. $\gamma_{ij}$ is the induced metric on $\mathbf{e}_n$ and $K_{ij}^x$ and $K_{ij}^t$ are the extrinsic curvatures. The dots in (2.85) denote higher order terms in $x, t$. The generalization of (2.85) to the metric of $\mathscr{M}_n/\mathbb{Z}_n$ is obtained as follows [113]. Choose polar coordinates $r, \phi$ for the directions transverse to $\mathbf{e}_n$. Due to the conical deficit, $\phi$ is identified as $\phi \sim \phi + 2\pi n$ and hence it is clear that the metric in the transverse directions must be of the form $n^2 dr^2 + r^2 d\phi^2$. On the other hand, the replica symmetry implies that the manifold $\mathscr{M}_n$ is composed out of $n$ identical parts that are identified with each other to get $\mathscr{M}_n/\mathbb{Z}_n$. Letting $\phi \to \phi + 2\pi$ moves from one part to the next in $\mathscr{M}_n$. Therefore, the metric components in the directions along $\mathbf{e}_n$ are $2\pi$-periodic in $\phi$. Thus for $n > 1$, the following metric appears in the vicinity of $\mathbf{e}_n$,

$$ds^2 = (n^2 dr^2 + r^2 d\phi^2) + (\gamma_{ij} + 2K_{ij}^x r^n \cos\phi + 2K_{ij}^t r^n \sin\phi)dy^i dy^i + \ldots \tag{2.86}$$

Einstein's field equations for this metric to leading order in $n-1$ are equivalent to [113]

$$K_{ij}^x \gamma^{ij} = K_{ij}^t \gamma^{ij} = 0. \tag{2.87}$$

Therefore the surface $\mathbf{e}_n$ must be extremal, $\mathbf{e}_n = \mathscr{E}_A$. Furthermore, evaluating the on-shell action for this solution of the Einstein equations gives a term proportional to the area of $\mathscr{E}_A$ [113]. In the saddle point approximation, the leading contribution to $e^{-S_{\text{grav}}}$ comes from the saddle point with smallest on-shell action if there are multiple saddle points. Other contributions are exponentially suppressed with $e^{-1/G_N}$ factors. Therefore from among all extremal surfaces $\mathscr{E}_A$, the leading contribution comes from the one with smallest area. The homology constraint has been shown to also follow from the above arguments as long as the manifolds $\mathscr{M}_n$ exist for all positive integers $n$ and are smooth (i.e. free of singularities) [115]. This proves the Ryu-Takayanagi formula subject to the assumption that the replica symmetry extends into the bulk[33] and of course assuming that the AdS/CFT correspondence holds.

[33] Note that this assumptions holds for most states of physical interest but not for all states. For the quantum corrected Ryu-Takayanagi formula from the quantum extremal surface prescription, it has been shown in [116, 117] that the assumption is valid if the boundary state $\rho$ is close to perfectly compressible, that is if there exists a reduced density matrix $\sigma$ that is close to $\rho$ (in the matrix norm) but which is a mixture involving a number of states that is only of order $S(\rho)$. Both pure states and thermal states which are the subject of study in this thesis are perfectly compressible.

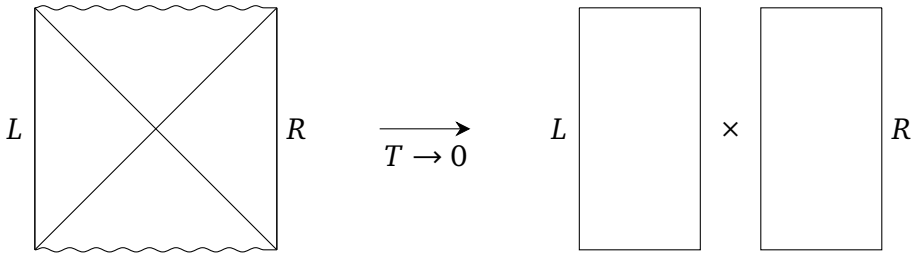


Figure 2.4.: In the limit of zero temperature, the two-sided black hole geometry whose Penrose diagram is depicted on the left reduces to two disconnected pure AdS spacetimes. In the dual CFT, the entangled thermofield double state becomes a product state $|0\rangle_L \times |0\rangle_R$ in this limit.

### 2.2.3. Entanglement builds geometry

The fact that the entanglement entropy is dual to a geometric object – the area of the Ryu-Takayanagi surface – has lead to a more general idea that the geometry of the asymptotically AdS space in AdS/CFT can be interpreted not as a fundamental object but as emergent from entanglement in the boundary theory [37, 38]. Equivalently, one may say that the classical bulk geometry is encoded in the entanglement structure of the boundary quantum state. This idea has been dubbed "entanglement builds geometry" or "it from qubit".

To examine this idea in more detail, let me first summarize an argument given in [38] to develop some intuition why entanglement and spacetime connectedness should be related in AdS/CFT. Consider a holographic conformal field theory which for concreteness is taken to live on a sphere and be in a particular quantum state $|\psi\rangle$. Divide this sphere into two parts. The entanglement entropy for this bipartition is dual to the area of the Ryu-Takayanagi surface in the dual asymptotically AdS spacetime. Now, manipulate the quantum state in such a way that the entanglement between the two halves decreases. This also lowers the area of the Ryu-Takayanagi surface. If the entanglement finally vanishes at the end of this procedure, the Ryu-Takayanagi surface is no longer existent. Then, the bulk dual disintegrates into two unconnected asymptotically AdS spaces. The quantum state $|\psi\rangle$ is now a product state which can be thought of as living on two disconnected hemispheres that are the boundaries of two unconnected asymptotically AdS spacetimes.

This procedure can be concretely implemented for instance in an AdS wormhole geometry, i.e. a maximally extended Schwarzschild-AdS spacetime. This spacetime, also known as the eternal black hole geometry, has two decoupled asymptotic boundaries on each end of the wormhole. By decoupled, I mean that the Hamiltonian is the sum of a "left" and "right" Hamiltonian on each of the two boundaries, $H = H_L + H_R$. The boundary CFT is in the thermofield double state (1.5) [39]. The reduced density matrix on either of the two asymptotic boundaries is a thermal mixture with temperature equal to the Hawking temperature of the wormhole in the bulk. Therefore, the bulk geometry is connected – even though the two-sides of the wormhole are decoupled – due to entanglement inherent in the thermofield double state.[34] Taking the zero temperature limit, the connection between the two asymptotic boundaries vanishes again (see figure 2.4). In this case, the system is in a product state dual to two disconnected (pure AdS) spacetimes in the bulk.

While the above arguments give some useful intuition into how entanglement and geometry are connected, they do not provide an obvious method for the reconstruction of bulk geometric objects from entanglement data of the field theory. And in fact, it is by now clear that such a

[34] Even though there is a connected spacetime between the two boundaries, no observer can send a signal from one end to the other because all signals sent into the wormhole end up in the singularity. Thus the spacetime connectedness is not in tension with the fact that the left and right CFT cannot communicate with each other.

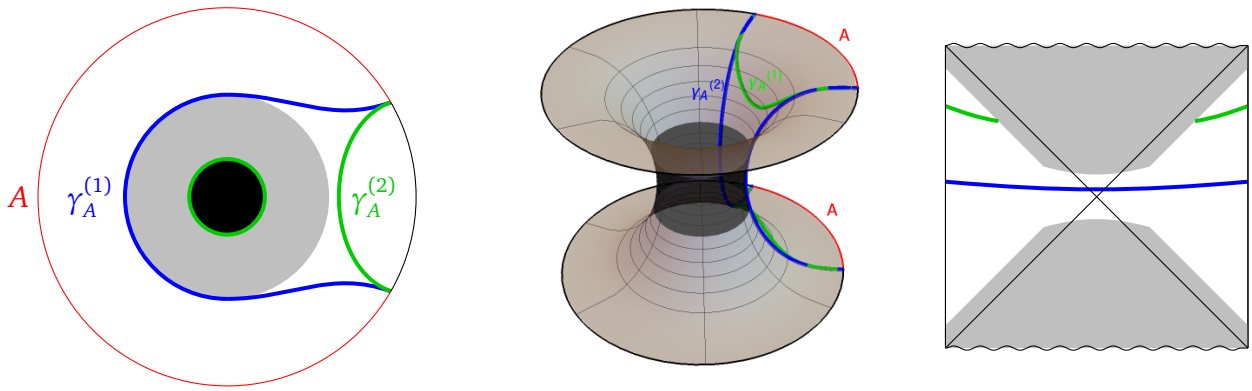


Figure 2.5.: Illustration of the entanglement shadow (in gray) of the BTZ black hole for a time-slice of the one-sided black hole (LHS) and two-sided black hole geometry including the Penrose diagram (RHS). The blue and green lines represent Ryu-Takayanagi surfaces in different phases. For the one-sided black hole, the Ryu-Takayanagi surface in blue is connected while the one in green is the union of a horizon wrapping piece and a boundary anchored geodesic. Similarly, Ryu-Takayanagi surfaces in blue for a two-sided black hole stretch through the wormhole for early times but are given by the union of two disconnected pieces in green outside the horizon for late times.

reconstruction runs into problems. The main problem is that there exist regions of spacetime known as entanglement shadows or entanglement holes which are not penetrated by any Ryu-Takayanagi surface [28, 44–47]. These entanglement shadows typically lie close to a black hole horizon or naked singularity. For example for Schwarzschild-AdS black holes, the entanglement shadow is a ball-shaped region extending to a finite distance above the black hole horizon [47] (see figure 2.5). Because no Ryu-Takayanagi surface enters these regions, one cannot probe this part of the bulk geometry with the entanglement entropy of spatial subregions $A$. Entanglement shadows arise due to phase transitions in the entanglement entropy at points where one extremal surface $\mathscr{E}_A$ becomes smaller than another one as the size of the subregion $A$ is varied.

A particular striking striking example of an entanglement shadow occurs in an asymptotically AdS wormhole. Consider a subregion $A$ consisting of the union of two subregions on either asymptotic boundary. As time evolves[35], at early times the entanglement entropy $S_A$ grows roughly linear in time [58]. In this phase, the two asymptotic boundaries are connected with a (spacelike) RT surface that stretches through the wormhole from one end to the other [58]. However, at some critical time $t_c$, there is phase transition where the entanglement entropy stops growing and reduces to a constant [58]. In this phase, the RT surface is given as the union of two disconnected surfaces that stay outside the wormhole in either exterior region [58]. See figure 2.5 for a visualization of these RT surfaces. Thus, an entanglement shadow forms: the region in the Penrose diagram close to the bifurcation surface is accessible with RT surfaces but not the wormhole interior (and a small region above the horizon) for later times. But a spacelike geodesic through the wormhole still keeps growing in time. Therefore, this feature of the bulk geometry (the behind-the-horizon region of the wormhole) is not accessible from the entanglement entropy in the dual boundary state.

[35]The time evolution here is with $H = H_L + H_R$ forwards in time on both boundaries. From the CFT point of view, it is also possible to choose the Hamiltonian as $H = H_L - H_R$ (evolution forwards in time on the left and backwards on the right side), however this leaves the thermofield double state invariant.

The "entanglement builds geometry" idea in AdS/CFT and entanglement shadows are one of the main topics investigated in this thesis. In chapter 3, I will develop generalized entanglement measures in $AdS_3/CFT_2$ to quantify the amount of entanglement between non-spatially organized degrees of freedom, i.e. entanglement between different fields as well as between spatial degrees of freedom. The gravity dual to these entanglement measures is given by a generalization of the Ryu-Takayanagi formula and allows for probing entanglement shadows of conical defects as well as one- and two-sided black hole geometries. Another idea, put forward in [51–54] to resolve the entanglement shadow subregion of a two-sided black hole, is that particular geometric features of this subregion can be probed by another quantity from quantum information theory known as computational complexity. Aspects of this idea will be studied in chapter 4. A detailed introduction to computational complexity and its proposed holographic interpretation may be found in the following section.

## 2.3. Quantum circuits, black holes and computational complexity

It is well known that the description of quantum effects in black hole systems is a difficult problem. A common approach to this problem is to start with classical gravity and then add quantum corrections on top, a method that famously leads to the black hole information paradox and the associated violations of unitarity [15]. However, it can often be useful to instead assume unitarity from the start and model the black hole as a quantum system. Although the microscopical description of such a system is only available in a complete theory of quantum gravity, upon construction of a general enough model it is nevertheless possible to study quantum features of black holes without having access to such a complete quantum gravity theory – assuming that unitarity holds of course.[36]

These kind of models have been used for example to study the time-evolution of the entanglement entropy between Hawking radiation and the remaining black hole [55], to argue that possible violations of the monogamy principle of entanglement put forward in [118, 119] might not actually be observable [120] or to investigate how quickly information thrown into an evaporating black hole leaks out again [57]. Let me now briefly summarize two such models in section 2.3.1 and 2.3.2 before explaining in detail the construction which forms the main motivation for the investigations in chapter 4 of this thesis and its relation to computational complexity in section 2.3.3. Finally, I will give an overview over computational complexity constructions in quantum field theory in section 2.3.4.

### 2.3.1. The Page curve

The first example yields an estimate of the entropy of the Hawking radiation with the black hole interior as time evolves (the so-called Page curve) [55] (see [33, 121] for reviews on this topic). In the setup of [55], the black hole together with its Hawking radiation is modeled by a pure state on the Hilbert space

$$\mathscr{H}_{\text{tot}} = \mathscr{H}_R \otimes \mathscr{H}_{BH} \tag{2.88}$$

while the states of the radiation subsystem $R$ and black hole subsystem $BH$ are mixed. Here, the size of the subsystems is assumed to be $|\mathscr{H}_R| = e^{S_{R,\text{coarse}}}$ and $|\mathscr{H}_{BH}| = e^{S_{BH,\text{coarse}}}$ where $S_{R,\text{coarse}}$ and $S_{BH,\text{coarse}}$ are the entropies of the radiation and of the black hole following from Hawking's

[36] In the AdS/CFT setting this assumption is valid because unitarity is built into the description from the start due to the unitarity of the dual field theory.

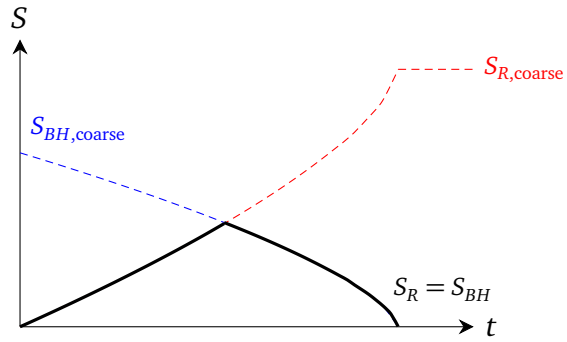


Figure 2.6.: Evolution of the entropy of the Hawking radiation and black hole subsystem in the semi-classical calculation (dashed lines) and in the quantum circuit model of [55] incorporating unitarity by construction. The dashed curves follow the estimates in [56] for large non-rotating black holes in flat space. Note that the shape of the solid black Page curve around the Page time is not entirely fixed by the quantum circuit construction of [55] and the sharp transition in this plot may not hold in a more realistic model.

calculation. These entropies are called coarse grained entropies to distinguish them from the fine-grained entropies $S_R$, $S_{\text{BH}}$ that are available only in a complete theory of quantum gravity and due to unitarity of course equal, $S_R = S_{BH}$. Due to our ignorance about the true theory of quantum gravity (which would in principle determine the states on the total system as well as the $R$ and $BH$ subsystems) the total state of the system is treated as being a random pure state

$$|\psi\rangle = U|\psi_0\rangle, \tag{2.89}$$

where $U$ is a unitary operator chosen randomly from the Haar measure on the unitary group acting on the total Hilbert space and $|\psi_0\rangle$ is a fixed state in this Hilbert space.[37] A state obtained in this way is called "Haar-random". For a general quantum system with $\mathscr{H}_{\text{tot}} = \mathscr{H}_A \otimes \mathscr{H}_B$ with $|\mathscr{H}_A| \ll |\mathscr{H}_B|$ and $|\mathscr{H}_A|, |\mathscr{H}_B| \gg 1$, the entanglement entropy averaged over all pure states of the total system is given by [123]

$$\int dU\, S_A = \log|\mathscr{H}_A| - \frac{1}{2}\frac{|\mathscr{H}_A|}{|\mathscr{H}_B|} + O(1/|\mathscr{H}_{A,B}|). \tag{2.90}$$

This implies that the entanglement entropy $S_R = S_{BH}$ (the von Neumann entropy of either the black hole or radiation subsystem) averaged over all pure states of the total system is given by $S_R \approx S_{R,\text{coarse}}$ at early times in the evolution while at late times it is given by $S_R \approx S_{BH,\text{coarse}}$. Therefore, the entanglement entropy shows an approximately linear increase until the Page time which is equal to roughly half of the evaporation time followed by a decrease until it reaches zero at the end of the evaporation process (see figure 2.6). This form of the entanglement entropy time evolution is called the Page curve. On the other hand, in Hawking's semiclassical calculation the von Neumann entropy of the Hawking radiation increases continuously until the end of the evaporation process. The calculation of the Page curve is an example for applications of a quantum circuit model, which is unitary by construction, to the study of black hole physics. The main feature of the construction of [55], modeling the dynamics by randomized time-evolution, is a

[37] By interpreting the real and imaginary directions of an $n$-dimensional Hilbert space as distinct directions in a $\mathbb{R}^{2n}$ Euclidean space, properly normalized states are points on the unit-sphere $S^{2n-1}$ in the $\mathbb{R}^{2n}$. The Haar measure on the unitary group acting on the Hilbert space then coincides with the area function on the $S^{2n-1}$ [122].

characteristic common to many quantum circuit models for black holes.

Finally, note that the arguments given above are agnostic about the sign of the cosmological constant and therefore apply more generally than only in AdS/CFT. Although a general derivation of the Page curve from quantum gravity calculations is still lacking, it has recently been shown that in AdS/CFT models of black holes coupled to non-gravitating bath systems the form of the Page curve can be derived directly from the gravity theory [31–33].

### 2.3.2. Firewalls and computational complexity

Another important example of applications of quantum circuits and in particular computational complexity to black hole physics comes from thought experiments uncovering an apparent inconsistency of a unitary black hole evaporation process with the applicability of a semi-classical description of an infalling observer at or close to the event horizon [118, 119] (see also [124] for earlier developments and [121, 125] for reviews). In more precise terms, the authors of [118, 119] argue for the inconsistency of the following postulates on black hole physics:

1. From the viewpoint of a distant observer, the black hole formation and evaporation process is a unitary process which can be described in ordinary quantum mechanics.

2. Up to about a Planck length outside of the black hole, the physics is described to good approximation by semi-classical field equations in which the system is modeled by quantum fields on a classical spacetime.

3. The black hole appears like a quantum system with discrete energy levels and an entropy equal to the Bekenstein-Hawking entropy.

4. The horizon is smooth in the sense that a free falling observer perceives nothing special when crossing it.

Briefly summarized, the basic problem uncovered in [118, 119] is that postulate 4 requires a high degree of entanglement between quantum field theory modes $A$ and $B$ inside and outside of the event horizon[38] due to the entanglement to all length scales inherent in all quantum field theories. Now consider a mode $B$ localized close to but outside the black hole horizon and in the process of propagating to an observer far away from the black hole. The postulates 1, 2 and 3 imply from the arguments summarized in section 2.3.1 that for a black hole which has evaporated to a substantial degree, the black hole subsystem $H$ together with the mode $B$ is highly entangled with the radiation subsystem $R$. However, these two facts are in tension with another due to the so-called monogamy property of entanglement [126, 127]: if the mode $B$ is highly entangled with some part of the radiation, it cannot at the same time be highly entangled with $A$. In particular, if $B$ is highly entangled both with $A$ as well as with some part $R_B \subset R$ of the radiation subsystem $R$, the strong subadditivity property of the entanglement entropy is violated, $S_{R_B \cup B} + S_{A \cup B} \ngeq S_B + S_{A \cup R_B \cup B}$ [128]. Assuming that postulate 4 is invalid and there is no entanglement between field theory modes across the horizon implies that at the horizon there is a singularity of some kind[39] even

[38] A mode in this context refers to a localized wave packet with associated creation and annihilation operators and a Fock space description.

[39] In general, QFT states are highly spatially entangled and therefore product states indicate a singularity. For example in scalar field theory in flat space, there is a large concentration of energy at the interface between complementary spatial subregions $A$ and $B$ for a product state $\rho_A \times \rho_B$ [121]. If there is no correlation between $A$ and $B$, the expectation value of the field difference $\phi$ at the interface between $A$ and $B$ is non-zero, i.e. the field is discontinuous. Therefore, the derivative $\partial_x \phi$ entering the Hamiltonian density is divergent, leading to a divergent energy density.

though for a large black hole the curvature is still small at the horizon and therefore no strong quantum effects are expected. This lead the authors of [118, 119] to propose that a free falling observer would encounter a so-called firewall comprised out of a large number of highly energetic particles at or close to the horizon. Whether the argument of [118, 119] actually holds up is unclear at the moment (see e.g. [121] for further discussions).

In particular, an interesting argument has been given in [120] that the violation of the monogamy of entanglement at the heart of the firewall proposal might actually not be observable because the computational complexity of the calculations necessary to prove the violation in a concrete experiment is so large that it prevents the experiment from being done. This argument is based on a quantum circuit description of the black hole system together with its Hawking radiation. Let the mode $B$, the next particle to be emitted by the black hole, be modeled by a single qubit, the remaining black hole system $H$ by $m$ qubits and the radiation $R$ by $n$ qubits. If the black hole has evaporated for sufficiently long, $n \gg m$ and the state of the total system $B \cup H \cup R$ is modeled by a random pure state while the state of the subsystem $B \cup H$ is a mixed state that is highly entangled with the radiation $R$. To observe the violation of the monogamy of entanglement, an observer which I will call Alice needs to do the following steps [120, 125]. First, Alice must act with a unitary operator on the radiation subsystem $R$ (which is the only part of the system she has access to) to bring the state into the form of a Bell pair between $B$ and one qubit of $R$. She must then perform a measurement on this qubit and wait until $B$ is emitted to confirm that $B$ and $R$ are indeed entangled in the form of a Bell pair. Alice then has to jump into the black hole where performing measurements on the remaining qubits in $H$ allows here to find entanglement between $B$ and a qubit $A$ in the subsystem $H$ in violation of the monogamy principle of entanglement.

The argument put forward in [120] is that the computational complexity of the first step, bringing the state into the form of a Bell pair, is so large that performing it would take much longer than the time needed for the black hole to evaporate completely. To be precise, the computational complexity was argued to be exponential in the initial black hole entropy $S$ while the evaporation time scales only polynomially in $S$. Note that this argument depends on some highly plausible but unproven statements from complexity theory, the details of which I will not discuss here (see e.g. [121, 125] for an introduction). The important point is that this argument introduces a concrete relation between complexity theory and black hole physics.

In fact, other relations of this kind in the AdS/CFT context motivate the construction of quantum circuits and the study of computational complexity in chapter 4 of this thesis. These relations emerged in part from investigations of the firewall proposal in AdS/CFT. In this direction, it was argued in [129] that the entanglement monogamy theorem underlying the firewall proposal is not applicable for two-sided black holes in AdS/CFT because the mode $A$ is not independent from the $R$ subsystem. This argument is based on mapping the bulk description of the black hole system to a boundary CFT description. For non-evaporating two-sided black holes in AdS spacetimes, the $R$ subsystem is identified with the CFT living on one of the two asymptotic boundaries[40] (say, the right one for concreteness) while the modes $A$ and $B$ are described by boundary operators [129]. The mode $B$ propagating in the left black hole exterior can be modeled by a CFT operator in the left subsystem while the CFT operator corresponding to $A$ propagating in the interior does not have support only in the left CFT. This lead the authors of [129] to conclude that the mode $A$ is encoded (in some complicated way) in the $R$ subsystem and that therefore the unperturbed two-sided black hole dual to the thermofield double state does not have a firewall. However, it has also been argued that in AdS/CFT, firewalls are typical in the sense that almost all states[41] in the

[40] Although the two-sided AdS black hole considered here does not evaporate, the $R$ subsystem plays the same role as the Hawking radiation subsystem for an evaporating black hole in flat space in that the total state is pure while the state on the $R$ subsystem is mixed and highly entangled with the remaining degrees of freedom.

[41] More precisely, consider an operator whose expectation value can be used to detect the presence of a firewall. The

microcanonical ensemble of states with fixed energy have a firewall [130]. Moreover, the authors of [129] state that unlike in the argument of [118], the presence of a firewall depends on what manipulations are done in the $R$ subsystem. According to [129], an experiment trying to prove a violation of the entanglement monogamy property will produce a firewall but this does not imply that the firewall would have been there had the experiment not been performed. From these arguments, interesting questions emerge: how difficult is it to create a firewall, i.e. how large is the computational complexity for this process in the AdS/CFT setting? Do firewalls exist for black holes created from realistic formation processes such as collapsing matter concentrations? These questions among other arguments lead to (conjectural) relations between computational complexity and geometric features of the dual AdS space [51–54] reviewed in the next subsection.

### 2.3.3. Computational complexity in holography

This subsection describes the computational complexity conjectures of [51–54] as well as the underlying quantum circuit alluded to in the previous subsection. These conjectures are motivated by the firewall arguments presented in the preceding subsection and by close similarities between the computational complexity and its conjectured dual in the bulk. Let me first start with a detailed description of the quantum circuit in consideration before briefly coming back to firewalls at the end.

The first question to ask in modeling a black hole as a quantum system is how many degrees of freedom, i.e. how many qubits do we need? In general, a quantum system of entropy $S$ must contain at least order $S$ qubits (the maximum entropy in a system with $K$ qubits scales like $K \log 2$). To keep the model simple, the assumption taken in [51–54] is that a system of size of the order of the black hole entropy $S$ is sufficient to model the features of the black hole that are of interest. Because a first principles description of the dynamics of the system requires a complete theory of quantum gravity, which is not available, the dynamics is modeled by a random Hamiltonian as in section 2.3.1. Moreover, [51–54] assumes that the Hamiltonian is approximately $k$-local (interaction terms in the Hamiltonian involve at most $k$ qubits) and all-to-all (there are $k$-qubit interactions between all possible subsets comprised of $k$ qubits in the system), where $k$ is a small fixed number.[42] The Hamiltonian generates evolution in Rindler time $\tau$ which is identified with the time coordinate along which the circuit evolves.[43]

Since black holes are thermal objects, it is important to know how quickly they thermalize in the circuit constructed thus far. It turns out that the thermalization time, sometimes also called scrambling time, is relatively short, scaling as a power of the entropy $S$.[44] The thermalization time is the time at which a one-sided black hole formed from collapse reaches maximum entropy[45] and also the time scale for perturbations of the one- and two-sided black hole to die down [57, 134]. This short thermalization time manifests itself in observables reaching stable values relatively quickly. For instance, the entanglement entropy of a spatial subregion consisting of the union of two parts on different asymptotic boundaries of the two-sided BTZ geometry geometry stops

expectation value of this operator in a randomly chosen pure state of a microcanonical ensemble is equal to the expectation value of the same operator in a state that contains a firewall up to corrections exponentially small in the entropy [121].

[42] This assumption can be rigorously shown in AdS/CFT models which are related to matrix theories, for instance for boundary theories like the SYK model or BFSS matrix theory [131, 132].

[43] In Rindler coordinates, the near-horizon geometry of a black hole takes on a universal form $ds^2 = -\rho^2 d\tau^2 + d\rho^2 + r(\rho)^2 d\Omega^2$ where $\rho$ is the proper distance from the horizon. This universality and the fact that $\tau$ is dimensionless make $\tau$ a natural candidate for the time coordinate of the circuit [133].

[44] For instance, for a Schwarzschild black hole, the thermalization time was estimated in [57] to be of order $O(r_S \log r_S) = O(\sqrt{S} \log S)$, where $r_S$ is the Schwarzschild radius.

[45] The two-sided black hole is in thermal equilibrium for the entire evolution.

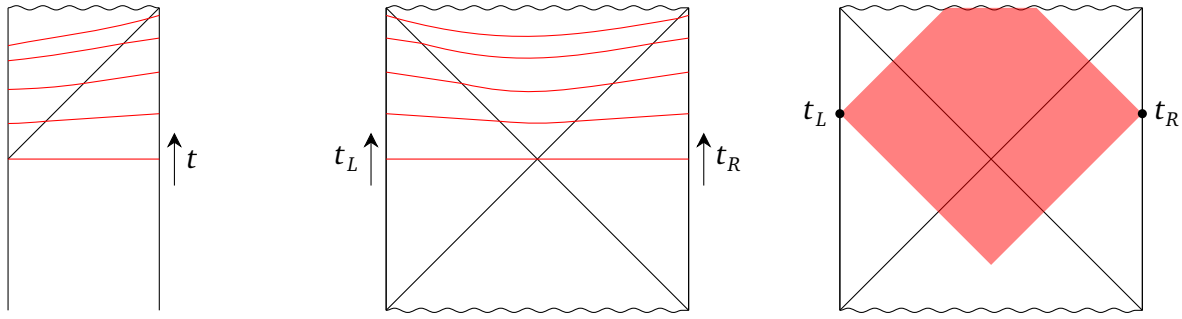


Figure 2.7.: Holographic probes of the growth of the behind-the-horizon region of AdS black holes. Shown are Penrose diagrams of one- and two-sided black hole geometries. Left and center: maximal volume slices in the one- and two-sided black hole. Right: bulk action on the Wheeler-de Witt patch (the red shaded region). $t_L$ and $t_R$ denotes the time on the left respectively right asymptotic boundaries of the two-sided black hole. Time evolves upward on both boundaries.

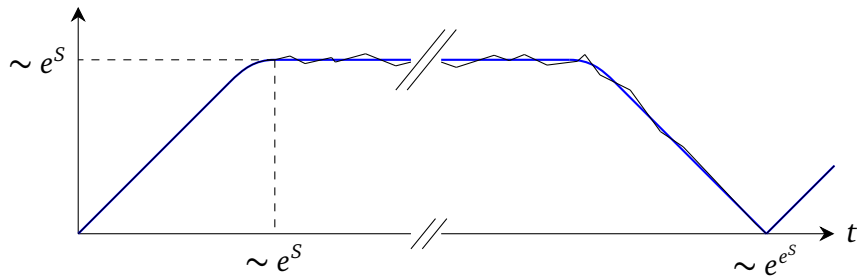


Figure 2.8.: Schematic time evolution behavior of observables probing the growth of the behind-the-horizon region of an AdS black hole. Up to a time scale exponential in the black hole entropy, the observables grow linearly after which quantum corrections lead to a saturation and fluctuation around the maximum value which also scales exponentially in the entropy. After a doubly exponential time, quantum recurrences lead to a decrease, the system returns to its starting point and the time evolution starts anew.

growing after a short time of order $O(S^0)$ [58].

On the other hand, there are important features of the bulk geometry that evolve way past the thermalization time. In particular, the "size" of the interior of a two-sided asymptotically AdS black hole grows for a very long time when evolving forward in time on both asymptotic boundaries. There are many observables that probe this growth and that thus can be used to define the size of the wormhole. For example, a spacelike extremal codimension-two surface stretching between two subregions on different asymptotic boundaries of the wormhole grows linearly in $t$ in the limit $t \to \infty$ [58]. Another meaning of size is determined by the volume of a maximal time slice asymptoting to constant time slices at equal time $t$ on both asymptotic boundaries [52] (see figure 2.7). This quantity likewise grows linear in time for large $t$ [52]. Further examples of observables that probe this kind of linear growth are given by the gravitational action on a Wheeler-de Witt patch[46] [53] or the general class of gravity observables recently investigated in [135].

In classical general relativity, all of the observables mentioned above exhibit a growth that continues for an infinite amount of time. However, when taking into account quantum effects the

[46]The Wheeler-de Witt patch is the spacetime region formed by the union of all spacelike slices in the bulk asymptoting to a fixed boundary time $t$ (see figure 2.7). Thus, by causality it is the region in which the CFT state at time $t$ is encoded.

growth stops after a finite amount of time. From the fact that the quantum system introduced above obeys the Poincaré recurrence theorem[47], it is clear that the growth cannot continue indefinitely. More precisely, from general arguments the description of quantum gravity by a classical spacetime is expected to become unreliable at a time that is exponential in the system size, i.e. in the case at hand the thermal entropy of the black hole. Therefore, once quantum effects are taken into account, the above observables (volume of a maximal codimension-one slice, geodesic distance, etc.) are expected to grow at most for a time that is exponential in the black hole entropy [59].[48] For times in between the thermalization time and the time scale at which the classical geometric description breaks down, the classical geometry is expected to still be a good approximation and hence a linear growth in time is expected [59]. More precisely, the maximal volume of a codimension-one hypersurface and the gravitational action on the WdW patch both grow in time proportional to the entropy $S$ times the temperature $T$ of the black hole [52, 54]. After the growth stops, the observables are expected to fluctuate close to the maximum value until they decrease again at the recurrence time and the process starts anew (see figure 2.8) [59].

Since ordinary thermodynamic variables reach their equilibrium value long before a time scale exponential in the entropy $S$, the growth of the observables introduced above (which loosely speaking leads to a growth of the behind-the-horizon region in the black hole geometry) must be encoded in subtle properties of the quantum state that evolve for very large time scales after the thermalization time. In particular, because the entanglement entropy dual to the area of a Ryu-Takayanagi surface saturates quickly to a maximum value [58], it cannot explain this time evolution behavior, calling into question the "entanglement builds geometry" idea.

A time evolution continuing for an exponentially long time scale in the system size as explained above closely resembles the time evolution properties of computational complexity, a quantity from computer science which I will now introduce (see e.g. [141] for a comprehensive treatment of this topic). In computer science, computational complexity is motivated by practical considerations. Assume for a moment that you had access to a computer which can perform a number of operations on its input state to perform a desired computation, the result of which is that the system finds itself in a particular target state. Then, the computational complexity between the reference and target state is defined to be the minimum number of operations necessary to perform the calculation. For a quantum computer, the operations are implemented by a fixed set of unitary operators (termed elementary gates) and the state of the computer is simply implemented by a Hilbert space element $|\psi\rangle$.[49]

For most quantum computers acting on $K$ qubits, starting from an unentangled reference state $|0\rangle^{\otimes K}$ almost all states are maximally complex[50] and the maximum complexity scales exponentially

[47] This theorem states that a non-integrable quantum system with finite density of states evolves almost periodically in the sense that the system periodically returns arbitrarily close to its starting point [136]. The average recurrence time for this process scales doubly exponential with the system size [137–139].

[48] The argument of [59] is based on the fact that the number of orthogonal vectors in the Hilbert space of the system is bounded by $e^S$ and that the time-scale for the system to reach a state orthogonal to $|\psi(t)\rangle$ is given by the Anandan-Ahanronov time [140] inversely proportional to the uncertainty in energy $\Delta E = \sqrt{\langle\psi(t)|H^2|\psi(t)\rangle - \langle\psi(t)|H|\psi(t)\rangle^2}$. For black holes, $\Delta E$ is proportional to the Planck time [59]. Therefore, after $e^S$ time steps, the system has exhausted the set of mutually orthogonal states and the state becomes a superposition of the states at earlier times.

[49] Oftentimes, the target state can only be reached exactly by applying an infinite number of gates. In this case, the computational complexity is usually defined as the minimum number of gates necessary to reach the target state up to to a small error, that is the norm of the state at the end of the evolution minus the target state is smaller than some number $\epsilon$ [142]. The tolerance $\epsilon$ then becomes part of the definition of computational complexity. In this thesis, I will use complexity definitions that are not based on a counting of discrete gates and for which the tolerance is not part of the definition.

[50] To be precise, the complexity scales exponentially in $K$ for all states except for a small fraction defined w.r.t. an appropriate measure that goes to zero as $K \to \infty$. For instance, in ref. [143] which considered a set of states

with $K$ [143–145]. Since each computation step takes a fixed amount of time, the quantum computer needs a time $\sim e^K$ to reach almost all target states.[51] This time scale is much larger than the thermalization time of a quantum system where it reaches maximum entropy, which scales polynomially with $K$ according to the assumptions on the quantum circuit reviewed above. Moreover, the number of gates applied at each time step in the quantum circuit scales with $S \sim K$ due to the $k$-local and all-to-all Hamiltonian. The circuit time is identified with the Rindler time $\tau$, related to the time coordinate $t$ at the asymptotic boundary by $\tau = 2\pi t T$. Therefore, it is proposed in [51] that the computational complexity increases linearly proportional to $TS$ up to a time scale exponential in $S$.

Comparing the time evolution behavior of the two quantities introduced above – the size of an AdS wormhole and the computational complexity of its dual quantum state – shows a qualitatively equivalent picture. In both cases, there is a large difference in the time scale between the thermalization time scaling polynomially in the system size and the time at which the respective quantities stop growing scaling exponentially in the system size. This motivated the conjecture made in [51–54] that computational complexity is related to the growth of the size of AdS wormholes (and in particular their behind the horizon region). In precise terms, the conjecture states that a suitable definition of computational complexity in the circuit modeling the black hole introduced above[52] is equal to a) the volume of an extremal codimension-one slice through a two-sided black hole asymptoting to a constant time on the asymptotic boundaries ("complexity=volume" conjecture) or b) the gravitational action on the Wheeler de-Witt patch of the two-sided black hole geometry ("complexity=action" conjecture). Due to this conjecture, the gravity observables are often termed *holographic complexity measures*. Because the circuit model of the black hole described above must be embedded in the boundary CFT, the computational complexity in the circuit must have a CFT counterpart. The complexity conjecture then states in a more general sense that the time evolution of gravitational observables probing the wormhole growth (such as the volume of an extremal slice or the action on the WdW patch) can be reproduced from a computational complexity definition in the boundary CFT but not from the entanglement structure of the CFT state [133].[53]

The statements above are made in the unperturbed two-sided black hole geometry where according to the arguments of [129] there is no firewall. What happens if the geometry is perturbed in order to create a high-energy shock wave behind the horizon, i.e. a firewall is created according to the arguments of [129]? On the boundary, this perturbation is implemented by applying a so-called precursor operator [151], which *in the Schrödinger picture* is given by

$$W(t) = U(t) W U^\dagger(t), \tag{2.91}$$

generated by unitaries from $SU(2^K)$, it was found for a number of distinct complexity measures that at most a double exponentially (in $K$) small fraction of points in $SU(2^K)$ had complexity smaller than some fixed value independent of $K$. The details depend on the complexity measure in question which in [143] is defined through a norm on $SU(2^K)$. The doubly exponentially small fraction considered is defined w.r.t. the Lebesgue measure on $SU(2^K)$.

[51] This statement can be put on a more rigorous footing in local random quantum circuits [146, 147] where progress has been made towards a proof in [148–150]. See also [125] for theorems relating the conjectured linear growth of complexity with mathematical results on the inclusion of different complexity classes with each other.

[52] That is a circuit composed out of gates that are all-to-all and $k$-local (for some small number $k$) acting on a number of qubits of the same order of magnitude as the black hole entropy $S$ [59]. The exact decomposition of the gate set and the number of qubits is not fixed by the conjecture.

[53] Note that [133] considers only entanglement between spatial subregions, where the claim that the corresponding entanglement entropy can only probe the wormhole growth for a short time indeed holds [58]. In chapter 3, I will investigate entanglement between not purely spatially organized degrees of freedom for which this claim does not seem to hold.

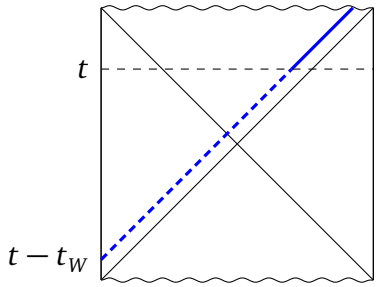


Figure 2.9.: The insertion of a precursor operator $W(t_W)$ at time $t$ simulates the insertion of the operator $W$ at time $t - t_W$. In the bulk, the operator $W$ creates a small localized excitation falling into the wormhole which after being blueshifted creates a shockwave behind the horizon drawn in blue. Note that there is no violation of causality here. Because the boundary CFT is dual to the bulk theory and thus contains full information about the entire state of the bulk theory, changing the state of the boundary CFT by applying the precursor $W(t_W)$ can change the metric arbitrarily deep into the bulk.

where $U(t)$ is the unitary time-evolution operator. The precursor operator simulates the effect of applying the operator $W$ at an earlier or later time: application of $W(t_W)$ onto a state at time $t$ leaves the system in the same state as if $W$ had been applied at time $t - t_W$ followed by ordinary time evolution until time $t$. Now, choose $W$ such that it creates a massless infalling excitation in one of the exterior regions of a two-sided black hole. Applying $W(t_W)$ for large $t_W$ simulates the effect of a small perturbation falling into the black hole at a very early time which is then blueshifted and appears to an infalling observer as a high-energy null shock wave behind the horizon on the right hand side of the Penrose diagram (see figure 2.9) [152]. Remarkably, the effect of the insertion of one or multiple precursors on the computational complexity and its conjectured holographic dual is the same. Identifying $W$ with an operator acting on a single qubit in the quantum circuit model, one finds that the computational complexity of $W(t_W)|\psi\rangle_{\text{TFD}}$ grows linearly in $t_W$ after a characteristic time delay for the scrambling time [52]. This time delay is reproduced in the bulk where the insertion leads to an ingoing null shock wave that increases for instance the volume of maximal slices stretching between two asymptotic boundaries of a wormhole [52, 152–157]. This striking agreement between the computational complexity and its proposed holographically dual realization lends further support for the conjecture of [51–54]. The characteristic time delay due to the insertion of a precursor has been called the switchback effect [52, 158].

Further support for the conjecture relating computational complexity and the gravity observables from figure 2.7 introduced above is obtained from the following observations. Firstly, computational complexity measures and holographic duals thereof have been studied in tensor networks which provide a discretized version of AdS/CFT and similar features as in the continuous setting have been found [52]. Moreover, the conjectured holographic duals to computational complexity obey and in many cases saturate universal bounds on the maximal rate of computation established in [159].[54]

Coming back to firewalls, the following conclusions can be drawn from the above arguments. Recall the following two statements made above. First, the computational complexity of almost all states is exponentially large in the system size [143–145] and second, almost all states have a firewall [130]. It is therefore argued in [59] that the presence of a firewall is related to exponentially large computational complexity of the state of the system. This requires time-evolution

[54]The bound is violated, however, in near-extremal AdS black holes [53]. See also [160] for criticism regarding the applicability of the results of [159] to the black hole system at hand.

for very large time scales or the application a very complex operator on the boundary such as the precursor operator which for large $t_W$ requires the simulating the effect of time-evolution for very long time scales. Black holes in our universe do not evolve for such long time scales and thus should not have firewalls according to [59]: the states which are likely to occur in nature are not the Haar-random states with exponentially large computational complexity.

### 2.3.4. Computational complexity in quantum field theory

In the previous subsection, the motivation for considering computational complexity in the boundary CFT was presented. In this section, I will review some of the previous work on computational complexity in conformal field theories and also quantum field theories in general. This topic has been a very active research field in recent years and hence there are already too many publications in this area to comprehensively summarize in this thesis. Therefore, I will review only those publications on this topic which are the most relevant for the remainder of this thesis and for applications to AdS/CFT in general. A more thorough treatment can be found for instance in the review article [142].

Let me start with some general remarks on the definition of computational complexity in quantum field theory. The task at hand is to quantify the amount of work needed to prepare a certain quantum state. This is commonly done in a setup developed in [143, 161, 162] which I will now describe. While the state preparation on an ordinary quantum computer is typically done using a sequence of discrete gates, in quantum field theory it is reasonable to model the time evolution from target to reference state by a Hamiltonian made up of a continuous set of gates $\mathcal{O}_I$,

$$H(t) = \sum_I Y^I(t)\mathcal{O}_I. \tag{2.92}$$

The time evolution between the reference state $|\psi_R\rangle$ and target state $|\psi_T\rangle$ is implemented by a unitary operator

$$U(t) = \overleftarrow{\mathcal{P}} \exp\left(i\int_0^t dt' H(t')\right) \tag{2.93}$$

such that

$$|\psi_T\rangle = U(t_f)|\psi_R\rangle, \tag{2.94}$$

where $t_f$ is the final time and $\overleftarrow{\mathcal{P}}$ denotes path ordering, i.e. time ordering with respect to the circuit time $t$ (which may be distinct from the physical time). To assign a cost to this circuit which is minimized by the complexity, define a cost functional $\mathcal{F}[U,Y] \equiv \mathcal{F}[U,\{Y^1,Y^2,...\}]$ quantifying how hard it is to apply the Hamiltonian $H = \sum_I Y^I\mathcal{O}_I$. The computational complexity is then defined as

$$\mathcal{C}[|\psi_T\rangle,|\psi_R\rangle] = \min_{\{Y\}} \int_0^{t_f} dt\, \mathcal{F}[U(t),Y(t)] \tag{2.95}$$

where the minimum is taken over all choices of $Y^I(t)$ that respect the condition $|\psi_T\rangle = U(t_f)|\psi_R\rangle$. For a physically sensible complexity definition, the cost function $\mathcal{F}$ should satisfy a number of conditions [143]; namely it should be continuous, positive ($\mathcal{F}[U,Y] \geq 0$), positively homogeneous ($\mathcal{F}[U,\alpha Y] = \alpha\mathcal{F}[U,Y]$ for all $\alpha > 0$) and obey the triangle inequality $\mathcal{F}[U,Y+Y'] \leq \mathcal{F}[U,Y]+\mathcal{F}[U,Y']$. This type of complexity definition – which is motivated by the simpler definition from counting of gates but in general not equivalent to it[55] – is the one which will be used

[55] Note that in many cases, the continuous version of computational complexity described above provides lower bounds on discrete versions [143].

in the rest of this thesis.

The exact form of the cost function $\mathscr{F}[U,Y]$ in the definition (2.95) is a choice to be made depending on the physics of the problem at hand. In the quantum computing setup, the cost function should be large for those $Y^I$ corresponding to gates which are hard to implement on the quantum computer (these gates are said to be penalized) and small otherwise. In the setting of the quantum circuits for black holes described in the previous section, it has been argued that the gates should be $k$-local, that is only involve $k$ qubits at most [59]. Therefore, the cost function in this setup should strongly penalize gates which act on more than $k$ qubits. Moreover, it was argued that the reference state in this setting should be a spatially unentangled state [53, 59].

There is an interesting class of circuits and cost functions for which the problem of determining the complexity is equivalent to finding a geodesic in a certain manifold $\mathscr{M}$ [143, 161, 162]. In this setup, the set of unitaries $U(t)$ forms a manifold[56] and the cost function is a so-called Finsler metric, a generalization of an ordinary Riemannian metric known from differential geometry. This Finsler metric is obtained by demanding that on top of the requirements on $\mathscr{F}[U,Y]$ specified above, $\mathscr{F}[U,Y]$ should be a smooth function, i.e. infinitely many times differentiable.[57] The complexity is then defined as the length of the shortest curve, i.e. the geodesic, between two points on the manifold. Examples of Finsler metric cost functions are given by functionals which I will call "$k$ norm cost functions",

$$\mathscr{F}_{k,\{p\}}[U,Y] = \left(\sum_I p_I |Y_I|^k\right)^{1/k}, \tag{2.96}$$

where $k \geq 1$ and $p_I$ are so-called penalty factors which give a higher cost to certain directions in the tangent space of the manifold of unitaries. The case $k = 2$ with all $p_I = 1$ is the standard Riemannian metric.

These Finsler metrics have been used in a number of works to investigate the computational complexity in free quantum field theories (see e.g. [164–171] for early work in this direction; a more comprehensive list of references may be found in [142]). Focusing on Gaussian states[58], in [164–167] some qualitative agreement between computational complexity definitions in free QFTs with holographic complexity proposals was obtained for suitable cost functions. For example, for free scalars and fermions in arbitrary number of dimensions the computational complexity between an unentangled reference state and the vacuum state was found to scale with the volume of the manifold in which the QFT lives for the cost function (2.96) with $k = 1$ [164, 166, 169]. This volume law divergence comes from building up the entanglement inherent in the vacuum state at all length scales. The same divergence is observed in holographic complexity proposals such as "complexity=volume" or "complexity=action" [172]. Furthermore, the computational complexity between an unentangled reference state and the time-evolved thermofield double state in free bosonic QFT (again for a cost function of the form (2.96) with $k = 1$) was found to also have similarities to holographic complexity proposals in two-sided black hole geometries with regard to the temperature dependence and divergence structure [167]. The time-dependence of computational complexity, one the other hand, does not match in this setting because the computational

[56] For example, this manifold is $U(2^N)$ for a circuit composed out of all possible unitary operators acting on $N$ qubits.

[57] To be precise, a Finsler metric $\mathscr{F}$ is defined as a function depending on a manifold point $U \in \mathscr{M}$ and a point $Y \in T_U\mathscr{M}$ in the tangent space into the positive real numbers such that $\mathscr{F}$ is a smooth function of $U$ and $Y$ for $Y \neq 0$ and such that at fixed $U$, $\mathscr{F}$ is a Minkowski norm on $T_U\mathscr{M}$ [163]. A Minkowski norm $N$ is a smooth function from $R^d$ to the positive real numbers, vanishing only at the origin of $R^d$, positively homogeneous and with strictly positive definite Hessian $H_{ij} = \frac{1}{2}\partial_i\partial_j N$ [163].

[58] The definition of a Gaussian state is that its wave function is a Gaussian function. These states are uniquely specified through their one- and two-point functions.

complexity in the QFT saturates quickly (at a time $t \sim \beta$) to a maximum [167] while holographic complexity proposals continue growing for a much longer time. This behavior is not surprising because holographic CFTs dual to a gravity theory in the semiclassical limit are generally strongly coupled while the QFT in [167] is a free theory.

The investigations reviewed above, while hinting at a duality between the holographic complexity proposals of [51–54] and computational complexity in the CFT, cannot be used to rigorously establish such dualities. To do this, it is in particular necessary to develop methods for the computation of computational complexity in strongly coupled quantum field theories. Moreover, to derive a duality from first-principles, the mapping of quantum circuits in the conformal field theory into their bulk duals (i.e. spacetimes interpolating between reference and target states) has to be developed. Chapter 4 makes progress towards this goal in the restricted setting of two-dimensional conformal field theories with a gate set composed out of Virasoro group transformations.

## 2.4. Geometric actions on coadjoint orbits

In chapter 4, I will make use of concepts from Lie group theory related to coadjoint orbits and geometric actions. Therefore, let me spend some time reviewing these concepts.

### 2.4.1. Coadjoint orbits in general

Let me first start with some definitions following [173, 174]. A Lie group $G$ is a group with a smooth manifold structure. The corresponding Lie algebra $\mathfrak{g}$ is given by elements of tangent space $T_{\mathbb{1}}G$ of the identity on the manifold. Algebra elements $g \in G$ and group elements $X \in \mathfrak{g}$ are related by the exponential map $X \to e^X$. Furthermore, let me introduce the dual space $\mathfrak{g}^*$, the space of linear maps $v : \mathfrak{g} \to \mathbb{R}$. The action of $v \in \mathfrak{g}^*$ on $X \in \mathfrak{g}$ is denoted by angle brackets in the following,

$$v(X) = \langle v, X \rangle. \tag{2.97}$$

The *adjoint action* of the group $G$ on elements of the Lie algebra $\mathfrak{g}$ is defined by[59]

$$\mathrm{Ad}_g(X) = \frac{d}{ds} g^{-1} h(s) g \bigg|_{s=0} \tag{2.98}$$

where $h$ parametrizes a curve in $G$ such that $h(0) = \mathbb{1}$ and $X$ is the tangent vector of $h(0)$. For matrix groups, this is succinctly written as

$$\mathrm{Ad}_g(X) = g^{-1} X g. \tag{2.99}$$

The adjoint action gives rise to a natural action of the group $G$ on elements of the dual space $\mathfrak{g}^*$, the *coadjoint action* $\mathrm{Ad}^*_g$, which is implicitly defined by the relation

$$\langle \mathrm{Ad}^*_g(v), X \rangle = \langle v, \mathrm{Ad}_{g^{-1}}(X) \rangle. \tag{2.100}$$

Due to the exponential map relating Lie group and Lie algebra elements, the coadjoint action also applies to Lie algebra elements $X$: the *coadjoint operator* $\mathrm{ad}^*_X$ is implicitly defined through the

[59] The adjoint action is used to define the perhaps more familiar adjoint representation of the group $G$ where every element group element $g$ is represented by an automorphism $\mathrm{Ad}_g$ of the Lie algebra $\mathfrak{g}$.

relation

$$\langle \mathrm{ad}_X^* v, Y\rangle = \langle v, [X,Y]\rangle. \tag{2.101}$$

Then, a *coadjoint orbit* is defined to be the set of elements of $\mathfrak{g}^*$ which are related by coadjoint transformations,

$$O_{v_0} = \{\mathrm{Ad}_g^*(v_0) \mid g \in G\}, \tag{2.102}$$

where $v_0$ is some fixed element of $\mathfrak{g}^*$. Different choices of $v_0$ define different orbits. The coadjoint orbit is a manifold itself, isomorphic to $G/H_{v_0}$ where $H_{v_0}$ is the stabilizer of the orbit comprised of all group elements that leave $v_0$ invariant under the coadjoint action.

### 2.4.2. The Virasoro group

The main Lie group considered in this thesis is the Virasoro group, the group $\mathrm{Diff}^+(S^1)$ of orientation-preserving diffeomorphisms of the circle together with a central extension. For conformal field theories, the central extension for the Virasoro group is related to the central charge $c$ in the sense that for $c = 0$ the symmetry group of the CFT reduces just to the $\mathrm{Diff}^+(S^1)$ part, i.e. the Virasoro group without the central extension. This subsection explains the structure of this group and its adjoint and coadjoint actions in detail. More complete treatments of the Virasoro group can be found for instance in [173–175].

First, let me explain the diffeomorphism group itself without the central extension. The group $\mathrm{Diff}^+(S^1)$ of orientation-preserving diffeomorphisms of the circle is built up from functions $\sigma \to f(\sigma)$ obeying

$$f(\sigma + 2\pi) = f(\sigma) + 2\pi \quad \text{and} \quad \partial_\sigma f(\sigma) > 0, \tag{2.103}$$

where $\sigma \in [0, 2\pi)$ parametrizes the $S^1$. The identity element is the trivial diffeomorphism $\sigma \to \sigma$. Group multiplication is defined through function composition,

$$(f_1 \circ f_2)(\sigma) = f_1(f_2(\sigma)). \tag{2.104}$$

I will denote inverse diffeomorphisms by capital letters, that is $f(F(\sigma)) = F(f(\sigma)) = \sigma$. The tangent space of the group at the identity defines the Lie algebra. An infinitesimal diffeomorphism close to the identity can be written as

$$f(\sigma) = \sigma + \epsilon X(\sigma) \tag{2.105}$$

for a small parameter $\epsilon$ and a periodic function $X(\sigma)$. Therefore, the Lie algebra of $\mathrm{Diff}^+(S^1)$ is identified with the space of vector fields

$$X(\sigma)\frac{\partial}{\partial\sigma} \tag{2.106}$$

generating infinitesimal diffeomorphisms. To compute the adjoint action $\mathrm{Ad}_f(X)$, let me define a group path $g_s(\sigma) = \sigma + sX(\sigma) + O(s^2)$. Then the adjoint action is given by

$$\begin{aligned}(\mathrm{Ad}_f(X))(\sigma) &= \frac{d}{ds}(F \circ g_s \circ f)(\sigma)\bigg|_{s=0} = \frac{d}{ds}F(g_s(f(\sigma)))\bigg|_{s=0} \\ &= F'(f(\sigma))X(f(\sigma)) = \frac{X(f(\sigma))}{f'(\sigma)}.\end{aligned} \tag{2.107}$$

The adjoint action simply describes the transformation of a vector field under a diffeomorphism,

$$X(\sigma)\frac{\partial}{\partial\sigma} \to X(f)\frac{\partial}{\partial f} = \frac{X(f(\sigma))}{f'(\sigma)}\frac{\partial}{\partial\sigma}. \tag{2.108}$$

From the identification of Lie algebra elements with vector fields, the Lie bracket follows immediately,

$$\left[X(\sigma)\frac{\partial}{\partial\sigma}, Y(\sigma)\frac{\partial}{\partial\sigma}\right] = (X(\sigma)Y'(\sigma) - Y(\sigma)X'(\sigma))\frac{\partial}{\partial\sigma}. \tag{2.109}$$

Expanding the vector fields in terms of Fourier modes defines the generators

$$l_m = e^{im\sigma}\frac{\partial}{\partial\sigma} \quad \text{for} \quad m \in \mathbb{Z} \tag{2.110}$$

from which the well-known Witt algebra emerges

$$i[l_m, l_n] = (m-n)l_{m+n}. \tag{2.111}$$

The dual space to the Lie algebra of $\mathrm{Diff}^+(S^1)$ is given by functions from the space of linear functions into the real numbers. This space may be parametrized by quadratic differentials $v(\sigma)d\sigma^2$ on the circle such that

$$\langle v, X\rangle = \frac{1}{2\pi}\int_0^{2\pi} d\sigma\, v(\sigma)X(\sigma). \tag{2.112}$$

Elements of the dual space must be given by quadratic differentials in order for the bracket $\langle v, X\rangle$ to be invariant under diffeomorphisms $\sigma \to f(\sigma)$ acting on both $v$ and $X$. The coadjoint action is easily obtained from the definition (2.100) and equation (2.107). Demanding equivalence of

$$\langle \mathrm{Ad}_f^*(v), X\rangle = \frac{1}{2\pi}\int_0^{2\pi} d\sigma\, (\mathrm{Ad}_f^*(v))(\sigma)X(\sigma) \tag{2.113}$$

and

$$\langle v, \mathrm{Ad}_F(X)\rangle = \frac{1}{2\pi}\int_0^{2\pi} d\sigma\, v(\sigma)\frac{X(F(\sigma))}{F'(\sigma)} = \frac{1}{2\pi}\int_0^{2\pi} d\sigma\, v(f(\sigma))X(\sigma)(f'(\sigma))^2 \tag{2.114}$$

yields

$$\mathrm{Ad}_f^*(v)(\sigma) = v(f(\sigma))(f'(\sigma))^2. \tag{2.115}$$

Again, this is simply the transformation of a quadratic differential $v(\sigma)d\sigma^2$ under diffeomorphisms.

Having described the $\mathrm{Diff}^+(S^1)$ part of the Virasoro group, let me now spend some time to discuss the central extension. The basic idea of a central extension is as follows [173, 174]. Consider a Lie group $\tilde{G}$ and a representation thereof given by unitary operators $U_g$ acting on a Hilbert space. Due to the $U_g$ forming a representation of $\tilde{G}$, these operators must fulfill $U_gU_h = U_{gh}$ for all $g, h \in \tilde{G}$. Central extensions arise from relaxing this condition and instead allowing $U_gU_h$ and $U_{gh}$ to differ by a phase $C(g,h)$,

$$U_gU_h = e^{iC(g,h)}U_{gh}. \tag{2.116}$$

A representation of $\tilde{G}$ satisfying (2.116) is called a projective representation. These representa-

tions arise from treating Hilbert space elements that differ only by a phase as equivalent physical states. The function $C : \tilde{G} \times \tilde{G} \to \mathbb{R}$ is called the 2-cocycle. It satisfies the cocycle condition

$$C(g_1, g_2) + C(g_1 g_2, g_3) = C(g_1, g_2 g_3) + C(g_2, g_3) \tag{2.117}$$

from associativity as well as the following properties

$$C(g, \mathbb{1}) = C(\mathbb{1}, g) = 0 \quad \text{and} \quad C(g, g^{-1}) = C(g^{-1}, g) \tag{2.118}$$

from demanding that $U_{\mathbb{1}} = \mathbb{1}$. Note that there exist trivial cocycles $C(g,h)$ which can be eliminated by redefining $U_g$. In general, any cocycle of the form

$$C(g,h) = K(gh) - K(g) - K(h) \tag{2.119}$$

fulfills the defining properties (2.117) and (2.118) but can be trivially set to zero be redefining $U_g \to e^{iK(g)} U_g$. Only non-trivial cocycles will be considered in the following.

Using the cocycle $C(g,h)$, a centrally extended group $G = \tilde{G} \otimes \mathbb{R}$ is defined by letting the elements of $G$ be given by pairs $(g, \alpha)$ where $g \in \tilde{G}$ and $\alpha \in \mathbb{R}$ and the group inverse and group multiplication be given by

$$(g, \alpha) \circ (h, \beta) = (g \circ h, \alpha + \beta + C(g,h)) \quad \text{and} \quad (g, \alpha)^{-1} = (g^{-1}, -\alpha - C(g, g^{-1})). \tag{2.120}$$

The projective representation of $\tilde{G}$ specified by $U_g$ and $C(g,h)$ is an exact, non-projective representation of the centrally extended group $G$. For the Virasoro group, the 2-cocycle is given by [176]

$$C(F_1, F_2) = -\frac{1}{48\pi} \int_0^{2\pi} d\sigma \log\left(F_1'(F_2(\sigma))\right) \frac{F_2''(\sigma)}{F_2'(\sigma)}. \tag{2.121}$$

It is easy to see that this satisfies (2.117) and (2.118) (in fact for the Virasoro group $C(F,f) = C(f,F) = 0$).

The central extension also applies to the Virasoro algebra. Similarly to the Virasoro group, the Virasoro algebra is represented by a pair $(X(\sigma)\partial_\sigma, r)$ where $X(\sigma)$ is a periodic function on $S^1$ and $r \in \mathbb{R}$. The Lie bracket, i.e. the commutator, of the Virasoro algebra is given by

$$[(X,r),(Y,s)] = \left((YX' - XY')\partial_\sigma, \int d\sigma XY'''\right). \tag{2.122}$$

Note that the central extension terms $r, s$ do not turn up on the right hand side of equation (2.122) because the central extension commutes with all other algebra elements. Elements of the Virasoro algebra may be expanded in terms of generators

$$L_n = (l_n, 0), \quad Z = (0, 1) \tag{2.123}$$

as $(X(\sigma)\partial_\sigma, r) = \sum_n X_n L_n + rZ$. From equation (2.122), the commutator of the generators is given by

$$i[L_n, L_m] = (n-m)L_{n+m} + \frac{Z}{12} n^3 \delta_{n+m,0}, \quad [Z, Z] = [Z, L_n] = 0. \tag{2.124}$$

Equation (2.124) is the Virasoro algebra in the form known from conformal field theory on the cylinder.[60] This form makes the origin of the Virasoro algebra as a central extension of the Witt

[60] The $L_n$ generators are the Fourier modes of the energy-momentum tensor on the cylinder, related to the coefficients in the Laurent expansion of the energy-momentum tensor on the plane by $L_0 \to L_0 - c/24$. The shift by $-c/24$

algebra clear.

For a centrally extended algebra, the dual space is centrally extended as well. Thus, elements of the dual space are denoted by $(v(\sigma)d\sigma^2, c)$ and the pairing to the elements of the Virasoro algebra is defined as

$$\langle (v,c),(X,r)\rangle = \frac{1}{2\pi}\int_0^{2\pi} d\sigma\, v(\sigma)X(\sigma) + cr. \tag{2.125}$$

Because the central extension terms act trivially, the coadjoint action of a general centrally extended group is given by

$$\mathrm{Ad}^*_{(g,\alpha)}(v,c) = (\widetilde{\mathrm{Ad}}^*_g(v) + c\gamma(g), c) \tag{2.126}$$

where $\gamma(g)$ is called the 1-cocycle. In general, a 1-cocycle valued in some vector space $V$ is associated with a representation $\mathscr{R}$ of $\tilde{G}$ in $V$. It is defined by the property[61]

$$\gamma(gh) = \mathscr{R}(g)\gamma(h) + \gamma(g) \tag{2.127}$$

as well as $\gamma(\mathbb{1}) = 0$. For the Virasoro group, the vector space is the space of quadratic differentials, the representation $\mathscr{R}$ the coadjoint representation $\mathscr{R}(f) = (\partial_\sigma f(\sigma))^2 d\sigma^2$ and the 1-cocycle is given by

$$\gamma(F) = -\frac{1}{24\pi}\{F,\sigma\}d\sigma^2 \tag{2.128}$$

where

$$\{F,\sigma\} = \frac{F'''(\sigma)}{F'(\sigma)} - \frac{3}{2}\left(\frac{F''(\sigma)}{F'(\sigma)}\right)^2 \tag{2.129}$$

is the Schwarzian derivative. The cocycle condition (2.127) is fulfilled due to the composition law

$$\{f_1(f_2(\sigma)),\sigma\} = (\partial_\sigma f_2)^2\{f_1,f_2\} + \{f_2,\sigma\}. \tag{2.130}$$

The coadjoint action written in terms of the inverse diffeomorphism $F(\sigma)$ reads

$$\mathrm{Ad}^*_F(v(\sigma)d\sigma^2, c) = \left(\left(v(F(\sigma))(\partial_\sigma F(\sigma))^2 - \frac{c}{24\pi}\{F,\sigma\}\right)d\sigma^2, c\right). \tag{2.131}$$

The coadjoint operator is accordingly given by

$$\mathrm{ad}^*_{(X\partial_\sigma,r)}(v d\sigma^2, c) = \left(\left(2vX' + Xv' - \frac{c}{24\pi}cX'''\right)d\sigma^2, 0\right), \tag{2.132}$$

obtained from (2.131) by the infinitesimal transformation $F(\sigma) = \sigma + \epsilon X(\sigma)$.

### 2.4.3. Coadjoint orbits of the Virasoro group

It is clear from (2.131) that elements of the dual space transform like holomorphic or anti-holomorphic energy-momentum tensor components $T_{zz}, \bar{T}_{\bar{z}\bar{z}}$ under conformal transformations in a CFT. Thus, the coadjoint orbit $O_{v_0}$ of the Virasoro group can be interpreted as the space of expectation values of the $T_{zz}, \bar{T}_{\bar{z}\bar{z}}$ components generated by applying conformal transformations onto some fixed expectation value determined by $v_0(\sigma) = T_{zz}(\sigma)$ or $v_0(\sigma) = \bar{T}_{\bar{z}\bar{z}}(\sigma)$. Let me now re-

modifies the central term from $(n^3 - n)\delta_{n+m,0}$ to $n^3\delta_{n+m,0}$.

[61] More generally, a $k$-cocycle is a smooth map $C$ onto a vector space $V$ with $k$ arguments such that $(d_k C)(g_1, \ldots g_{k+1}) = \mathscr{R}(g_1)C(g_2, \ldots, g_{k+1}) + (-1)^{k+1}C(g_1, \ldots, g_k) + \sum_{i=1}^k (-1)^i C(g_1, \ldots, g_i g_{i+1}, \ldots, g_{k+1}) = 0$ [174]. Here, $d_k C$ is analogous to an exterior derivative mapping a function with $k$ arguments to one with $k+1$ arguments. For the trivial representation $\mathscr{R}(g) = \mathbb{1}$ and $k = 2$, the 2-cocycle condition (2.117) emerges.

view the classification of the coadjoint orbits of the Virasoro group first determined in [177, 178] (see also [173–175, 179]).[62]

Recall that a coadjoint orbit $O_{v_0}$ in the group $G$ is a quotient of $G$ by the stabilizer $H_{v_0}$ that leaves $v_0$ invariant. To determine this stabilizer, consider an infinitesimal coadjoint transformation generated by $f(\sigma) = \sigma + \epsilon X(\sigma)$. From equation (2.131), this leaves $(v_0(\sigma)d\sigma^2, c)$ invariant if

$$X v_0' + 2X' v_0 - \frac{c}{12} X''' = 0. \tag{2.133}$$

Since this is a third order differential equation, the stabilizer is at most three-dimensional. Consider first coadjoint orbits whose representative $v_0$ is a constant. In this case, (2.133) reduces to

$$X' - \frac{c}{24 v_0} X''' = 0 \tag{2.134}$$

and the general solution is given by

$$X(\sigma) = A + B e^{i\omega\sigma} + C e^{-i\omega\sigma} \tag{2.135}$$

where $\omega^2 = -\frac{24 v_0}{c}$. Periodicity restricts the allowed stabilizer transformations further. For generic values of $v_0$, the coefficients $B$ and $C$ have to vanish. In this case, the only allowed solution is $X(\sigma) = \text{const}$ which generates transformations by $L_0$. The coadjoint orbit for this representative is of the form $(\text{Diff}^+(S^1)/U(1)) \times \mathbb{R}$ where the $U(1)$ group is generated by the $L_0$ generator. On the other hand, if $v_0 = -\frac{n^2 c}{24}$ for $n \in \mathbb{N}$, (2.135) is valid for generic $B = C^*$. In this case, the stabilizer generates transformations by $L_0, L_{\pm n}$ forming the $PSL^{(n)}(2,\mathbb{R})$ group and the coadjoint orbit is of the form $(\text{Diff}^+(S_1)/PSL^{(n)}(2,\mathbb{R})) \times \mathbb{R}$. These orbits are the only possible coadjoint orbits with constant representatives $v_0$ and in fact the only orbits containing a constant coadjoint vector $v(\sigma) = \widetilde{\text{Ad}}^*_f(v_0)$. Further coadjoint orbits are possible for non-constant representatives. Their classification is more involved than that of the orbits for constant $v_0$ and therefore I will just state the final result (see e.g. [174] for a derivation). Non-constant orbit representatives $v_0$ are given by

$$v_0^{n,\alpha}(\sigma) = \frac{c\alpha^2}{6} + \frac{c}{12}\frac{n^2 + 4\alpha^2}{F_{n,\alpha}(\sigma)} - \frac{c}{8}\frac{n^2}{F_{n,\alpha}(\sigma)^2} \tag{2.136}$$

where $\alpha \in \mathbb{R}_+$, $n \in \mathbb{N}$ and $F_{n,\alpha}(\sigma) = \cos^2(n\sigma/2) + \left(\sin(n\sigma/2) + \frac{2\alpha}{n}\cos(n\sigma/2)\right)^2$ as well as

$$v_0^{n,\pm}(\sigma) = \frac{c}{12}\frac{n^2}{H_{n,\pm}(\sigma)} - \frac{c}{8}\frac{n^2(1 \pm 1/(2\pi))}{H_{n,\pm}(\sigma)^2} \tag{2.137}$$

where again $n \in \mathbb{N}$ and $H_{n,\pm}(\sigma) = 1 \pm \sin^2(n\sigma/2)/(2\pi)$. Orbits with representatives of the types given above exhaust the entire set of coadjoint orbits of the Virasoro group.

Finally, note that not all of the orbits are physically sensible descriptions of the space of expectation values of the energy-momentum tensor components: not in every coadjoint orbits is the energy

$$E[v] = \frac{1}{2\pi}\int_0^{2\pi} d\sigma\, v(\sigma) \tag{2.138}$$

bounded from below. It can be shown that the only orbits with energy bounded from below are the ones with constant representative $v_0 \geq -c/24$ as well the one with representative $v_0^{1,-}(\sigma)$

[62] I will restrict to the physically interesting case $c \neq 0$ in the following. The set of coadjoint orbits of $\text{Diff}^+(S^1)$, the Virasoro group for $c = 0$, is much larger than the one for $c \neq 0$ and can be found for instance in [174].

from (2.137). In a conformal field theory, the orbits with $v_0 = h - c/24 \geq -c/24$ are of course the spaces of energy-momentum tensor expectation values for states in the Verma module of a primary with weight $h$. The stabilizer groups are the familiar groups generated by Virasoro generators for which the primary state $|h\rangle$ is an eigenstate, i.e. the groups generated by $L_0$ for $h > 0$ and $L_0, L_{\pm 1}$ for $h = 0$. The remaining orbit with representative $v_0^{1,-}(\sigma)$ from (2.137), while valid from the group theory viewpoint, does not occur in conformal field theory. Any orbit associated to a Verma module must contain a constant representative because the expectation value of the energy-momentum tensor in a primary state $|h\rangle$ is constant.

### 2.4.4. Geometric actions

Geometric actions are natural action functionals in the classical mechanics sense defined on coadjoint orbits, which I will now introduce. The presentation in this section largely follows [174], see also [180].

The existence of geometric actions follows from the fact that coadjoint orbits are symplectic manifolds: each orbit $O_{v_0}$ admits a $G$ invariant symplectic form[63], the Kirillov-Kostant form. Applied onto two elements $a_X$, $a_Y$ of the tangent space to $v \in O_{v_0}$, the Kirillov-Kostant form reads

$$\omega(a_X, a_Y) = \langle v, [X, Y] \rangle \tag{2.139}$$

where $[X, Y]$ denotes the Lie bracket. A Lie algebra element $X$ is associated to an element $a_X$ of the tangent space of $v \in O_{v_0}$ such that acting with $\mathrm{Ad}^*_{e^X}$ onto $v$ generates translations along the $a_X$ direction along $O_{v_0}$. It is clear from its definition that $\omega$ fulfills the defining properties of a symplectic form. Therefore, coadjoint orbits admit a phase space structure.

The Kirillov-Kostant form $\omega$, a two-form on the orbit $O_{v_0}$, induces a two-form $\omega_G$ on the group $G$ such that mapping group elements into orbit elements using the coadjoint action $g \to Ad^*_g(v)$ maps $\omega_G$ to $\omega$. More explicitly, the two-form $\omega_G$ may be written in terms of the Maurer-Cartan form $\theta$, the (unique) Lie algebra valued[64] one-form that maps elements in the tangent space $T_g G$ of some group element $g$ to elements in the tangent space $T_{\mathbb{1}} G$ of the identity [181]. For matrix groups, the Maurer-Cartan form is simply defined as $\theta = g^{-1} \circ dg$.[65] The embedding $\omega_G$ of the Kirillov-Kostant form is given by

$$\omega_G(X_g, Y_g) = \langle v, [\theta(X_g), \theta(Y_g)] \rangle, \tag{2.140}$$

where $v = \mathrm{Ad}^*_g(v_0)$ and $X_g, Y_g \in T_g G$ while $[\theta(X_g), \theta(Y_g)]$ denotes the Lie bracket. Note that $\omega_G$ is degenerate and therefore there is no symplectic structure on the group $G$, only on coadjoint orbits of the group.

The symplectic structure may be used to define an action functional on the coadjoint orbit. The Kirillov-Kostant form is closed and therefore defines a symplectic potential $\alpha$ such that $\omega = d\alpha$. Then, an action is defined as follows on the coadjoint orbit,

$$I = \int \alpha. \tag{2.141}$$

[63] A symplectic form $\omega$ is a mapping $O_{v_0} \times O_{v_0} \to \mathbb{R}$ that is bilinear in both its arguments, alternating ($\omega(X, X) = 0$) and non-degenerate (if $\omega(X, Y) = 0$ for all $Y$, then $X = 0$).

[64] A Lie algebra valued differential form is a linear mapping from vectors to Lie algebra elements, unlike the more commonly encountered differential forms that map vectors to numbers.

[65] This form is also known as the "left Maurer-Cartan form". One can define similarly a right Maurer-Cartan form which for matrix groups is given by $\theta = dg \circ g^{-1}$.

Equation (2.141) is called "geometric action" or sometimes "coadjoint orbit action".[66] More concretely, the geometric action may be written in terms of a group path $g(t)$ as follows. Since $\omega_G$ is closed, there is a one-form $\alpha_G(X_g) = -\langle v, \theta(X_g)\rangle$ such that $\omega_G = d\alpha_G$. On the path $g(t)$, the Maurer-Cartan reduces to

$$\theta = \theta_{g(t)} dt = \frac{d}{ds}\left(g^{-1}(t)g(s)\right)\Big|_{s=t} dt. \tag{2.142}$$

and therefore the geometric action is written in terms of the path $g(t)$ as

$$I = \int \alpha_G = -\int dt \langle \mathrm{Ad}^*_{g(t)}(v_0), \theta_{g(t)}\rangle = -\int dt \langle v_0, \dot{g}(t)g^{-1}(t)\rangle. \tag{2.143}$$

For centrally extended groups, the Maurer-Cartan form (2.142) is given by

$$\theta = \theta_{(g(t),\beta(t))} dt = (\theta_g, m_\theta) dt = \frac{d}{ds}\left(g^{-1}(t)\circ g(s), -\beta(t) + \beta(s) + C(g^{-1}(t), g(s))\right)\Big|_{s=t} dt. \tag{2.144}$$

Therefore, the geometric action for centrally extended groups reads

$$I = -\int dt \langle (v,c), (\theta_g, m_\theta)\rangle = -\int dt \left(\langle \widetilde{\mathrm{Ad}}^*_g(v_0), \theta_g\rangle + c\langle \gamma(g), \theta_g\rangle + c m_\theta\right). \tag{2.145}$$

Note the presence of the additional terms $c\langle \gamma(g), \theta_g\rangle$ and $c m_\theta$ compared to the geometric action for non-centrally extended groups. For the Virasoro group, the Maurer-Cartan form is given by

$$\theta = (\theta_F, m_\theta) dt = \left(\frac{\dot{F}}{F'}\frac{\partial}{\partial\sigma}, \frac{1}{48\pi}\int_0^{2\pi} d\sigma \frac{\dot{F}}{F'}\left(\frac{F''}{F'}\right)'\right) dt. \tag{2.146}$$

Inserting this into the general form (2.145) yields the geometric action for the Virasoro group,

$$I = \int d\sigma dt \left(-v_0(F)F'\dot{F} + \frac{c}{48\pi}\frac{\dot{F}}{F'}\left(\frac{F'''}{F'} - 2\frac{(F'')^2}{(F')^2}\right)\right). \tag{2.147}$$

Equation (2.147) is also known as the Alekseev-Shatashvili action [182]. Note that the Hamiltonian associated to the geometric action defined by (2.141) vanishes.[67] In general, choosing a Hamiltonian function $H : O_{v_0} \to \mathbb{R}$ on the coadjoint orbit defines a more general type of geometric action,

$$I = \int \alpha - \int dt\, H(t). \tag{2.148}$$

If the term geometric action is used without qualifiers in the following, the form (2.141) with vanishing Hamiltonian is meant.

Finally, let me mention as a side note that there is a quantization procedure for the classical phase space defined by the coadjoint orbit. In this procedure, known as geometric quantization [180, 183], characters of group representations can be evaluated via a path integral over the exponentiated geometric action $\exp(iI)$. This topic has extensive connections to three-dimensional

[66] I will use the term geometric action throughout this thesis to prevent confusion of the geometric action (an action functional in the classical mechanics sense) with coadjoint actions $\mathrm{Ad}^*_g(v)$ (maps from $G \times \mathfrak{g}^*$ to $\mathfrak{g}^*$).

[67] As an example for this, consider $\omega = dq^i \wedge dp^i$ for which the action is given by $I = \int dt\, p_i \dot{q}^i$. The Legendre transformation of the Lagrangian $p_i\dot{q}^i$ obviously vanishes.

gravity, both with negative as well as zero cosmological constant (see e.g. [184–186]). For instance, geometric quantization of Virasoro coadjoint orbits has been used to propose a path integral formulation of pure $AdS_3$ gravity (i.e. gravity without matter fields) [185]. These connections to $AdS_3$ gravity will be explained in more detail in section 4.3.5.

# 3. Generalized entanglement measures

This chapter is dedicated to the study of entanglement between different fields as well as between spatial degrees of freedom in $AdS_3/CFT_2$. The bipartitions of the degrees of freedom chosen in this chapter generalize the purely spatial bipartitions investigated previously in the AdS/CFT context and hence the quantities studied in this chapter are referred to as *generalized entanglement measures*.

I will start in section 3.1 by motivating the proposed generalized entanglement measures from gravity arguments, conjecturing a dual holographic description and providing an intuitive but imprecise description of the bipartition of the degrees of freedom whose entanglement is studied in the following. Section 3.2 then rigorously defines this bipartition as well as the associated entanglement entropy, providing in particular a manifestly gauge invariant definition of the entanglement entropy. Following this, I will explain how to compute this generalized entanglement entropy in section 3.3 for the relevant examples of states dual to conical defect and black hole geometries in the bulk. Actually performing this computation for the states dual to black holes necessitates a diversion from the main theme of this chapter to present monodromy methods for the calculation of conformal blocks in section 3.4. These methods are subsequently applied to the computation of the entanglement entropy for spatial and non-spatial bipartitions in section 3.5 and section 3.6 respectively.

## 3.1. Introduction and motivation

In section 2.2.3, it was found that Ryu-Takayanagi surfaces do not probe the entire bulk geometry of many asymptotically AdS spacetimes, leaving behind so-called entanglement shadows that are not penetrated by any RT surface. The goal of this section is to identify generalizations of RT surfaces in asymptotically $AdS_3$ geometries that probe these entanglement shadows and conjecture dual realizations thereof as generalized entanglement entropies in the boundary field theory.

An important aid in this endeavor is the fact that the Einstein equations in three spacetime dimensions admit only constant curvature solutions whose Riemann tensor is maximally symmetric [187],

$$R_{\mu\nu\rho\sigma} = \Lambda(g_{\mu\rho}g_{\nu\sigma} - g_{\mu\sigma}g_{\nu\rho}) \,, \qquad R_{\mu\nu} = 2\Lambda g_{\mu\nu}. \tag{3.1}$$

Locally the spacetime looks flat ($\Lambda = 0$) or like a de Sitter ($\Lambda > 0$) or anti de Sitter ($\Lambda < 0$) space. Non-trivial spacetimes only differ in their global topology. All three-dimensional spacetimes with asymptotically AdS boundary conditions are obtained as quotients of pure $AdS_3$ by splitting up the pure $AdS_3$ geometry into multiple parts that are identified with with each other (see figure 3.1 for an example). Each of these parts is called a fundamental domain.

Ryu-Takayanagi surfaces in three dimensions are minimal-length geodesics stretching between two points on a constant time slice of the asymptotic boundary. The restriction on the geodesic to have minimal length is the crucial constraint that prevents these RT surfaces from probing the entire bulk geometry. This can be seen as follows. Any bulk geometry in three dimensions is obtained as a quotient of a pure $AdS_3$ covering space. Since the quotient action maps multiple

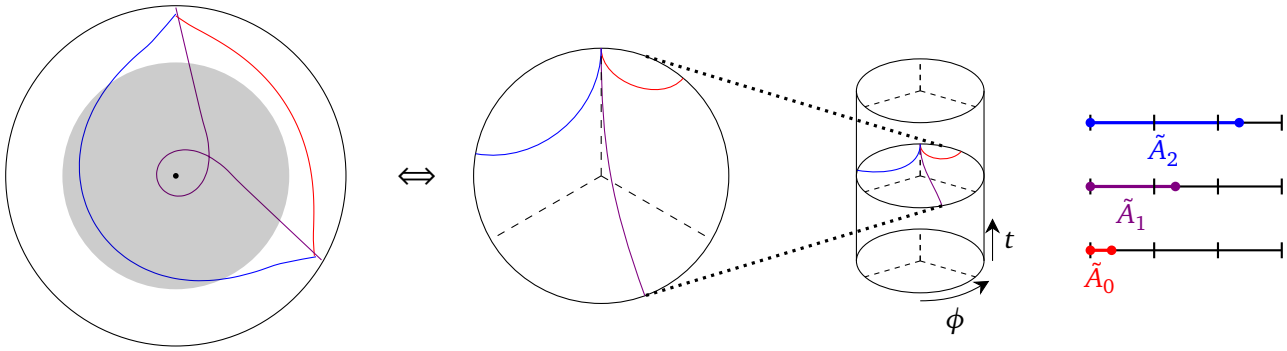


Figure 3.1.: The conical defect geometry is obtained by partitioning pure $AdS_3$ into $n$ wedges (shown here is the case $n = 3$) which are identified with each other. Geodesics on the covering $AdS_3$ space descend to geodesics on the conical defect under the identification. The endpoints of the geodesic shown in red span a boundary interval $\tilde{A}_0$ that is smaller than half of the boundary of a fundamental domain. Therefore, this geodesic descends to a geodesic with winding number $w = 0$ in the conical defect. Ryu-Takayanagi surfaces, that is geodesics with winding number zero, do not penetrate the entanglement shadow indicated in gray. However, the remaining geodesics with winding number $w > 0$ shown in blue and purple probe the entire constant time slice of the conical defect.

points on the covering space to a single point on the quotient geometry, in general there are multiple geodesics stretching between two points on the boundary of an asymptotically $AdS_3$ spacetime. Because all points of the bulk covering space can be reached by boundary anchored geodesics and geodesics on the covering space descend to geodesics on the quotient geometry, any entanglement shadow in the quotient geometry disappears upon including geodesics with non-minimal length. These non-minimal geodesics differ in their topology from RT surfaces. The set of non-minimal geodesics includes for instance geodesics that wind a non-zero number of times around a black hole horizon or naked singularity.

Therefore, it is natural to identify geodesics with non-zero winding numbers as the candidates for the bulk dual to the generalized entanglement entropy that is studied in this chapter. Then, assuming that this identification holds, what is bipartition of the field theory degrees of freedom underlying this entanglement entropy?

It is instructive to start with a simple example: conical defects in $AdS_3$, that is asymptotically $AdS_3$ spacetimes with a naked conical singularity in the middle. In this case, the quotient group is $\mathbb{Z}_n$ and there are $n$ geodesics attached to every boundary interval $A$ (see figure 3.1). Generalized entanglement entropy dual to non-minimal geodesics has been studied in this system in [46, 188–190] under the name of *entwinement*. Entwinement was defined in [46] to be $n$ times the entanglement entropy of a boundary interval $\tilde{A}_w$ on the covering space. $\tilde{A}_w$ is given by the union of $w$ fundamental domains and an interval $A$ contained in a single fundamental domain (see figure 3.1),

$$E_{A,w} = -n\mathrm{Tr}(\rho_{\tilde{A}_w} \log \rho_{\tilde{A}_w}). \tag{3.2}$$

With this definition, $E_{A,w}$ times $4G_N$ is equal to the length of a geodesic with winding number $w$ in the conical defect. While the degrees of freedom in consideration are localized in $\tilde{A}_w$ on the covering space, they are not localized in a single subregion in the quotient space. Thus, it is clear that entwinement measures entanglement between different fields as well as between spatial degrees of freedom [46].

To be more specific, the subset of degrees of freedom underlying the entwinement definition

can be specified as follows. Let $X^i$, $i = 1, ..., n$ stand collectively for the set of fields living on the $i$-th fundamental domain in the covering space. Equivalently, one may split up the set of fields of the CFT on the boundary of the conical defect into $n$ groups $X^1$,...,$X^n$.[1] The subset of degrees of freedom then consists of $w$ groups $X^1, ..., X^w$ on the entire boundary together with one group $X^{w+1}$ in the subregion $A$. The CFT state dual to the conical defect is a state from the twisted sector of a $\mathbb{Z}_n$ orbifold introduced in section 2.1.4.[2] Therefore, the fields $X^i(\phi)$ [3] obey twisted boundary conditions, $X^i(\phi + 2\pi) = X^{(i+1) \bmod n}(\phi)$ where $\phi \in [0, 2\pi]$ is the spatial coordinate on the boundary of the conical defect. As will become clear in the following, resolving the contribution to the entanglement entropy of Hilbert space sectors with different twisted boundary conditions is necessary to find a dual to the length of geodesics with non-zero winding numbers.

Of course, more general bipartitions of the degrees of freedom may be chosen to define further generalized entanglement measures than those obtained from the entwinement definition above. The most general bipartition comes from a subsystem consisting of the degrees of freedom of each field $X^i$ in a separate subregion $A_i$. The entanglement entropy for this bipartition will be denoted as $S_{\{A_i\}}$. This generalization encompasses both the ordinary entanglement entropy as well as the entwinement from [46, 188–190]. In the following, I will drop the name entwinement and refer to the entanglement measures studied in the following as "generalized entanglement measures". If the particular configuration of subregions $A_i$ corresponding to entwinement is considered, I will note such in the text.

Another asymptotically $AdS_3$ geometry I will consider for the study of the generalized entanglement entropy is the BTZ black hole. Again, there is an entanglement shadow which no Ryu-Takayanagi surface penetrates (see figure 2.5). In the one-sided black hole case, the entanglement shadow is a disk-shaped region that includes the black hole interior and extends to a finite distance above the horizon. For the maximally extended two-sided black hole geometry, the entanglement shadow includes a large part of the black and white hole interiors. Thus, RT surfaces can only probe the spacetime up to a finite distance from the black hole horizon in the one-sided black hole geometry case respectively the singularity in the two-sided wormhole geometry. However, geodesics that wind a non-zero amount of times around the black hole horizon probe the entire bulk geometry. In section 3.2, I will define a generalized entanglement entropy whose dual is given by the length of such winding geodesics. Let me give a brief overview here how this definition works and where it differs from the one for the conical defect.

In general in AdS/CFT, black holes are described in the field theory by thermal states for the one-sided black hole respectively the thermofield double state for two-sided black hole. These states are mixtures and superpositions of states with all possible different boundary conditions, in particular including all twisted sectors of the boundary CFT. The generalized entanglement entropy studied in this thesis for states dual to black holes uses two new ingredients compared to the ordinary entanglement entropy for a spatial subregion. As before, I will consider entanglement between different fields as well as between spatial degrees of freedom. In addition, I will also

[1] This splitting is well-defined due to the structure of the boundary CFT, see section 3.2 for details.

[2] The bottom-up field theory model of the conical defect as a state in the twisted sector of an otherwise unspecified orbifold theory described above is believed to be the correct description of a conical defect in $AdS_3/CFT_2$ in general. For example, the conical defect is implemented in the top-down D1/D5 system construction from section 2.1.3 by the ground state of the $(n)^{N/n}$ twisted sector in the $S_N$ orbifold CFT [191–193]. The ground state breaks the $S_N$ gauge group down to $(\mathbb{Z}_n)^{N/n}/S_{N/n}$ and therefore a $\mathbb{Z}_n$ symmetry emerges as part of the gauge group. The groups of fields $X^i$ contain the bosonic fields $x_a^{kn+i}$ of the $S_N$ orbifold theory as well as the fermionic ones $\psi_a^{kn+i}$ for $k \in \mathbb{N}$. If $n$ is not a divisor of $N$, there may be additional twist cycles than the ones in $(n)^{N/n}$, however in the large $N$ limit at fixed $n$ these additional cycles only lead to subleading corrections to observables in the $N$ expansion.

[3] To be precise, $X^i(\phi)$ here stands for the eigenvalue of the field operator $\hat{X}^i(\phi)$ when applied onto the state dual to the conical defect.

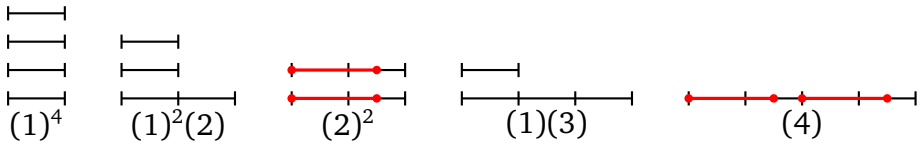


Figure 3.2.: Illustration of the subset of degrees of freedom marked in red underlying the generalized entanglement entropy definition for thermal states dual to a geodesic length in the BTZ black hole geometry. The figure illustrates an example with $N = 4$ fields in total and choice of parameters $m = 2$, $w = 1$ and $A = [0, \pi)$. Fields connected by twisted boundary conditions are drawn as adjacent intervals. The subset in consideration distinguishes between twisted sectors. None of the degrees of freedom of sectors with cycles that are not a multiple of $m = 2$ (i.e. the $(1)^4, (1)^2(2)$ and $(1)(3)$ sectors) are contained in the subset. For the remaining sectors, the subset consists of a single field $X^i$ in the full space $[0, 2\pi]$ (due to $w = 1$) together with a field $X^j$ in $A$, where $X^j$ is connected to $X^i$ by the boundary conditions, $X^i(\phi + 2\pi) = X^j(\phi)$.

restrict to a subset of the twisted sectors of the boundary CFT. These two ingredients are specified by a choice of subregions $A_i$ for the fields $X^i$ and a choice of twisted sectors defined by a set of conjugacy classes $C_k$ of the (permutation) gauge group of the boundary CFT.

There is considerable freedom in the choice of these two ingredients which leads to a large number of possible generalized entanglement entropy definitions. In this thesis, I will concentrate on the $S_N$ orbifold theory of the D1/D5 system introduced in section 2.1.4 as a particular example of a top-down AdS/CFT construction in which the field content and in particular the structure of the twisted sectors is explicitly known. For this system, in order to find a generalized entanglement entropy which is equal to the length of a winding geodesic in the BTZ black hole geometry the ingredients are chosen as follows. First, restrict to twisted sectors containing only cycles whose length is a multiple of some fixed integer $m$, that is conjugacy classes $(m)^{n_m}(2m)^{n_{2m}}(3m)^{n_{3m}}\ldots$ in the notation from section 2.1.4. Then, consider the degrees of freedom of $w < m$ fields in the full space ($\phi \in [0, 2\pi]$) together with the degrees of freedom of a single field in a subregion ($\phi \in A$). Moreover, choose these degrees of freedom such that all of the $w + 1$ fields whose degrees of freedom comprise the subset considered are continuously connected by the twisted boundary conditions. See figure 3.2 for an illustration of this bipartition. The parameter $w$ will again be identified with the winding number of the dual geodesic while $m$ parametrizes the size of the subset in consideration: as $m$ becomes smaller, the generalized entanglement entropy probes a smaller subset of the Hilbert space. While the restriction to a subset of the twisted sectors may seem somewhat ad-hoc at the moment, it will naturally emerge when considering the measurements that an observer could do if he had only access to the subset of degrees of freedom described above.

Note that the specification of the subset of degrees of freedom made so far is somewhat imprecise because it ignores the gauge invariance of the problem at hand. The $\mathbb{Z}_n$ orbifold for the state dual to the conical defect as well as the $S_N$ orbifold theory of the D1/D5 system both contain permutation gauge groups. Because these gauge groups identify groups of fields with each other, strictly speaking it is not correct to state that a subset of the degrees of freedom belongs to a particular field. Consequently, the textbook definition (2.69) of the entanglement is not applicable in this setting, as was already pointed out for the conical defect case in [46]. In the subsequent section 3.2, I will show how to circumvent this issue and present a definition of the generalized entanglement entropy that is manifestly gauge invariant and reduces to the textbook definition (2.69) if the gauge invariance plays no role.

## 3.2. Definition of generalized entanglement entropy

In this section, I will show how to rigorously define the generalized entanglement entropy which was introduced using informal arguments in the previous section. The basic difficulty for finding such a rigorous definition is that the textbook definition of entanglement entropy as the von Neumann entropy of reduced density matrices is not applicable for orbifold conformal field theories. The reason for this is that the Hilbert space does not factorize into tensor factors,

$$\mathscr{H} \neq \mathscr{H}_A \otimes \mathscr{H}_B. \tag{3.3}$$

In the following, I will present a manifestly gauge invariant definition of the entanglement entropy for theories with discrete gauge symmetries such as the orbifold conformal field theories introduced in section 2.1.4. The construction generalizes previously known constructions based on algebraic methods [194] and of course also the textbook definition of the entanglement entropy as the von Neumann entropy of a reduced density matrix. Similar work in on entanglement entropy for non-factorizing Hilbert spaces can be found for example in [195, 196] whose connections to the work presented here will be explained in detail below.

### 3.2.1. Hilbert space structure of orbifold conformal field theories

To start out, let me summarize the Hilbert space structure of orbifold CFTs and explain why this structure does not allow for tensor factorizations. This non-factorization property affects both spatial and non-spatial bipartitions of the degrees of freedom. Let me first consider the simplest case of a $\mathbb{Z}_2$ permutation orbifold and a spatial bipartition. The Hilbert space of this theory is given by a direct sum of the Hilbert spaces of the two twisted sectors,

$$\mathscr{H} = \mathscr{H}_{g_1} \oplus \mathscr{H}_{g_2}, \tag{3.4}$$

where $g_1 = \mathbb{1}$ and $g_2$ denotes the non-identity permutation of the $\mathbb{Z}_2$ group. I will use field eigenstates $|X^1, X^2\rangle_g$ to define an (overcomplete) basis for the Hilbert spaces that will be introduced in the following. These field eigenstates are defined such that

$$\hat{X}^i(\phi)|X^1,X^2\rangle_g = X^i(\phi)|X^1,X^2\rangle_g \quad \text{for } i = 1,2 \quad \text{and} \quad X^i(\phi + 2\pi) = X^{g(i)}(\phi), \tag{3.5}$$

where field operators $\hat{X}^i(\phi)$ and their corresponding eigenvalues $X^i(\phi)$ have been distinguished by the presence of a hat to make the difference between these two objects clear.[4] The Hilbert spaces $\mathscr{H}_{g_1}, \mathscr{H}_{g_2}$ are spanned by symmetric superpositions of these field eigenstates[5],

$$\mathscr{H}_g \equiv \mathscr{H}_g^+ = \{\ |X^1,X^2\rangle_g + |X^2,X^1\rangle_g\ \} = \{\ P_+|X^1,X^2\rangle_g\ \}, \tag{3.6}$$

where the projector $P_+$ is defined by $P_+ = (g_1 + g_2)/2$. Antisymmetric superpositions, on the other hand, span a Hilbert space of unphysical states denoted by $\mathscr{H}_g^-$,

$$\mathscr{H}_g^- = \{\ |X^1,X^2\rangle_g - |X^2,X^1\rangle_g\ \} = \{\ P_-|X^1,X^2\rangle_g\ \}, \tag{3.7}$$

where $P_- = (g_1 - g_2)/2$ is the orthogonal projector to $P_+$, i.e. $P_+P_- = 0$. Now, let me pick out one of the twisted sectors and drop the subscript $g$ for the moment. Consider a subregion $A$, its

[4] If the difference between these two objects is clear from context, I will drop the hat from the notation.

[5] To keep the notation simple, I am not including normalization factors for the states as was already done in section 2.1.4.

complement $B$ and the Hilbert space of (anti)symmetrized states in these subregions

$$\mathscr{H}_A^{\pm} = \left\{ |X_A^1, X_A^2\rangle \pm |X_A^2, X_A^1\rangle \right\}, \quad \mathscr{H}_B^{\pm} = \left\{ |X_B^1, X_B^2\rangle \pm |X_B^2, X_B^1\rangle \right\}. \tag{3.8}$$

Tensoring a state of $\mathscr{H}_A^+$ with a state of $\mathscr{H}_B^+$ gives[6]

$$(|X_A^1, X_A^2\rangle + |X_A^2, X_A^1\rangle) \otimes (|X_B^{1'}, X_B^{2'}\rangle + |X_B^{2'}, X_B^{1'}\rangle) = P_+(|X_A^1 X_B^{1'}, X_A^2 X_B^{2'}\rangle + |X_A^1 X_B^{2'}, X_A^2 X_B^{1'}\rangle) \tag{3.9}$$

which is manifestly in $\mathscr{H}^+$. But tensoring a state of $\mathscr{H}_A^-$ with one of $\mathscr{H}_B^-$ also gives a state of $\mathscr{H}^+$,

$$(|X_A^1, X_A^2\rangle - |X_A^2, X_A^1\rangle) \otimes (|X_B^{1'}, X_B^{2'}\rangle - |X_B^{2'}, X_B^{1'}\rangle) = P_+(|X_A^1 X_B^{1'}, X_A^2 X_B^{2'}\rangle - |X_A^1 X_B^{2'}, X_A^2 X_B^{1'}\rangle). \tag{3.10}$$

From the explicit form of the r.h.s. of (3.9), (3.10), it is obvious that pairs of these states span all of $\mathscr{H}^+$ and hence $\mathscr{H}^+$ is given as a direct sum

$$\mathscr{H}^+ = (\mathscr{H}_A^+ \otimes \mathscr{H}_B^+) \oplus (\mathscr{H}_A^- \otimes \mathscr{H}_B^-). \tag{3.11}$$

Therefore, the physical Hilbert space $\mathscr{H}^+$ of $\mathbb{Z}_2$ symmetric states decomposes not into tensor factors but only into a direct sum of tensor factors. Reinstating the twisted sectors, one obtains the decomposition

$$\mathscr{H} = \bigoplus_{g\in\mathbb{Z}_2} \mathscr{H}_g = \bigoplus_{g\in\mathbb{Z}_2} \left[ (\mathscr{H}_{A,g}^+ \otimes \mathscr{H}_{B,g}^+) \oplus (\mathscr{H}_{A,g}^- \otimes \mathscr{H}_{B,g}^-) \right]. \tag{3.12}$$

However, including additional unphysical non-gauge invariant states yields a larger Hilbert space that admits a tensor factorization in each twisted sector,

$$\begin{aligned} \tilde{\mathscr{H}} &= \bigoplus_{g\in\mathbb{Z}_2} \left[ (\mathscr{H}_{A,g}^+ \otimes \mathscr{H}_{B,g}^+) \oplus (\mathscr{H}_{A,g}^+ \otimes \mathscr{H}_{B,g}^-) \oplus (\mathscr{H}_{A,g}^- \otimes \mathscr{H}_{B,g}^+) \oplus (\mathscr{H}_{A,g}^- \otimes \mathscr{H}_{B,g}^-) \right] \\ &= \bigoplus_{g\in\mathbb{Z}_2} (\tilde{\mathscr{H}}_{A,g} \otimes \tilde{\mathscr{H}}_{B,g}), \end{aligned} \tag{3.13}$$

where $\tilde{\mathscr{H}}_{A,g} = \mathscr{H}_{A,g}^+ \oplus \mathscr{H}_{A,g}^-$. The additional Hilbert space sectors $\mathscr{H}_{A,g}^+ \otimes \mathscr{H}_{B,g}^-$ and $\mathscr{H}_{A,g}^- \otimes \mathscr{H}_{B,g}^+$ contain only unphysical states that are not gauge invariant as can be shown easily by an analogous calculation to (3.9), (3.10).

The $\mathbb{Z}_n$ case for $n > 2$ is a simple generalization of the above story. Let me define projection operators

$$P_r = \frac{1}{n} \sum_{j=0}^{n-1} e^{2\pi i r j/n} g_j. \tag{3.14}$$

These operators are pairwise orthogonal and square to themselves, $P_r P_s = \delta_{rs} P_r$. The physical Hilbert space decomposes as

$$\mathscr{H} = \bigoplus_{g\in\mathbb{Z}_n} \mathscr{H}_g = \bigoplus_{g\in\mathbb{Z}_n} \bigoplus_{r=0}^{n-1} (\mathscr{H}_{A,g}^r \otimes \mathscr{H}_{B,g}^{n-r}), \tag{3.15}$$

where a Hilbert space with superscript $r$ is obtained by application of the $P_r$ projection operator.[7] This Hilbert space contains eigenstates of $g_j \in \mathbb{Z}_n$ with eigenvalue $e^{-2\pi i r j/n}$. Again, one can intro-

[6] The state $|X_A^1 X_B^{1'}\rangle$ denotes a state with $\hat{X}^1(\phi)$ eigenvalue $X_A^1(\phi)$ for $\phi \in A$ and $X_B^{1'}(\phi)$ for $\phi \in B$.

[7] Strictly speaking there is a separate projection operator for the Hilbert spaces corresponding to the subregions $A$ and $B$ that acts only locally in $A$ or $B$ respectively.

duce an enlarged Hilbert space $\tilde{\mathscr{H}}$ containing unphysical non-gauge invariant states but which factorizes into tensor factors in each twisted sector,

$$\tilde{\mathscr{H}} = \bigoplus_{g\in\mathbb{Z}_n} \bigoplus_{r=0}^{n-1} \bigoplus_{s=0}^{n-1} (\mathscr{H}^r_{A,g} \otimes \mathscr{H}^s_{B,g}) = \bigoplus_{g\in\mathbb{Z}_n} (\tilde{\mathscr{H}}_{A,g} \otimes \tilde{\mathscr{H}}_{B,g}), \tag{3.16}$$

where $\tilde{\mathscr{H}}_{A,g} = \bigoplus_{r=0}^{n-1} \mathscr{H}^r_{A,g}$.

The Hilbert space of $S_N$ orbifold theories is structured similar to the one for $\mathbb{Z}_n$ orbifolds. Recall from section 2.1.4 that the twisted sectors of the $S_N$ orbifold are defined by conjugacy classes $C(h) = \{ g^{-1}hg \mid g \in S_N \}$ of $S_N$ containing $n_m$ cycles of length $m = 1,...,N$. The states in a twisted sector are obtained by symmetrizing over elements of the stabilizer subgroup $N_h$,

$$P_{N_h}|X^1,...,X^N\rangle_h = \frac{1}{|N_h|} \sum_{g\in N_h} g|X^1,...,X^N\rangle_h, \tag{3.17}$$

where $|N_h| = \prod_m m^{n_m} n_m!$ is the cardinality of $N_h$. The action of an $S_N$ element on a state is given by $g|X^1,...,X^N\rangle_h = |X^{g(1)},...,X^{g(N)}\rangle_{g^{-1}hg}$. For $g \in N_h$, conjugation by $g$ leaves $h$ invariant, i.e. $g^{-1}hg = h$. The stabilizer subgroup $N_h \simeq \prod_m (\mathbb{Z}_m)^{n_m} \times S_{n_m}$ decomposes into cyclic permutations inside the cycles of length $m$ and symmetric permutations of the cycles with equal length. Using these permutations from $N_h$, a maximal set of pairwise orthogonal projectors $P_r$ can be formed. The projector $P_0 = P_{N_h}$ implements the symmetrization procedure in (3.17). Acting with the projection operators $P_r$ locally in $A$ and $B$ defines Hilbert space subsectors $\mathscr{H}^r_{A,C(h)}$ and $\mathscr{H}^s_{B,C(h)}$. An enlarged Hilbert space is given by

$$\tilde{\mathscr{H}} = \bigoplus_{C(h)} \bigoplus_{r} \bigoplus_{s} \mathscr{H}^r_{A,C(h)} \otimes \mathscr{H}^s_{B,C(h)} = \bigoplus_{C(h)} \tilde{\mathscr{H}}_{A,C(h)} \otimes \tilde{\mathscr{H}}_{B,C(h)} \tag{3.18}$$

which contains the physical Hilbert space $\mathscr{H}$ formed by states that can be written as $P_0$ applied onto some element of $\tilde{\mathscr{H}}$ as a subspace. While $\tilde{\mathscr{H}}$ factorizes in each twisted sector $C(h)$ into $\tilde{\mathscr{H}}_{A,C(h)} = \bigoplus_r \mathscr{H}^r_{A,C(h)}$ and $\tilde{\mathscr{H}}_{B,C(h)} = \bigoplus_r \mathscr{H}^r_{B,C(h)}$, the physical Hilbert space $\mathscr{H} \subset \tilde{\mathscr{H}}$ does not factorize into tensor products. A decomposition of the physical Hilbert space $\mathscr{H}$ into a direct sum of tensor factors can be derived from a similar argument as the one leading to the decomposition (3.15) for the $\mathbb{Z}_n$ orbifold. Concretely, one has to look for combinations of projectors acting locally in $A$ and $B$ that taken together can be written as $P_0$ acting on $A \cup B$ times a projector acting only locally in either $A$ or $B$. This yields for instance, for $N = 3$

$$\mathscr{H} = \left( \bigoplus_{r=0}^{2} \mathscr{H}^r_{A,(3)} \otimes \mathscr{H}^{3-r}_{B,(3)} \right) \otimes \left( \bigoplus_{r=0}^{1} \mathscr{H}^r_{A,(1)(2)} \otimes \mathscr{H}^r_{B,(1)(2)} \right) \otimes \left( \bigoplus_{r=0}^{1} \mathscr{H}^r_{A,(1)^3} \otimes \mathscr{H}^r_{B,(1)^3} \right). \tag{3.19}$$

The projectors defining the Hilbert space factors in (3.19) are given by (3.14) with $n = 3$ and $n = 2$ for the (3) and (1)(2) twisted sectors respectively, while the two projectors in the untwisted sector denoted by $(1)^3$ are given by $P_0 = \frac{1}{3!}\sum_{g\in S_3} g$ and $P_1 = \frac{1}{3!}\sum_{g\in S_3} \mathrm{sgn}(g) g$.

For non-spatial bipartitions, i.e. bipartitions where the subsystem consists of the degrees of freedom in a different subregion $A_i$ for each field $X^i$, the Hilbert space is even less structured than for spatial bipartitions. While in the latter case, the physical Hilbert space decomposes into a direct sum of tensor factors from equation (3.15) and (3.19), this no longer holds for non-spatial bipartitions. Consider again the enlarged Hilbert space $\tilde{\mathscr{H}}$. It is obvious that this Hilbert space factorizes into tensor factors

$$\tilde{\mathscr{H}} = \tilde{\mathscr{H}}_{\{A_i\}} \otimes \tilde{\mathscr{H}}_{\{B_i\}} \tag{3.20}$$

associated to the subsystem and its complement, for instance for $\mathbb{Z}_n$

$$\tilde{\mathscr{H}}_{\{A_i\}} = \bigotimes_{i=1}^{n} \tilde{\mathscr{H}}_{A_i} \ , \quad \tilde{\mathscr{H}}_{\{B_i\}} = \bigotimes_{i=1}^{n} \tilde{\mathscr{H}}_{B_i} . \tag{3.21}$$

$\tilde{\mathscr{H}}_{\{A_i\}}$ may be decomposed into field eigenstates $|X^1_{A_1}, ..., X^n_{A_n}\rangle$. However, it is not possible to form symmetrized or antisymmetrized combinations of these field eigenstates as was done previously because the $A_i$ intervals differ from one another. Therefore, one cannot combine the field eigenstates of the subsystem and those of the complement in the same way as before to form a gauge-invariant state of the full system. When restricting to gauge invariant states one has to dispense altogether with the notion of a Hilbert space factorization, even only for a factorization of some term in a direct sum. Therefore, another method to identify a subset of the degrees of freedom that is not based on a factorizing Hilbert space is needed. The development of such a method is the subject of the following subsection.

### 3.2.2. $\mathbb{Z}_n$ orbifolds

I will now explain how the entanglement entropy is defined for the $\mathbb{Z}_n$ orbifold theory.

#### Ordinary entanglement entropy

Let me start with the ordinary entanglement entropy of a spatial subregion $A$. For spatial bipartitions, there are two options to deal with the non-factorization of the Hilbert space described above[8]:

1. Embedding the density matrix into the larger Hilbert space $\tilde{\mathscr{H}}$ containing unphysical states and taking a partial trace in $\tilde{\mathscr{H}}$.
   This method will be called the "embedding approach" in the following. It is applicable if the state is not composed out of a superposition of states in different twisted sectors. This holds in particular for the states of interest dual to conical defects in the bulk. Because I will work entirely in a single twisted sector, I will drop again the $g$ subscripts of the Hilbert spaces, i.e. in the following $\mathscr{H} \equiv \mathscr{H}_g$ and $\tilde{\mathscr{H}} \equiv \tilde{\mathscr{H}}_g$ for some fixed $g \in \mathbb{Z}_n$. Formally, the embedding of $\rho \in \mathscr{H}$ is implemented by $\tilde{\rho} = \rho \oplus 0 \in \tilde{\mathscr{H}}$. Then, due to $\tilde{\mathscr{H}}$ factorizing into tensor factors, a reduced density matrix can be defined by the usual partial trace formula,

   $$\tilde{\rho}_A = \mathrm{Tr}_{\tilde{\mathscr{H}}_B}(\tilde{\rho}) \in \tilde{\mathscr{H}}_A. \tag{3.22}$$

   The entanglement entropy is defined as the von Neumann entropy of this reduced density matrix,

   $$S_A = -\mathrm{Tr}_{\tilde{\mathscr{H}}_A}(\tilde{\rho}_A \log \tilde{\rho}_A). \tag{3.23}$$

   While this procedure works very well for explicit calculations, the problem with it is that to implement it, one has to use non-gauge invariant states throughout. Thus, it is not clear

[8] Note that some of the formulas shown below are only valid for finite dimensional Hilbert spaces. Although the Hilbert space of a QFT is of course infinite, this is not a problem for the calculation of the entanglement entropy because the entanglement entropy for all finite energy states in quantum field theories is infinite anyway due to entanglement between modes at all energy scales. Therefore a regularization procedure is needed to define the entanglement entropy in any case and in the following I will implicitly take the QFTs in consideration to be regularized to a quantum system on a finite dimensional Hilbert space.

how an observer – that of course has access only to gauge invariant states and operators – would measure the entanglement entropy defined in this way.[9]

2. Modeling the subsystem $A$ not through a tensor factor of the Hilbert space, but instead by the set of operators acting locally on $A$.
This viewpoint on quantum mechanics is well-known in the context of algebraic quantum field theory [197]. A detailed discussion in the context of entanglement entropy can be found in the textbook [194] and in the appendix of [198]. For the $\mathbb{Z}_n$ orbifold CFTs considered here, the set of operators acting locally in $A$ is comprised of operators of the form (again dropping the dependence on the twisted sector)

$$P_{\mathbb{Z}_n}(\mathcal{O}_{\mathcal{H}_A} \otimes \mathbb{1}_{\mathcal{H}_B})P_{\mathbb{Z}_n} = \sum_{r=0}^{n-1} \mathcal{O}_{\mathcal{H}_A^n} \otimes \mathbb{1}_{\mathcal{H}_B^{n-r}}. \tag{3.24}$$

From the definition (3.24), it is clear that the set of these operators is closed under addition, multiplication and Hermitean conjugation. Thus, it forms a von Neumann algebra $M_A$.[10] A von Neumann algebra admits a unique density matrix $\rho_A \in M_A$ defined by the property that the expectation value of all operators in the algebra for $\rho_A$ is equal to the expectation value for the global density matrix $\rho$ [194, 198],

$$\mathrm{Tr}_{\mathcal{H}}(\rho\,\mathcal{O}_A) = \mathrm{Tr}_{\mathcal{H}}(\rho_A \mathcal{O}_A) \quad \forall\ \mathcal{O}_A \in M_A. \tag{3.25}$$

Note that here $\rho_A$ acts on the Hilbert space $\mathcal{H}$ in contrast to the usual definition of a reduced density matrix which acts only on a tensor factor $\mathcal{H}_A$. This definition of $\rho_A$ reduces to the ordinary one obtained from a partial trace if the algebra is associated to a tensor factor, that is for $\mathcal{H} = \mathcal{H}_A \otimes \mathcal{H}_B$ the von Neumann algebra $M_A$ contains the operators $\mathcal{O}_{\mathcal{H}_A} \otimes \mathbb{1}_{\mathcal{H}_B}$ and $\rho_A = \mathrm{Tr}_{\mathcal{H}_B}(\rho) \otimes \frac{\mathbb{1}_{\mathcal{H}_B}}{|\mathcal{H}_B|}$ [198]. In the algebraic approach, the existence of a tensor factorization is related to triviality of the center $Z_A$ of $M_A$. $Z_A$ is defined to be the intersection of $M_A$ with its commutant $M_A'$ (the set of operators commuting with all elements of $M_A$),

$$M_A \cap M_A' = Z_A. \tag{3.26}$$

If and only if $Z_A$ contains only the identity operator, there is a tensor factorization associated to $M_A$ and $M_A$ is called a factor algebra [198].

For $\mathbb{Z}_n$ orbifold conformal field theories, it is clear from the definition (3.24) of $M_A$ that the center is spanned by the projectors $P_{\mathcal{H}_A^r \otimes \mathcal{H}_B^{n-r}}$ onto the Hilbert space $\mathcal{H}_A^r \otimes \mathcal{H}_B^{n-r}$.[11] The

[9] Of course, the entanglement entropy is not a property accessible through a single projective measurement and thus not an observable in the usual sense in quantum mechanics. However, the entanglement entropy is nevertheless accessible to an observer that has access to a large number of identical copies of a quantum state $\rho$. When speaking of an observer measuring a von Neumann entropy of a density matrix $\rho$ in the following, it is implicitly understood that the observer has access to a enough identical copies of $\rho$ to completely determine $\rho$ and therefore also the von Neumann entropy $S(\rho)$.

[10] The precise definition of a von Neumann algebra is given as a set of bounded operators on a Hilbert space closed under addition, multiplication and Hermitean conjugation, containing the identity operator and being closed under a limit in the weak operator topology [197]. This limit will however not play a role in the following. For the purpose of this thesis it suffices to know that the algebras are closed under addition and multiplication.

[11] In terms of the $\mathbb{Z}_n$ group elements this projector is defined by the product of projectors composed out of group elements acting locally in $A$ and $B$ as $P_{\mathcal{H}_A^r \otimes \mathcal{H}_B^{n-r}} = P_{r,A} P_{n-r,B}$.

reduced density matrix $\rho_A$ is given by

$$\rho_A = \bigoplus_{r=0}^{n-1} \left( \rho_A^r \otimes \frac{\mathbb{1}_{\mathscr{H}_B^{n-r}}}{|\mathscr{H}_B^{n-r}|} \right) \tag{3.27}$$

where

$$\rho_A^r = \mathrm{Tr}_{\mathscr{H}_B^{n-r}}(P_{\mathscr{H}_A^r \otimes \mathscr{H}_B^{n-r}} \rho P_{\mathscr{H}_A^r \otimes \mathscr{H}_B^{n-r}}). \tag{3.28}$$

Then, the entanglement entropy in this setup is defined as the von Neumann entropy of $\rho_A$ [198],

$$S_A = -\hat{\mathrm{Tr}}_{\mathscr{H}}(\rho_A \log \rho_A) = -\sum_{r=0}^{n-1} \mathrm{Tr}_{\mathscr{H}_A^r}(\rho_A^r \log \rho_A^r). \tag{3.29}$$

Here, $\hat{\mathrm{Tr}}$ is a modified trace functional defined via the right hand side of (3.29). This modification is needed because the trace runs over the entire Hilbert space $\mathscr{H}$ instead of just a tensor factor.[12] The advantage of this procedure is that the entire calculation manifestly uses only gauge invariant states. Therefore, the physical interpretation of the result (as well as the method an observer would need to use to obtain it) is clear. Moreover, the algebraic approach also applies to states which are superpositions of states from distinct twisted sectors which the embedding approach cannot deal with, although I will not make use of this fact in this thesis.

Finally, let me note that the two options described above give the same result for the entanglement entropy for a spatial bipartition in $\mathbb{Z}_n$ orbifolds. To see, this consider again first the special case $n = 2$. Assuming for the moment that the global density matrix $\rho$ contains only states from a single twisted sector, it can be schematically expanded in field eigenstates as[13]

$$\rho = \int DX^1 DX^2 \int DX^{1\prime} DX^{2\prime} \rho(X^1, X^2, X^{1\prime}, X^{2\prime}) |X^1, X^2\rangle \langle X^{1\prime}, X^{2\prime}| \tag{3.30}$$

where the expansion coefficients $\rho(X^1, X^2, X^{1\prime}, X^{2\prime})$ obey

$$\rho(X^1, X^2, X^{1\prime}, X^{2\prime}) = \rho(X^2, X^1, X^{1\prime}, X^{2\prime}) = \rho(X^1, X^2, X^{2\prime}, X^{1\prime}) = \rho(X^2, X^1, X^{2\prime}, X^{1\prime}) \tag{3.31}$$

due to gauge invariance $\rho = g\rho = \rho g$ for all $g \in \mathbb{Z}_2$. Due to the Hilbert space decomposition (3.11), the density matrix is given as a direct sum $\rho = (\rho_A^+ \otimes \rho_B^+) \oplus (\rho_A^- \otimes \rho_B^-)$ where $\rho_A^\pm$ are expanded in field eigenstates

$$\begin{aligned} \rho_A^\pm &= \mathrm{Tr}_{\mathscr{H}_B^\pm}(P_{\mathscr{H}_A^\pm \otimes \mathscr{H}_B^\pm} \rho P_{\mathscr{H}_A^\pm \otimes \mathscr{H}_B^\pm}) \\ &= \frac{1}{8} \int DX_A^1 DX_A^2 \int DX_A^{1\prime} DX_A^{2\prime} (|X_A^1, X_A^2\rangle \pm |X_A^2, X_A^1\rangle)(\langle X_A^{1\prime}, X_A^{2\prime}| \pm \langle X_A^{2\prime}, X_A^{1\prime}|) \\ &\quad \times \int DX_B^1 DX_B^2 (\rho(X^1, X^2, X_A^{1\prime} X_B^1, X_A^{2\prime} X_B^2) \pm \rho(X^1, X^2, X_A^{1\prime} X_B^2, X_A^{2\prime} X_B^1)). \end{aligned} \tag{3.32}$$

[12] More formally, $\hat{\mathrm{Tr}}$ is the unique linear functional on the algebra $M_A$ obeying $\hat{\mathrm{Tr}}(ab) = \hat{\mathrm{Tr}}(ba)$ for all $a, b \in M_A$ and $\hat{\mathrm{Tr}}(p) = 1$ for minimal projections $p \in M_A, p \neq 0$. A projection operator $p$ is called minimal if the only projections $q \in M_A$ with $q\mathscr{H} \subseteq p\mathscr{H}$ are $q = 0$ and $q = p$ [198].

[13] The notation $\int DX^1$ denotes an integral over the value of $X^1$ at each point $\phi$, $DX^1 = \prod_{\phi=0}^{2\pi} dX^i(\phi)$.

Using (3.31) and renaming some of the integration variables yields

$$\rho_A^+ \oplus \rho_A^- = \int DX^1 DX^2 \int DX_A^{1\prime} DX_A^{2\prime}\, \rho(X_A^1 X_B^1, X_A^2 X_B^2, X_A^{1\prime} X_B^1, X_A^{2\prime} X_B^2) |X_A^1, X_A^2\rangle \langle X_A^{1\prime}, X_A^{2\prime}|. \tag{3.33}$$

In this equation, $\rho_A^+ \oplus \rho_A^-$ is expanded in terms of basis elements $|X_A^1, X_A^2\rangle$ of $\tilde{\mathscr{H}}_A$ to facilitate comparison with the embedding approach. From (3.29), it is easy to see that the von Neumann entropy of $\rho_A^+ \oplus \rho_A^-$ in the Hilbert space $\mathscr{H}_A^+ \oplus \mathscr{H}_A^-$ is equal to the entanglement entropy associated to $M_A$ in the algebraic approach. Moreover, the same result is obtained in the embedding approach. The reduced density matrix (3.22) obtained by first embedding $\rho$ into $\tilde{\mathscr{H}}$ and then taking a partial trace yields (3.33) by definition and therefore $\tilde{\rho}_A = (\rho_A^+ \oplus \rho_A^-) \oplus 0$. Thus, the results for the entanglement entropy, (3.23) and (3.29), agree with each other for $\mathbb{Z}_2$ orbifolds and an analogous calculation shows the same agreement for the $n > 2$ case as well.

Note that this agreement between the embedding approach and the algebraic approach is a special property of the discrete gauge symmetry that I am working with and does not hold in general. The two approaches described above are applicable as well to continuous gauge groups where the same non-factorization problems occur as in the discrete setting. This has been studied in detail for lattice gauge theories [199–206] where it was found that the choice of algebra associated to a subregion $A$ is not unique. The ambiguity in the choice of algebra lies in whether to include link operators between lattice sites at the boundary of $A$ in the algebra $M_A$ or not. This ambiguity manifests itself in contributions to the entanglement entropy localized on the boundary the subregion $A$ that depend on which choice for the algebra is made. This is a choice that an observer wanting to measure the entanglement entropy would have to make as well, but which is not obvious how to implement in the embedding approach.

### Generalized entanglement entropy

Let me now go on to describe the definition of the generalized entanglement entropy. As for the entanglement of spatial degrees of freedom, there is no Hilbert space factorization for the $\mathbb{Z}_n$ orbifolds in consideration. While for the entanglement entropy of spatial subregions it was possible to circumvent this problem with the algebraic approach, this does not work for the generalized entanglement entropy: as will become clear below, the set of operators acting locally on the subset of degrees of freedom in consideration does not form an algebra for the generalized entanglement entropy because the set is not closed under multiplication. Again, I will consider two options to deal with the non-factorization problem:

1. Embedding the state in the larger factorizing Hilbert space $\tilde{\mathscr{H}}$ and taking the partial trace there.
   This method works in the same way as for the ordinary entanglement entropy and is the method originally used in [46] to define entwinement. Again, let me restrict to states contained in a single twisted sector and drop the $g$ subscripts. The Hilbert space $\tilde{\mathscr{H}}$ decomposes into tensor products associated to the degrees of freedom in the subregion $A_i$ for the field $X^i$, see (3.20). A reduced density matrix $\tilde{\rho}_{\{A_i\}}$ is obtained from a partial trace of $\tilde{\rho}$ over the complementary Hilbert space $\tilde{\mathscr{H}}_{\{B_i\}}$ and the generalized entanglement entropy as the von Neumann entropy of this density matrix. However, this method suffers from the same violations of gauge symmetry as for the ordinary entanglement entropy.

2. Modeling the subset of degrees of freedom whose entanglement with the rest of the system is to be computed by the set $M_{\{A_i\}}$ of operators acting locally the subset.
   As observed in [190], this set does not form an algebra like in the ordinary entanglement

entropy case but instead only a linear subspace closed under addition but not multiplication. To see this, consider the $\mathbb{Z}_2$ case. The set of operators consists of operators acting locally in different subregions for different fields, symmetrized over $\mathbb{Z}_2$ transformations,

$$P_{\mathbb{Z}_2}\mathcal{O}_{A_1,A_2}P_{\mathbb{Z}_2} \sim \mathcal{O}_{A_1,A_2} + \mathcal{O}_{A_2,A_1} \in M_{\{A_i\}}, \tag{3.34}$$

where $\mathcal{O}_{A_1,A_2}$ acts locally in $A_1$ on $X^1$ and in $A_2$ on $X^2$. It is easy to see that addition of two of these operators gives another operator of the form (3.34). Multiplication of operators, on the other hand, gives an operator of the form

$$P_{\mathbb{Z}_2}\mathcal{O}_{A_1\cup A_2,A_1\cup A_2}P_{\mathbb{Z}_2} \notin M_{\{A_i\}} \tag{3.35}$$

acting locally in the union of $A_1$ and $A_2$ for both fields. Analogous arguments apply to the $\mathbb{Z}_n$ case.

Nevertheless, it is possible to associate an entropy to the subset $M_{\{A_i\}}$ generalizing the entanglement entropy in the algebraic approach which itself generalizes the textbook definition (2.69). The basic idea is to make use of the fact that projective measurements with operators from $M_{\{A_i\}}$ increase the von Neumann entropy of the state $\rho$ to define the entanglement entropy as the entropy of $\rho$ after a measurement, minimized over all possible measurements with operators from $M_{\{A_i\}}$.

To be concrete, let me write the density matrix $\rho$ in terms of a spectral decomposition

$$\rho = \sum_i p_i |\psi_i\rangle\langle\psi_i|, \tag{3.36}$$

where the $|\psi_i\rangle$ form a complete orthonormal basis for the Hilbert space of the system and $p_i \in [0,1]$. Performing a projective measurement with a Hermitean operator $\mathcal{O}$ decomposed into another complete orthonormal basis $|\chi_j\rangle$ as $\mathcal{O} = \sum_j \alpha_j |\chi_j\rangle\langle\chi_j|$ yields the state

$$\rho_{\mathcal{O}} = \sum_{i,j} p_i |\langle\chi_j|\psi_i\rangle|^2 |\chi_j\rangle\langle\chi_j| = \sum_j p_{\mathcal{O},j}|\chi_j\rangle\langle\chi_j|, \tag{3.37}$$

where $p_{\mathcal{O},j}$ is the probability of measuring the state $|\chi_j\rangle$. The von Neumann entropy of $\rho_{\mathcal{O}}$ is in general larger than the von Neumann entropy of $\rho$ [100],

$$S(\rho_{\mathcal{O}}) = -\sum_j p_{\mathcal{O},j}\log p_{\mathcal{O},j} \geq S(\rho) = -\sum_i p_i \log p_i. \tag{3.38}$$

Equality is obtained when the eigenbases of $\mathcal{O}$ and $\rho$ agree, $|\psi_i\rangle = |\chi_i\rangle$. One can make use of this fact to measure the von Neumann entropy of an arbitrary quantum state $\rho$ by looking for the infimum of $S(\rho_{\mathcal{O}})$ over the set of all Hermitean operators acting on the quantum system (or equivalently over the set of bases $|\chi_j\rangle$),

$$S(\rho) = \inf\{S(\rho_{\mathcal{O}}) \mid \{|\chi_j\rangle\} \text{ is a basis for the Hilbert space of } \rho\}. \tag{3.39}$$

The same procedure can be applied if one has access not to the entire set of Hermitean operators acting on the quantum system but only to a linear subspace $M_{\{A_i\}}$ thereof. For the $\mathbb{Z}_n$ orbifolds considered here, $M_{\{A_i\}}$ is spanned by a set of basis operators of the form

$$\mathcal{O}_j = P_{\mathbb{Z}_n}\mathcal{O}_{\{A_i\}}P_{\mathbb{Z}_n} = P_{\mathbb{Z}_n}(|\chi_j\rangle\langle\chi_j| \otimes \mathbb{1})P_{\mathbb{Z}_n}, \tag{3.40}$$

where $\mathcal{O}_{\{A_i\}}$ is an operator on the enlarged Hilbert space $\tilde{\mathcal{H}}$ that acts locally in the subregion $A_i$ for the field $X^i$. The $|\chi_j\rangle$ form a complete orthonormal basis for the Hilbert space factor $\tilde{\mathcal{H}}_{\{A_i\}}$. Again, measurements using the operators $\mathcal{O}_j$ yield a probability distribution given by

$$p_{\mathcal{O},j} = \mathrm{Tr}_{\mathcal{H}}(\rho\mathcal{O}_j) \tag{3.41}$$

and a corresponding entropy $S(\rho_{\mathcal{O}}) = -\sum_j p_{\mathcal{O},j}\log p_{\mathcal{O},j}$. Then, the generalized entanglement entropy is defined to be the infimum of $S(\rho_{\mathcal{O}})$ over all bases $\{\mathcal{O}_j\}$,

$$S_{\{A_i\}} = \inf\left\{S(\rho_{\mathcal{O}}) \mid \mathcal{O} = \sum_j \alpha_j\mathcal{O}_j \text{ and } \{\mathcal{O}_j\} \text{ is a basis for } M_{\{A_i\}}\right\}. \tag{3.42}$$

Note that this procedure is manifestly gauge invariant: the operators $\mathcal{O}_j$ are gauge invariant and the measurement procedure from (3.41) also does not depend on the introduction of non-gauge invariant states. By construction, the generalized entanglement entropy defined in this way is a measure for the amount of information that can be obtained about the density matrix $\rho$ from measurements with operators in the linear subspace $M_{\{A_i\}}$.

As for the ordinary entanglement entropy, the two options for the definition of the generalized entanglement entropy give equal results in the $\mathbb{Z}_n$ orbifold theory. This follows from the equality of the probability distribution (3.41) for measurements in the physical Hilbert space $\mathcal{H}$ to the probability distribution

$$p_{\tilde{\mathcal{O}},j} = \mathrm{Tr}_{\tilde{\mathcal{H}}}(\tilde{\rho}\tilde{\mathcal{O}}_j) = \mathrm{Tr}_{\tilde{\mathcal{H}}_{\{A_i\}}}(\tilde{\rho}_{\{A_i\}}|\chi_j\rangle\langle\chi_j|) \tag{3.43}$$

for measurements in the enlarged Hilbert space $\tilde{\mathcal{H}}$. Here, $\tilde{\mathcal{O}}_j = |\chi_j\rangle\langle\chi_j| \otimes \mathbb{1}$ and the $|\chi_j\rangle$ form a basis for the Hilbert space factor $\tilde{\mathcal{H}}_{\{A_i\}}$. Due to the von Neumann entropy of the reduced density matrix $\tilde{\rho}_{\{A_i\}}$ being obtainable by the infimum of the entropy of $p_{\tilde{\mathcal{O}},j}$ over all bases $|\chi_j\rangle$, the two entanglement entropy definitions agree with each other if

$$p_{\mathcal{O},j} = p_{\tilde{\mathcal{O}},j}. \tag{3.44}$$

Equation (3.44) follows immediately as a consequence of $g\rho = \rho g = \rho \ \forall g \in \mathbb{Z}_n$ and $\rho|\psi\rangle = 0$ for non-gauge invariant states ($|\psi\rangle \in \tilde{\mathcal{H}}$ but $|\psi\rangle \notin \mathcal{H}$),

$$p_{\mathcal{O},j} = \mathrm{Tr}_{\mathcal{H}}\left(\rho\mathcal{O}_j\right) = \mathrm{Tr}_{\mathcal{H}}(\rho P_{\mathbb{Z}_n}\tilde{\mathcal{O}}_j P_{\mathbb{Z}_n}) = \mathrm{Tr}_{\mathcal{H}}(\rho\tilde{\mathcal{O}}_j) = \mathrm{Tr}_{\tilde{\mathcal{H}}}(\tilde{\rho}\tilde{\mathcal{O}}_j) = p_{\tilde{\mathcal{O}},j}. \tag{3.45}$$

Finally, let me point out that entanglement entropy definitions from a linear subspace of observables have been explored previously in the literature in [195, 196]. Let me briefly discuss the connection of these works to the definition introduced above. In [195, 196], entanglement has been defined with respect to a convex cone $C$ of states, i.e. a set of operators representing density matrices that is closed under taking convex linear combinations $\lambda\rho_1 + (1-\lambda)\rho_2$, where $\lambda \in [0,1]$. Pure states are unit trace elements of $C$ that cannot be written as convex combinations of other elements of $C$. Furthermore, a second cone $C'$ is introduced together with a map $\pi$ from $C$ to $C'$. Then, a pure state $\rho \in C$ is called generalized unentangled relative to $C'$ if $\pi(\rho)$ is pure as well. The authors of [195, 196] also introduce an entanglement measure on states $\rho' \in C'$ as

$$S(\rho) = \inf\left\{S(\mathbf{p}) \mid \rho' = \pi(\rho) = \sum_i p_i\rho'_i \text{ with } \rho'_i \text{ pure}\right\}, \tag{3.46}$$

where $S(\mathbf{p})$ is an entropy measure on the probability distribution $\{p_i\}$, e.g. the Shannon entropy

$S(\mathbf{p}) = -\sum_i p_i \log p_i$. This definition is equivalent to the ordinary entanglement entropy if $C'$ is the set of operators acting on a tensor factor of the Hilbert space that $C$ acts on and $\pi$ the partial trace [195, 196]. It is also equivalent to the generalized entanglement entropy if $C$ is identified with the set of operators acting on $\mathscr{H}$ and $C'$ with $M_{\{A_i\}}$. In this case, the map $\pi$ takes an element of $C$ to an element of $C'$ by embedding it in the enlarged Hilbert space $\tilde{\mathscr{H}}$, taking the partial trace over $\tilde{\mathscr{H}}_{\{A_i\}}$ to obtain $\tilde{\rho}_{\{A_i\}}$ and projecting onto a $\mathbb{Z}_n$ invariant operator as $P_{\mathbb{Z}_n}(\tilde{\rho}_{\{A_i\}} \otimes \mathbb{1}/|\tilde{\mathscr{H}}_{\{B_i\}}|)P_{\mathbb{Z}_n}$. Using the convex cone formalism, one can in fact show in general that a restriction to measurements using a subspace of observables implies the existence of a pair of cones $C$ and $C'$ for which the generalized entanglement described above can be defined [195].

The entanglement measure (3.46) is extended to mixed states in [195, 196] using the convex hull construction familiar from entanglement of formation. In general, the convex hull construction defines a mixed state entanglement measure from a pure state entanglement measure by an infimum over convex decompositions $\rho = \sum_i p_i \rho_i$ of the state $\rho$ into pure states $\rho_i$, $S_{\text{mixed}}(\rho) = \inf \sum_i p_i S_{\text{pure}}(\rho_i)$. For the construction in [195, 196], $S_{\text{pure}}$ is given by (3.46) and $\rho, \rho_i \in C$. I will not extend the generalized entanglement entropy definition in the same way, since I do not aim to separate quantum correlations due to entanglement from classical correlations due to a mixed global density matrix. Rather, in holography one is mostly interested in quantifying the total amount of correlations between subsystems: for instance although the ordinary entanglement entropy quantifies the total amount of correlations in a given subsystem and not those from entanglement alone, its holographic dual is simply given as the area of the Ryu-Takayanagi surface for both mixed and pure states. In fact, even the entropy of a thermal density matrix with no quantum correlation part at all acquires an interesting holographic dual as the Bekenstein-Hawking entropy of the dual black hole.

### 3.2.3. $S_N$ orbifolds and mixed states

The goal of this section is to develop generalized entanglement entropy definitions applicable to mixtures of states in different twisted sectors. In particular, thermal states which are dual to black holes are examples of such mixtures. Because the definition I will develop depends on a detailed knowledge of the twisted sectors of the boundary theory, I will restrict to the $S_N$ orbifold theory of the D1/D5 system as an example of a top-down AdS/CFT model in which this information is known in detail.

Recall from section 3.1 that there are two new "ingredients" in the generalized entanglement entropy. First, the aim is to characterize entanglement for a subset consisting of different fields localized in different subregions and second, there is a restriction to a subset of the twisted sectors. Using the embedding approach introduced above, the generalized entanglement entropy for these ingredients is defined as follows. The starting point is the restriction onto the subset $C_1, C_2 \ldots$ of twisted sectors, which is implemented by applying projection operators onto the corresponding Hilbert space subsets,

$$\rho_{\{C_i\}} = (P_{\mathscr{H}_{\{C_i\}}} \rho P_{\mathscr{H}_{\{C_i\}}})/\text{Tr}(P_{\mathscr{H}_{\{C_i\}}} \rho P_{\mathscr{H}_{\{C_i\}}}), \tag{3.47}$$

where $\mathscr{H}_{\{C_i\}} = \bigoplus_i \mathscr{H}_{C_i}$. Here, $C_i$ denotes a conjugacy class of $S_N$ and $\mathscr{H}_{C_i}$ the corresponding twisted sector. If the density matrix is block diagonal, $\rho = \bigoplus_C p_C \rho_C$, $\rho_{\{C_i\}}$ is given by

$$\rho_{\{C_i\}} = \bigoplus_i p_{C_i} \rho_{C_i} \tag{3.48}$$

embedded into the total density matrix as

$$\rho = p_{\{C_i\}} \rho_{\{C_i\}} \oplus p_{\{C_i\}^c} \rho_{\{C_i\}^c}, \tag{3.49}$$

where $\{C_i\}^c$ denotes the complement of the set $\{C_i\}$. Note that all density matrices are normalized to one, $\mathrm{Tr}\rho_C = \mathrm{Tr}\rho_{\{C_i\}} = \mathrm{Tr}\rho_{\{C_i\}^c} = 1$, and therefore it is necessary to introduce the probability factors $p_C, p_{\{C_i\}}, p_{\{C_i\}^c} \in [0,1]$. At this point, $\rho_{\{C_i\}}$ is defined in a Hilbert space of gauge invariant states of the $S_N$ orbifold theory which does not factorize into tensor products. Therefore, the next step is to embed $\rho_{\{C_i\}}$ into an enlarged factorizing Hilbert space $\tilde{\mathscr{H}}$ and to trace out the complement to define a reduced density matrix

$$\tilde{\rho}_{\{A_i\},\{C_i\}} = \mathrm{Tr}_{\tilde{\mathscr{H}}_{\{B_i\}}}(\rho_{\{C_i\}}). \tag{3.50}$$

The generalized entanglement entropy is then defined as the von Neumann entropy of $\tilde{\rho}_{\{A_i\},\{C_i\}}$,

$$S_{\{A_i\},\{C_i\}} = -\mathrm{Tr}_{\tilde{\mathscr{H}}_{\{A_i\}}}(\tilde{\rho}_{\{A_i\},\{C_i\}} \log \tilde{\rho}_{\{A_i\},\{C_i\}}). \tag{3.51}$$

Again, it is easy to find an equivalent gauge invariant definition by considering the set of operators acting locally on the subset of the degrees of freedom in consideration. In fact, in this viewpoint the restriction on the subset of twisted sectors emerges naturally: simply choose operators that map states in twisted sectors other than $\{C_i\}$ to zero. In other words, the set of operators available to an observer in the subsystem is comprised out of block diagonal operators $\mathscr{O}_{\{C_i\}} \oplus 0_{\{C_i\}^c}$. Moreover, let the operators $\mathscr{O}_{\{C_i\}}$ act locally on the degrees of freedom in the subregions $\{A_i\}$. As before, this set of operators forms a linear subspace $M_{\{A_i\},\{C_i\}}$ and therefore the same gauge invariant definition of the generalized entanglement entropy as for the $\mathbb{Z}_n$ orbifolds is possible,

$$S_{\{A_i\},\{C_i\}} = \inf\left\{ S(\rho_{\mathscr{O}}) \mid \mathscr{O} = \sum_j \alpha_j \mathscr{O}_j \text{ and } \{\mathscr{O}_j\} \text{ is a basis for } M_{\{A_i\},\{C_i\}} \right\}. \tag{3.52}$$

Let me close with some remarks on the operators in the subset $M_{\{A_i\},\{C_i\}}$. First, note that in the above definition the subregions $A_i$ always have to be chosen in conjunction with a particular boundary condition $C_i$ as is done for instance in figure 3.2. The Hilbert space of orbifold theories is structured in such a way that it is not enough to specify a set of subregions $A_i$ on which an operator $\mathscr{O}$ acts locally to uniquely determine $\mathscr{O}$ without also specifying the boundary conditions, i.e. the twisted sectors $C_i$, alongside $A_i$. Unless the set of operators treats all fields in the same way (for instance by choosing the subregions $A_i$ to be the same for all $i$), it is necessary to choose $A_i$ and $C_i$ together to uniquely specify a linear subspace of operators. Finally, let me also note that in order to distinguish between different twisted boundary conditions it is necessary to employ non-local operators: none of the field operators $X^i(\phi)$ evaluated at a single point can distinguish between different twisted sectors. Therefore, due to the restriction to a subset of the twisted sectors, $M_{\{A_i\},\{C_i\}}$ contains non-local operators involving field operators at multiple points. Although this might look strange at first, the same issue applies to an observer that wants to measure the total density matrix; they can also do this only if they have access to operators distinguishing between twisted sectors.

## 3.3. Calculation of the generalized entanglement entropy

Let me now explain how to obtain explicit expressions for the generalized entanglement entropy in order to test that the proposed duality to winding geodesic lengths indeed holds. I will consider states in a generic $\mathbb{Z}_n$ orbifold theory dual to conical defects as well as thermal states of the $S_N$ orbifold theory of the D1/D5 system which are dual to black holes. This section only contains an

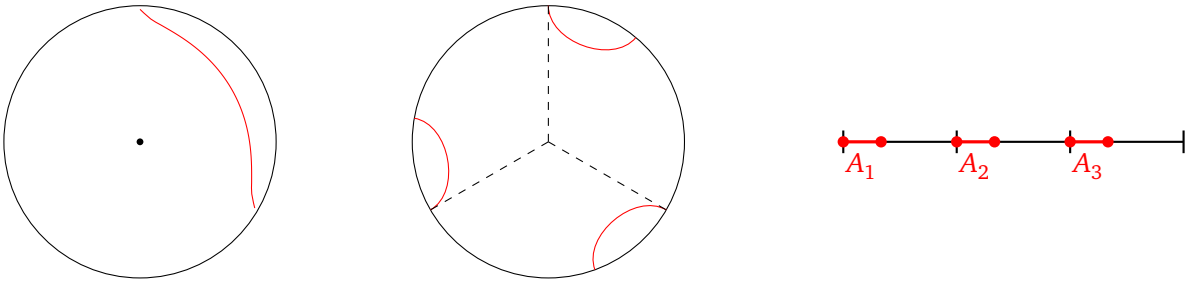


Figure 3.3.: The entanglement entropy of the subregion $A$ in the conical defect geometry is obtained as the entanglement entropy of the union of $n$ copies of $A$ in the each fundamental domain of the covering space.

overview over the calculation methods in general. The results for thermal states are presented in section 3.6 after developing necessary calculation techniques for conformal blocks in section 3.4 and applying them to the ordinary entanglement entropy in section 3.5.

First, let me briefly summarize why the generalized entanglement entropy in states dual to conical defects is dual to the length of a winding geodesic as this argument can be made without complicated calculations. The conical defect is dual to a state in a twisted sector of the $\mathbb{Z}_n$ orbifold. Because the fields $X^1, ..., X^n$ of the orbifold theory are continuously connected by the boundary conditions, this state may equivalently be interpreted as a state of another CFT, the covering theory, which lives on an $n$ times larger spatial circle $\phi \in [0, 2\pi n]$ than the $\mathbb{Z}_n$ orbifold. The $n$ fields $X^1, ..., X^n$ of the orbifold are combined into a single field of the covering theory. Therefore, the central charge $c/n$ of the covering theory is $n$ times smaller than that of the orbifold theory. From the bulk perspective, the covering theory is simply the CFT living on the boundary of the covering space of the conical defect. For a conical defect of empty $\mathrm{AdS}_3$, the state of the orbifold theory is the ground state of the twisted sector and the covering theory is in the ground state as well.

In the embedding approach to the computation of the generalized entanglement, $S_{\{A_i\}}$ reduces to the ordinary entanglement entropy of a subregion $\bigcup_i A_i$ of the covering theory, where now $A_i$ is interpreted to be a part of the region $[2\pi(i-1), 2\pi i]$ in the covering space. For the particular choice of $A_i$ corresponding to $w$ full subregions $[0, 2\pi]$ and a single interval $A$, i.e. $\bigcup_i A_i = [0, 2\pi w + |A|] = \tilde{A}_w$, and a choice of state corresponding to the ground state of the covering theory it is obvious that the generalized entanglement entropy is proportional to the length of a geodesic in the conical defect (see figure 3.1),

$$S_{\{A_i\}} = \frac{1}{n} \frac{\mathrm{Length}[\gamma_A^w]}{4G_N}. \tag{3.53}$$

Here, $\gamma_A^w$ is a geodesic winding $w$ times around the naked singularity of the conical defect geometry and ending on $\partial A$ on the boundary. Equivalently, $\gamma_A^w$ is a geodesic in the covering empty $\mathrm{AdS}_3$ space between $\phi = 0$ and $\phi = 2\pi w + |A|$. The arguments above have been confirmed by explicit calculation of the generalized entanglement entropy via the replica trick in [189].

Note that the final result for the generalized entanglement entropy is equal to the geodesic length divided by $4G_N$ only up to a prefactor of $1/n$. Unlike in the definition of entwinement from [46], I will not choose a generalized entanglement entropy definition that multiples the result with $n$ in order to compensate for this prefactor. As seen in the previous section, $S_{\{A_i\}}$ is a measure for the amount of correlations in the subsystem specified by $\{A_i\}$. Therefore, there is no reason to multiply this correlation measure by another prefactor. In fact, by choosing the subsystem $\{A_i\}$ as above the subsystem is in a sense smaller than for the case where all $A_i$ are equal. Consequently,

the generalized entanglement entropy probes finer details of the entanglement structure and it therefore comes as no surprise that the prefactor is smaller than for the ordinary entanglement entropy. For a purely spatial bipartition with all $A_i$ equal, the entanglement entropy is dual to the length of $n$ identical geodesics in the covering space of the conical defect [46] (see figure 3.3) and the factor of $n$ is recovered naturally.

For thermal states of the $S_N$ orbifold, the calculation method I am using briefly summarized works as follows. Again, for explicit computations I will use the embedding approach for the definition of the generalized entanglement entropy so that the gauge symmetry can be neglected. The actual calculation of the generalized entanglement entropy proceeds via the replica trick: first calculate the Rényi entropy

$$S^{(n)}_{\{A_i\},\{C_i\}} = \frac{1}{1-n} \log \mathrm{Tr} \rho^n_{\{A_i\},\{C_i\}} \tag{3.54}$$

for integer $n$ and then analytically continue to $n \to 1$ to obtain (3.51). The Rényi entropy is in turn obtained from the partition function $Z^{\{C_i\}}_{n,\text{replica}}(\{A_i\})$ constructed by gluing together $n$ copies of the system along the entangling interval determined by $\{A_i\}$,

$$S_{\{A_i\},\{C_i\}} = -\lim_{n\to 1} \partial_n \frac{Z^{\{C_i\}}_{n,\text{replica}}(\{A_i\})}{(Z^{\{C_i\}}_{1,\text{replica}}(\{A_i\}))^n}. \tag{3.55}$$

Because the states in consideration are thermal and the horizon of the dual BTZ black hole is compact, both finite temperature and finite size effects must be included. Therefore, the boundary CFT lives on a torus in Euclidean signature. The torus is specified by its modular parameter $\tau$ and without loss of generality, the space direction of the torus is taken to be of size $2\pi$. The gluing procedure in the replica trick happens along the entangling interval which is placed on a fixed time slice of this torus. The difference between the replica trick for the generalized entanglement entropy and the one for the ordinary entanglement entropy explained in section 2.2.1 is that now this gluing happens in different subregions $A_i$ for different fields $X^i$. Therefore, for the generalized entanglement entropy the partition function is no longer defined on a single higher genus surface as in the ordinary replica trick. The replica partition function $Z^{\{C_i\}}_{n,\text{replica}}(\{A_i\})$ decomposes into conformal blocks,

$$Z^{\{C_i\}}_{n,\text{replica}}(\{A_i\}) = \sum_{p,q} a_{p,q} \mathscr{F}_n(h_p, h_q; \{A_i\}, \{C_i\}) \bar{\mathscr{F}}_n(h_p, h_q; \{A_i\}, \{C_i\}), \tag{3.56}$$

where $a_{p,q}$ denotes the contribution of the OPE coefficients and multiplicities. At large central charge $c$, it is expected that the conformal blocks exponentiate[14],

$$\mathscr{F}(h_p, h_q; \{A_i\}, \{C_i\}) = e^{-c/6 f_{\text{cl.}}(h_p/c, h_q/c; \{A_i\}, \{C_i\})}. \tag{3.57}$$

The so-called semiclassical conformal blocks $f_{\text{cl.}}$ are obtained by a monodromy method developed in the next section. For a large class of conformal field theories, the replica partition function is dominated by a single conformal block (up to corrections of order $e^{-c}$). These CFTs are characterized by a sparse spectrum of light operators and OPE coefficients that grow at most exponentially with the central charge $c$. It has been argued that these properties are characteristic of holographic CFTs with a classical gravity limit [103, 209].

[14] This exponentiation was first conjectured in [207] and recently shown in [208] for the conformal block of the four-point function on the plane.

For the ordinary entanglement entropy, the dominant conformal block is the vacuum block with $h_p = h_q = 0$. For the generalized entanglement entropy the restriction on a subset of the twisted sectors projects out the vacuum block and thus a certain conformal block with $h_q > 0$ dominates. Moreover, for the particular choice of subregions $A_i$ described in section 3.1 near figure 3.2 corresponding to a generalized entanglement entropy dual to the length of a winding geodesic in the BTZ geometry, the gluing along the $A_i$ intervals can be treated effectively as an entangling interval winding multiple times around the space direction of the torus. See section 3.6 for more details.

Note that this calculation procedure is necessary for thermal states because – unlike for the pure states dual to conical defects – the projection onto the subset of twisted sectors $\{C_i\}$ is non-trivial, $\rho_{\{C_i\}}(\beta) \neq \rho(\beta)$. After the projection, the state $\rho_{\{C_i\}}(\beta)$ is still a mixture of states from different twisted sectors. Therefore, a priori it is not clear whether $\rho_{\{C_i\}}(\beta)$ has a natural interpretation in terms of a covering CFT like for the conical defect.

## 3.4. Monodromy methods for conformal blocks

In two-dimensional conformal field theories, any correlation or partition function decomposes into a sum over conformal blocks with prefactors built up from OPE coefficients $C_{qr}^{p}$ and conformal weights $h_p$. The conformal blocks are fixed completely by conformal symmetry and can be computed in a number of different ways. Apart from a not very practical direct evaluation in a series expansion by applying the Virasoro algebra, recursion relations have been developed first for four-point blocks on the complex plane in [210, 211] and later for other conformal blocks in e.g. [212, 213]. The method I am going to use in the following is based on imposing a certain monodromy condition on solutions of an auxiliary differential equation. This equation is obtained by inserting a degenerate operator in the correlation function whose conformal block is to be calculated. I will first review the standard monodromy method for conformal blocks on the plane before generalizing it to the case of conformal blocks on the torus. Finally, I will explain how to derive a monodromy method for zero-point blocks of the partition function on the replica surface relevant to the computation of entanglement entropy on the torus.

### 3.4.1. Conformal blocks on the plane

The starting point for the derivation of the monodromy method for the calculation of four-point (semiclassical) conformal blocks on the plane (see [207, 211] and also [214] for a more detailed explanation) is the correlation function of four primary fields $\mathcal{O}_i$,

$$\langle \mathcal{O}_1(z_1,\bar{z}_1)\mathcal{O}_2(z_2,\bar{z}_2)\mathcal{O}_3(z_3,\bar{z}_3)\mathcal{O}_4(z_4,\bar{z}_4)\rangle. \tag{3.58}$$

Let me parametrize the central charge as $c = 1 + 6(b + 1/b)^2$ and take the semiclassical limit $c \to \infty, b \to 0$ in which the conformal weights $h_i$ of the operators $\mathcal{O}_i$ as well as the internal conformal weight $h_p$ scale proportional to the central charge. Then, insert a degenerate operator $\Psi(z,\bar{z})$ with conformal weight $h_\Psi = -1/2 - 3b^2/4 \sim \mathcal{O}(c^0)$ into the correlation function (3.58). The degenerate operator obeys

$$\left(\hat{L}_{-2} + \frac{1}{b^2}\hat{L}_{-1}^2\right)\Psi(z,\bar{z}) = 0, \tag{3.59}$$

where the action of a Virasoro generator $\hat{L}_{-n}$ on the field $\Psi(z,\bar{z})$ is given by

$$\hat{L}_{-n}\Psi(z,\bar{z}) = \int \frac{dw}{2\pi i}\frac{1}{(w-z)^{n-1}}T(w)\Psi(z,\bar{z}). \tag{3.60}$$

From the conformal Ward identities, this yields the following differential equation known as the decoupling equation,

$$\left[\frac{1}{b^2}\partial_z^2 + \sum_i\left(\frac{h_i}{(z-z_i)^2} + \frac{\partial_{z_i}}{z-z_i}\right)\right]\langle \mathcal{O}_1\mathcal{O}_2\Psi\mathcal{O}_3\mathcal{O}_4\rangle = 0. \tag{3.61}$$

Without loss of generality, I will restrict to the $s$-channel conformal block in the following. This channel arises from applying the operator product expansion between $\mathcal{O}_1$ and $\mathcal{O}_2$,

$$\mathcal{O}_1(z_1,\bar{z}_1)\mathcal{O}_2(z_2,\bar{z}_2) = \sum_p C_{21}^p \sum_{k,\bar{k}}(z_2-z_1)^{h_p-h_1-h_2+|k|}(\bar{z}_2-\bar{z}_1)^{\bar{h}_p-\bar{h}_1-\bar{h}_2+|\bar{k}|}\beta_{21}^{pk}\beta_{21}^{p\bar{k}}\mathcal{O}_p^{\{k,\bar{k}\}}(z_1,\bar{z}_1). \tag{3.62}$$

Here $k = k_1, k_2, \ldots$ is a collection of ordered indices with $k_i \geq k_{i+1}$, $|k| = \sum_i k_i$ and $\mathcal{O}^{\{k,\bar{k}\}}(z,\bar{z}) = (\hat{L}_{-k_1}\hat{L}_{-k_2}\ldots)(\hat{\bar{L}}_{-\bar{k}_1}\hat{\bar{L}}_{-\bar{k}_2}\ldots)\mathcal{O}(z,\bar{z})$. The $\beta_{ij}^{pk}$ coefficients depend on the central charge as well as $h_i, h_j$ and $h_p$. They are fixed by conformal symmetry but their explicit form is not needed in the following. Inserting the OPE (3.62) into the correlation function yields terms containing $\langle \mathcal{O}_p^{\{k,\bar{k}\}}\Psi\mathcal{O}_3\mathcal{O}_4\rangle$ which at large central charge can be approximated by

$$\langle \mathcal{O}_p^{\{k,\bar{k}\}}\Psi\mathcal{O}_3\mathcal{O}_4\rangle \approx \Psi_p\langle \mathcal{O}_p^{\{k,\bar{k}\}}\mathcal{O}_3\mathcal{O}_4\rangle, \tag{3.63}$$

where $\Psi_p$ is defined by

$$\Psi_p = \frac{\langle \mathcal{O}_p\Psi\mathcal{O}_3\mathcal{O}_4\rangle}{\langle \mathcal{O}_p\mathcal{O}_3\mathcal{O}_4\rangle}. \tag{3.64}$$

This can be shown by employing the form of $\langle \mathcal{O}_p^{\{k,\bar{k}\}}\Psi\mathcal{O}_3\mathcal{O}_4\rangle$ in terms of a string of differential operators $\mathcal{L}_{k_i}, \bar{\mathcal{L}}_{k_i}$ acting on $\langle \mathcal{O}_p\Psi\mathcal{O}_3\mathcal{O}_4\rangle$, where

$$\mathcal{L}_{-k_i}^{\Psi} = -\sum_{j=3,4,\Psi}\left(\frac{(1-k_i)h_j}{(z_j-z_1)^{k_i}} + \frac{1}{(z_j-z_1)^{k_i-1}}\partial_{z_j}\right). \tag{3.65}$$

Now $\langle \mathcal{O}_p\mathcal{O}_3\mathcal{O}_4\rangle$ scales as $e^{-c/6S_{\text{cl.}}}$ in the semiclassical limit where $S_{\text{cl.}} \sim O(c^0)$ while $\Psi_p \sim O(c^0)$ and $h_\Psi \sim O(c^0)$. Hence, the derivatives acting on $\Psi_p$ and on the $h_\Psi$ term can be neglected to obtain (3.63) in the leading order in $c$. Next, use a conformal transformation to send $z_1 \to 0$, $z_3 \to 1$, $z_4 \to \infty$ and $z_2$ to the cross ratio

$$x = \frac{(z_1-z_2)(z_4-z_3)}{(z_4-z_2)(z_1-z_3)} \tag{3.66}$$

This implies

$$\langle \mathcal{O}_1\mathcal{O}_2\Psi\mathcal{O}_3\mathcal{O}_4\rangle \approx \sum_p \Psi_p(z,x,\bar{x})C_{21}^pC_{43}^p\mathcal{F}_{12,34}^p(x)\bar{\mathcal{F}}_{12,34}^p(\bar{x}), \tag{3.67}$$

where $\mathcal{F}_{12,34}^p(x)$ is the desired conformal block which in the semiclassical limit scales as $\mathcal{F}_{12,34}^p(x) \sim e^{-\frac{c}{6}f_{\text{cl.}}(x)}$ [207, 208]. The semiclassical conformal block $f_{\text{cl.}}$ depends only on the cross ratio $x$ and

on $b^2h_i, b^2h_p$. The decoupling equation (3.61) then yields at leading order in $c$

$$\left[\partial_z^2 + \sum_i \left(\frac{b^2h_i}{(z-z_i)^2} - \frac{\partial_{z_i} f_{\text{cl.}}(x)}{z-z_i}\right)\right]\Psi_p = 0. \tag{3.68}$$

There is one separate decoupling equation for each term in the sum over $p$ since generically, each term has a different monodromy around paths encircling the operator insertion points and thus must vanish separately. All terms involving derivatives of $\Psi_p$ vanish to leading order due to $\Psi_p \sim O(c^0)$. From the expression for the cross ratio (3.66), a number of linear relations among the $\partial_{z_i} f_{\text{cl.}}$ are obtained,

$$\sum_i \partial_{z_i} f_{\text{cl.}} = \sum_i (z_i \partial_{z_i} f_{\text{cl.}} - b^2h_i) = \sum_i (z_i^2 \partial_{z_i} f_{\text{cl.}} - 2z_i b^2 h_i) = 0. \tag{3.69}$$

These follow from $\partial_{z_i} f_{\text{cl.}} = (\frac{\partial x}{\partial z_i})\partial_x f_{\text{cl.}}$ and $\sum_i \frac{\partial x}{\partial z_i} = \sum_i \frac{\partial x}{\partial z_i} z_i = \sum_i \frac{\partial x}{\partial z_i} z_i^2 = 0$ as can easily be shown from the definition of $x$ and the conformal transformation properties of correlation functions of primary operators. This yields the final form of the decoupling equation,

$$\left[\partial_z^2 + \frac{b^2h_1}{z^2} + \frac{b^2h_2}{(z-x)^2} + \frac{b^2h_3}{(z-1)^2} - \frac{b^2(h_1+h_2+h_3-h_4)}{z(z-1)} + \frac{x(1-x)\partial_x f_{\text{cl.}}}{z(z-x)(z-1)}\right]\Psi_p = 0. \tag{3.70}$$

The fact that the solutions $\Psi_p$ must have a certain monodromy when $z$ is taken in a loop around $0, x$ can be used to obtain $f_{\text{cl.}}$ from the decoupling equation (3.70). This monodromy can be derived from the decoupling equation of $\langle \mathcal{O}_p \Psi \mathcal{O}_3 \mathcal{O}_4 \rangle$,

$$\left[\frac{1}{b^2}\partial_z^2 + \left(\frac{h_p}{(z-z_1)^2} + \frac{1}{z-z_1}\partial_{z_1}\right) + \sum_{i=3,4}\left(\frac{h_i}{(z-z_i)^2} + \frac{1}{z-z_i}\partial_{z_i}\right)\right]\langle \mathcal{O}_p \Psi \mathcal{O}_3 \mathcal{O}_4 \rangle = 0. \tag{3.71}$$

As $z \to z_1$, the leading coefficient of the OPE between $\Psi$ and $\mathcal{O}_p$ is given by $(z-z_1)^\kappa \mathcal{O}_p'(z_1)$ where $\kappa$ can be determined by inserting this coefficient into (3.71),

$$\begin{aligned}\Bigg[\frac{1}{b^2}\kappa(\kappa-1)(z-z_1)^{\kappa-2} + \sum_{i=3,4}\left(\frac{h_i}{(z-z_i)^2} + \frac{1}{z-z_i}\partial_{z_i}\right)(z-z_1)^\kappa \\ + h_p(z-z_1)^{\kappa-2} - \kappa(z-z_1)^{\kappa-2}\Bigg]\langle \mathcal{O}_p' \mathcal{O}_3 \mathcal{O}_4 \rangle = 0.\end{aligned} \tag{3.72}$$

The leading contribution in $z \to z_1$ is given by

$$\left[\frac{1}{b^2}\kappa(\kappa-1) + h_p - \kappa\right](z-z_1)^{\kappa-2} = 0. \tag{3.73}$$

Thus as $b^2 \to 0$ and $z \to z_1$,

$$\kappa = \frac{1}{2}\left(1 \pm \sqrt{1-4h_p b^2}\right) \quad \text{and} \quad \Psi_p \sim (z-z_1)^{\frac{1}{2}(1\pm\sqrt{1-4h_p b^2})}. \tag{3.74}$$

Therefore, the monodromy matrix around $0, x$ is given by

$$M_{0,x} = \begin{pmatrix} e^{i\pi(1+\sqrt{1-4h_p b^2})} & 0 \\ 0 & e^{i\pi(1-\sqrt{1-4h_p b^2})} \end{pmatrix}. \tag{3.75}$$

The trace of the monodromy matrix, which is independent of the basis in which the two solutions of (3.70) are decomposed, is given by

$$\mathrm{Tr}M_{0,x} = -2\cos\left(\pi\sqrt{1-4h_p b^2}\right). \tag{3.76}$$

Thus, the derivative of the conformal block can be extracted from (3.70) by choosing $\partial_x f_{\mathrm{cl.}}$ such that the monodromy of the solution $\Psi_p$ around a loop enclosing $z_1$ and $z_2$ is given by (3.76).[15] Finally, the conformal block is obtained by integrating the chosen $\partial_x f_{\mathrm{cl.}}$.

The four point conformal block in other channels is obtained from the same decoupling equation by imposing different monodromy conditions. For example, the $t$-channel block is obtained by imposing the monodromy condition $\mathrm{Tr}M_{1,x} = -2\cos\left(\pi\sqrt{1-4h_p b^2}\right)$ around the insertion points of $\mathcal{O}_2$ and $\mathcal{O}_3$. Higher point conformal blocks on the plane are computed from similar monodromy methods derived analogously to the four-point case. For $n$ point blocks, the decoupling equation contains $n-3$ independent derivatives fixed by $n-3$ monodromy conditions around the operator insertion points which are contracted in the OPE.

### 3.4.2. Conformal blocks on the torus

I now continue with the derivation of a monodromy method for conformal blocks on the torus. The derivation of this monodromy method proceeds in a very similar way to the one on the plane. I will illustrate the derivation using the two-point function on the torus

$$\langle \mathcal{O}_1(z_1)\mathcal{O}_2(z_2)\rangle_\tau = \mathrm{Tr}[e^{2\pi i\tau(L_0-c/24)}e^{-2\pi i\bar{\tau}(\bar{L}_0-c/24)}\mathcal{O}_1(z_1)\mathcal{O}_2(z_2)], \tag{3.77}$$

however conformal blocks for other correlation functions on the torus are obtained in a similar fashion, as I will briefly discuss as the end of this section. The modular parameter of the torus is denoted by $\tau$, related to the inverse temperature by $\beta = -2\pi i\tau$ for vanishing chemical potential. I will also introduce the parameter

$$Q = e^{-\beta} = e^{2\pi i\tau}, \tag{3.78}$$

the square of the "nome" $e^{\pi i\tau}$, written with an uppercase $Q$ instead of the standard lowercase $q$ to distinguish it from the conformal dimension $h_q$ of the internal index of the conformal block to be derived in the following.

As on the plane, the first step is to insert the degenerate operator $\Psi(z,\bar{z})$ into (3.77). The derivation of the corresponding decoupling equation uses the conformal Ward identity on the torus [215] [16],

$$\langle T(z)\prod_i \mathcal{O}_i(z_i)\rangle_\tau = \left[\sum_i\left(h_i\left(\wp(z-z_i)+2\eta_1\right)+\left(\zeta(z-z_i)+2\eta_1 z_i\right)\partial_{z_i}\right)+2\pi i\partial_\tau\right]\langle\prod_i \mathcal{O}_i(z_i)\rangle_\tau. \tag{3.79}$$

Here, $z\sim z+1\sim z+\tau$ are the coordinates on the torus with modular parameter $\tau$ and $\wp(z),\zeta(z)$ denote Weierstraß elliptic functions with associated $\eta_1$ parameter (see appendix A for the conventions used for the Weierstraß functions). Using the conformal Ward identity (3.79) as well as

[15] The loop needs to enclose both $z_1$ and $z_2$ in order for the OPE between $\mathcal{O}_1(z_1)$ and $\mathcal{O}_2(z_2)$ to converge.

[16] Note that [215] uses a convention where correlation functions on the torus are normalized by the inverse of the partition function $Z(\tau)$ and thus the expression for the conformal Ward identity in [215] contains an additional term $(2\pi i\partial_\tau Z(\tau))\langle\prod_i \mathcal{O}_i(z_i)\rangle_\tau$.

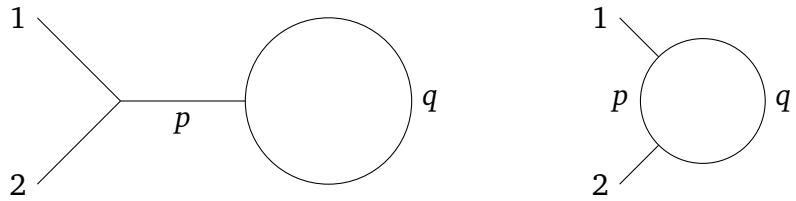


Figure 3.4.: Conformal blocks for the two point function on the torus. Left: OPE channel, right: projection channel.

(3.60), it is easy to see that

$$\begin{aligned}\langle\prod_i \mathcal{O}_i(z_i)\hat{L}_{-2}\Psi(z)\rangle_\tau = \Big[\sum_i \big(h_i(\wp(z-z_i)+2\eta_1)+(\zeta(z-z_i)+2\eta_1 z_i)\partial_{z_i}\big) \\ +2\eta_1 z\partial_z + 2h_\Psi\eta_1 + 2\pi i\partial_\tau\Big]\langle\prod_i \mathcal{O}_i(z_i)\Psi(z)\rangle_\tau\end{aligned} \tag{3.80}$$

and

$$\langle\prod_i \mathcal{O}_i(z_i)\hat{L}_{-1}\Psi(z)\rangle_\tau = \partial_z\langle\prod_i \mathcal{O}_i(z_i)\Psi(z)\rangle_\tau. \tag{3.81}$$

Thus, $\langle\prod_i \mathcal{O}_i(z_i)\Psi(z)\rangle_\tau$ obeys the decoupling equation

$$\begin{aligned}\Big[\frac{1}{b^2}\partial_z^2 + \sum_i \big(h_i(\wp(z-z_i)+2\eta_1)+(\zeta(z-z_i)+2\eta_1 z_i)\partial_{z_i}\big) \\ +2\eta_1 z\partial_z + 2h_\Psi\eta_1 + 2\pi i\partial_\tau\Big]\langle\prod_i \mathcal{O}_i(z_i)\Psi(z)\rangle_\tau = 0.\end{aligned} \tag{3.82}$$

To relate $\langle\mathcal{O}_1(z_1)\mathcal{O}_2(z_2)\Psi(z)\rangle_\tau$ to a conformal block, the trace over states in (3.77) is decomposed into contributions from a primary $\mathcal{O}_q$ and its descendants and the appropriate OPE contractions are inserted. For the two-point function, there are two possible channels (see figure 3.4). The *projection block* is obtained by OPE contracting $\mathcal{O}_2$ and $\mathcal{O}_q$. On the other hand, for the *OPE block* which I will derive first, $\mathcal{O}_2$ and $\mathcal{O}_1$ are contracted,

$$\begin{aligned}\langle\mathcal{O}_1(z_1)\mathcal{O}_2(z_2)\Psi(z)\rangle_\tau &= \sum_q\sum_l Q^{h_q-c/24+|l|}\langle\mathcal{O}_q^{\{l\}}(z_0)\mathcal{O}_1(z_1)\mathcal{O}_2(z_2)\Psi(z)\mathcal{O}_q^{\{l\}}(z_\infty)\rangle(\text{c.c.}) \\ &= \sum_{p,q} C_{21}^p \sum_{k,l}(z_2-z_1)^{h_p-h_1-h_2+|k|}Q^{h_q-c/24+|l|}\beta_{21}^{pk}\langle\mathcal{O}_q^{\{l\}}(z_0)\mathcal{O}_p^{\{k\}}(z_1)\Psi(z)\mathcal{O}_q^{\{l\}}(z_\infty)\rangle(\text{c.c.}),\end{aligned} \tag{3.83}$$

where (c.c.) denotes schematically the antiholomorphic parts of the expression and $z_0 \to -i\infty$ while $z_\infty \to +i\infty$. Defining

$$\Psi_{pq} = \frac{\langle\mathcal{O}_q(z_0)\Psi(z)\mathcal{O}_p(z_1)\mathcal{O}_q(z_\infty)\rangle}{\langle\mathcal{O}_q(z_0)\mathcal{O}_p(z_1)\mathcal{O}_q(z_\infty)\rangle}. \tag{3.84}$$

one obtains as on the plane in the large $c$ limit

$$\langle\mathcal{O}_q^{\{l\}}(z_0)\mathcal{O}_p^{\{k\}}(z_1)\Psi(z)\mathcal{O}_q^{\{l\}}(z_\infty)\rangle(\text{c.c.}) \approx \Psi_{pq}\langle\mathcal{O}_q^{\{l\}}(z_0)\mathcal{O}_p^{\{k\}}(z_1)\mathcal{O}_q^{\{l\}}(z_\infty)\rangle(\text{c.c.}). \tag{3.85}$$

This yields

$$\langle \mathcal{O}_1 \mathcal{O}_2 \Psi \rangle_\tau \approx \sum_{p,q} C_{21}^p C_{pq}^q \Psi_{pq} \mathcal{F}_{21,pq} \bar{\mathcal{F}}_{21,pq}, \tag{3.86}$$

where $\mathcal{F}_{21,pq}$ is the conformal block to be calculated. Assuming that exponentiation of the conformal blocks in the semiclassical limit holds, $\mathcal{F}_{21,pq} \sim e^{-c/6 f_{\text{cl.}}}$, and using that $\partial_{z_1} f_{\text{cl.}} = -\partial_{z_2} f_{\text{cl.}}$ gives

$$\left[\partial_z^2 + \sum_{i=1,2} \left(b^2 h_i (\wp(z-z_i) + 2\eta_1) + \partial_{z_2} f_{\text{cl.}} (-1)^{i+1} (\zeta(z-z_i) + 2\eta_1 z_i)\right) - 2\pi i \partial_\tau f_{\text{cl.}}\right] \Psi_{pq} = 0. \tag{3.87}$$

From the definition of $\Psi_{pq}$ the monodromy conditions are derived in the same way as on the plane. For the OPE block, these are

$$\text{Tr} M_{z_1,z_2} = -2\cos(\pi\sqrt{1-4h_p b^2}),\ \text{Tr} M_{z_0} = -2\cos(\pi\sqrt{1-4h_q b^2}). \tag{3.88}$$

The subscripts of the monodromy matrices show around which cycles the monodromy is taken. The derivation for the projection block works analogously. Here $\mathcal{O}_q(z_0)\mathcal{O}_2(z_2)$ are contracted,

$$\begin{aligned} &\langle \mathcal{O}_1(z_1)\mathcal{O}_2(z_2)\Psi(z)\rangle_\tau \\ &= \sum_{p,q} C_{2q}^p \sum_{k,l} (z_2-z_0)^{h_p-h_q-h_2+|k|} Q^{h_q-c/24+|l|} \beta_{2q}^{pk} \langle \mathcal{O}_p^{\{k\}}(z_0)\mathcal{O}_1(z_1)\Psi(z)\mathcal{O}_q^{\{l\}}(z_\infty)\rangle (\text{c.c.}). \end{aligned} \tag{3.89}$$

Using $\Psi_{pq}$ defined by

$$\Psi_{pq} = \frac{\langle \mathcal{O}_p(z_0)\Psi(z)\mathcal{O}_1(z_1)\mathcal{O}_q(z_\infty)\rangle}{\langle \mathcal{O}_p(z_0)\mathcal{O}_1(z_1)\mathcal{O}_q(z_\infty)\rangle} \tag{3.90}$$

and related to the two point correlator by

$$\langle \mathcal{O}_1 \mathcal{O}_2 \Psi \rangle_\tau \approx \sum_{p,q} C_{2q}^p C_{1p}^q \Psi_{pq} \mathcal{F}_{2q,1p} \bar{\mathcal{F}}_{2q,1p} \tag{3.91}$$

one finds the same decoupling equation (3.87) as for the OPE block. However, the monodromy conditions differ. For the projection block, they are given by

$$\text{Tr} M_{z_0,z_2} = -2\cos(\pi\sqrt{1-4h_p b^2}),\ \text{Tr} M_{z_\infty} = -2\cos(\pi\sqrt{1-4h_q b^2}). \tag{3.92}$$

To solve the decoupling equation, it is useful to perform a coordinate transformation $u = e^{-2\pi i z}$. Using the transformation properties of primary operators under conformal transformations as well as the series representations of the Weierstrass elliptic functions from appendix A, the decoupling equation becomes

$$\begin{aligned} &\Bigg[\partial_u^2 + y(h_2 - (1+y)\partial_y f_{\text{cl.}}) \sum_{m=-\infty}^{\infty} \frac{Q^m}{u(u-Q^m)(u-Q^m(1+y))} + \frac{1/4 - Q\partial_Q f_{\text{cl.}}}{u^2} \\ &+ h_1 \sum_{m=-\infty}^{\infty} \frac{Q^m}{u(u-Q^m)^2} + h_2 \sum_{m=-\infty}^{\infty} \frac{Q^m(1+y)}{u(u-Q^m(1+y))^2}\Bigg] \Psi_{pq} = 0, \end{aligned} \tag{3.93}$$

where I have chosen w.l.o.g. $z_1 = 0$ and $e^{-2\pi i z_2} = 1+y$. In these coordinates, the monodromy

conditions become

$$\begin{aligned}
\mathrm{Tr}M_{1,1+y} &= -2\cos(\pi\sqrt{1-4h_p b^2}) \quad , \ \mathrm{Tr}M_0 = -2\cos(\pi\sqrt{1-4h_q b^2}) \qquad \text{(OPE block)} \\
\mathrm{Tr}M_{0,1+y} &= -2\cos(\pi\sqrt{1-4h_p b^2}) \quad , \ \mathrm{Tr}M_\infty = -2\cos(\pi\sqrt{1-4h_q b^2}) \quad \text{(projection block)}
\end{aligned} \tag{3.94}$$

This representation of the decoupling equation is immediately applicable for the calculation of the OPE block, which is defined through a series expansion in $y$ and $Q$,

$$\begin{aligned}
\mathscr{F}^{\mathrm{OPE}}_{21,pq} = y^{h_p-h_1-h_2}Q^{h_q-c/24}\sum_{n,m=0}^{\infty} y^n Q^m \sum_{\substack{|k_1|=|k_2|=n \\ |l_1|=|l_2|=m}} & [G_n(h_p)]^{k_1k_2}[G_m(h_q)]^{l_1l_2}\langle h_p|L_{\{k_1\}}\mathscr{O}_1(1)|h_2\rangle \\
& \times \langle h_q|L_{\{l_1\}}(\hat{L}_{-\{k_2\}}\mathscr{O}_p(1))L_{-\{l_2\}}|h_q\rangle.
\end{aligned} \tag{3.95}$$

Here, $[G_n(h)]_{k_1k_2}$ is the Gram matrix with entries $\langle h|L_{\{k_1\}}L_{-\{k_2\}}|h\rangle$ and $[G_n(h_p)]^{k_1k_2}$ the inverse thereof. Series expanding $f_{\mathrm{cl.}}$ in $y, Q$ and employing a WKB approximation for large $h_p, h_q$, equation (3.93) can be solved order by order in $y$ and $Q$. For example, to first order the OPE block is given by

$$f^{\mathrm{OPE}}_{\mathrm{cl.}} = -b^2(h_p-h_1-h_2)\log y - (b^2h_q-1/4)\log Q + \frac{1}{2}b^2(h_p+h_2-h_1)y - b^2\frac{h_p^2}{2h_q}Q + \ldots \tag{3.96}$$

The projection block is naturally expanded in a series in $q_1 = Q/(1+y)$ and $q_2 = 1+y$,

$$\begin{aligned}
\mathscr{F}^{\mathrm{projection}}_{2q,1p} = q_1^{h_q-c/24}q_2^{h_p-h_2-c/24}\sum_{n,m=0}^{\infty} q_1^n q_2^m \sum_{\substack{|k_1|=|k_2|=n \\ |l_1|=|l_2|=m}} & [G_n(h_q)]^{k_1k_2}[G_m(h_p)]^{l_1l_2}\langle h_p|L_{\{l_1\}}\mathscr{O}_1(1)L_{-\{k_1\}}|h_q\rangle \\
& \times \langle h_q|L_{\{k_2\}}\mathscr{O}_2(1)L_{-\{l_2\}}|h_p\rangle.
\end{aligned} \tag{3.97}$$

The decoupling equation can then be solved in the same way as for the OPE block order by order in $q_1$ and $q_2$ by expressing (3.93) in these variables and applying a WKB approximation. For example, to first order in $q_1$ and $q_2$ the projection block is given by

$$\begin{aligned}
f^{\mathrm{projection}}_{\mathrm{cl.}} = & -(b^2h_q-1/4)\log q_1 - (b^2(h_p-h_2)-1/4)\log q_2 \\
& - b^2\frac{(h_1-h_p+h_q)(h_2-h_p+h_q)}{2h_q}q_1 - b^2\frac{(h_1+h_p-h_q)(h_2+h_p-h_q)}{2h_p}q_2 + \ldots
\end{aligned} \tag{3.98}$$

I have checked that the results for both the OPE and the projection block are in agreement with the recursion formulas derived in [213] (see app. B for detailed expressions) as well as explicit evaluation of (3.95),(3.97) up to third order in $Q, y$ and $q_1, q_2$ respectively.

It is clear that the above derivation can be easily generalized to other conformal blocks on the torus. The simplest case is the zero-point block on the torus, i.e. the Virasoro character. Performing a similar derivation as above or equivalently taking the limit $h_{1,2,p} \to 0$ in (3.93), one arrives at the following decoupling equation,

$$\left[\partial_u^2 + \frac{1/4 - Q\partial_Q f_{\mathrm{cl.}}}{u^2}\right]\Psi_q = 0, \tag{3.99}$$

together with the monodromy condition $\mathrm{Tr}M_0 = -2\cos(\pi\sqrt{1-4h_q b^2})$. In this case, it is possible to give the full solution without resorting to series expansions in $Q$. The decoupling equation is solved by $\Psi_q = u^{1/2\pm\sqrt{Q\partial_Q f_{\mathrm{cl.}}}}$, from which one obtains $f_{\mathrm{cl.}} = (1/4 - b^2h_q)\log Q$. This correctly

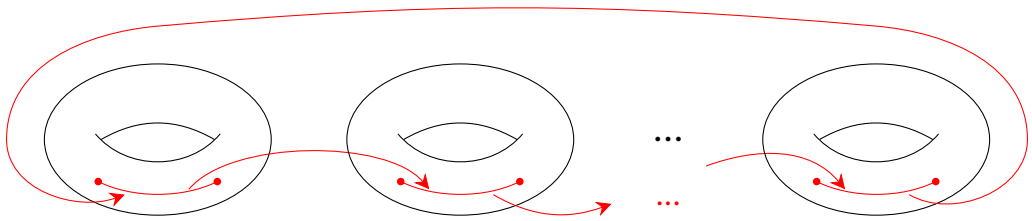

Figure 3.5.: Illustration of the replica surface $\mathscr{R}_n$ for the computation of the ordinary entanglement entropy at finite size and finite temperature: $n$ copies of a torus are cyclically glued together along the entangling interval $A$ to form a genus $n$ Riemann surface, i.e. a manifold with $n$ handles.

reproduces the leading order contribution in $c$ of the Virasoro character $\chi_q = \frac{1}{\eta(\tau)} Q^{h_q-(c-1)/24} \sim e^{-c/6 f_{\text{cl.}}}$. For a general $n$-point conformal block, the decoupling equation is given by

$$\left[\partial_z^2 + \sum_{i=1}^{n} \left(b^2 h_i(\wp(z-z_i)+2\eta_1) + \partial_{z_i} f_{\text{cl.}}(\zeta(z-z_i)+2\eta_1 z_i)\right) - 2\pi i \partial_\tau f_{\text{cl.}}\right]\Psi = 0, \tag{3.100}$$

and there are $n$ monodromy conditions around non-trivial cycles determined by the OPE contractions. By conformal transformations, the insertion point of one of the operators can be fixed, for example to $z_1 \to 0$. Then, there are $n$ independent accessory parameters $\partial_\tau f_{\text{cl.}}$ and $\partial_{z_i} f_{\text{cl.}}$ for $i \geq 2$ fixed by these monodromy conditions.

### 3.4.3. Partition function on the replica surface

The replica trick relates the entanglement entropy of a spatial subregion $A$ at finite size and finite temperature to the partition function on a higher genus Riemann surface $\mathscr{R}_n$, the *replica surface*, constructed by gluing $n$ copies of a torus along the entangling interval $A$ (see figure 3.5). This section explains how to calculate the conformal blocks of the partition function on $\mathscr{R}_n$ via a monodromy method.

But before doing so, let me first clarify why it is necessary to develop these monodromy methods in the first place. Since at zero temperature the replica partition function is equal to a correlation function of twist operators, naively one might think that it would be enough to calculate a correlation function of twist operators on the torus (for example using the monodromy methods from the last subsection) and relate that correlator to the entanglement entropy. In the small interval limit, this method indeed works and the replica partition function is identical to the correlation function of two twist operators inserted at the endpoints of the entangling interval on the torus (see e.g. [216–219]), analogous to the zero temperature case. For large intervals, on the other hand, the replica partition function does not agree with a correlation function of local twist operators, as can be seen by the following argument. It is well known that for a pure state $\rho$, the entanglement entropy for $A$ is equal to the entanglement entropy of the complement $B$, $S_A = S_B$. However, for mixed states such as the thermal states described by the CFT on the torus, this property no longer holds. Since the correlation function of local twist operators contains no information about whether the entanglement entropy is calculated for $A$ or for $B$ (the location of the branch cuts between the twist operators is not fixed by the twist correlator), it cannot give the correct answer on the torus. Note that this issue can be resolved by defining non-local twist operators on the torus as in [220], however I will not do this and instead phrase the calculation directly in terms of the replica partition function. In the following the term "twist operator" will always refer to a local operator of scaling dimension $h = \bar{h} = c/24(n-1/n)$.

Fortunately, however, the monodromy method for the partition function on $\mathscr{R}_n$ is a close cousin to that of the two-point function of twist operators on the torus, as I will explain in the following. In general, the partition function on any higher genus Riemann surface can be expanded in zero-point conformal blocks, which can again be calculated via a monodromy method. This monodromy method can be derived by inserting the degenerate operator directly on the higher genus Riemann surface – in contrast to the last section, where the degenerate operator was inserted in a correlation function on the torus – and putting in projection operators at appropriate places. The difficulty of this approach is of course that deriving the decoupling equation for an arbitrary Riemann surface is quite hard. However, as will become clear in a moment, things simplify for the special higher genus surface $\mathscr{R}_n$ that is of interest for the computation of the entanglement entropy. Assuming that the dominant contribution to the partition function depends only on the temperature and size of the entangling interval and not on any other moduli of $\mathscr{R}_n$, the same decoupling equation as for the twist operator correlator on the torus is found. The difference to the monodromy method from the last subsection lies in the monodromy conditions. The zero-point block on $\mathscr{R}_n$ admits more general monodromy conditions (corresponding to different channels) than the conformal block on the torus. One of these more general monodromy conditions will give the dominant contribution to the entanglement entropy for large intervals.

Before deriving the decoupling equation on $\mathscr{R}_n$, let me collect some facts about the topology and moduli of $\mathscr{R}_n$. For simplicity, I specialize again to the single interval case. The replica surface is given by $n$ copies of a torus with modular parameter $\tau$, joined at a branch cut along the entangling interval $A$. Coordinates $z, \bar{z}$ with identifications $z \sim z+1$ and $z \sim z+\tau$ are used to parametrize $\mathscr{R}_n$. In these coordinates, $\mathscr{R}_n$ is described by a branched cover of the torus with branch points located at $z = z_{1,2} + k + l\tau$ for $k, l \in \mathbb{Z}$. Near the branch points, the covering map is given by $y^n \propto (z - z_1 - k - l\tau)$ and $y^n \propto 1/(z - z_2 - k - l\tau)$. The genus of $\mathscr{R}_n$ can be found by the Riemann-Hurwitz theorem. Since the ramification index at each branch point is equal to $n$ the genus $g$ is also equal to $n$. Because the Euler characteristic is $\chi < 0$, there are no conformal Killing vectors. This implies by the Riemann-Roch theorem that there exist $3(n-1)$ holomorphic quadratic differentials $\omega_{zz}^{(i)}$ parametrizing deformations of the complex structure of the Riemann surface. The $\omega_{zz}^{(i)}$ are meromorphic doubly periodic functions that are regular everywhere on the covering surface, i.e. $\omega_{yy}^{(i)} dy^2 = \omega_{zz}^{(i)} \left(\frac{dz}{dy}\right)^2 dz^2$ is non-singular for all $y$. Simple examples include $\omega_{zz}^{(1)} = \text{const.}$ which is trivially regular and doubly periodic as well as $\omega_{zz}^{(2)} = \zeta(z - z_1) - \zeta(z - z_2) + 2\eta_1(z_1 - z_2)$. $\omega_{zz}^{(2)}$ is regular since $\omega_{yy}^{(2)} \propto y^{n-2}$ near $z = z_1 + k + l\tau$ and thus $\omega_{yy}^{(2)}$ is regular at $y = 0$ for $n \geq 2$. Near $z = z_2 + k + l\tau$ regularity can be shown in an analogous way. In fact, the two holomorphic quadratic differentials $\omega_{zz}^{(1)}$ and $\omega_{zz}^{(2)}$ are the only ones relevant for the following arguments since they are the only ones that respect the $\mathbb{Z}_n$ replica symmetry permuting the different copies of the torus with each other.[17]

The derivation of the decoupling equation on the replica surface then proceeds in a similar fashion as in the previous section. Assuming exponentiation of the zero-point block in the semiclassical limit, the conformal Ward identities for a general Riemann surface [215] imply a decoupling equation of the form

$$\left[\partial_z^2 + \langle T_{zz} \rangle + \sum_{i=1}^{n} \omega_{zz}^{(i)} \partial_{w_i} f_{\text{cl.}}\right] \Psi(z) = 0, \tag{3.101}$$

where $w_i$ are the modular parameters associated to $\omega_{zz}^{(i)}$. $\langle T_{zz} \rangle$ is the expectation value of the

[17] This can be seen as follows. The replica symmetry acts as $y \to y e^{2\pi i/n}$. Therefore, only the $\omega_{zz} \sim (z - z_i)^{\alpha_i}$ with $\alpha_i \in \mathbb{Z}$, $i = 1, 2$ are invariant under this symmetry. The case $\alpha_i < -1$ is singular at $z = z_i$. $\alpha_i > 0$ is singular at some other point since any non-constant elliptic function has at least two poles inside the fundamental parallelogram, which lead to singularities in $\omega_{yy}$. This leaves only $\alpha_i = 0, -1$ which are the two examples described above.

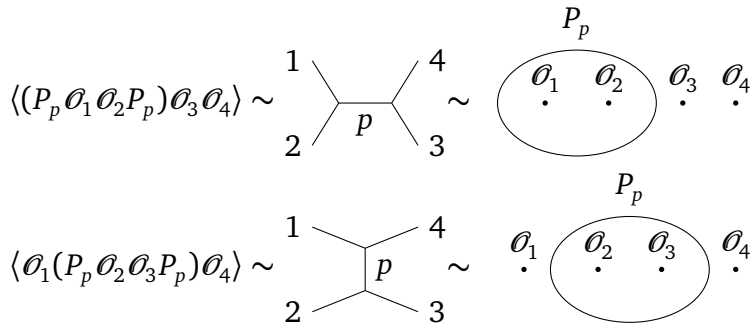


Figure 3.6.: Inserting projection operators $P_p$ onto the Verma module of a primary $\mathcal{O}_p$ into a correlator yields the conformal block with internal weight $h_p$.

energy momentum tensor. It can be derived along the lines of [221]: $\langle T_{zz} \rangle$ transforms with a Schwarzian derivative,

$$\langle T_{yy} \rangle = \left( \frac{\partial z}{\partial y} \right)^2 \langle T_{zz} \rangle + \frac{nc}{12} \{z, y\}, \tag{3.102}$$

and $\langle T_{yy} \rangle$ must be regular. The Schwarzian derivative term comes with a $nc/12$ prefactor since the stress-energy tensor on the replica surface is given as the sum of the stress-energy tensors of the $n$ tori. Therefore, the Schwarzian for the transformation of the stress-energy tensor on the replica surface is given by the sum of $n$ identical Schwarzian terms with prefactor $c/12$. Together with the requirement that $\langle T_{zz} \rangle$ be doubly periodic, regularity of $\langle T_{yy} \rangle$ implies

$$\langle T_{zz} \rangle = \frac{c}{24} \left( n - \frac{1}{n} \right) \sum_i (\wp(z - z_i) + 2\eta_1). \tag{3.103}$$

The $1/(z-z_i)^2$ poles in $\wp(z-z_i)$ give a $1/y^2$ contribution to $\langle T_{yy} \rangle$ that cancels with the Schwarzian derivative term.[18] Letting the sum over $i$ in (3.101) run only over $i = 1, 2$, the decoupling equation (3.87) for the twist correlator is recovered. Restricting the sum to this range means that I assume $\partial_{w_i} f_{\text{cl.}} = 0$ for $i > 2$, i.e. I assume that the result for the partition function on the replica surface does not depend on other moduli of the replica surface than the size of the torus $\tau$ and the length of the entangling interval $z_2 - z_1$.

However, as mentioned in the beginning of this section, the admitted monodromy conditions for the decoupling equation (3.101) are more general than those of (3.87) for the twist correlator. To see this, recall that conformal blocks of any correlation function can be obtained in two equivalent ways. Either one can perform OPE contractions between two or more operators and then keep only terms of particular primaries and their descendants in the OPE or equivalently one can insert projection operators onto the Verma modules of these primaries in the correlation function at appropriate places. The projectors of the latter approach can be thought of as non-local operators acting in a closed line around the operators whose OPE contractions are performed in the former approach (see figure 3.6). For the zero-point block on an arbitrary higher genus Riemann surface, there are in general $3(n-1)$ projectors to be inserted corresponding to $3(n-1)$ monodromy conditions. However, as mentioned above I assume that the partition function on the higher genus Riemann surface depends only on two of the moduli and thus I consider only two of the $3(n-1)$ monodromy conditions.

Which monodromy conditions are appropriate for the calculation of the entanglement entropy?

[18] For ease of comparison with the previous subsection I have also added a constant term $\frac{c}{24}\left(n - \frac{1}{n}\right) 4\eta_1$ to $\langle T_{zz} \rangle$ which is not strictly necessary for regularity and could be absorbed into the prefactor of $\omega_{zz}^{(1)}$.

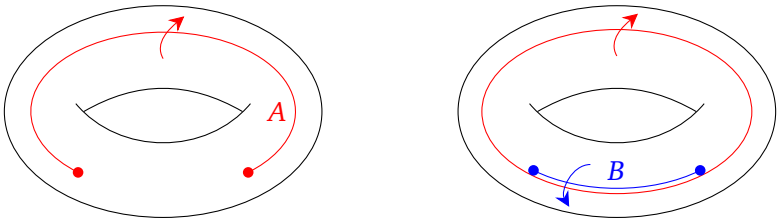


Figure 3.7.: Branch cut structure for large intervals. The branch cut along $A$ (denoted in red on the left) is decomposed into a branch cut along the full spatial circle (denoted in red on the right) and a branch cut in the opposite direction along $B$ (denoted in blue on the right).

For the conformal block of the two-point function of twist operators on the torus, the monodromy conditions must be taken around the spatial circle and around $z_1, z_2$.[19] On the other hand, for the zero-point block on the replica surface the prescription described in this section still leaves open the question of where to put the monodromy conditions – i.e. which channel to choose – in order to obtain the dominant contribution to the partition function from the vacuum block. Taking the limits of high and low temperature, it is clear that for small intervals one of the monodromy conditions must be taken around the spatial circle for low temperatures and the time circle for high temperatures, while the other monodromy condition must be imposed around the entangling interval $A$ between $z_1$ and $z_2$ (see figure 3.8). For large intervals, the correct monodromy condition is obtained by reformulating the problem along the lines of [218, 222]. First, separate the branch cut on the torus along $A$ yielding the replica surface into a branch cut along the full spatial circle and a branch cut in the opposite direction along $B$ (see figure 3.7). Then, impose trivial monodromy around $B$ to fix the dependence on the size of the entangling interval. For small temperatures, the monodromy condition around the spatial circle remains unchanged. However, for high temperatures the monodromy condition around the time circle is now transformed into a monodromy condition around a time circle of size $n\tau$, since the branch cut along the full spatial circle connects all $n$ replica copies together to effectively create a torus with modular parameter $n\tau$.

Note again that it is perfectly valid to use any of the above monodromy conditions for all values of the temperature and entangling interval size. However, outside of the regimes of validity described above, the vacuum block is not expected to give the dominant contribution in the semi-classical limit and thus the partition function in this case would be obtained by summing up all of the conformal blocks for different values of the dimensions of the exchanged operators. The cross-over point between the regimes must be determined by an analysis of these contributions from the exchange of non-identity operators.

Let me also note that explicit calculations for the free fermion case support the arguments presented in this section with regards to the differences between twist correlators and partition functions on $\mathscr{R}_n$ and with regards to the monodromy condition for large intervals. Namely, in [223] based on previous work [224–226] it was observed that the twist correlator on the torus does not give the correct answer for the entanglement entropy and in particular violates Bose-Fermi equivalence and modular covariance. This was traced back in [227] to the way in which different spin structures of the replica surface $\mathscr{R}_n$ combine to give the total answer for the partition function $Z_{n,\text{replica}}$. The replica surface, being composed of $n$ copies of a torus, has $2n$ nontrivial cycles around which the fermions have either periodic or antiperiodic boundary conditions. To

[19] It is also possible to calculate the modular transformed block for the twist correlator, which is expected to be the dominant contribution at large temperature and small intervals. In this case, the monodromy conditions are taken around $z_1, z_2$ and around the time circle.

calculate the total partition function $Z_{n,\text{replica}}$ on the replica surface, it is necessary to sum over all possible spin structures each of which corresponds to a particular choice of boundary conditions around the nontrivial cycles of the replica surface. For small intervals, the replica surface essentially factorizes into $n$ unconnected torus copies. In this limit, it was shown in [227] that $Z_{n,\text{replica}}$ is given by an "uncorrelated" sum where the summation over spin structures is performed for each of the $n$ tori separately. For large intervals, $Z_{n,\text{replica}}$ is given by a "correlated" sum where only one sum over spin structures is performed, i.e. equal boundary conditions are imposed around the time respectively space circles of each of the $n$ replica copies [227]. In this case, the partition function $Z_{n,\text{replica}}$ of the replica surface is essentially given by the partition function on a torus with modular parameter $n\tau$.

## 3.5. Ordinary entanglement entropy at finite size and finite temperature

Before considering the generalized entanglement entropy, it is instructive to first apply the monodromy methods developed in the preceding section to the entanglement entropy of a spatial subregion $A$ on the torus at large central charge. The generalized entanglement entropy will then be a relatively simple generalization of the discussion in this section. For previous work relevant to entanglement at finite size and finite temperature in holographic CFTs, see [220, 222, 228, 229].

As explained in the previous section, the entanglement entropy can be obtained from the partition function $Z_{n,\text{replica}}$ on the replica surface $\mathscr{R}_n$ which decomposes into zero-point conformal blocks. The claim I would like to investigate is that at large central charge $c \to \infty$ and for $n \to 1$ the dominant contribution to $Z_{n,\text{replica}}$ comes from the vacuum block with $h_p = h_q = 0$. The derivation of this statement proceeds as follows. First, it is necessary to show that the semiclassical limit is well-defined not only for $h_{p,q} = O(c)$ but also for $h_{p,q} = O(c^0)$. This means that for $h_{p,q} = \gamma c$ the limits $\lim_{c\to\infty}$ and $\lim_{\gamma\to 0}$ of the conformal block commute. A discussion of this point starting from the recursion relation for torus conformal blocks is relegated to app. B. In the next step, I will solve the decoupling equation (3.87) perturbatively in $\varepsilon = n - 1$ up to first order. Imposing the monodromy conditions derived in section 3.4.2 then yields the conformal block from which finally the entanglement entropy is extracted.

I will first consider the limits of high and low temperature as well as small and large entangling interval size in section 3.5.1. Each combination of these limits comes with different monodromy conditions as explained in the previous section. The results are in agreement with the known universal results in the limits where the torus degenerates into a cylinder. As a byproduct of this analysis, I will determine in which limits the replica partition function reduces to a correlation function of twist operators on the torus. I will then examine the conditions on the CFT spectrum and OPE coefficients under which these results extend to intermediate temperature and interval size regimes in section 3.5.2, leading to the conclusion that for holographic CFTs the results from section 3.5.1 are valid for all temperatures and interval sizes. Moreover, I will consider the case of multiple entangling intervals on the torus in section 3.5.3. Finally, I will numerically check the assumption on the dominance of the vacuum block in section 3.5.4.

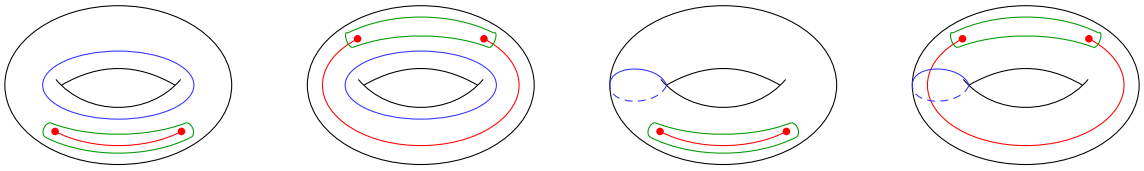

$\beta \gg 1, |A| \ll 1$ $\beta \gg 1, |A| \gg 1$ $\beta \ll 1, |A| \ll 1$ $\beta \ll 1, |A| \gg 1$

Figure 3.8.: Illustration of the monodromy conditions imposed for the calculation of ordinary entanglement entropy via the partition function on the replica surface $\mathscr{R}_n$. Shown here is one of the $n$ tori that are glued together to form $\mathscr{R}_n$. Monodromy conditions for $h_q$ are imposed around the blue path and those for $h_p$ around the green path. The entangling interval $A$ is drawn in red.

### 3.5.1. Limiting cases

#### Low temperature and small intervals

In the low temperature limit $\beta \to \infty$ the torus degenerates into a cylinder with periodic space direction. For the cylinder, the entanglement entropy of a single interval can be obtained directly by mapping this cylinder to the plane and using the known formula for the entanglement entropy on the plane [97],

$$S_A = \frac{c}{3} \log\left(\sin(\pi(z_2 - z_1))\right) + \text{const.} \tag{3.104}$$

To obtain the same result from the monodromy method for the replica partition function on the torus, first series expand $\Psi_{pq}$ and $f_{\text{cl.}}$ in $\epsilon = n-1$: $\Psi_{pq} = \sum_k \Psi_{pq}^{(n)}(n-1)^k$ and $f_{\text{cl.}} = \sum_k f_n (n-1)^k$. The decoupling equation (3.87) at zeroth order in $n-1$ becomes

$$[\partial_z^2 - 2\pi i \partial_\tau f_0]\Psi_{pq}^{(0)}(z) = 0. \tag{3.105}$$

This is solved by

$$\Psi_{pq}^{(0)}(z) = \exp(\pm\sqrt{2\pi i \partial_\tau f_0} z). \tag{3.106}$$

By a coordinate transformation $u = \exp(-2\pi i z)$, this transforms to $\tilde{\Psi}_{pq}^{(0)}(u) = u^{h_\Psi}\Psi_{pq}^{(0)}(z = i\log(u)/(2\pi))$. Imposing trivial monodromy of $\tilde{\Psi}_{pq}^{(0)}(u)$ around $u = 0$ is equivalent to antiperiodic monodromy conditions for $\Psi_{pq}^{(0)}(z)$ around the spatial circle of the torus, $\Psi_{pq}^{(0)}(z+1) = -\Psi_{pq}^{(0)}(z)$. As expected, this implies that $f_0$ is equal to the leading order in $c$ of the vacuum character on the torus,

$$f_0 = \pi i \tau/2 = -\beta/4 \qquad \Leftrightarrow e^{-c/6 f_0} = e^{c/24\beta} = \chi_{h=0}(\beta)|_{c\to\infty}\,. \tag{3.107}$$

At first order in $n-1$, the decoupling equation is given by

$$[\partial_z^2 - 2\pi i \partial_\tau f_0]\Psi_{pq}^{(1)}(z) + m(z)\Psi_{pq}^{(0)}(z) = 0, \tag{3.108}$$

yielding

$$\Psi_{pq}^{(1)}(z) = \frac{e^{-i\pi z}}{2\pi i}\int^z dx\, m(x) e^{i\pi x}\Psi_{pq}^{(0)}(x) - \frac{e^{i\pi z}}{2\pi i}\int^z dx\, m(x) e^{-i\pi x}\Psi_{pq}^{(0)}(x), \tag{3.109}$$

where $m(z)$ is given by

$$m(z) = \sum_i \left( \frac{1}{2}(\wp(z-z_i) + 2\eta_1) + (-1)^{i+1}(\zeta(z-z_i) + 2\eta_1 z_i)\partial_{z_2} f_1 \right) - 2\pi i \partial_\tau f_1. \tag{3.110}$$

To compute the conformal block I will impose trivial monodromy around $z_1, z_2$ which is equivalent to the vanishing of

$$\oint_{z_1,z_2} dx\, m(x) e^{\pm i\pi x} \Psi^{(0)}_{pq}(x). \tag{3.111}$$

This gives the $z_1, z_2$ dependence of $f_1$,

$$f_1 = \log(\sin(\pi(z_2 - z_1))) + C_1(\tau). \tag{3.112}$$

From trivial monodromy around $u = 0$ one finds the $\tau$ dependence to be $\partial_\tau f_1 = 0$, which implies that $C_1(\tau) = \text{const.}$ is independent of $\tau$. The antiholomorphic conformal block $\bar{f}_1$ gives the same result as the holomorphic one. Then the entanglement entropy is given by $S_A = \frac{c}{6}(f_1 + \bar{f}_1)$, in agreement with (3.104). In this limit, the OPE vacuum block of the twist correlator gives the same results, since it is given by the same monodromy method as the zero-point vacuum block of the replica partition function computed in this section.

### Low temperature and large intervals

In this limit, it is necessary to demand trivial monodromy around the spatial circle (i.e. around $u = e^{-2\pi i z} = 0$) as well as trivial monodromy around $B$, the conjugate of $A$ (i.e. $[z_1, z_2 - 1]$). This gives the same vacuum block and thus the same entanglement entropy (3.104) as in the small interval case at low temperature. Also in this case, the twist correlator gives the correct result.

### High temperature and small intervals

In the high temperature limit $\beta \to 0$ the torus again degenerates into a cylinder, now with periodic time direction. As in the low temperature case, the entanglement entropy of a single interval can be obtained by mapping this cylinder to the plane [97],

$$S_A = \frac{c}{3} \log\left( \frac{\beta}{2\pi^2} \sinh\left( \frac{2\pi^2}{\beta}(z_2 - z_1) \right) \right) + \text{const.} \tag{3.113}$$

In the monodromy method, one has to impose trivial monodromy around the time circle and around $z_1, z_2$. As in the low temperature limit, the decoupling equation (3.87) is solved in a series expansion around $\epsilon = n - 1$. An analogous calculation as above yields

$$f_{\text{cl.}} = -\frac{\pi i}{2\tau} + \epsilon \log\left( \tau \sinh\left( \frac{\pi i}{\tau}(z_2 - z_1) \right) \right) + \text{const.} = f_0 + \epsilon f_1 \tag{3.114}$$

At zeroth order in $\epsilon$ the leading order in $c$ of the modular transformed vacuum character $\chi_{h=0}\left(\frac{4\pi^2}{\beta}\right) = e^{\frac{c}{24}\frac{4\pi^2}{\beta}} = e^{-\frac{c}{6}(-\frac{\pi i}{2\tau})}$ is recovered. The entanglement entropy given by the first order contribution, $S_A = \frac{c}{6}(f_1 + \bar{f}_1)$, agrees with the result from the cylinder (3.113).

From the twist correlator point of view, the high temperature limit is obtained by a modular transformation $\tau \to -1/\tau$ from the low temperature result. The two point function on the torus

transforms covariantly,

$$\langle \mathcal{O}_1(-z_1/\tau,-\bar{z}_1/\bar{\tau})\mathcal{O}_2(-z_2/\tau,-\bar{z}_2/\bar{\tau})\rangle_{-1/\tau} = (-\tau)^{h_1+h_2}(-\bar{\tau})^{\bar{h}_1+\bar{h}_2}\langle \mathcal{O}_1(z_1,\bar{z}_1)\mathcal{O}_2(z_2,\bar{z}_2)\rangle_\tau. \quad (3.115)$$

If the two point function of twist operators is dominated by a single conformal block, the conformal block for the modular transformed $\tau$ is obtained from the modular transformation properties of the correlation function as

$$f_{\text{cl.}}^{-1/\tau}(-z_1/\tau,-z_2/\tau) = -b^2(h_1+h_2)\log(-\tau) + f_{\text{cl.}}^{\tau}(z_1,z_2). \quad (3.116)$$

Therefore, one can immediately read off the high temperature behavior of the twist correlator from

$$f_{\text{cl.}}^{\tau}(z_1,z_2)\Big|_{\tau\to\infty} = \left[f_{\text{cl.}}^{-1/\tau}(-z_1/\tau,-z_2/\tau) + b^2(h_1+h_2)\log(-\tau)\right]_{\tau\to\infty} \quad (3.117)$$

For $h_1 = h_2 = 1/2\epsilon$ and $f_{\text{cl.}}^{\tau}(z_1,z_2)\Big|_{\tau\to 0} = \frac{\pi i\tau}{2} + \epsilon\log(\sin(\pi(z_2-z_1))) + \text{const.}$ equation (3.114) is obtained again. Thus the twist correlator agrees with the replica partition in this limit.

Let me note that is also possible to determine the high temperature expansion of the twist correlator by applying the modular transformation to the monodromy conditions instead of the final result for the conformal block. At low temperatures, trivial monodromy around the spatial circle of the torus is imposed. Since the modular transformation $\tau \to -1/\tau$ exchanges the time and space directions of the torus, the high temperature behavior of the twist correlator is obtained by demanding trivial monodromy around the time circle of the torus, showing directly the equivalence between the twist correlator result and the replica partition function in the limit of high temperature and small entangling intervals.

### High temperature and large intervals

As explained in section 3.4.3, the correct monodromy condition of the zero-point block on the replica surface for large intervals imposes trivial monodromy around $B$ (the complement of the entangling interval $A$) and $z \to z + n\tau$ ($n$ times the spatial circle). To zeroth order in $n-1$ the decoupling equation (3.87) is solved by $\Psi_{pq}^{(0)}(z) = \exp(\pm\sqrt{2\pi i\partial_\tau f_0})$. Imposing $\Psi_{pq}^{(0)}(z+n\tau) = -\Psi_{pq}^{(0)}(z)$ yields

$$f_0 = -\frac{\pi i}{2n^2\tau}. \quad (3.118)$$

To first order, the solution reads

$$\Psi_{pq}^{(1)}(z) = n\tau\frac{e^{-\frac{i\pi z}{n\tau}}}{2\pi i}\int^z dx\, m(x)e^{\frac{i\pi x}{n\tau}}\Psi_{pq}^{(0)}(x) - n\tau\frac{e^{\frac{i\pi z}{n\tau}}}{2\pi i}\int^z dx\, m(x)e^{-\frac{i\pi x}{n\tau}}\Psi_{pq}^{(0)}(x). \quad (3.119)$$

Imposing trivial monodromy around $B$ and expanding in $\epsilon = n-1$, one obtains

$$f_{\text{cl.}} = -\frac{\pi i}{2\tau} + \epsilon\left(\frac{i\pi}{\tau} + \log\left(\tau\sinh\left(\frac{i\pi}{\tau}(1-(z_2-z_1))\right)\right)\right) + \text{const.} \quad (3.120)$$

giving

$$S_A = \frac{c}{3}\left(\frac{2\pi^2}{\beta} + \log\left(\frac{\beta}{2\pi^2}\sinh\left(\frac{2\pi^2}{\beta}(1-(z_2-z_1))\right)\right)\right) + \text{const.} \quad (3.121)$$

As expected from general arguments [216, 218], the difference between the entanglement entropy for $A$ and for the complement $B$ in the limit of large interval size is given by the thermal entropy $S(\beta) = -\beta^2\partial_\beta(\beta^{-1}f\,or\,\log Z(\beta)) = \frac{c}{3}\frac{2\pi^2}{\beta}$, using the partition function $Z(\beta\to 0) =$

$\exp(\frac{c}{12}\frac{4\pi^2}{\beta})$ from the Cardy formula. The twist correlator, on the other hand, cannot reproduce this feature as is easy to see by applying the modular transformation argument from the last section which gives again (3.114), in disagreement with (3.120).

### 3.5.2. Holographic CFTs

I will now argue that the results in the limits considered in the previous section are valid for all temperatures and interval sizes in holographic CFTs. This statement holds if the vacuum block computed in the previous section gives the dominant contribution to the partition function on the replica manifold $\mathscr{R}_n$ in the large central charge limit.

Let me first consider the case $n = 1$, i.e. the zeroth order in the $n-1$ expansion. In this order, the monodromy method calculates the vacuum character to leading order in $c$. If this vacuum character dominates the partition function, $Z(\beta)$ takes on the universal form

$$Z(\beta) = \begin{cases} \exp\left(\frac{c}{12}\beta\right) & , \beta > 2\pi \\ \exp\left(\frac{c}{12}\frac{4\pi^2}{\beta}\right) & , \beta < 2\pi \end{cases} \tag{3.122}$$

for all temperatures. For consistency of the computation method, dominance of the conformal block to first order in $n-1$ also requires dominance of the zeroth order in $n-1$. It has been argued in [209] that a partition function of the form (3.122) is characteristic of a holographic CFT. Thus it is a necessary condition that the CFT in question be holographic in order for the results of section 3.5.1 to hold at arbitrary temperatures.

More explicit conditions on the CFT in question can be given following an argument for dominance of the vacuum block in the zero temperature case that proceeds as follows [103]. This argument holds for CFTs with OPE coefficients $C_{21}^p$ that grow at most exponentially with $c$ [20] and a density of states for light operators that does not grow with $c$. Here, light operators mean operators with conformal weight $h, \bar{h} < h_{\text{gap}}$ where $h_{\text{gap}}$ is of the order of the central charge. In the large central charge limit, the conformal block expansion in the $s$-channel of the four-point twist correlator on the plane takes on the form

$$\langle \sigma_n(0)\sigma_n(x)\sigma_n(1)\sigma_n(\infty)\rangle = \sum_p C_{21}^p \exp\left(-\frac{c}{6}\left(f_{\text{cl.}}(h_{\sigma_n}/c, h_p/c, x) + \bar{f}_{\text{cl.}}(\bar{h}_{\sigma_n}/c, \bar{h}_p/c, \bar{x})\right)\right). \tag{3.123}$$

On account of the cluster decomposition principle, the vacuum exchange is the leading contribution in the $s$-channel around $x = 0$ and in the $t$-channel around $x = 1$. This implies that the contribution of the heavy operators with $h, \bar{h} > h_{\text{gap}}$ in the $s$-channel in some finite region around $x = 0$ is suppressed exponentially and similarly for the $t$-channel around $x = 1$. The sparse spectrum of the light operators allows ignoring the multiplicity factors for $h, \bar{h} < h_{\text{gap}}$. Consider first the scenario that the OPE coefficients grow subexponentially with $c$. In this case, it is also possible to ignore the coefficient $C_{21}^p$ and the sum over the light operators in (3.123) is dominated exponentially in $e^{-c}$ by its largest term. If the semiclassical conformal block $f_{\text{cl.}}$ is a monotonically increasing function with $h_p/c$, this implies that the vacuum block with the lowest possible $h_p/c = 0$ dominates. In the case that the OPE coefficients grow exponentially with $c$, the sum over the light operators gives

$$\int_0^{h_{\text{gap}}} dh_p d\bar{h}_p \exp\left(\frac{c}{6}\left(g(h_p/c, \bar{h}_p/c) - f_{\text{cl.}}(h_{\sigma_n}/c, h_p/c, x) - \bar{f}_{\text{cl.}}(\bar{h}_{\sigma_n}/c, \bar{h}_p/c, \bar{x})\right)\right), \tag{3.124}$$

[20] This is equivalent to the requirement that correlation functions obey the cluster decomposition principle and are smooth in a neighborhood of the point where multiple operator insertion points coincide [103].

where $g(h_p/c, \bar{h}_p/c)$ contains the contribution of the OPE coefficients and multiplicities. This integral is dominated either by the endpoints of the integration or by a saddle point. Near coincident points, the leading universal term in any correlation function is given by the vacuum exchange. Therefore, in a finite region around $x = 0$ and $x = 1$, the integral in (3.124) is dominated by the endpoint at $h_p = 0$. However, now – unlike for subexponentially growing OPE coefficients – it is not possible to exclude saddle points dominating the integral (3.124) in some finite subset of $x \in [0, 1]$. Examples of such saddle points have been found in [230] for genus two partition functions computing the third Rényi entropy on the plane.

In summary, the vacuum block dominates correlation functions in a finite region around coincident operator insertion points if the conformal block $f_{\text{cl.}}$ increases monotonically with the internal conformal weights $h_{p,q}$. In section 3.5.4, I will present numerical evidence that this is indeed the case. Therefore, the results of section 3.5.1 are valid for all temperatures and interval sizes assuming subexponentially growing OPE coefficients and a sparse spectrum of light operators. For exponentially growing OPE coefficients, the results are still valid in a finite region around the respective limiting points. The points at which the different limits exchange dominance are obtained as follows. From the requirement of consistency of our results at $n = 1$ with the partition function (3.122) it is clear that the low and high temperature regimes exchange dominance at the Hawking-Page phase transition point $\beta = 2\pi$. The transition between small and large interval behavior in the high temperature regime is estimated by equating the results for the conformal block in the small and large interval regime. The dominant contribution comes from the smaller conformal block.

Assuming the aforementioned restrictions on the CFT spectrum and OPE coefficients, the results match perfectly with the predictions from the RT formula [27, 216]. There is also a direct way to implement the monodromy computation for the calculation of the entanglement entropy in the dual gravity theory, as was shown in [221] at zero temperature. This was generalized to the finite temperature case in [222, 229]. I obtain the same monodromy method as [222, 229] from the CFT side. This clearly shows that my results are valid for holographic CFTs.

Furthermore, the high temperature and large interval size result (3.120) agrees with a CFT calculation of the vacuum sector contribution to the entanglement entropy done in [222] using complementary techniques to obtain the vacuum block. Specifically, the conformal block is obtained in [222] by an explicit construction of the Virasoro generators and descendant states in the twisted sector of a $\mathbb{Z}_n$ orbifold. This allows for a series expansion of the Rényi entropy. Moreover, in the limit $n \to 1$, the authors of [222] find that the leading order of the semiclassical vacuum block is given by an expression in terms of the four-point function of twist-operators on the plane, which gives the same conformal block (3.120) that I obtain using the monodromy method.

Let me also note that the universal form of the partition function (3.122) in holographic theories can be derived from the same vacuum block dominance argument as the universal form of the entanglement entropy. The partition function can be expanded in zero-point blocks on the torus either in a low temperature expansion (zero-point blocks are Virasoro characters) or in a high temperature expansion (zero-point blocks are modular transformed Virasoro characters). From the known form of the Virasoro characters, the leading order contribution in the central charge of the characters is given by $\chi \sim Q^{h_q - c/24}$ where $Q = e^{2\pi i \tau}$ respectively $Q = e^{-2\pi i/\tau}$ in the low and high temperature expansions. Since $(-6/c)\log\chi$ is an increasing function of $h_q$, the same arguments as for the entanglement entropy given above apply to the partition function which is dominated by the vacuum character with $h_q = 0$.

### 3.5.3. Multiple intervals

The generalization to an entangling interval consisting of the union of multiple intervals, $A = [z_1, z_2] \cup [z_3, z_4] ... [z_{2N-1}, z_{2N}]$, is straightforward. The decoupling equation is given by

$$\left[\partial_z^2 + \sum_{i=1}^{2N}\left(\frac{1}{4}(n-1/n)(\wp(z-z_i)+2\eta_1) - \partial_{z_i} f_{\text{cl.}}(\zeta(z-z_i)+2\eta_1 z_i)\right) - 2\pi i \partial_\tau f_{\text{cl.}}\right]\Psi(z) = 0. \tag{3.125}$$

Imposing trivial monodromy around $N$ pairs $(i, j)$ of interval endpoints $z_i, z_j$ fixes the $\partial_{z_i} f_{\text{cl.}}$ parameters. The temperature dependence is fixed by demanding trivial monodromy around either the spatial circle, a time circle of size $\tau$ or a time circle of size $n\tau$ depending on the temperature and total entangling interval size $|A| = \sum_i |z_{2i} - z_{2i-1}|$. This yields

- low temperature: trivial monodromy for $z \to z + 1$

$$S_A = \frac{c}{3}\sum_{(i,j)} \log\left(\sin(\pi(z_i - z_j))\right) + \text{const.} \tag{3.126}$$

- high temperature and small total interval size: trivial monodromy for $z \to z + \tau$

$$S_A = \frac{c}{3}\sum_{(i,j)} \log\left(\frac{\beta}{2\pi^2}\sinh\left(\frac{2\pi^2}{\beta}(z_i - z_j)\right)\right) + \text{const.} \tag{3.127}$$

- high temperature and large total interval size: trivial monodromy for $z \to z + n\tau$

$$S_A = \frac{c}{3}\left(\frac{2\pi^2}{\beta} + \sum_{(i,j)} \log\left(\frac{\beta}{2\pi^2}\sinh\left(\frac{2\pi^2}{\beta}(z_i - z_j)\right)\right)\right) + \text{const.} \tag{3.128}$$

Which monodromy condition and which combination of pairs $(i, j)$ to take, i.e. in which channel to expand the conformal block, depends on the interval size. The dominant contribution is expected to come from the channel with the smallest $f_{\text{cl.}}$, in which case agreement with the RT formula is found. However, I caution that this argument depends on the vacuum block dominating the partition function, which I have checked only for a single interval.

One particular interesting special case of the above calculation is the time dependence of the entanglement entropy between two intervals on opposite boundaries of a two-sided BTZ black hole. Correlation functions of operators inserted on opposite asymptotic boundaries of the two-sided black hole are evaluated in a path integral formalism from operator insertions on the torus where the operators from one asymptotic boundary are inserted at time-offset $\tau/2$ compared to the operators from the other boundaries. Similarly, the entanglement entropy is obtained by positioning the two intervals at a distance $\tau/2$ in the time coordinate on the torus [58]. To obtain the time evolution of the entanglement entropy, it is necessary to perform an analytic continuation of the endpoints [58],

$$\begin{aligned} z_1 = \bar{z}_1 = 0 \qquad & z_2 = \bar{z}_2 = L \\ z_3 = 2t + L + \tau/2, \bar{z}_3 = -2t + L + \bar{\tau}/2 \qquad & z_4 = 2t + \tau/2, \bar{z}_4 = -2t + \bar{\tau}/2, \end{aligned} \tag{3.129}$$

where $L$ is the size of the entangling interval taken to be equal on both boundaries and $t$ is the time coordinate at which both parts of the entangling interval are placed on the asymptotic boundaries

of the wormhole[21] (see [58] for more details on the setup). For small interval size $L$, there are two conformal blocks to consider. At early times, i.e. for small $t$, the dominant contribution comes from imposing trivial monodromy around $z_1, z_4$ and $z_2, z_3$, while at late times the vacuum block with trivial monodromy around $z_1, z_2$ and $z_3, z_4$ dominates. Taking into account that due to the analytic continuation $f_{\text{cl.}} \neq \bar{f}_{\text{cl.}}$, the corresponding entanglement entropy is given by

$$S_A = \frac{2c}{3} \log\left(\frac{\beta}{2\pi^2} \cosh\left(\frac{4\pi^2}{\beta} t\right)\right) + \text{const.} \tag{3.130}$$

at early times and by

$$S_A = \frac{2c}{3} \log\left(\frac{\beta}{2\pi^2} \sinh\left(\frac{2\pi^2}{\beta} L\right)\right) + \text{const.} \tag{3.131}$$

at late times. This reproduces the phase transition in the dual RT surfaces from geodesics that connect the two boundaries through the interior of the two-sided black hole at early times to disconnected geodesics on opposite boundaries that do not enter the black hole interior at late times [58].

### 3.5.4. Vacuum block dominance

In this section, I provide numerical evidence that the vacuum block exponentially dominates the twist correlator in the large $c$ limit. For simplicity, I restrict to the single interval case. Assuming the same conditions on the spectrum and OPE coefficients of the CFT detailed in the last section, it is necessary to show that the conformal block monotonically increases with the weight of the internal operators $h_{p,q}$.

For the zero temperature case, this was done numerically in [103] for arbitrary $n$, giving evidence that the Rényi entropies are given by the vacuum conformal block contribution only. However, the calculation is much simpler if one restricts to $n$ close to one which implies $h_p/c \gg h_i/c \to 0$ for $i = 1, 2, 3, 4$. In this limit, the conformal block can be obtained in closed form from the monodromy calculation by a WKB expansion in $1/(h_p/c)$ [211],

$$\frac{c}{6} f_{\text{cl.}}(0, h_p/c, x) = h_p \left(\pi \frac{K(1-x)}{K(x)} - \log 16\right), \tag{3.132}$$

where $K(x)$ is the complete elliptic integral of the first kind. Thus, $f_{\text{cl.}}$ is an increasing function of $h_p/c$ if $\pi K(1-x)/K(x) - \log 16 > 0$ which can easily be checked to be fulfilled for $x < 1/2$. In fact, $f_{\text{cl.}}(0, h_p/c, x) - f_{\text{cl.}}(0, h_p/c, 1-x)$ reaches its crossover point exactly at $x = 1/2$, confirming that at this point dominance is exchanged from the $s$ to the $t$-channel block.

Applying the same arguments as on the plane to the case of the torus, it is clear that the vacuum block dominates if the semiclassical block is an increasing function of $h_p$ and $h_q$. Without loss of generality, I take $z_1 = 0$ in the following. Restricting again to $n \approx 1$, the semiclassical block in the limit $h_{p,q}/c \gg h_{1,2}/c \to 0$ needs to be computed. Unlike on the plane, however, $f_{\text{cl.}}$ can not easily be obtained in a closed form expression from the monodromy calculation in this limit.[22] Thus, it is necessary apply a series expansion in $y = e^{-2\pi i z_2} - 1$ and $Q = e^{2\pi i \tau}$ on top of the WKB approximation in $1/(h_{p,q}/c)$.

[21] Note that this time coordinate has nothing to do with the euclidean time coordinate on the torus on which the finite temperature correlator in the euclidean CFT is calculated.

[22] The reason for this is that the solution of the decoupling equation on the torus takes on the schematic form of an integral over $\sqrt{A\partial_{z_2} f_{\text{cl.}} + B\partial_\tau f_{\text{cl.}}}$ for some functions $A$ and $B$, from which it is not easily possible to extract $\partial_{z_2} f_{\text{cl.}}$ and $\partial_\tau f_{\text{cl.}}$. The solution of the decoupling equation on the plane, on the other hand, is given by an integral over $\sqrt{A\partial_x f_{\text{cl.}}}$ from which $\partial_x f_{\text{cl.}}$ can be factored out immediately.

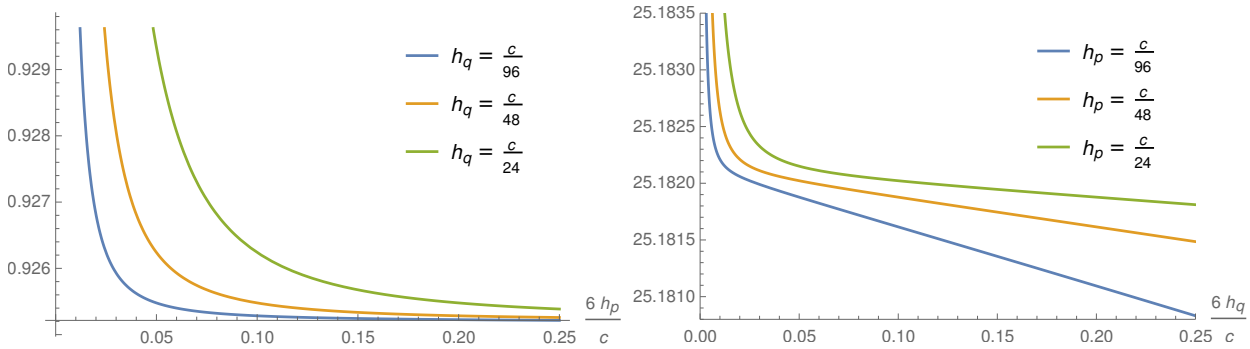


Figure 3.9.: Derivative of the semiclassical conformal block $f_{\text{cl.}}$ w.r.t. $h_p$ (left) and $h_q$ (right) for $z_2 = 0.1$, $\beta = 4\pi$ and different values of $h_p$ and $h_q$ in the range $[0, c/24]$. Note that the plotted value is greater than zero in all cases, showing that the semiclassical conformal block increases with $h_p$ and $h_q$. The series expansion used in this figure was truncated at order 10 in both $y$ and $Q$.

While this yields a very precise numerical approximation to the true value of the conformal block if enough terms are included in the series, the expansion has a restricted domain of validity in the $y, Q$ plane. In particular, the series expansion in the cross-ratio $x$ of the four-point block on the plane converges for $|x| < 1$ [211], therefore it is natural to expect the series expansion of the two-point block on the torus to have a convergence radius of $|y| = 1$ (the torus block reduces to the block on the plane in the limit $Q \to 0$). The numerics confirm this expectation. For $|y| > 1$, large fluctuations in the value of the conformal block are observed as more terms are included in the series expansion. The numerics for the convergence radius in $Q$ is less clear, but also in this variable large fluctuations are observed close to $Q = e^{-2\pi}$. Thus, one can check the vacuum block dominance only in a restricted region around the origin in $y$, corresponding to small intervals. The restricted convergence radius in $Q$ is not a limiting factor for the calculation of the entanglement entropy since above the Hawking-Page transition temperature given by $Q = e^{-2\pi}$, the block in the high temperature expansion is expected to dominate. The high temperature expansion of the conformal block is given by a series expansion in $e^{2\pi i z_2/\tau} - 1$ and $e^{-2\pi i/\tau}$. In the $h_{p,q}/c \gg h_{1,2}/c$ limit, the series coefficients are equal to those of the low temperature expansion. Moreover, in the same limit at high temperatures and for $n \to 1$ the conformal block in the large interval limit (where the monodromy condition is taken around a time circle of size $n\tau$) is equivalent to the conformal block in the small interval limit with the replacement $z_2 \to 1 - z_2$.

Some plots of $\frac{\partial f_{\text{cl.}}}{\partial h_p}$ and $\frac{\partial f_{\text{cl.}}}{\partial h_q}$ are shown in figure 3.9 for small temperatures and values of $y$ and $Q$ inside the convergence radius. The plots for the conformal block in the high temperature limit show no significant differences from the ones in the low temperature limit. I find in all cases that inside the convergence radius of the series expansion $\frac{\partial f_{\text{cl.}}}{\partial h_{p,q}} > 0$, i.e. the assumption of vacuum block dominance is satisfied.

While it is not possible to find an analytic continuation for the conformal block from a truncated series expansion, it is possible to use a Padé approximant to get a heuristic approximation of the series outside its convergence radius. The Padé approximation works by replacing the truncated series expansion by a rational function whose Taylor expansion agrees with the series expansion up to the order in which the truncation was performed [231]. In many cases, this approximation has a better radius of convergence than the original series expansion due to poles in the function limiting the radius of convergence of its Taylor expansion being taken into account in the Padé approximation. The Padé approximant of $f_{\text{cl.}}$ is plotted in the special case $h_p = h_q$ for different orders of the denominator polynomial in figure 3.10 depending on $z_2$ (the size of the entangling

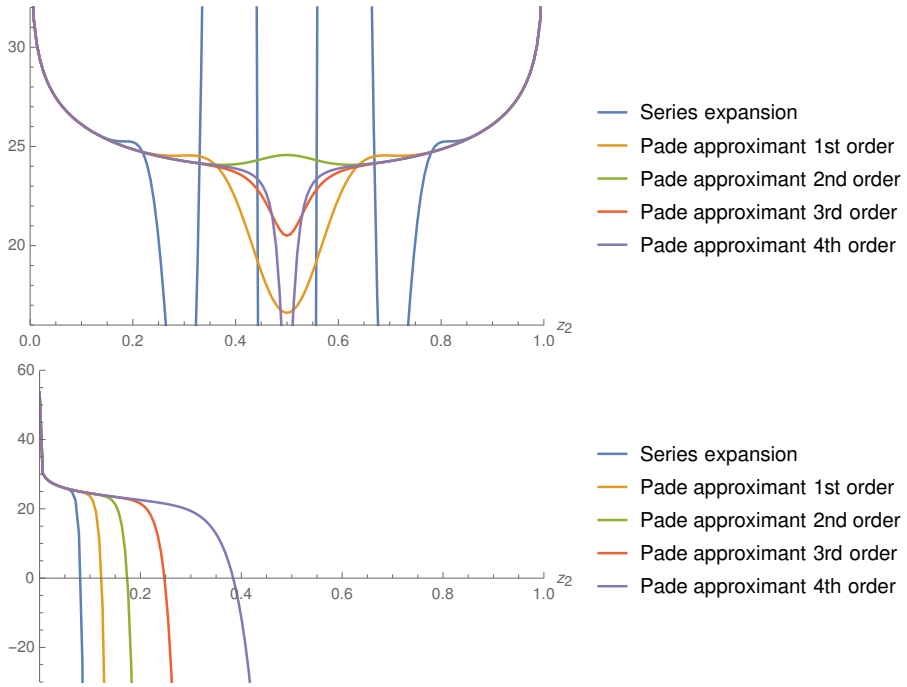


Figure 3.10.: Derivative of the Padé approximation of the semiclassical conformal block w.r.t. the internal conformal weight plotted against the entangling interval size $z_2$. The upper plot shows the conformal block at $\beta = 4\pi$ in the low temperature expansion and the lower plot the block at $\beta = \pi$ in the high temperature expansion. For plotting convenience $h_p$ and $h_q$ are equal such that the derivative of $f_{\text{cl.}}$ is constant for all $h_p$. As the order of the denominator polynomial in the Padé approximation is increased, the fluctuations in $f_{\text{cl.}}$ outside of the convergence radius of the series expansion decrease. Moreover, multiple Padé approximants converge to the same value outside of the convergence radius. The convergence radius $|y| = 1$ is located at $z_2 = 1/6$ in the upper plot and $z_2 = \frac{\log(2)}{4\pi} = 0.0552$ in the lower plot. The series expansion approximated by the Padé approximants in this figure was truncated at order 10 in both $y$ and $Q$.

interval). I find that different Padé approximants for $f_{\text{cl.}}$ converge to the same value and yield $\frac{\partial f_{\text{cl.}}}{\partial h_{p,q}} > 0$ in a finite region outside of the convergence radius $|y| = 1$ of the series expansion of $f_{\text{cl.}}$. While this is not a formal proof, it does indicate that vacuum block dominance holds also outside of the convergence radius.

## 3.6. Generalized entanglement entropy at finite size and finite temperature

In this section, I discuss the generalized entanglement entropy for thermal states. As shown figure 3.2, I will consider a subset of the degrees of freedom specified by twisted sectors $C_i = \prod_{k=1}^{N/m}(km)^{n_{km}^{(i)}}$ and subregions $A_i$ consisting of $w$ full intervals $[0, 2\pi]$ continuously connected together with a single interval interval $A$. I will work in the large $N$ limit and assume $m$ to be of order $O(N^0)$.[23] The calculation of the generalized entanglement entropy for this subset is a

[23] Strictly speaking, $m$ should be a divisor of $N$ in order for the twisted sectors shown above to be well-defined such that the total number of cycles is given by $N$. However, the number of additional cycles needed to get to $N$ cycles is

straightforward generalization of the calculation in section 3.5 for the ordinary entanglement entropy of a spatial subregion. Let me briefly discuss in the following where the calculation here differs from the one in the previous section.

### 3.6.1. Results

#### Low temperatures

The first important difference is that in the sum over states in the thermal partition function, the untwisted sector and thus the character for the identity operator is projected out for the subset $\{C_i\}$. Therefore, by the vacuum block dominance argument the leading contribution to the thermal partition function at low temperature comes from the character of the operator with lowest conformal weight that is not projected out. In the case at hand this is the twist operator $\Sigma$ creating the ground state of the $(m)^{N/m}$ twisted sector with conformal weight

$$h_\Sigma = \bar{h}_\Sigma = \frac{N}{m}\frac{\tilde{c}}{24}\left(m - \frac{1}{m}\right). \tag{3.133}$$

This is confirmed by a direct calculation of the contribution of the $\{C_i\}$ subset to the thermal partition function of the $S_N$ orbifold theory in appendix C.

Therefore, at low temperature the leading contribution to the replica partition function for the $\{C_i\}$ subset comes from the zero-point block where the weight $h_q$ of the internal operator originating from the sum over states in the thermal partition function is given by $h_q = h_\Sigma$ instead of $h_q = 0$ as for the vacuum block. The projection onto the subset of twisted sectors does not spoil the argument that this conformal block is dominant up to $e^{-c}$ corrections since projecting out a part of the spectrum can only decrease the multiplicities and does not change the OPE coefficients. Note that all descendants of a primary operator $\Sigma$ are in the same twisted sector as $\Sigma$, thus the projection does not change the conformal blocks themselves. The modification of the entangling intervals also necessitates a change in the monodromy conditions used to derive the conformal block: instead of trivial monodromy around an entangling interval $A = [0, L]$, trivial monodromy around a path encircling $w$ times the spatial circle combined with the interval $[0, L]$ is imposed (see figure 3.11). Due to the projection onto the subset $\{C_i\}$ of twisted sectors considered, this choice of monodromy conditions is well defined since all of the fields touched by this path are sewn together into a continuous cycle by the twisted boundary conditions.

To compute the entanglement entropy, the next step is to derive the zero-point conformal block on the replica surface for internal operators with weight $h_p = 0$ and $h_q = h_\Sigma$. This may be achieved in a perturbation expansion in $n-1$ using the monodromy method derived in section 3.4. The zeroth order in $n-1$ gives the $h_\Sigma$ character $\chi_\Sigma(\tau)$ as expected. The first order in $n-1$ yields the semiclassical zero-point block on the replica surface, analytically continued in $n$,

$$f_1 = \frac{1}{m}\log(\sin(\pi(L+w)/m)), \tag{3.134}$$

related to $Z^{\{C_i\}}_{n,\text{replica}}$ by

$$Z^{\{C_i\}}_{n,\text{replica}} \propto \chi_\Sigma(\tau)\bar{\chi}_\Sigma(\bar{\tau})e^{-c/6(n-1)(f_1+\bar{f}_1)}. \tag{3.135}$$

of order $O(N^0)$ and therefore these additional cycles produce only $O(N^0)$ corrections to the entanglement entropy, no matter how these cycles are chosen. These $O(N^0)$ corrections are neglected in the following. Therefore, in the notation below $N/m$ is implicitly rounded to an integer with the understanding that the rounding procedure only produces negligible $O(N^0)$ corrections.

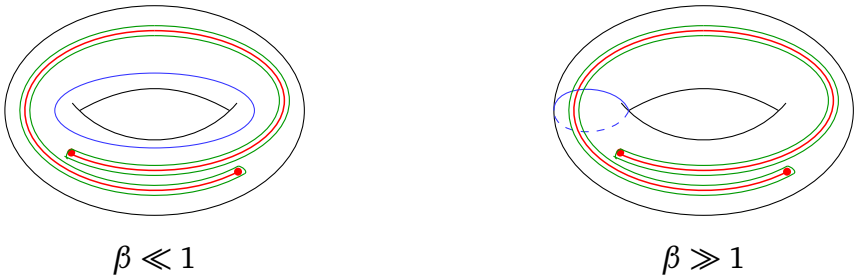


Figure 3.11.: Monodromy conditions for the calculation of the generalized entanglement entropy. Monodromy conditions for $h_q$ are imposed around the blue path and those for $h_p$ around the green path. The effective entangling interval winds $w = 1$ times around the space direction of the torus. Shown here is only the case of $w$ small compared to $m$ in which trivial monodromy is imposed for the green path encircling the effective entangling interval. For larger $w$, trivial monodromy is imposed around a path encircling the space direction of the torus $m - w$ times together with the complement of the effective entangling interval.

The proportionality constant includes OPE coefficients and multiplicity factors which drop out in the end. Thus, the generalized entanglement entropy is obtained from (3.55) to be

$$S_{\{A_i\},\{C_i\}} = \frac{N}{m}\frac{\tilde{c}}{3}\log\left[\frac{m}{\epsilon_{\text{UV}}}\sin\left(\frac{\pi(L+w)}{m}\right)\right] \quad (\beta > 2\pi m). \tag{3.136}$$

The crossover point $\beta = 2\pi m$ between the low and high temperature limits can be derived from the thermal partition function (see equation (C.28)). The result (3.136) is proportional to the length of a geodesic in thermal $\text{AdS}_3$ with opening angle $2\pi(L+w)/m$. Note that the proportionality constant between the geodesic length and the entanglement entropy is smaller by a factor of $1/m$ compared to the RT formula due to there being only $N/m$ branch cuts in the replica surface in total, compared to $N$ branch cuts in the ordinary entanglement entropy of spatial subregions.

### High temperatures

In the high temperature case, the leading contribution to the replica partition function comes from the identity block as for the ordinary entanglement entropy of a spatial subregion. This can be seem from the fact that the modular transformed identity character $\chi_{\mathbb{1}}(-1/\tau)$ includes contributions from all twisted sectors, which implies that the high temperature result for the thermal partition function of the $\{C_i\}$ subset is equal to the one for the full $S_N$ theory – up to a proportionality constant that drops out for the entanglement entropy in normalizing the reduced density matrix to one. Because the modular transformed character is obtained from trivial monodromy around the time circle, the entanglement entropy for the $\{C_i\}$ subset at high temperature is also given by a conformal block with trivial monodromy for $h_q$ around the time circle of the torus. The monodromy for $h_p$ is obtained by the same argument as for low temperatures: trivial monodromy is imposed around a path encircling $w$ times the spatial circle combined with the interval $[0, L]$ (see figure 3.11).

At high temperatures and for small intervals, the generalized entanglement entropy is given by

$$S_{\{A_i\},\{C_i\}} = \frac{N}{m}\frac{\tilde{c}}{3}\log\left[\frac{\beta}{2\pi^2\epsilon_{\text{UV}}}\sinh\left(\frac{2\pi^2(L+w)}{\beta}\right)\right] \quad (\beta < 2\pi m). \tag{3.137}$$

This is proportional to the length of a geodesic in the BTZ geometry with opening angle $2\pi L$ and winding number $w$, again with a proportionality factor $1/m$ times smaller than that of the RT formula. Note that for $2\pi m > \beta > 2\pi$, the dual geometry is in fact thermal $AdS_3$ while the entanglement entropy is still dual to the length of a geodesic in the BTZ black hole.

For large intervals, there is phase transition as in the ordinary entanglement entropy case,

$$S_{\{A_i\},\{C_i\}} = \frac{N\tilde{c}}{3}\frac{2\pi^2}{\beta} + \frac{N}{m}\frac{\tilde{c}}{3}\log\Big[\frac{\beta}{2\pi^2\epsilon_{\mathrm{UV}}}\sinh\Big(\frac{2\pi^2(m-L-w)}{\beta}\Big)\Big]. \tag{3.138}$$

Eq. (3.138) is dual to the thermal entropy of the BTZ black hole plus the length of a geodesic in the black hole geometry with opening angle $2\pi(1-L)$ and winding number $m-w-1$. Under the assumption that vacuum block dominance holds for all values of $L$ and $w$, the entanglement entropy is given by the minimum of (3.137) and (3.138) with a sharp crossover point.

### Multiple intervals

Let me now consider a subset $\{A_i\}$ of the degrees of freedom consisting of multiple disconnected components along a continuously connected cycle of $m$ fields. This subset is specified by a collection of an even number of coordinates $z_a \in [0,m]$ with $z_a < z_{a+1}$. If the coordinate $z = \phi + j$ belonging to the field $X^{i+j}$ for some $i \in (N/n)\mathbb{N}$ is contained in one of the intervals $[z_{2a}, z_{2a-1}]$, then the degrees of freedom of the field $X^{i+j}$ at the coordinate $\phi$ belong to the subset $\{A_i\}$ in consideration. The arguments given above then generalize to the multiple interval case in the same way as for the ordinary entanglement entropy, giving

$$S_{\{A_i\},\{C_i\}} = \frac{N}{m}\frac{\tilde{c}}{3}\sum_{(i,j)}\log\Big[\frac{m}{\epsilon_{\mathrm{UV}}}\sin\big(\pi(z_i - z_j)/m\big)\Big] \tag{3.139}$$

for low temperature ($\beta < 2\pi m$) and

$$S_{\{A_i\},\{C_i\}} = \frac{N}{m}\frac{\tilde{c}}{3}\sum_{(i,j)}\log\Big[\frac{\beta}{2\pi^2\epsilon_{\mathrm{UV}}}\sinh\Big(\frac{2\pi^2(z_i - z_j)}{\beta}\Big)\Big] \tag{3.140}$$

for high temperature ($\beta > 2\pi m$) and small intervals. Moreover, there is a phase transition for high temperatures and large intervals analogous to (3.138). Which combination of pairs $(i,j)$ to take depends on the interval sizes. As for the ordinary entanglement entropy, the combination that gives the lowest entanglement entropy dominates the replica partition function $Z^{\{C_i\}}_{n,\mathrm{replica}}$ if the vacuum block dominance property holds.

### Two-sided black holes

Of particular interest is the case of two intervals on opposite sides of a two-sided black hole. This is obtained by placing one of the two intervals at an offset $+\tau/2$ on the torus of the boundary theory. For two intervals of equal size $L < 1$ and with equal $w$, the generalized entanglement entropy is given by

$$S_{\{A_i\},\{C_i\}} = \begin{cases} \frac{N}{m}\frac{2\tilde{c}}{3}\log\Big[\frac{\beta}{2\pi^2\epsilon_{\mathrm{UV}}}\cosh\Big(\frac{4\pi^2 t}{\beta}\Big)\Big], & t < t_c \\ \frac{N}{m}\frac{2\tilde{c}}{3}\log\Big[\frac{\beta}{2\pi^2\epsilon_{\mathrm{UV}}}\sinh\Big(\frac{2\pi^2(w+L)}{\beta}\Big)\Big], & t > t_c \end{cases} \tag{3.141}$$

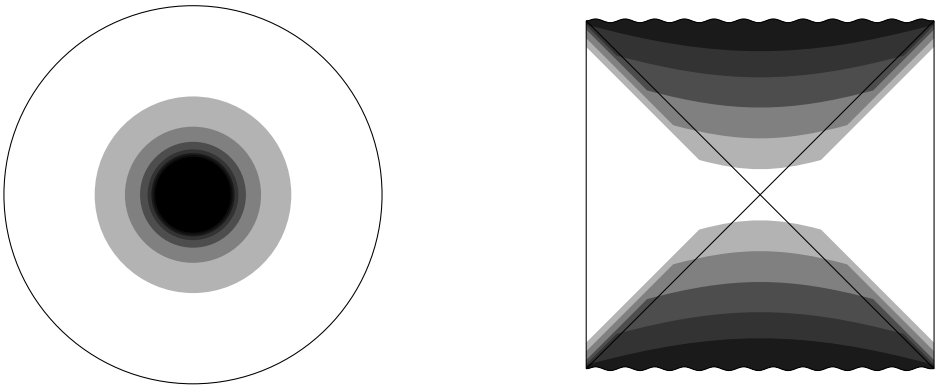

Figure 3.12.: Illustration of entanglement shadows for different winding numbers $w$ in a constant time-slice of the one-sided BTZ black hole (LHS) and the Penrose diagram of the two-sided BTZ black hole (RHS). As $w$ increases and the subset of the degrees of freedom for the generalized entanglement entropy becomes smaller, the entanglement shadow becomes smaller as indicated in progressively darker shades of gray.

where $t_c = \frac{\beta}{4\pi^2}\text{arcosh}\sinh(2\pi^2(w+L)/\beta) \approx (w+L)/2$. For early times $t < t_c$, eq. (3.141) is proportional to the length of two geodesics stretching from the endpoints of the entangling interval through the wormhole to the other side, while for late times $t > t_c$, the dual picture is given by two geodesics that do not enter the wormhole and wind $w$ times around the horizon.

### 3.6.2. Bulk geometry reconstruction

Let me now discuss the implications of the above results for the reconstruction of the bulk geometry from field theory entanglement data.

The winding geodesics dual to the generalized entanglement entropy probe a larger subregion of the BTZ geometry than the (non-winding) Ryu-Takayanagi surfaces dual to the ordinary entanglement entropy. The entanglement shadow decreases as the winding number $w$ (and with it the $m$ parameter) increases (see figure 3.12). For the one-sided black hole, geodesics with fixed winding number probe the spacetime up to a finite distance above the horizon. This distance decreases with increasing $w$. Likewise, the generalized entanglement entropy can probe a larger and larger region of the two-sided black hole interior as $w$ increases. The generalized entanglement entropy dual to the length of geodesics stretching through the interior of the two-sided BTZ geometry increases up to a critical time $t_c$ which is linear in $w$ while the ordinary entanglement entropy is restricted to $w = 0$.

In the strict $N \to \infty$ limit, $m$ and $w$ are unbounded from above and therefore it is possible to probe the the BTZ geometry up to the horizon in the one-sided case and in the entire space in the two-sided case. The black hole horizon is known to be an extremal surface barrier [232] for the one-sided black hole which means that the region behind the horizon is not accessible using any extremal surface anchored at only one asymptotic boundary. That the black hole interior cannot be probed for the one-sided black hole is likely a feature of the description of the black hole as a thermal average and might not hold for actual black hole microstates.

For large but finite $N$, the generalized entanglement entropy results are valid in a series expansion in $N$ to the leading order if $m = O(N^0)$. To go beyond the leading order in $N$ it would be in particular necessary to consider projections onto a smaller subset of the twisted sectors with $m = O(N)$ for which the results are no longer universal since multiple conformal blocks contribute to the partition function. Therefore, at large but finite $N$ the generalized entanglement entropy can only probe a part of the entire space and the approximation of the entanglement entropy as a

geodesic length becomes less and less accurate as the parameters $m$ and $w$ increase. It is striking that $1/N$ corrections to the entanglement entropy start to become important at the point where the geodesics dual to the generalized entanglement entropy probe close to the singularity in the two-sided case or the black hole horizon in the one-sided case. In particular, near the singularity strong quantum effects are expected to lead to a breakdown of the classical geometric spacetime description. This seems to find its counterpart in a large disagreement between geodesic lengths and entanglement entropies. From the CFT viewpoint, the limit on the winding number $w$ comes from a limit on how small the subset of degrees of freedom for the generalized entanglement entropy can be chosen. One can project out all twisted sectors apart from the maximally twisted sector but not more. Roughly speaking one might say that the size of the Hilbert space limits how small of a subset can be considered in the boundary field theory which corresponds to a limited resolution achievable for resolving the bulk geometry. This effect disappears for infinite $N$ where the classical spacetime description is valid.

### 3.6.3. String theory interpretation of twisted sectors

This section explains the interpretation of the projection onto twisted sectors $\{C_i\}$ in the dual string theory picture. Recall from section 2.1.4 that at the orbifold point, the string theory is in the tensionless limit in which the moduli of the torus worldsheets localize on holomorphic covering spaces of the boundary torus for the computation of the torus partition function from the gravity side [83, 86, 87]. In other words, the only contribution of torus worldsheets to this partition function comes from strings that wind an integer number of times around the time or space circle of the boundary torus.

From the equality of boundary field theory and string theory partition functions derived in [87], it can be seen that each cycle of length $m_i$ in a twisted sector of the boundary theory corresponds to a string with winding number $m_i$ around the space circle of the boundary torus.[24] Therefore, the restriction to certain twisted sectors in the boundary theory amounts to considering only string worldsheets with particular winding numbers around the spatial circle. For example, the untwisted sector corresponds to $N$ strings winding once around the spatial circle. The $\{C_i\}$ subset considered in this section corresponds to projecting onto the gravity degrees of freedom consisting of strings with winding number $km$ for $k \in \mathbb{N}$.

This clarifies why the projection onto twisted sectors in the boundary theory leads to geodesics with non-zero winding number in the bulk: only strings with non-zero winding numbers are considered. These strings form the natural probe of the non-contractible cycle in the bulk geometry from the gravity side. Note, however, that of course the classical geometric description of the bulk spacetime for which the notion of a geodesic makes sense is not a good description in the tensionless limit and thus this interpretation is somewhat limited in its applicability.

### 3.6.4. Entanglement entropy for single twisted sectors

Up to now, the generalized entanglement entropy was studied only for a very particular subset $\{C_i\}$ of twisted sectors. This section contains a discussion about the entanglement entropy resolved for a single twisted sector of the $S_N$ orbifold theory, i.e. the set $\{C_i\}$ contains only a single element

[24] Note that the partition function in consideration is in the canonical ensemble with fixed "particle number" $N$ [87]. In string perturbation theory it is more common to work in the grand-canonical ensemble in which $N$ is allowed to fluctuate. The canonical ensemble leads to an upper bound on the number of strings as well as on the winding number unlike in the grand-canonical ensemble where both quantities are unbounded. A related upper bound on the $R$-charge of chiral primaries in two-dimensional holographic CFTs which is not visible from the classical gravity theory has been dubbed the "stringy exclusion principle" [233].

$(1)^{n_1}...(N)^{n_N}$. In particular, I will discuss for which subsystems $\{A_i\}$ universal results independent of the seed theory of the $S_N$ orbifold are obtained in the limit $N \to \infty$.

The most general set of subregions $\{A_i\}$ one might consider for a single twisted sector consists of the union of an arbitrary number of intervals $[z^{(j)}_{m,2i-1}, z^{(j)}_{m,2i}]$ in the $j$-th cycle of length $m$ where $1 \leq j \leq n_m$. As in above, I will use the convention that an interval may contain the degrees of multiple fields connected by the boundary conditions if the size of the interval $|z^{(j)}_{m,2i} - z^{(j)}_{m,2i-1}|$ is larger than one. The contribution of a particular twisted sector to the thermal partition function is determined from (C.11), which decomposes into a product of contributions

$$Z_{(m)^{n_m}}(\tau) = \frac{1}{n_m} \sum_{k=1}^{n_m} Z_{(m)}(k\tau) Z_{(m)^{n_m-k}}(\tau) \tag{3.142}$$

from cycles of the same length $m$. This product structure extends to the replica partition function, thus it is sufficient to consider the contribution $S_{\{A_i\},\{C_i\},m}$ to the entanglement entropy of cycles with the same length $m$ separately. The total entanglement entropy is then obtained by summing over all $m$,

$$S_{\{A_i\},\{C_i\}} = \sum_m S_{\{A_i\},\{C_i\},m}. \tag{3.143}$$

I will first consider the case of a number $n_m$ of short cycles of length $m = O(N^0)$. As shown in appendix C, the contribution $Z_{(m)^{n_m}}$ of these cycles to the thermal partition function becomes universal if $n_m = O(N)$ (see equation (C.20)). If the same methods as above can be used to argue for vacuum block dominance of the contribution $Z_{(m)^{n_m},n,\text{replica}}$ to the replica partition function, then the universality extends to this contribution. For a general $\{A_i\}$, this is not possible because the methods used above rely on the entangling interval to be equal in each cycle, i.e. the $z^{(j)}_{m,i} \equiv z_{m,i}$ are equal for all $j$. That is, treating $Z_{(m)^{n_m},n,\text{replica}}$ as the partition function of a large central charge CFT on a branched cover of the torus and then applying the decomposition of this partition function into conformal blocks only works if the branch cuts for the fields of this auxiliary CFT all lie at the same position. If this holds, then for instance for a single interval the following universal contribution to the entanglement entropy is obtained,

$$S_{\{A_i\},\{C_i\},m} = \frac{\tilde{c}}{3} n_m \log\left(\frac{1}{\epsilon_{\text{UV}}} \sin\left(\frac{\pi(z_{m,2} - z_{m,1})}{m}\right)\right). \tag{3.144}$$

For long cycles of length $m = O(N)$, the contribution to the entanglement entropy is determined from the replica partition function $Z_{(m)^{n_m},n,\text{replica}}$ which decomposes into a number of (replica) seed partition functions with modular parameter that goes to zero as $N \to \infty$. For a general collection of entangling intervals, this will again not give a universal result. However, if the entangling intervals are small in the sense that $|z^{(j)}_{m,2i} - z^{(j)}_{m,2i-1}| = O(N^0)$, then the size of corresponding entangling intervals in the replica seed partition function goes to zero and the entangling intervals become well separated as $N \to \infty$. For example, in the case of a single interval $[z^{(j)}_{m,1}, z^{(j)}_{m,2}]$, the leading contribution to the replica partition function in limit $n \to 1$ is given by $\prod_j \tilde{Z}^{(j)}_{n,\text{replica}}(\tau/m)$ where $\tilde{Z}^{(j)}_{n,\text{replica}}(\tau/m)$ includes a single entangling interval from $z^{(j)}_{m,1}/m$ to $z^{(j)}_{m,2}/m$ the size of which goes to zero as $m \to \infty$. Contributions from other $\tilde{Z}_{n,\text{replica}}$, for instance $\tilde{Z}^{(j,k)}_{n,\text{replica}}(2\tau/m)$ which includes two entangling intervals $[z^{(j)}_{m,1}/m, z^{(j)}_{m,2}/m]$ and $[(z^{(k)}_{m,1} + \tau)/m, (z^{(k)}_{m,2} + \tau)/m]$, are suppressed by $e^{-N}$ factors as in the thermal partition function (see appendix C). The corresponding entanglement

entropy contribution is equal to

$$S_{\{A_i\},\{C_i\},m} = \frac{\tilde{c}}{3}\sum_j \log\left(\frac{\beta}{2\pi^2\epsilon_{\text{UV}}}\sinh\left(\frac{2\pi^2(z_{m,2}^{(j)} - z_{m,1}^{(j)})}{\beta}\right)\right). \tag{3.145}$$

Note that (3.144) and (3.145) are valid for all temperatures. The phase transition observed above comes only into play if one considers the contribution of a large number of twisted sectors including both those with long and those with short cycles.

### 3.6.5. Probability factors and fluctuation entropy

The thermal density matrix of the $S_N$ orbifold theory decomposes into twisted sector contributions,

$$\rho(\beta) = \bigoplus_C p_C(\beta)\rho_C(\beta), \tag{3.146}$$

with normalized density matrices $\text{Tr}\rho_C = 1$ and probability factors $p_C \in [0,1]$. These probability factors determine the relation between the total entanglement entropy $S_A$ and the entanglement entropy contribution $S_{A,C}$ resolved w.r.t. a single twisted sector,

$$S_A = \sum_C (p_C S_{A,C} - p_C \log p_C). \tag{3.147}$$

Block diagonal decompositions of the form (3.146) occur in a number of different contexts (see for instance [234–238]), where the first term of (3.147) has been called configurational or accessible entropy, while the second term is known as fluctuation, measurement or number entropy defined by

$$S_{\text{fluct.}} = -\sum_C p_C \log p_C. \tag{3.148}$$

Since this fluctuation entropy contributes to the total entanglement entropy, one might wonder whether this contribution plays an important part if projections onto twisted sectors come into play as in the generalized entanglement entropy considered above. In this section, I will determine the probability factors $p_C$ as well as the corresponding fluctuation entropy and show that their contribution to the total entanglement entropy is not important in the $S_N$ orbifold theory.

The $p_C$ factors are given by

$$p_C = \frac{1}{Z(\tau)} Z_{(1)^{n_1}\ldots(N)^{n_N}}(\tau), \tag{3.149}$$

where the twisted sector is specified by the conjugacy class $C$ containing $n_m$ cycles of length $m$. Using the results of app. C, it is easy to evaluate (3.149) in the large $N$ limit. For $\beta > 2\pi$, only the untwisted sector contributes, therefore $p_C$ is one for the untwisted sector and zero otherwise. For $\beta < 2\pi$, $p_C$ vanishes if the $C$ sector contains a large number of short cycles, i.e. if one of the $n_m$ is proportional to $N$. Otherwise, $p_C = (\prod_m m^{n_m} n_m!)^{-1}$. Note that $\sum_C (\prod_m m^{n_m} n_m!)^{-1} = 1$ as is appropriate for a probability distribution. The above formulas for $p_C$ hold up to corrections of order $e^{-N}$.

The corresponding fluctuation entropy vanishes for $\beta > 2\pi$ and scales sublinearly in $N$ (roughly proportional to $\sqrt{N}$) for $\beta < 2\pi$. Note that this entropy contribution drops out in the total thermal entropy, which is given by

$$S(\beta) = -\text{Tr}(\rho(\beta)\log\rho(\beta)) = -\sum_C \text{Tr}(p_C\rho_C \log(p_C\rho_C)) = \sum_C p_C S_C(\beta) + S_{\text{fluct.}}, \tag{3.150}$$

where $S_C(\beta)$ is the thermal entropy of the $Z_{(1)^{n_1}\ldots(N)^{n_N}}(\tau)$ contribution to $Z(\tau)$. This can be seen from the definition of the thermal entropy in terms of the partition function,

$$S(\beta) = \log Z(\tau) - \beta \frac{\partial \log Z(\tau)}{\partial \beta} = \begin{cases} 0, & \beta > 2\pi \\ \dfrac{2\tilde{c}N}{3\beta}, & \beta < 2\pi. \end{cases} \tag{3.151}$$

For $\beta > 2\pi$, the fluctuation entropy vanishes identically. For $\beta < 2\pi$, $Z_{(1)^{n_1}\ldots(N)^{n_N}}(\tau) = p_C e^{\frac{\tilde{c}N}{12}\frac{4\pi^2}{\beta}}$ and the $p_C$ prefactor cancels with the $S_{\text{fluct.}}$ contribution. Since the reduced density matrix $\rho_A$ for the ordinary entanglement entropy of a spatial subregion in the full $S_N$ theory is obtained by tracing out the complement of $A$ in each of the twisted sectors separately, the entanglement entropy contains the same fluctuation entropy contribution as the thermal entropy and therefore the same cancellation happens for the entanglement entropy.

### 3.6.6. Deformations of the $S_N$ orbifold

In section 3.6.1, it was found that the generalized entanglement entropy for thermal states of the $S_N$ orbifold theory is proportional to the length of a geodesic in the BTZ geometry. At first glance this is somewhat surprising because at the orbifold point the boundary CFT is weakly coupled and dual to a strongly coupled gravity theory. Therefore, at this point in the moduli space the description by classical supergravity, in which the notion of a geodesic makes sense, is not applicable. In this section, I will investigate which properties of the generalized entanglement entropy expressions derived in section 3.6.1 survive the deformation away from the orbifold point.[25] Due to the need to use perturbation theory, the deformation is parametrically small and does not take us all the way to the supergravity point. Nevertheless, it provides some indication as to whether the generalized entanglement entropy results from section 3.6.1 can also hold at the supergravity point.

Recall from section 2.1.4 that the $S_N$ orbifold theory possesses 20 exactly marginal operators which can be used to deform the boundary theory to another CFT. 16 of those operators are in the untwisted sector. These are simple to handle since they leave the orbifold structure invariant: they just deform the CFT to a $S_N$ orbifold of a different seed theory. But since the results of section 3.6.1 are independent of the seed theory, these deformations do not change the entanglement entropy.

The remaining four exactly marginal two-cycle twist operators are more interesting because they deform the CFT away from the weak coupling point. In the following, I will derive how this deformation affects the entanglement entropy to the first non-trivial order in conformal perturbation theory and at leading order in the large $N$ limit. The derivation is based on the assumption that the deformed theory possesses the same vacuum block dominance properties (i.e. sparse spectrum of low dimension operators and at most exponentially growing OPE coefficients) as the $S_N$ orbifold. The fact that the RT formula at strong coupling gives the same entanglement entropy result as is obtained here at the weakly coupled orbifold point indicates that this assumption is likely justified, although I have not proven it from first principles. Under this assumption, the entanglement entropy is obtained from the conformal block whose internal operators have the lowest dimension compatible with the projection onto the subset $\{C_i\}$ of twisted sectors, since the same operators in the deformed theory are projected out as in the $S_N$ orbifold.

Therefore, it remains to determine the anomalous dimensions of the primaries of the $S_N$ orbifold theory. The conformal weight of the identity operator in the deformed theory is given by $h = \bar{h} = 0$ as in the $S_N$ orbifold. Moreover, from arguments given below I will argue that the anomalous di-

[25] For previous work on deformations of the $S_N$ orbifold, see [99, 239–255].

mension of operators in twisted sectors that consist of $\lfloor N/m \rfloor = O(N)$ cycles of length $m$ together with an arbitrary collection of cycles for the remaining $N - \lfloor N/m \rfloor$ fields vanishes up to $O(N^0)$ corrections to second order in conformal perturbation theory. Under the assumption of vacuum block dominance, this implies that the partition functions considered in section 3.6.1 are invariant under deformations up to $O(N^0)$ corrections. This holds for both the contribution of the $\{C_i\}$ subset to the thermal partition function function as well as for the replica partition function $Z^{\{C_i\}}_{n,\text{replica}}$ since these partition functions are dominated by characters or conformal blocks of the aforementioned operators which only receive small corrections to the conformal weight in the large $N$ limit.[26] Note that while the insertion of two-cycle twist operators into the replica partition function changes the boundary conditions for some of the fields of the $S_N$ orbifold and thus the monodromy conditions for the conformal blocks may differ from those of section 3.6.1, as long as only an $O(N^0)$ number of such operators are inserted this will not change the leading order in $N$ of the entanglement entropy result.

These arguments imply that the entanglement entropy is invariant up to corrections of order $O(N^0)$ for deformations to second order in conformal perturbation theory. It is likely that similar arguments can be used to show invariance also to higher orders, although the growing complexity of the involved conformal blocks and OPE coefficients quickly makes the calculation intractable.

### Anomalous dimensions for primaries of the $S_N$ orbifold

In this subsection, I will determine bounds on the scaling with $N$ of the anomalous dimension of a general primary $\Sigma$ in an arbitrary twisted sector of the $S_N$ orbifold theory.

Let me first consider the untwisted sector. It is easy to see that the contribution of the untwisted sector to the thermal or replica partition function is invariant under deformations to all orders in perturbation theory. Every CFT possesses an identity operator with conformal weight $h = \bar{h} = 0$ which must be in the untwisted sector since twisting the boundary conditions incurs an energy cost. Since conformal blocks of the identity operator give the dominant contribution to the ordinary entanglement entropy of spatial subregions under the assumption of vacuum block dominance, this implies that the ordinary entanglement entropy is invariant under deformations.

To determine the anomalous dimension of an operator $\Sigma$ in some other twisted sector of the $S_N$ orbifold, the deformation operator $\exp\left(\lambda \int d^2w\, \Phi(w,\bar{w})\right)$ is inserted in the two-point function $\langle \Sigma(z_1,\bar{z}_1)\Sigma(z_2,\bar{z}_2)\rangle$ and expanded in the deformation parameter $\lambda$,

$$\begin{aligned}\langle \Sigma(z_1,\bar{z}_1)\Sigma(z_2,\bar{z}_2) e^{\lambda \int d^2w\, \Phi(w,\bar{w})}\rangle = \langle \Sigma(z_1,\bar{z}_1)\Sigma(z_2,\bar{z}_2)\rangle &+ \lambda \int d^2w \langle \Phi(w,\bar{w})\Sigma(z_1,\bar{z}_1)\Sigma(z_2,\bar{z}_2)\rangle \\ &+ \frac{\lambda^2}{2}\int d^2w_1 d^2w_2 \langle \Phi(w_1,\bar{w}_1)\Phi(w_2,\bar{w}_2)\Sigma(z_1,\bar{z}_1)\Sigma(z_2,\bar{z}_2)\rangle \\ &+ O(\lambda^3).\end{aligned} \tag{3.152}$$

Here, $\Phi(z,\bar{z})$ denotes one of the exactly marginal two-cycle twist operators of the $S_N$ orbifold theory. To determine the anomalous dimensions $h_\Sigma(\lambda)$ and $\bar{h}_\Sigma(\lambda)$, this is to be compared with the

[26] Strictly speaking, for the high temperature phase this argument assumes that the projection onto the $\{C_i\}$ subset in the deformed theory does not project out exactly those twisted sectors that are responsible for the leading order contribution to the thermal partition function at high temperatures. It seems unlikely for this to happen, because projections with different $m$ project out different subsets of the twisted sectors and thus the leading order for the thermal partition function would have to come from the contributions of a very small subset of the twisted sectors that includes neither the vacuum (which is known not to be dominant for high temperature) nor any of the sectors that are projected onto for any value of $m \in \mathbb{N}$. At the orbifold point, it is known from appendix C that this subset does not give the leading order contribution of the partition function at large $N$.

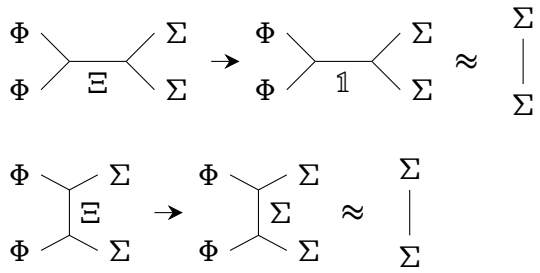


Figure 3.13.: The leading contribution to the anomalous dimension of $h_\Sigma$ comes from the conformal block where $\Phi\Phi$ fuse together into $\Xi = \mathbb{1}$ (upper part) or $\Phi\Sigma$ fuse together into $\Xi = \Sigma$ (lower part). Due to the conformal weight of $\Phi$ being of order $N^0$, these blocks are approximately equal to the two-point function $\langle\Sigma\Sigma\rangle$ in the large $N$ limit.

expansion of the two-point function in the deformed theory,

$$\langle\Sigma(z_1,\bar{z}_1)\Sigma(z_2,\bar{z}_2)\rangle_\lambda = \frac{1}{(z_1-z_2)^{2h_\Sigma(\lambda)}(\bar{z}_1-\bar{z}_2)^{2\bar{h}_\Sigma(\lambda)}}. \tag{3.153}$$

The $n$-th order in the series expansion of the anomalous dimension is then obtained from the $n+2$-point function of $\Sigma$ and $\Phi$ in (3.152). The first order in $\lambda$ of the anomalous dimension vanishes because the OPE coefficient $C^{\Phi}_{\Sigma\Sigma}$ vanishes between the two-cycle twist operator $\Phi$ and any $\Sigma$. For the second order, the four-point function in (3.152) is expanded in conformal blocks (see figure 3.13),

$$\begin{aligned}\langle\Phi(w_1,\bar{w}_1)\Phi(w_2,\bar{w}_2)\Sigma(z_1,\bar{z}_1)\Sigma(z_2,\bar{z}_2)\rangle &= \sum_\Xi (C^\Xi_{\Phi\Sigma})^2 \mathscr{F}^\Xi_{\Phi\Sigma,\Phi\Sigma}\bar{\mathscr{F}}^\Xi_{\Phi\Sigma,\Phi\Sigma} \\ &= \sum_\Xi C^\Xi_{\Sigma\Sigma}C^\Xi_{\Phi\Phi}\mathscr{F}^\Xi_{\Sigma\Sigma,\Phi\Phi}\bar{\mathscr{F}}^\Xi_{\Sigma\Sigma,\Phi\Phi}.\end{aligned} \tag{3.154}$$

In the large $N$ limit the conformal blocks exponentiate, $\mathscr{F} \sim e^{-c/6 f_{\text{cl.}}}$. The fact that the semiclassical blocks $f_{\text{cl.}}$ increase with increasing weight $h_\Xi$ of the internal primary operator $\Xi$ [27] ensures that the leading contribution comes from the conformal block with lowest $h_\Xi$. Note that conformal blocks in different channels exchange dominance as $z_1, z_2, w_1, w_2$ are varied, thus all possible channels need to be considered. This is essentially a vacuum block dominance argument, only this time applied to the four-point function on the plane. Conformal blocks for other $\Xi$ are suppressed by factors of $e^{-N}$. The leading contribution at large $N$ is then equal to the two-point function $\langle\Sigma\Sigma\rangle$ without insertions of $\Phi(z,\bar{z})$ (see fig. 3.13).

However, in general other contributions to the anomalous dimension at linear order in $N$ come from the OPE coefficients and multiplicities. Below, I will show that such contributions are absent for states in twisted sectors that consist of $\lfloor N/m\rfloor = O(N)$ cycles of length $m$ together with an arbitrary collection of cycles for the remaining $N - \lfloor N/m\rfloor$ fields. Thus the conformal weight of the corresponding operators $\Sigma$ is invariant up to $O(N^0)$ corrections.

I will now determine the combinatorical factors for the OPE coefficients contributing to the anomalous dimension of the deformed $S_N$ orbifold. To second order in conformal perturbation theory, the relevant OPE coefficients come from the decomposition (3.154). Therefore, the task at hand is to determine the scaling with $N$ of the OPE coefficients

$$C^\Xi_{\Phi\Sigma}, C^\Xi_{\Sigma\Sigma}, C^\Xi_{\Phi\Phi} \tag{3.155}$$

[27] This can be seen numerically from the series expansion of the conformal blocks [103].

and the multiplicity factor, i.e. the number of operators $\Xi$ with lowest weight $h_\Xi$ which are not suppressed by $e^{-N}$ factors from the conformal block.

The computation of the large $N$ scaling properties is achieved using combinatorics of the $S_N$ group. A gauge invariant operator $\Sigma$ of the $S_N$ orbifold theory is obtained from a reference operator $\hat{\Sigma}$ by conjugating with elements of the $S_N$ gauge group,

$$\Sigma = \frac{1}{\sqrt{A_\Sigma}} \sum_{g \in S_N} g \hat{\Sigma} g^{-1}, \tag{3.156}$$

where $A_\Sigma$ is a normalization factor. The twist selection rule of the $S_N$ orbifold theory states that an n point function $\langle \hat{\Sigma}_1 ... \hat{\Sigma}_n \rangle$ with boundary conditions for the operators $\hat{\Sigma}_i$ determined by the $S_N$ group element $g_i$ is non-vanishing only if the product of all $g_i$ is the identity,

$$\prod_i g_i = \mathbb{1}. \tag{3.157}$$

Therefore, the combinatorical factors of interest are computed by employing the twist selection rule (3.157) to count how many terms of the sum in (3.156) contribute to the three-point function determining the OPE coefficients (3.155). See for instance [230, 256] for related computations of OPE coefficients of the $S_N$ orbifold theory using the same techniques.

First, I will determine the normalization factor $A_\Sigma$ for a general $\Sigma$ in the twisted sector determined by $\{n_m^\Sigma\} \equiv \{n_m\}$ by demanding that the two-point function $\langle \Sigma(0)\Sigma(\infty) \rangle$ be equal to one. It is easy to see that one of the two operators in $\langle \Sigma(0)\Sigma(\infty) \rangle$ can be fixed to the reference operator $\hat{\Sigma}$, i.e. one of the two sums over $g \in S_N$ drops out. This yields an $N!$ factor. The boundary conditions for the other operator must be inverse to those of $\hat{\Sigma}$. This happens only if the $g$ element in the remaining sum over $S_N$ is in the stabilizer subgroup $N_\Sigma$ of $\hat{\Sigma}$. This subgroup is of size $|N_\Sigma| = \prod_m m^{n_m} n_m!$, yielding in total

$$A_\Sigma = N! \prod_m m^{n_m} n_m!. \tag{3.158}$$

In the next step, I will determine the OPE coefficients. Let $\Sigma$ be in a generic $(1)^{n_1} ... (N)^{n_N}$ twisted sector in the following. I will use the shorthand notation

$$\hat{C}^{\Sigma_1}_{\Sigma_2 \Sigma_3} \sim \sqrt{A_{\Sigma_1} A_{\Sigma_2} A_{\Sigma_3}} \frac{C^{\Sigma_1}_{\Sigma_2 \Sigma_3}}{N! |N_{\Sigma_2}| |N_{\Sigma_3}|}. \tag{3.159}$$

The $\sim$ symbol denotes that only the combinatorical factors from the $S_N$ orbifold are considered and not further dependencies on excitations in the seed theory.

Let me start with $C^\Xi_{\Phi\Sigma}$. The action of the two-cycle twist operator $\Phi$ on $\Xi$ is to either splice together two cycles $(m1)(m2) \to (m1{+}m2)$ or to split apart a single cycle $(m1{+}m2) \to (m1)(m2)$. If two cycles of the same length $m$ are spliced together, this gives a contribution $\hat{C}^\Xi_{\Phi\Sigma} = m^2 \frac{1}{2}(n_m + 1)(n_m + 2)$ since for $C^\Xi_{\Phi\Sigma}$ to be non-vanishing there must be $n_m + 2$ cycles of length $m$ in $\Xi$ and there are $\binom{n_m+2}{2} = \frac{1}{2}(n_m + 1)(n_m + 2)$ possibilities to choose two cycles to splice together and $m$ possibilities to choose an element inside each cycle. Thus,

$$C^\Xi_{\Phi\Sigma} \sim \sqrt{\frac{m^3 n_{2m}(n_m + 1)(n_m + 2)}{N(N-1)}}. \tag{3.160}$$

Splicing two cycles of different lengths $m_1, m_2$ together yields $\hat{C}^\Xi_{\Phi\Sigma} = m_1 m_2 (n_{m_1} + 1)(n_{m_2} + 1)$ with

an analogous counting argument,

$$C^{\Xi}_{\Phi\Sigma} \sim \sqrt{\frac{2m_1m_2(m_1+m_2)n_{m_1+m_2}(n_{m_1}+1)(n_{m_2}+1)}{N(N-1)}}. \tag{3.161}$$

Similarly, for splitting apart a cycle into two cycles of equal length $m$, one gets $\hat{C}^{\Xi}_{\Phi\Sigma} = m(n_{2m}+1)$ for cycles with the same length $m$ since there are $n_{2m}+1$ cycles to choose and in each cycle there are $m$ possible splittings, yielding

$$C^{\Xi}_{\Phi\Sigma} \sim \sqrt{\frac{m^3 n_m(n_m-1)(n_{2m}+1)}{N(N-1)}}. \tag{3.162}$$

Splitting apart a cycle into two cycles of different lengths $m_1, m_2$ gives $\hat{C}^{\Xi}_{\Phi\Sigma} = (m_1+m_2)(n_{m_1+m_2}+1)$,

$$C^{\Xi}_{\Phi\Sigma} \sim \sqrt{\frac{2m_1m_2(m_1+m_2)n_{m_1}n_{m_2}(n_{m_1+m_2}+1)}{N(N-1)}}. \tag{3.163}$$

Next, let me consider $C^{\Xi}_{\Sigma\Sigma}$ and $C^{\Xi}_{\Phi\Phi}$. The latter OPE coefficient only allows

$$\Xi \in \{(1)^N, (1)^{N-3}(3), (1)^{N-4}(2)^2\}, \tag{3.164}$$

thus $C^{\Xi}_{\Sigma\Sigma}$ needs to be computed only for these $\Xi$. The case $\Xi \in (1)^N$ is simple since for the identity operator all combinatorical factors drop out,

$$C^{\Xi}_{\Sigma\Sigma} \sim C^{\Xi}_{\Phi\Phi} \sim 1. \tag{3.165}$$

In the other two cases, $C^{\Xi}_{\Phi\Phi}$ is obtained as a special case of the $C^{\Xi}_{\Phi\Sigma}$ OPE coefficient derived above, giving

$$\begin{aligned} C^{\Xi}_{\Phi\Phi} &\sim \sqrt{\frac{12(N-2)}{N(N-1)}}, \quad \Xi \in (1)^{N-3}(3) \\ C^{\Xi}_{\Phi\Phi} &\sim \sqrt{\frac{2(N-2)(N-3)}{N(N-1)}}, \quad \Xi \in (1)^{N-4}(2)^2 \end{aligned} \tag{3.166}$$

It remains to compute $C^{\Xi}_{\Sigma\Sigma}$. In order for $C^{\Xi}_{\Sigma\Sigma}$ to be non-vanishing $\Xi$ applied to $\Sigma$ must give an operator in the same conjugacy class as $\Sigma$. For the case $\Xi \in (1)^{N-3}(3)$, the non-trivial 3 cycle permutation in $\Xi$ applied onto a single cycle of length $m \geq 3$ again yields a cycle of length $m$ in $\binom{m}{3}$ cases. Moreover, the 3 cycle can also act on two cycles $(m_1)(m_2)$ with $m_1 < m_2$ at the same time, giving again another two $(m_1)(m_2)$ cycles in $m_1m_2$ cases. Thus, for $\Xi \in (1)^{N-3}(3)$ the combinatorical factors of the OPE coefficient are given by

$$C^{\Xi}_{\Sigma\Sigma} \sim \sqrt{\frac{3}{N(N-1)(N-2)}}\left[\sum_{m=3}^{N} n_m \binom{m}{3} + \sum_{m_1=1}^{N}\sum_{m_2=m_1+1}^{N} n_{m_1}n_{m_2}m_1m_2\right]. \tag{3.167}$$

Finally, for the $\Xi \in (1)^{N-4}(2)^2$ case, the two non-trivial 2 cycle permutations can act on either 1, 2 or 3 cycles simultaneously to give the same cycle structure again. For one cycle $(m) \to (m)$, there are $\binom{m}{4}$ possibilities. For two cycles $(m_1)(m_2) \to (m_1)(m_2)$ there are $m_1m_2(m_2-2)$ possibilities for $m_1 < m_2$ and $\frac{1}{2}m^2(m-1)$ possibilities for $m_1 = m_2 = m$. In the three cycle case $(m_1)(m_2)(m_1+m_2) \to (m_1)(m_2)(m_1+m_2)$, one of the 2 cycle permutations splices $(m_1)(m_2)$

together into a $(m_1+m_2)$ cycle while the other 2 cycle permutation splits apart $(m_1+m_2)$ into $(m_1)(m_2)$. There are $m_1m_2(m_1+m_2)$ possibilities in this case if $m_1<m_2$ and $m^3$ possibilities if $m_1=m_2=m$. In total, the combinatorical factors of the OPE coefficient are given by

$$\begin{aligned} C^{\Xi}_{\Sigma\Sigma} \sim \sqrt{\frac{8(N-4)!}{N!}}\Bigg[ &\sum_{m=4}^{N} n_m \binom{m}{4} + \sum_{m_1=1}^{N}\sum_{m_2=m_1+1}^{N} n_{m_1}n_{m_2}m_1m_2(m_2-1) \\ &+ \sum_{m=1}^{N}\frac{1}{4}n_m(n_m-1)m^2(m-1) \\ &+ \sum_{m_1=1}^{N}\sum_{m_2=m_1+1}^{N/2-m_1} n_{m_1}n_{m_2}n_{m_1+m_2}m_1m_2(m_1+m_2) \\ &+ \sum_{m=1}^{N/4}\frac{1}{2}n_m(n_m-1)n_{2m}m^3\Bigg]. \end{aligned} \tag{3.168}$$

Let me now consider an operator $\Sigma$ comprised of $\lfloor N/m\rfloor = O(N)$ cycles of length $m=O(N^0)$ and any number of cycles in the remaining $N-\lfloor N/m\rfloor$ elements. For this operator, $n_k=\lfloor N/m\rfloor\delta_{k,m}+O(N^0)$. Inserting this in the above expressions, it is easy to see that all OPE coefficients scale at most as $O(N^0)$. I further note that $h_\Xi \geq h_\Sigma + O(N^0)$ for the $C^{\Xi}_{\Phi\Sigma}$ coefficients and $h_\Xi \geq 0$ for the $C^{\Xi}_{\Phi\Phi}C^{\Xi}_{\Sigma\Sigma}$ coefficients. At the minimum value for $h_\Xi$, the conformal block reduces to the two-point function $\langle\Sigma\Sigma\rangle$ times the OPE coefficients and a multiplicity factor. Moreover, the multiplicity factor for the $\Sigma$ in consideration is also of order $O(N^0)$: there are only an $O(N^0)$ number of twisted sectors in which $\Xi$ can lie. Any $O(N)$ number of excitations on top of the ground states of these twisted sectors will also cause $h_\Xi$ to shift by an $O(N)$ term. The contribution of these excited $\Xi$ is suppressed by powers of $e^{-N}$ from the conformal blocks and can be neglected.

More general $\Sigma$, however, may receive large corrections. For instance all $\Sigma$ that are in a twisted sector containing at least one long cycle of length $m=O(N)$ have multiplicities and OPE coefficients that scale with $O(N)$. Thus, it is not possible use the above techniques to argue for the absence of $O(N)$ corrections to the anomalous dimension for operators in these twisted sectors.

Nevertheless, a partition or correlation function that for $\lambda=0$ is dominated by conformal blocks with operators whose scaling dimension is invariant under deformations will be dominated by the same conformal blocks in a perturbation expansion in $\lambda$. Let for instance the partition function $Z_\lambda(\tau)$, given by

$$Z_\lambda(\tau) = \sum_{\Sigma}\chi_{\Sigma,\lambda}(\tau)\bar{\chi}_{\Sigma,\lambda}(\bar{\tau}), \tag{3.169}$$

be dominated by $\Sigma_0$ for $\lambda=0$,

$$Z_0(\tau) \approx \chi_{\Sigma_0}(\tau)\bar{\chi}_{\Sigma_0}(\bar{\tau}). \tag{3.170}$$

Then, the logarithm of $Z_\lambda(\tau)$ is expanded in $\lambda$ as follows,

$$\log Z_\lambda(\tau) = \log Z_0(\tau) + \frac{\partial_\lambda Z_\lambda(\tau)|_{\lambda=0}}{Z_0(\tau)}\lambda + O(\lambda^2), \tag{3.171}$$

where (using that in the large $N$ limit $\chi_\Sigma(\tau)\approx e^{-\beta(h_\Sigma - c/24)}$)

$$\partial_\lambda Z_\lambda(\tau)|_{\lambda=0} \approx -\beta\sum_{\Sigma} e^{-\beta(h_\Sigma(0)+\bar{h}_\Sigma(0)-\frac{c}{12})}\,\partial_\lambda(h_\Sigma(\lambda)+\bar{h}_\Sigma(\lambda))\big|_{\lambda=0}. \tag{3.172}$$

Due to $h_\Sigma(0)$ scaling with $O(N)$ and $h_\Sigma(0) > h_{\Sigma_0}(0)$ together with analogous statements for $\bar{h}_\Sigma$,

$\partial_\lambda Z_\lambda(\tau)|_{\lambda=0}$ is dominated by the $\Sigma = \Sigma_0$ term non withstanding any polynomial corrections in $N$ to $h_\Sigma(\lambda)$ for $\Sigma \neq \Sigma_0$. It is easy to see that similar arguments work for any correlation function which obeys the vacuum block dominance property for $S_N$ orbifold theory.

# 4. Quantum circuits of the Virasoro group and computational complexity in AdS/CFT

Recent years have seen a surge of interest in the implementation of quantum circuits in AdS/CFT, following conjectures in [51–54] that relate features of two-sided AdS black hole geometries to the computational complexity of corresponding quantum circuits. In this chapter, I will study aspects of quantum circuits composed out of conformal group transformations, in particular their mapping to gravity and computational complexity measures as well as their holographic duals in these circuits.

I will start in section 4.1 with a brief introduction and an explanation of the motivation behind choosing conformal symmetry transformations for the quantum circuits considered in this chapter. I will subsequently present the construction of these quantum circuits in detail in section 4.2 before studying examples of computational complexity measures based on geometric actions on coadjoint orbits in section 4.3 and the Fubini-Study metric in section 4.4. Finally, to go beyond examples and facilitate the study of relations between computational complexity measures and dual quantities in the gravity theory, it becomes necessary to derive the bulk dual to the quantum circuits studied in this chapter which is presented in section 4.5.

## 4.1. Introduction and motivation

In section 2.3, an introduction to quantum circuits for the study of quantum aspects of black holes was given. In particular, the conjecture from [51–54] that computational complexity in quantum circuits is related to geometric properties of black holes in AdS was explained in detail. The conjecture states that the time evolution of computational complexity is dual to the growth of the behind-the-horizon region of an AdS black hole or wormhole geometry. It is this conjecture that forms the main motivation for the investigations in this chapter into computational complexity in the boundary CFT and more generally implementing quantum circuits in AdS/CFT. However, I will not limit myself to exactly the same setup as in [51–54]. Instead, the aim is more generally to implement quantum circuits and computational complexity measures in AdS/CFT even if those circuits deviate somewhat from what was considered in [51–54].

Performing an analysis of computational complexity in AdS/CFT is not an easy task to do in full generality, especially due to the strong coupling in the boundary CFT. Previous work on computational complexity in quantum field theory has focused heavily on free theories, see for example [164–171] as well as the references in the review [142]. Here, I will pursue a different direction by restricting to a special class of quantum circuits built up from conformal transformations in two-dimensional conformal field theories. Although with these transformations one can explore only a part of the quantum circuits that are possible in general (the circuits which move only between states in the same Verma module), there are a number of advantages to this approach. First, note that the conformal transformations form a subspace of the operator set of all holographic quantum field theories and even in many interesting non-holographic field theories

such as the Ising model at the critical point. Therefore, universal results may be obtained which are valid for all AdS/CFT models which would not necessarily be the case if for instance circuits generated by a scalar operator were considered. Moreover, the approach is applicable for interacting and in particular also strongly coupled field theories.[1] Finally, further work [265–269] in these circuits has found some interesting connections between computational complexity measures and holographic complexity proposals in the gravity theory which deserve to be explored in more detail as is done in this chapter.

The goal of this chapter is to develop dualities between computational complexity measures in the boundary CFT and geometric features of the dual bulk geometry. In particular, the aim will be to investigate if these geometric features can probe the wormhole growth to verify the conjecture of [51–54] in the special case of our setup.

Let me now summarize the most important aspects of the computational complexity measures studied in the rest of this chapter. The complexity measures in this chapter are all based on the continuous gate counting approach reviewed in section 2.3.4 where the set of gates is infinite dimensional and a cost is assigned to the infinitesimal gates applied at each time step such that the computational complexity is given by the minimum of the total cost. Therefore, two choices have to be made to define a computational complexity measure: a set of elementary gates comprising the basic "computing elements" in the circuit as well as a cost function $\mathscr{F}$ specifying how complicated it is to apply a certain gate. In this chapter, the gate set is chosen as the set of Virasoro generators $L_n$ such that at each time step the circuit generator $Q(\tau) = \sum_n \epsilon_n(\tau) L_{-n}$ is applied where the prefactors $\epsilon_n(\tau)$ parametrize the circuit (see section 4.2 for details).

I will consider multiple cost functions in the following. First, in [266, 270] the choice

$$\mathscr{F}(\tau) = |\langle\psi(\tau)|Q(\tau)|\psi(\tau)\rangle| \tag{4.1}$$

was investigated and close connections with geometric actions on coadjoint orbits were found. These connections are extended in section 4.3 by showing that a suitable modification of (4.1) yields a computational complexity measure that is given exactly by the geometric action on the coadjoint orbit corresponding to the Verma module in which the circuit lives. Subsequently, the viability of these geometric actions as complexity measures is investigated. This investigation largely rules out the possibility put forward in [266] that geometric actions on coadjoint orbits can implement a "complexity=action" type duality, i.e. a duality between a computational complexity measure and a gravity action evaluated on some part of the bulk manifold.

Another interesting choice of cost function is determined from the Fubini-Study metric, a metric on a projective Hilbert space[2] with line element [271]

$$ds^2_{\text{FS}} = \frac{\langle\delta\psi|\delta\psi\rangle}{\langle\psi|\psi\rangle} - \frac{\langle\delta\psi|\psi\rangle\langle\psi|\delta\psi\rangle}{\langle\psi|\psi\rangle^2}. \tag{4.2}$$

The Fubini-Study metric is the unique Riemannian metric on a projective Hilbert space invariant under the unitary group acting on Hilbert space elements.[3] For canonically normalized states

[1] Studies of computational complexity in interacting QFTs are much less common than those in free theories. An example which does not make use of symmetry groups (as is done in this thesis) can be found in [257] where a scalar field theory with a weak $\phi^4$ interaction was considered. In quantum mechanics, there have been a number of studies of computational complexity for chaotic interacting systems (see [258–264]) such as random matrix theories or the Sachdev-Ye-Kitaev model which in AdS/CFT are related to two-dimensional gravity.

[2] A projective Hilbert space arises from a Hilbert space by identifying states related by multiplication with complex numbers, $|\psi\rangle = \lambda|\chi\rangle$ for $\lambda \in \mathbb{C}$. For normalized states $\langle\psi|\psi\rangle = \langle\chi|\chi\rangle = 1$, this identifies two states related by phase changes. Thus, projective Hilbert space is the space of physically distinct states.

[3] Note that there also exists a generalization of the Fubini-Study metric to mixed states which is known as the Bures metric. The geodesic distance for the Bures metric is given by $D(\rho,\sigma) = \arccos\sqrt{F(\rho,\sigma)}$ where

$|\psi\rangle = |\psi(\tau)\rangle$ and $|\delta\psi\rangle = \partial_\tau|\psi(\tau)\rangle$ related by time evolution with $Q(\tau)$, i.e. $|\psi(\tau + d\tau)\rangle = e^{iQ(\tau)d\tau}|\psi(\tau)\rangle \approx |\psi(\tau)\rangle + |\delta\psi\rangle d\tau$, the Fubini-Study line element is given by the variance of $Q(\tau)$,

$$ds^2_{\text{FS}} = |\langle\psi(\tau)|Q(\tau)^2|\psi(\tau)\rangle| - |\langle\psi(\tau)|Q(\tau)|\psi(\tau)\rangle|^2. \tag{4.3}$$

The Fubini-Study line element was investigated as the cost function in a computational complexity measure first in [165] for Gaussian states of free quantum field theories and then for the Virasoro circuits considered in this chapter in [268, 269]. From the latter analysis, connections with the "complexity=volume" proposal [51, 52] emerged (using the results of [265, 272]), showing an equivalence between these quantities for small conformal transformations at leading order in perturbation theory. These connections are further investigated in section 4.4 by extending the calculation to higher orders in perturbation theory. This rules out a direct equivalence between "complexity=volume" and the Fubini-Study complexity functional for Virasoro circuits.

Finally, in section 4.5 bulk duals to the circuits considered in this chapter are constructed. By a quantum circuit, a sequence of states $|\psi(\tau)\rangle$ together with the corresponding Hamiltonian time-evolution operator $Q(\tau)$ is meant. The bulk dual to the circuit corresponds to an asymptotically $\text{AdS}_3$ geometry chosen such that the boundary states on constant time slices $t = \tau$ of the geometry are given by $|\psi(\tau)\rangle$. This is implemented by placing the boundary CFT on a non-trivial background metric such that the time-evolution with the physical Hamiltonian $H(t)$ in this metric implements the same time-evolution as that with the circuit generator $Q(t)$. The dual bulk geometry then evolves from the geometry dual to the reference state (generally pure $\text{AdS}_3$ or a conical defect dual to a primary state) to a Bañados geometry[4] dual to the target state.

The bulk dual to the circuit derived in section 4.5 enables us to study gravity duals to cost functions form first principles. By using the basic AdS/CFT relations derived in section 2.1.2, cost functions such as the Fubini-Study line element (4.3) can be mapped directly to geometric bulk quantities. In this way, a geometric realization of the Fubini-Study line element is determined as a functional in terms of the lengths of geodesics, integrated over the endpoints. Applying this geometric realization to the two-sided BTZ geometry shows that the main properties expected for a cost function of a computational complexity measure are fulfilled, in particular with regards to the time-evolution behavior of computational complexity. Therefore, the goals set up for this chapter are to a large extent achieved. Nevertheless, many open questions remain in regards to the conjecture of [51–54] as will be discussed in chapter 5.

## 4.2. Quantum circuits from Virasoro group transformations

This section explains in detail the construction of circuits implementing a sequence of consecutive conformal transformations. Circuits composed out of consecutive conformal transformations have been considered before in [266, 268, 269], whose notation I will follow closely in this section.

As for all quantum circuits, the circuit in question is specified by a reference state $|\psi_R\rangle$ (the starting point), a target state $|\psi_T\rangle$ (the endpoint) as well as a time-dependent Hamiltonian which

$F(\rho,\sigma) = \text{Tr}[\sqrt{\sqrt{\rho}\sigma\sqrt{\rho}}]^2$ is the fidelity, generalizing the geodesic distance for the Fubini-Study metric, $\gamma(|\psi\rangle,|\chi\rangle) = \arccos(|\langle\psi|\chi\rangle|/\sqrt{\langle\psi|\psi\rangle\langle\chi|\chi\rangle})$.

[4] Bañados geometries are the most general asymptotically $\text{AdS}_3$ geometries corresponding to pure states in the dual field theory. There is a one-to-one mapping between expectation values of the energy-momentum tensor in a state in some Verma module and Bañados geometries.

I will denote as $Q(\tau)$ that implements the evolution between $|\psi_R\rangle$ and $|\psi_T\rangle$,

$$|\psi(\tau)\rangle = U(\tau)|\psi_R\rangle \quad \text{with} \quad U(\tau) = \overleftarrow{\mathscr{P}} \exp\left(-\int_0^\tau d\tilde{\tau}\, Q(\tilde{\tau})\right) \tag{4.4}$$

where $|\psi(\tau_f)\rangle = |\psi_T\rangle$, $\overleftarrow{\mathscr{P}}$ denotes path ordering (i.e. time ordering w.r.t. $\tau$) and $\tau_f$ is the final time. Note that the time scale $\tau$ is an auxiliary parameter whose choice is in principle arbitrary. If the distinction between $\tau$ and the physical time $t$ is of importance, I will refer to $\tau$ as the *circuit parameter*. Likewise, if $Q(\tau)$ is to be distinguished from the physical Hamiltonian $H(t)$, then $Q(\tau)$ is called the *circuit generator*. The quantum theory in question is a two-dimensional conformal field theory in Euclidean signature on a unit-radius spatial circle parametrized by $\phi$. Therefore the time-translation generator $U(\tau)$ is the analytic continuation of a unitary operator to Euclidean signature. In most cases, the reference state will be chosen to be a primary state $|h\rangle$.

For circuits composed out of conformal transformations, the circuit generator $Q(\tau)$ can be expanded in Virasoro generators as

$$Q(\tau) = \sum_n \epsilon_n(\tau) L_{-n}. \tag{4.5}$$

For simplicity, I will mostly consider only one copy of the Virasoro algebra. Because the holomorphic and anti-holomorphic Virasoro generators $L_n$ and $\bar{L}_n$ commute, the generalization to two copies is trivial. The circuit generator $Q(\tau)$ can be equivalently written by smearing the holomorphic component of the energy-momentum tensor,

$$Q(\tau) = \int_0^{2\pi} \frac{d\phi}{2\pi}\, T(z)\, \epsilon(\tau, z), \tag{4.6}$$

where $\epsilon(\tau, z) = \sum_n \epsilon_n(\tau) e^{nz}$ and $z = t + i\phi$ with $t$ being the Euclidean time variable. Throughout this chapter, the notation $T(z)$, $\bar{T}(\bar{z})$ denotes an operator acting on a Hilbert space defined in terms of Virasoro generators as

$$T(z) = \sum_n \left(L_n - \frac{c}{24}\delta_{n,0}\right) e^{nz}, \quad \bar{T}(\bar{z}) = \sum_n \left(\bar{L}_n - \frac{c}{24}\delta_{n,0}\right) e^{n\bar{z}}. \tag{4.7}$$

Here, $L_n$, $\bar{L}_n$ are the ordinary Virasoro generators with algebra

$$\begin{aligned} [L_n, L_m] &= (n-m)L_{n+m} + \frac{c}{12}(n^3 - n)\delta_{n+m,0} \\ [\bar{L}_n, \bar{L}_m] &= (n-m)\bar{L}_{n+m} + \frac{c}{12}(n^3 - n)\delta_{n+m,0} \\ [L_n, \bar{L}_m] &= 0. \end{aligned} \tag{4.8}$$

It is important to clearly distinguish the operators $T(z)$, $\bar{T}(\bar{z})$ from energy-momentum tensor components. Only in coordinates such that $ds^2 = dz d\bar{z}$ the relation $T_{zz} = T(z)$, $T_{\bar{z}\bar{z}} = \bar{T}(\bar{z})$ holds, but for instance diffeomorphisms $z \to w(z)$ lead to $T_{ww} = T(w)(\partial_z w)^2 \neq T(w)$. In the notation adopted in this thesis $T(z)$ and $\bar{T}(\bar{z})$ refer to scalar operators that do not transform under coordinate changes.

In the following, two closely related circuits are constructed that implement the sequence of consecutive conformal transformations. The two circuits are distinguished by the interpretation of the circuit time parameter. In the first construction (case (a)), the circuit parameter $\tau$ is an auxiliary parameter independent on the physical time coordinate $t$ on the manifold in which the conformal field theory lives, while in the second construction (case (b)) the physical time

coordinate and circuit parameter are identical.

The circuit implements at each time step $\tau$ an infinitesimal conformal transformation $z \to z + \epsilon(\tau, z)$ acting on the state $|\psi(\tau)\rangle$. Together, these infinitesimal transformations implement the total conformal transformation $z \to f(\tau, z)$ acting on the reference state. Since the conformal transformations form a group with group action realized by composition of functions, the parameter $\epsilon(\tau, z)$ is related to $f(\tau, z)$ by

$$\epsilon(\tau, f(\tau, z)) = \frac{d}{d\tau} f(\tau, z). \tag{4.9}$$

The two constructions of the circuit mentioned above are distinguished by the value of $\epsilon(\tau, z)$. If the circuit parameter $\tau$ is an auxiliary parameter independent of $z$ (case (a)), the solution of (4.9) is given by

$$\epsilon_{(a)}(\tau, z) = \dot{f}(\tau, F(\tau, z)), \tag{4.10}$$

where $F(\tau, z)$ is the inverse of $f(\tau, z)$ defined by $f(\tau, F(\tau, z)) = z$ and $\dot{f}$ denotes the derivative of $f$ w.r.t. its first argument, i.e. the $\tau$-derivative at a fixed value of $z$. On the other hand, if the circuit parameter $\tau$ is given by the physical time $t$ then the holomorphic coordinate $z$ that is transformed by the conformal transformations depends on $\tau$ such that the solution of (4.9) is given by

$$\epsilon_{(b)}(t, z) = \dot{f}(t, F(t, z)) + f'(t, F(t, z)), \tag{4.11}$$

where $f'$ denotes the derivative of $f$ w.r.t. its second argument. The energy-momentum tensor at circuit time $\tau$ in both constructions is given by

$$U^\dagger(\tau) T(z) U(\tau) = f'(\tau, z)^2 T(f(\tau, z)) + \frac{c}{12}\{f(\tau, z), z\}. \tag{4.12}$$

Therefore, the action of one layer of the circuit between some $\tau$ and $\tau + d\tau$ is as follows. If $\tau$ is treated as an independent auxiliary parameter, the energy-momentum tensor transforms as

$$e^{Q_{(a)}(\tau) d\tau} U^\dagger(\tau) T(z) U(\tau) e^{-Q_{(a)}(\tau) d\tau} = f'(\tau + d\tau, z)^2 T(f(\tau + d\tau, z)) + \frac{c}{12}\{f(\tau + d\tau, z), z\}, \tag{4.13}$$

while for $\tau = t$,

$$e^{Q_{(b)}(t) dt} U^\dagger(t) T(z) U(t) e^{-Q_{(b)}(t) dt} = f'(t + dt, z + dt)^2 T(f(t + dt, z + dt)) + \frac{c}{12}\{f(t + dt, z + dt), z\}. \tag{4.14}$$

Equations (4.13) and (4.14) further illustrate the difference between the two circuit constructions. In case (a) the state $|\psi(\tau)\rangle$ lives on the same time slice in physical time (say at $t = 0$) for all $\tau$. The circuit evolution in this case creates a sequence of states dual to the $t = 0$ slices of Bañados geometries. On the other hand, in case (b) the states $|\psi(t)\rangle$ live on different time slices of the same geometry (see figure 4.1). Therefore, in this case time evolution also has to include evolution in the holomorphic coordinate $z$. Equations (4.13) and (4.14) may also be used to derive $Q_{(a)}$ and $Q_{(b)}$ by expanding to linear order in, respectively, $d\tau$ and $dt$ and applying the Virasoro algebra. This recovers, respectively, (4.10) and (4.11). Of course, the sequence of states described by these circuits differs between the two constructions since the circuit generators $Q_{(a)}$ and $Q_{(b)}$ are different.

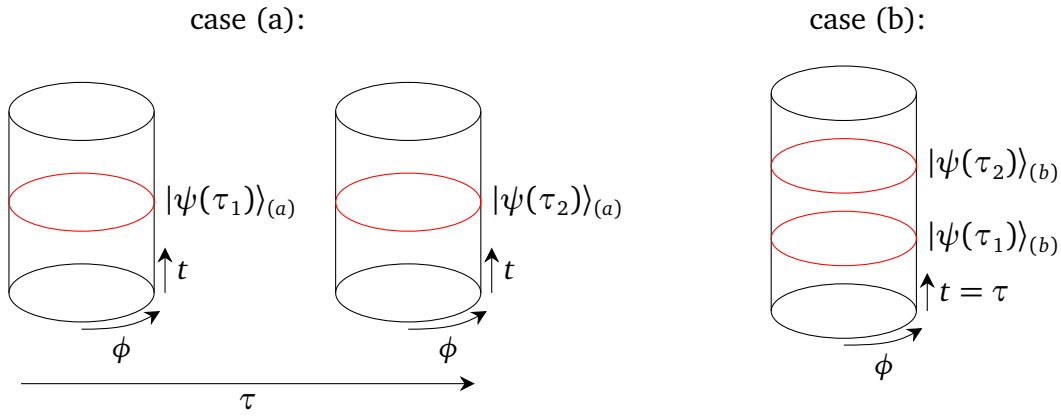


Figure 4.1.: Depiction of the two circuits in consideration. In case (a), the circuit evolution proceeds through a sequence of states living on time slices of different spacetimes (marked in red). There is no associated evolution with respect to physical time $t$. In case (b), the states live on different time slices of the same spacetime. In holography, case (a) is dual to a sequence of independent bulk geometries, whereas case (b) is dual to a single bulk geometry.

## 4.3. Computational complexity and geometric actions on coadjoint orbits

This section concerns itself with the study of computational complexity measures in the Virasoro circuits of section 4.2 related to geometric actions on coadjoint orbits of the Virasoro group. This topic is motivated by the results of [266] showing a close connection between computational complexity for the one-norm cost function (4.1) and geometric actions on coadjoint orbits. I will review these connections in section 4.3.1. Afterwards, in section 4.3.2 I will show that a modification of the cost function (4.1) taking into account the central extension of the Virasoro group allows for defining a computational complexity functional that is exactly equal to the geometric action on coadjoint orbits of the Virasoro group. Following this, I will investigate the viability of the geometric action as a complexity definition in section 4.3.3, finding significant issues with this proposal. Determining the optimal path for the geometric action as a complexity functional shows that the geometric action identified as computational complexity only measures phase changes. Finally, I will summarize relations between the geometric action and Berry phases as well as gravitational actions and Liouville theory in section 4.3.4 and 4.3.5.

### 4.3.1. Complexity for symmetry groups

Let me start by briefly summarizing the general approach for defining complexity with a gate set built out of symmetry transformations developed in [270]. This method when applied to the Virasoro group gives a computational complexity functional closely related to the geometric action on a coadjoint orbit of the Virasoro group [266].[5]

The definition of computational complexity developed in [270] fits in the general framework based on continuous gate counting approach described in section 2.3.4. Its basic ingredients, the elementary gates and the cost function, are defined as follows. Consider a $d$-dimensional quantum field theory with a global symmetry given by a Lie group $G$. Then, [270] chooses the

[5] See also [273, 274] for further work relating geometric actions on coadjoint orbits to computational complexity.

gate set to be the set of unitary operators[6] forming the representation of $G$ on the Hilbert space of the theory. That is, in Euclidean signature which I will exclusively work in in this section, the gate set is given by operators of the form (4.4) where the circuit generator is given by a sum over generators $T_i$ of the Lie algebra $\mathfrak{g}$ associated to $G$,

$$Q(\tau) = \sum_i \epsilon_i(\tau) T_i. \tag{4.15}$$

Here $\epsilon_i(\tau)$ specifies which generator is applied at time $\tau$ and may be related to a path $g(\tau)$ in the group by

$$g(\tau + d\tau) = e^{Q(\tau)d\tau} g(\tau). \tag{4.16}$$

Of course, by restricting the set of allowed gates to symmetry transformations, the set of possible target states is restricted to those reachable by symmetry transformations. The Virasoro circuits introduced in section 4.2 are a special case of this setup where $G$ is the Virasoro group with the conserved current being the energy-momentum tensor. Concerning the other choice to be made, the cost function $\mathscr{F}$, it is argued in [270] that the $\mathscr{F}$ should be chosen such that the penalty factors in (2.96) are all equal. Because the system of interest is invariant under symmetry transformations, all infinitesimal symmetry transformations should be equally difficult to apply. Moreover, it is also argued in [270] that the cost function for the operator $e^{-Q(\tau)d\tau}$ implementing infinitesimal time evolution at time $\tau$ should not assign any cost to operators that do not change the state, i.e. to operators that vanish when applied onto $|\psi(\tau)\rangle$. For instance, when considering the Virasoro group and decomposing $Q(\tau)$ into Virasoro modes, no cost should be assigned to $L_n$ modes for which $L_n|\psi(\tau)\rangle = 0$. This can be implemented by state-dependent cost functions such as the "one-norm cost function"

$$\mathscr{F}_1 = |\langle\psi(\tau)|Q(\tau)|\psi(\tau)\rangle| \tag{4.17}$$

or the "two-norm cost function"

$$\mathscr{F}_2 = \sqrt{|\langle\psi(\tau)|Q^2(\tau)|\psi(\tau)\rangle|}. \tag{4.18}$$

A more extensive study of cost functions with different choices of state dependence and norm can be found in [273]. Here, I will consider only the two examples $\mathscr{F} = \mathscr{F}_1$ or $\mathscr{F} = \mathscr{F}_2$. The total cost of a possible path connecting the reference and target state is then given by integrating the cost function over $\tau$, $\mathscr{C} = \int d\tau\, \mathscr{F}$ as usual.

I will now review the application of the above method to the Virasoro group based on [266]. The circuits considered in [266] are of type (a) in the language of section 4.2, that is the circuit parameter $\tau$ is an auxiliary parameter independent of the physical time $t$. Therefore, without loss of generality the physical time $t$ may be set to zero such that only a dependence on the spatial coordinate remains. Keeping in line with the notation from Virasoro group theory from 2.4 the spatial coordinate is denoted by $\sigma \in [0, 2\pi]$, related to the holomorphic and antiholomorphic coordinates by $z = i\sigma$, $\bar{z} = -i\sigma$. To simplify the notation, diffeomorphisms defining Virasoro group elements as well as their analogues for Virasoro algebra elements are redefined compared to section 4.2 such that $f(\tau, z) \to f(\tau, -iz) = f(\tau, \sigma)$. In these conventions, the circuit generator (4.5) is written as

$$Q(\tau) = \sum_n \epsilon_n(\tau) L_{-n} = \frac{1}{2\pi} \int d\sigma\, \epsilon(\tau, \sigma) T(\sigma). \tag{4.19}$$

The parameter $\epsilon(\tau, \sigma)$ can be read off either from equation (4.16) specialized to the Virasoro

[6] Or the analytic continuation thereof for Euclidean signature.

group or from (4.10),

$$\epsilon(\tau, f(\tau,\sigma)) = \dot{f}(\tau,\sigma) \quad \Leftrightarrow \quad \epsilon(\tau,\sigma) = -\frac{\dot{F}(\tau,\sigma)}{F'(\tau,\sigma)}. \tag{4.20}$$

To derive the complexity functional, it is useful to note that the circuit implements a symmetry transformation. This allows for relating the expectation value of the circuit generator $Q(\tau)$ in the state $|\psi(\tau)\rangle$ to the expectation value of an operator $\tilde{Q}(\tau) = U(\tau)^\dagger Q(\tau) U(\tau)$ in the reference state $|\psi_R\rangle$ [266],

$$\mathscr{F}_1 = |\langle\psi(\tau)|Q(\tau)|\psi(\tau)\rangle| = |\langle\psi_R|\tilde{Q}(\tau)|\psi_R\rangle|. \tag{4.21}$$

From the transformation of the energy-momentum tensor under conformal transformations[7],

$$T(\sigma) \to \tilde{T}(\sigma) = F'^2 T(F(\sigma)) + \frac{c}{12}\{F,\sigma\}, \tag{4.22}$$

the operator $\tilde{Q}(\tau)$ is given by

$$\tilde{Q}(\tau) = \frac{1}{2\pi}\int d\sigma\, \epsilon(\tau,\sigma)\tilde{T}(\sigma). \tag{4.23}$$

Therefore, the computational complexity for the one-norm cost function (4.17) is found to be [266]

$$\mathscr{C} = \int d\tau\, \mathscr{F}_1 = \frac{1}{2\pi}\int d\tau \left| \int d\sigma \left[ -\dot{F}F'\langle\psi_R|T(F)|\psi_R\rangle - \frac{c}{12}\frac{\dot{F}}{F'}\{F,\sigma\}\right]\right|. \tag{4.24}$$

Comparison with the geometric action on a coadjoint orbit in equation (2.147) shows clear similarities: up to the absolute value, identifying the orbit representative $v_0(\sigma)$ with the expectation value of the energy-momentum tensor in the reference state gives a matching first term in (2.147) and (4.24). However, the second term in (2.147) does not match with (4.24). The reason for this mismatch is determined in the following subsection. For explicit calculations with the complexity functional (4.24), it will be useful to relate the inverse group path determined by $F(\tau,\sigma)$ to the group path $f(\tau,\sigma)$ which is simply a change of integration variable $\sigma \to f(\tau,\sigma)$. Furthermore choosing the reference state as a primary state, $|\psi_R\rangle = |h\rangle$, such that $\langle\psi_R|T(\sigma)|\psi_R\rangle = h - c/24$, the complexity functional (4.24) becomes [266]

$$\mathscr{C} = \frac{c}{24\pi}\int d\tau \left| \int d\sigma\, \frac{\dot{f}}{f'}\left[\frac{1}{2}\left(1 - \frac{24h}{c}\right) + \{f,\sigma\}\right]\right|. \tag{4.25}$$

The two-norm cost function (4.18) for the Virasoro group is proportional to the one-norm cost function (4.17) up to order $1/c$ corrections [266]: as for the one-norm, the expectation value of $Q^2(\tau)$ in the state $|\psi(\tau)\rangle$ is equal to the expectation value of $\tilde{Q}^2(\tau)$ in the reference state $|\psi_R\rangle$

[7] In order to keep the notation consistent with that of [266], the conventions for conformal transformations of the energy-momentum tensor differ from those of section 4.2, compare (4.12) and (4.22). This is essentially the replacement of the transformation $f$ by its inverse $F$, although note that the definition of $\epsilon(\tau,\sigma) = \dot{f}(\tau, F(\tau,\sigma))$ used in [266] is the same as in section 4.2.

and therefore

$$\mathscr{F}_2^2 = \left(\frac{c}{24\pi}\right)^2 \left| \left( \int d\sigma \frac{\dot{f}}{f'} \left[ \frac{1}{2}\left(1 - \frac{24h}{c}\right) + \{f,\sigma\} \right] \right)^2 \right.$$
$$\left. + \frac{12}{c} \sum_n n(n^2 - 1 + 24h/c) \int d\sigma_1 d\sigma_2 \frac{\dot{f}_1}{f_1'} \frac{\dot{f}_2}{f_2'} \left(\frac{\sigma_2}{\sigma_1}\right)^n \right|, \tag{4.26}$$

where $f_1 = f(\tau, \sigma_1)$ and $f_2 = f(\tau, \sigma_2)$. Thus, at leading order in the large central charge limit the one-norm and two-norm cost functions yield equivalent complexity functionals.

### 4.3.2. From complexity to geometric actions

Let me now determine the relation between the complexity functional (4.24) and the geometric action (2.147) on a coadjoint orbit of the Virasoro group in more detail.

In the first step, I will show that the geometric action is equal to the complexity functional (4.24) up to terms arising from the central extension of the Virasoro group. To be concrete, recall from section 2.4.4 and in particular equation (2.145) that the geometric action for a centrally extended group $G$ contains the geometric action for the non-centrally extended group $\tilde{G}$ together with two additional terms coming from the 1-cocycle $\gamma(g)$ as well as the central extension part $m_\theta$ of the Maurer-Cartan form. The complexity functional in (4.24) is – up to the absolute value in $\mathscr{F}_1$ – given only by the first two terms, the geometric action for $\tilde{G}$ and the contribution from the 1-cocycle,

$$\mathscr{C} \sim -\int d\tau \left( \langle \widetilde{\mathrm{Ad}}_g^*(v_0), \theta_g \rangle + c\langle \gamma(g), \theta_g \rangle \right) = -\int d\tau \, \langle \mathrm{Ad}^*_{(g,\alpha)}(v_0, c), (\theta_g, 0) \rangle. \tag{4.27}$$

Group theoretic quantities entering the geometric action are identified as follows. As already seen above, the expectation value of the energy-momentum tensor in the reference state is identified with the orbit representative,

$$v_0(\sigma) = -\frac{1}{2\pi} \langle \psi_R | T(\sigma) | \psi_R \rangle. \tag{4.28}$$

This expectation value is related to the expectation value of $T(\sigma)$ in the state $|\psi(\tau)\rangle$ by the coadjoint action (2.131),

$$(\mathrm{Ad}_F^*(v_0))(\sigma) = -\frac{1}{2\pi} \langle \psi(\tau) | T(\sigma) | \psi(\tau) \rangle. \tag{4.29}$$

The 1-cocycle $\gamma(g)$ is of course given by the Schwarzian derivative, as is clear from the definition (2.128). The Maurer-Cartan form $\theta_{g^{-1}}$ in terms of the inverse group element $g^{-1}$ is related to the parameter $\epsilon(\tau, \sigma)$ determining which conformal transformations are applied at each time step. From (4.9), finite transformations of group elements are determined by

$$g(\tau_2) = e^{\int_{\tau_1}^{\tau_2} \epsilon(\tau) d\tau} g(\tau_1). \tag{4.30}$$

Here, $\epsilon(\tau) \equiv \epsilon(\tau, \sigma)$ is interpreted as an element of the Virasoro algebra. Multiplication by the inverse $g^{-1}(\tau_2)$ and differentiating with respect to $\tau_2$ gives

$$\theta_{g^{-1}(\tau_1)} = \frac{d}{d\tau_2} (g(\tau_1) \circ g^{-1}(\tau_2)) \Big|_{\tau_2 = \tau_1} = -\epsilon(\tau_1). \tag{4.31}$$

That $\epsilon(\tau)$ is related the Maurer-Cartan form for the inverse group element $g^{-1}$ is easily understood from the complexity point of view. The Maurer-Cartan form relates an element of the tangent space at some point $g(\tau)$ in the group manifold to the tangent space at the identity. However, when computing the complexity, the starting point is the identity and one aims to relate an element of the tangent space at $\tau = 0$ to an element of the tangent space of some point close by. In the complexity case, one is thus moving forward in time along the path, whereas the Maurer-Cartan form by definition moves us backward. Consequently, the Maurer-Cartan form in the complexity calculation must be written in terms of the inverse transformation in order to reverse the direction of the mapping to move forward in $\tau$.

### Recovering the central term

The question now arises if it is possible to adjust the cost function (4.17) to obtain the full geometric action (2.147) for the complexity functional (4.24). This is possible by letting the additional phase from the two-cocycle $C(g,h)$ contribute to the cost function.

In group theoretic terms, it is necessary to extend the parameter $\epsilon(\tau)$, an element of the Lie algebra of the non-centrally extended group $\tilde{G}$, to an element of the full group $G$. The extended parameter $(\epsilon(\tau), \beta(\tau))$ is sensitive to contributions from the central extension. To derive $\beta(\tau)$, the starting point is equation (4.30) which relates two elements of $\tilde{G}$ on two points $\tau_1$ and $\tau_2$ along the path that do not necessarily have to be close. Rather than just considering a path through the transformations $g$, the new transformation includes a path through the real numbers $\alpha(\tau)$ as well,

$$(g(\tau_2), \alpha(\tau_2)) = e^{\int_{\tau_1}^{\tau_2} d\tau(\epsilon(\tau),\beta(\tau))}(g(\tau_1), \alpha(\tau_2)). \tag{4.32}$$

Multiplying by $(g(\tau_1), \alpha(\tau_1))^{-1}$ and taking a derivative with respect to $\tau_1$ yields the central extension of the Maurer-Cartan form according to (2.142),

$$(\theta, m_\theta)_{g^{-1}} = -(\epsilon(\tau_2), \beta(\tau_2)) = \frac{d}{d\tau_1}\left((g(\tau_2), \alpha(\tau_2)) \circ (g^{-1}(\tau_1), -\alpha(\tau_1))\right)\Big|_{\tau_1=\tau_2}. \tag{4.33}$$

Using (2.120), this gives

$$(\theta, m_\theta)_{g^{-1}} = -(\epsilon(\tau_2), \beta(\tau_2)) = \frac{d}{d\tau_1}\left(g(\tau_2) \circ g^{-1}(\tau_1), C(g(\tau_2), g^{-1}(\tau_1))\right)\Big|_{\tau_1=\tau_2}. \tag{4.34}$$

Then, the new cost function is defined for the parameter $\epsilon(\tau)$ and $\beta(\tau)$ in the extended group as the sum of two contributions[8],

$$\tilde{\mathscr{F}}_1 = \int d\sigma \epsilon(\tau,\sigma)\langle\psi(\tau)|T(\sigma)|\psi(\tau)\rangle + c\beta(\tau). \tag{4.35}$$

The first contribution from $\epsilon(\tau)$ is just the cost function (4.17) used previously, which does not include the central extension. The second contribution is given by $\beta(\tau)$ times a constant which is identified with the central charge $c$ to achieve an equality of the resulting complexity functional with the geometric action, although this is of course not the only possible choice. Physically speaking, the additional contribution arises from assigning a cost to phase changes $|\psi(\tau)\rangle \to e^{i\beta(\tau)}|\psi(\tau + d\tau)\rangle$.

[8]Note that the absolute values around $\langle\psi(\tau)|T(\sigma)|\psi(\tau)\rangle$ have also been dropped in order to obtain a strict equality with the geometric action. This absolute value does not significantly affect the conclusions drawn in section 4.3.3 as can be seen by choosing a path $g(\tau)$ where $\langle\psi(\tau)|T(\sigma)|\psi(\tau)\rangle$ is always positive.

From (4.35) as well as the definition (2.145) of the geometric action from the Maurer-Cartan form it is obvious that the computational complexity following from the cost function $\widetilde{\mathscr{F}}_1$ is equal to the geometric action,

$$\mathscr{C} = \int d\tau \widetilde{\mathscr{F}}_1 = I, \tag{4.36}$$

where $I$ denotes the geometric action for the Virasoro group from (2.147). Written in terms of the group element $f(\tau,\sigma)$ instead of the inverse $F(\tau,\sigma)$ by a change of integration variable, the complexity functional for $\widetilde{\mathscr{F}}_1$ is given by

$$\mathscr{C} = \int d\tau d\sigma \frac{\dot{f}}{f'}\left(v_0(f) + \frac{c}{48\pi}\left(\frac{f''}{f'}\right)'\right). \tag{4.37}$$

Two comments are in order. First, note that the real number valued part $\alpha$ of the group path is chosen to be a constant, $\alpha(\tau_1) = \alpha(\tau_2) = \text{const}$. This choice is necessary to avoid contributions that are solely determined by the path through the real numbers and are thus independent of the transformation $g$ applied. The cost, however, should always depend on the symmetry transformation. Hence, the only contribution from the central extension should arise from the cocycle $C(g_1, g_2)$, which depends on the transformations $g$ alone, and not from derivatives of $\alpha$, which are independent of $g$. Moreover, derivatives of $\alpha$ would of course also lead to additional contributions that spoil the equivalence of the complexity functional to a geometric actions.

Second, before proceeding, let me verify that the cost function (4.35) still assigns zero cost to the identity. This is clear from the definition (4.32) since for $\tau_1 = \tau_2$, the integral in the exponential is zero. From a physical point of view, it is also clear that for two identical points $\tau_1 = \tau_2$ the Maurer-Cartan form (4.34) vanishes. Mathematically, the vanishing of (4.34) comes about since for the non-centrally extended component $\epsilon(\tau)$ the derivative of a constant $g(\tau)g^{-1}(\tau) = 1$ is taken and for the central extension piece $\beta(\tau) = m_\theta = 0$ due to $C(g(\tau), g^{-1}(\tau)) = \text{const}$ according to (2.121).

### Gauge invariance

The fact that the phase of a quantum state is not measurable in general leads to an important subtlety in the interpretation of geometric actions as complexity functionals that was not yet addressed. The issue is that symmetry transformations that only change the phase of the state, such as $|h\rangle \to |\psi_T\rangle = e^{iaL_0}|h\rangle$, transform between physically indistinguishable states, i.e. these unitary operators generate gauge transformations. Thus, applying a certain symmetry transformation $f$ onto the reference state should be equivalent to applying the same $f$ together with such a phase changing gauge transformation, since the states $U_f|h\rangle$ and $U_f e^{iaL_0}|h\rangle$ obtained in this way are physically equivalent representations of the target state in the Hilbert space.[9] As it turns out, the on-shell value of the geometric action is not invariant under such gauge transformations.

In the language of coadjoint orbits, the gauge transformations are represented by transformations which leave the orbit invariant. Recall from section 2.4 that the coadjoint orbits are isomorphic to manifolds $G/H_{v_0}$, where $H_{v_0}$ is the stabilizer of the orbit, i.e. the set of transformations that leave the reference state invariant. In terms of the the coadjoint element $v_0$ defining

[9] Note that this issue is independent of the question whether to include the central extension in the complexity functional. The gauge symmetry relevant here amounts to a total phase that relates the target state to the reference state. On the other hand, the central extension term in the complexity functional counts relative phase differences between two infinitesimally related states. Since these infinitesimally related states are physically inequivalent, the relative phase between them is observable. In contrast, the total phase between reference and target state is not observable in general, for example if reference and target state coincide up to the phase difference.

the reference state,

$$\mathrm{Ad}_h^* v_0 = v_0 \quad \text{for} \quad h \in H_{v_0}. \tag{4.38}$$

The coadjoint orbit action and with it the complexity should be invariant under transformations $h(\tau)$ from the stabilizer subgroup. As discussed in section 2.4.4, the geometric actions are defined not on the full group manifold $G$, but only on the orbit $G/H_{v_0}$. In particular, only the projection of the group path $g(\tau)$ onto the coadjoint orbit is relevant for the complexity. Consequently, paths that are non-trivial in $G$ should result in vanishing complexity if they are trivial projections on the coadjoint orbit. This includes paths $h(\tau)$ belonging to the stabilizer since these are projected onto points and thus always have vanishing complexity.

It turns out that this gauge invariance property is indeed satisfied – up to the appearance of a total derivative term in the action [174]. This term does not change the equations of motion. However, for the on-shell value of the action, this total derivative term leads to an additional contribution, such that the on-shell action is not gauge invariant. Our complexity definition, however, is defined in terms of the on-shell action. As such, the on-shell action is assigned a role as a physically meaningful and in principle measurable object. Therefore the boundary terms arising from the total derivative terms cannot be neglected.

As an example, consider the Virasoro group for which the coadjoint orbits fall into two different classes, those with representative $v_0 = -c/24$ and $v_0 > -c/24$. The representatives define the reference states $|0\rangle$ and $|h\rangle$ with $h > 0$ in the complexity functional. While the former state is invariant under $PSL(2,\mathbb{R})$ transformations generated by $L_{0,\pm 1}$, the latter states are invariant only under the $U(1)$ subgroup of the Virasoro group generated by $L_0$. The corresponding orbits are $\mathrm{Diff}(S^1)/PSL(2,\mathbb{R})$ and $\mathrm{Diff}(S^1)/U(1)$ respectively, see section 2.4.3.

Now consider a gauge transformation given by a $U(1)$ stabilizer parametrized by $a(\tau)$,

$$f(\tau,\sigma) \to f(\tau,\sigma) + a(\tau). \tag{4.39}$$

Since $a(\tau)$ is independent of $\sigma$, it leads to an action of the $L_0$ generator only. Inserting this in the action (4.37) yields a change of

$$S \to S + \delta S \quad \text{with} \quad \delta S = \int d\tau d\sigma \frac{\dot{a}}{f'}\left(v_0 + \frac{c}{48\pi}\left(\frac{f''}{f'}\right)'\right). \tag{4.40}$$

By expressing (4.40) in terms of the inverse diffeomorphism $F$, $\delta S$ can be integrated in $\sigma$. Since $F(\sigma + 2\pi, \tau) = F(\sigma,\tau) + 2\pi$, only a constant contribution is obtained from the integral over $\sigma$. The remaining integral is over a constant times $\dot{a}$. Therefore, it is trivially solvable to obtain

$$S \to S + 2\pi v_0 (a(\tau_f) - a(0)), \tag{4.41}$$

where the $\tau$-integration range goes from $\tau = 0$ to $\tau = \tau_f$. Thus, it is possible that symmetry transformations which are pure gauge and change only the phase of the reference state lead to a non-vanishing complexity.[10]

As mentioned above, a gauge invariant complexity functional is obtained by introducing suitable boundary terms in the action. These boundary terms are presented in section 4.3.4. Section 4.3.4 also reviews results from [275] showing that the geometric action with these boundary terms can be interpreted as a Berry phases. But before introducing these topics, it is useful to first determine the on-shell value of the geometric action. This calculation is presented in the following section 4.3.3.

[10] Note that this is independent of whether one takes into account the central extension in the cost function. Equation (4.25) suffers from the same problem.

### 4.3.3. Constructing optimal transformations and computing complexity

The arguments given above show that for a suitable choice of cost function, the computational complexity can be identified with the geometric action on a coadjoint orbit of the Virasoro group. To provide some intuition for this rather abstract object, I will explicitly calculate the computational complexity for some examples.

This involves determining the value of the complexity functional for the optimal path of minimal cost, i.e. the on-shell value of the geometric action. Therefore, the equations of motion and their solutions are determined for the complexity functional (4.37). This determines the full set of optimal transformations for the complexity functional. Upon calculating the complexity from these solutions, several issues are encountered as already anticipated above. Not only is there a large class of optimal transformations for which (4.37) counts only phase changes, but there are also examples of optimal transformations in which different costs are assigned to the same unitary transformation. These problems can be traced back to the fact that the gauge symmetry resulting from changes in the phase of a quantum state is not taken into account in the complexity proposal. Upon adding suitable boundary terms, gauge invariance is restored but the complexity vanishes as shown in section 4.3.4.

#### General solution to the equations of motion

The equations of motion of the complexity functional (4.37) are derived by varying this functional with respect to $f$ which gives after a straightforward but tedious calculation (see e.g. [276])

$$\nu_0\left(\frac{\dot{f}}{f'}\right)' - \frac{c}{48\pi}\left(\frac{\dot{f}}{f'}\right)''' = 0. \tag{4.42}$$

This equation is simple enough to be solved in the general case. In fact, in terms of $(\dot{f}/f')'$, equation (4.42) is just the equation of motion for a harmonic oscillator with frequency $\omega_h = \sqrt{1-24h/c}$. The solution is

$$\frac{\dot{f}}{f'} = A(\tau)\sigma + B(\tau)e^{i\omega_h\sigma} + C(\tau)e^{-i\omega_h\sigma} + D(\tau), \tag{4.43}$$

where $A, B, C, D$ are arbitrary functions of $\tau$ satisfying $B(\tau) = C^*(\tau)$. However, the requirement that $f$ be a diffeomorphism (at constant $\tau$) and hence that $\dot{f}$ and $f'$ be periodic imposes $A(\tau) = 0$. For $h > 0$, $\omega_h \notin \mathbb{Z}$ and thus in this case also $B(\tau) = C(\tau) = 0$.

Note that if $f(\tau,\sigma) = f_0(\tau,\sigma)$ is a solution of (4.43), then

$$f(\tau,\sigma) = g(f_0(\tau,\sigma)) \tag{4.44}$$

is another solution of (4.43) for a diffeomorphism $g(\sigma) \in \mathrm{Diff}^+(S^1)$. Therefore, it is sufficient to first determine a simple solution $f_0(\tau,\sigma)$ of (4.43). The general solution then follows by composition with an arbitrary $g(\sigma)$.

Concentrate first on the case $h > 0$, where (4.43) reduces to

$$\dot{f} = D(\tau)f'. \tag{4.45}$$

It is simple to see that

$$f_0(\tau,\sigma) = \sigma + \delta(\tau) \tag{4.46}$$

provides a solution of this differential equation for $D(\tau) = \dot{\delta}(\tau)$. Inserting the general solution $f(\tau,\sigma) = g(f_0(\tau,\sigma))$ into (4.37), it is clear that the complexity depends only on the value of $\delta(\tau)$ at $\tau = 0$ and $\tau = \tau_f$,

$$\mathscr{C} = \int d\sigma d\tau\, \dot{\delta}(\tau)\left(\nu_0 + \frac{c}{48\pi}\left(\frac{f''}{f'}\right)'\right) = 2\pi\nu_0(\delta(\tau_f) - \delta(0)). \tag{4.47}$$

For $\delta(t_f) = \delta(0)$, the complexity vanishes. As expected for a consistent interpretation, in this case the unitary transformation $U_f$ acting on the reference state is just the identity. To see this, note that $F(\tau,\sigma) = G(\sigma) - \delta(\tau)$ and thus $\epsilon(\tau,\sigma) = -\dot{F}/F' = \dot{\delta}(\tau)/G'(\sigma)$, where $G(g(\sigma)) = \sigma$. Therefore, the time integral of $U_f = \overleftarrow{\mathscr{P}} e^{\int\int d\tau d\sigma\, \epsilon(\tau,\sigma)T(\sigma)}$ is trivially solvable and $U_f$ is just an exponential of a sum over $L_n$ symmetry generators with prefactor $\delta(\tau_f) - \delta(0)$. When $\delta(\tau_f) = \delta(0)$, this prefactor vanishes and the exponential yields the identity.

For $h = 0$, one solution to (4.43) is given by[11]

$$f_0(\tau,\sigma) = 2\arctan\left(\frac{a(\tau)\tan(\sigma/2) + b(\tau)}{c(\tau)\tan(\sigma/2) + d(\tau)}\right), \tag{4.48}$$

where $ad - bc = 1$, i.e. $a, b, c, d$ together form a $PSL(2,\mathbb{R})$ element. The functions $a, b, c, d$ are related to $B, C, D$ by

$$\begin{aligned} B &= \frac{1}{2}\Big[\dot{b}d - b\dot{d} - \dot{a}c + a\dot{c} - i(\dot{b}c - b\dot{c} + \dot{a}d - a\dot{d})\Big] = C^* \\ D &= \dot{b}d - b\dot{d} + \dot{a}c - a\dot{c}. \end{aligned} \tag{4.49}$$

In this case, the complexity cannot be derived in closed form in general. Inserting the general solution $f(\tau,\sigma) = g(f_0(\tau,\sigma))$ into the complexity action functional (4.37) yields

$$\begin{aligned} \mathscr{C}[f] &= \mathscr{C}[f_0] + \frac{c}{48\pi}\int d\sigma d\tau\, \frac{\dot{f}_0}{f_0'}\left(\frac{g''}{g'}\right)' \\ &= \int d\tau\, D 2\pi\nu_0 + \frac{c}{48\pi}\int d\sigma d\tau\, (Be^{i\sigma} + Ce^{-i\sigma})\left(\frac{f_0''}{f_0'} + \frac{g''}{g'}\right)'. \end{aligned} \tag{4.50}$$

How do we interpret the above solutions (4.46) and (4.48) from the perspective of complexity? First, let me note that the $f_0(\tau,\sigma)$ are in the stabilizer subgroup of the respective reference state, i.e. $U_{f_0(\tau)}$ only generates a phase shift in $|h\rangle$. Moreover, $g$ is independent of $t$. The above solutions are given by a composition of $g$ with $f_0(t)$, hence

$$U_{f(\tau)} = U_{g\cdot f_0(\tau)} \sim U_g U_{f_0(\tau)}, \tag{4.51}$$

where $\sim$ denotes equality up to a phase $e^{i\alpha}$. Therefore, the state $|\psi(\tau)\rangle$ at computation time $\tau$ is reached by first applying a time-dependent phase shift $U_{f_0(\tau)}$ followed by a time independent conformal transformation $U_g$. Thus, up to a phase, the target state is reached instantaneously at time $\tau = 0$, [12]

$$|\psi_T\rangle \sim U_{f(0)}|h\rangle \sim U_g|h\rangle. \tag{4.52}$$

At later times $\tau > 0$, only this phase changes. What cost is associated with these two contribu-

[11] This can be equivalently represented as $f(\tau,\sigma) = \frac{1}{i}\ln\left[\frac{\alpha(\tau)e^{i\sigma} + \beta(\tau)}{\bar{\beta}(\tau)e^{i\sigma} + \bar{\alpha}(\tau)}\right]$.

[12] If one additionally requires that $U_{f(0)} = \mathbb{1}$ as in [266], instantaneous transitions are forbidden. Then $g$ must be the identity and only phase shifts can be generated.

tions to $U_{f(\tau)}$? For $h > 0$, from (4.47) it is obvious that the complexity is independent of $g$ and counts only the phase change generated by $U_{f_0(\tau)}$. Thus, it follows that in this case, the complexity definition given by the on-shell value of the geometric action (4.37) counts only phase changes, while it assigns zero cost to the (most certainly more interesting) contribution that actually produces a physically distinct state! For the special case of $h = 0$, equation (4.50) shows that the complexity is in general not independent of $g$. In this case, $U_g$ contributes to the cost of the total transformation $U_{f(\tau)}$ as does the phase shift generated by $U_{f_0(\tau)}$.

In the following, the cost assigned to these phase shifts is derived by considering solutions to the equations of motion where $g$ is the identity, i.e. solutions for which only a phase change is generated. The transformations for these solutions are generated by stabilizer subgroups $U(1)$ and $PSL(2,\mathbb{R})$ of the Virasoro group. I will show that the cost is non-vanishing and proportional to the phase shift.

### Example: $U(1)$ subgroup of the Virasoro group

For $f(\tau,\sigma) = f_0(\tau,\sigma) = \sigma + \delta(\tau)$, only the $L_0$ generator forming a $U(1)$ subgroup of the Virasoro group acts on the reference state,

$$\epsilon(\tau,\sigma) = -\dot{F}/F' \equiv \epsilon(\tau) = \dot{\delta}(\tau). \tag{4.53}$$

For a reference state $|h\rangle$ with well-defined scaling dimension $h$, the complexity then counts only the change in phase as

$$|h\rangle \to \overleftarrow{\mathscr{P}} \exp\left(2\pi \int d\tau\, \epsilon(\tau)(L_0 - c/24)\right)|h\rangle. \tag{4.54}$$

As was already seen, the complexity is determined entirely by the boundary conditions for $\delta(\tau)$ at $\tau = 0$ and $\tau = \tau_f$,

$$\mathscr{C} = \left(h - \frac{c}{24}\right)\left(\delta(\tau_f) - \delta(0)\right). \tag{4.55}$$

Thus, despite the fact that only the phase of the state changes, which is a gauge symmetry, the complexity is still non-vanishing. As explained in section 4.3.3, the same result for the complexity from equation (4.55) is obtained for a general optimal transformation $f(\tau,\sigma) = g(f_0(\tau,\sigma))$. Hence, for reference states with $h > 0$, equation (4.55) is the general expression valid for the complexity between $|h\rangle$ and any target state.

### Example: $PSL(2,\mathbb{R})$ subgroup of the Virasoro group

As a further example, consider optimal transformations belonging to the $PSL(2,\mathbb{R})$ subgroup of the Virasoro group, i.e. $f(\tau,\sigma)$ from (4.48). The inverse $F(\tau,\sigma)$ has the same form with $a,b,c,d$ replaced by $d,-b,-c,a$, which are the elements of the inverse of the $PSL(2,\mathbb{R})$ element corresponding to $a,b,c,d$. Thus, $\epsilon(\tau,\sigma)$ is given by

$$\epsilon(\tau,\sigma) = \tilde{B}(\tau)e^{i\sigma} + \tilde{C}(\tau)e^{-i\sigma} + \tilde{D}(\tau), \tag{4.56}$$

where $\tilde{B},\tilde{C},\tilde{D}$ are functions of $\tau$ related to $a,b,c,d$ by

$$\begin{aligned} \tilde{B} &= \frac{1}{2}\Big[-\dot{b}a + b\dot{a} + \dot{d}c - d\dot{c} - i(\dot{b}c - b\dot{c} + \dot{d}a - d\dot{a})\Big] = \tilde{C}^* \\ \tilde{D} &= -\dot{b}a + b\dot{a} - \dot{d}c + d\dot{c}. \end{aligned} \tag{4.57}$$

Therefore, only $L_0, L_{\pm 1}$ forming a $PSL(2,\mathbb{R})$ subgroup of the Virasoro group act on the reference state $|0\rangle$,

$$|\psi_T\rangle = U_{f(\tau_f,\sigma)}|0\rangle = \exp\left(2\pi i \int_0^{\tau_f} d\tau \left(\tilde{B}(\tau)L_{-1} + \tilde{C}(\tau)L_1 + \tilde{D}(\tau)\left(L_0 - \frac{c}{24}\right)\right)\right)|0\rangle. \tag{4.58}$$

Since $|0\rangle$ is $PSL(2,\mathbb{R})$ invariant, this gives only a phase change that arises from the zero mode $L_0 - c/24$. Like for the $U(1)$ case, the complexity for these phase changing transformations does not vanish in general as can be seen from (4.50).

Let me now consider a particular example of a $PSL(2,\mathbb{R})$ transformation for which the complexity does vanish. Consider a diffeomorphism that was introduced in the context of Virasoro Berry phases in [275] where $f(\tau,\sigma)$ is chosen such that the corresponding bulk diffeomorphism gives an $\mathrm{AdS}_3$ boost with rapidity $\lambda$,

$$f(\tau,\sigma) = \frac{1}{i}\ln\left[\frac{\cosh\left(\frac{\lambda}{2}\right)e^{i\sigma} + \sinh\left(\frac{\lambda}{2}\right)}{\sinh\left(\frac{\lambda}{2}\right)e^{i\sigma} + \cosh\left(\frac{\lambda}{2}\right)}\right] + \omega\tau. \tag{4.59}$$

The inverse transformation $F(\tau,\sigma)$ is a function of $\sigma - \omega\tau$, thus the only non-vanishing mode of $\epsilon(\tau)$ is the zero mode

$$\epsilon(\tau,\sigma) = \epsilon_0 = \omega\,. \tag{4.60}$$

The complexity follows from a straightforward calculation by inserting (4.59) into the action (4.37),

$$\mathscr{C} = h\tau_f\omega\cosh(\lambda)\,. \tag{4.61}$$

For general $h$, this would imply that the cost induced by $|h\rangle \to \exp\left(i\int d\tau\,\epsilon_0(L_0 - c/24)\right)|h\rangle$ grows linearly with the angular velocity $\omega$ and computation time $\tau_f$. However, for the vacuum we have $h = 0$ such that the complexity actually vanishes. This is certainly a puzzling result in light of the fact that in one could have taken $\delta(\tau) = \omega\tau$ in the $U(1)$ case from above and derived a non-vanishing complexity (4.55) for exactly the same unitary (phase changing) transformation (4.54) as is used here. This discrepancy, which exists only for the vacuum state due to the fact that it is the only $PSL(2,\mathbb{R})$ invariant state, shows again that it is essential to take into account the gauge symmetry to obtain a consistent interpretation of geometric actions as complexity.

### Example: $PSL^{(n)}(2,\mathbb{R})$ subgroup of the Virasoro group

Finally, let me consider transformations arising from the $SL^{(n)}(2,\mathbb{R})$ subgroup of the Virasoro group. Note that these do not solve the equations of motion (4.42) and are thus not optimal. It is interesting to compare the cost and target state with the results for optimal $PSL(2,\mathbb{R})$ transformations above.

An example for a non-optimal transformation is given by a generalization of (4.59),

$$f(\tau,\sigma) = \frac{1}{in}\ln\left[\frac{\alpha e^{in\sigma} + \beta}{\bar{\beta}e^{in\sigma} + \bar{\alpha}}\right] + \omega\tau, \tag{4.62}$$

where $n \in \mathbb{N}$. Equation (4.62) is not a solution to the equations of motion (4.42) due to the fact that $\dot{f}, f'$ contains terms proportional to $e^{\pm in\sigma}$. The transformation arises from modes $L_0, L_{\pm n}$ forming $PSL^{(n)}(2,\mathbb{R})$ subgroup of the Virasoro group.[13] $PSL^{(n)}(2,\mathbb{R})$ is an $n$-fold cover of $PSL(2,\mathbb{R})$.

[13] This is the stabilizer group of so-called exceptional coadjoint orbits of the Virasoro group. For $n > 1$, these orbits

The associated cost is non-minimal and therefore not a measure for complexity.

Since the inverse transformation $F(\tau,\sigma)$ is a function of $\sigma-\omega\tau$, the only non-vanishing mode for this transformation is again the zero mode

$$\epsilon(\tau,\sigma)=\epsilon_0=\omega. \tag{4.63}$$

Thus, the unitary operator $U_f$ implementing the transformation $f(\tau,\sigma)$ in the Hilbert space generates the same state as the $PSL(2,\mathbb{R})$ transformation considered above. The cost of this transformation is given by

$$\mathscr{C}=h\tau_f\,\omega\cosh(\lambda)+\omega\tau_f\frac{c}{24}\left(n^2-1\right)\cosh(\lambda). \tag{4.64}$$

As expected, the complexity of non-optimal transformations is larger than that of optimal $PSL(2,\mathbb{R})$-transformations in equation (4.61). However, the corresponding unitary operator $U_f$ acting on the Hilbert space still contains only the $L_0$ generator and is exactly equivalent to the one for the (optimal) $PSL(2,\mathbb{R})$ path above. Thus, one sees again that without taking the gauge invariance into account, the complexity definition assigns different costs (4.64) and (4.61) to the same unitary transformation $U_f$.

### 4.3.4. Boundary terms and Berry phases

As seen in the previous subsection, without taking the gauge invariance of states under phase changes into account, the geometric action does not give sensible results as a computational complexity functional. However, not all phase changes are unphysical: as is well known, a type of phase change known as Berry phase or geometric phase is actually measurable. Berry phases also arise on coadjoint orbits of the Virasoro group [275] (see also [277, 278]) and are in fact equal to geometric actions up to the addition of a boundary term. This boundary term is the one necessary to restore gauge invariance of the geometric action as a computational complexity functional. Therefore, let me now review the connections between Berry phase and geometric actions uncovered in [275].[14]

A Berry phase generally arises from adiabatic evolution around a closed loop in a system depending on external parameters (the canonical example is evolution in an external magnetic field). The Hamiltonian in the system depends on the external parameters $\gamma(\tau)$ which evolve in time. The Berry phase for such a system is given by

$$\theta_\gamma=i\int_0^{\tau_f}d\tau\,\langle\psi(\gamma(\tau))|\partial_\tau|\psi(\gamma(\tau))\rangle. \tag{4.65}$$

For closed paths $\gamma(\tau)$, the phase $\theta_\gamma$ is unambiguously defined and can be measured by interference experiments with two copies of the system, one of which evolves along $\gamma(\tau)$ while the parameters for the other system are kept fixed. The Berry phase can be written as the integral of a one-form $A$ called the Berry connection,

$$\theta_\gamma=\int_\gamma A. \tag{4.66}$$

The Berry connection $A$ itself is ambiguous and transforms as a $U(1)$ gauge field under gauge

are unphysical with energy unbounded from below (see section 2.4.3), thus they are not considered in the rest of this work.

[14] For further work relating Virasoro Berry phases to the original complexity functional of [266] without the central extension piece see [267].

transformations $|\psi(\gamma)\rangle \to e^{i\phi(\gamma)}|\psi(\gamma)\rangle$, however the integral of $A$ along a closed path $\gamma(\tau)$ is invariant under these transformations and hence unambiguously defined.

In the context of symmetry groups, the Berry phase arises as follows [275]. Consider a global symmetry group given by a Lie group $G$ containing time translations, i.e. let the Hamiltonian $\hat{H}$ be a generator of the Lie algebra of $G$. Furthermore, let $U_g$ denote elements of a unitary representation of $G$ on the Hilbert space. What happens to the Hamiltonian if we use a symmetry transformation $g \in G$ to transform to another frame? An observer in the new frame will perceive time-evolution to be generated by the operator $U_g \hat{H} U_g^{-1}$. Thus, symmetry transformations define a family of Hamiltonians $U_g \hat{H} U_g^{-1}$ labeled by group elements $g$ which play the role of the external parameters $\gamma$ above. Evolution with these Hamiltonians along a closed path $g(t)$ yields a Berry phase[15]

$$\theta_g = i \int_0^{\tau_f} d\tau \, \langle \psi | U^\dagger_{g(\tau)} \partial_\tau U_{g(\tau)} | \psi \rangle, \tag{4.67}$$

where $|\psi\rangle$ is the state of the system at the start of the evolution. However, demanding that the path $g(\tau)$ be closed is too restrictive in this setup. After all, unitary representations $U_g$ may be projective and include phase changes themselves. Therefore, it is enough to demand that

$$U_{g(\tau_f)} |\psi\rangle = e^{i\phi} U_{g(0)} |\psi\rangle \tag{4.68}$$

for some real number $\phi$ in order for the states at the start and end of the evolution to be equivalent. Thus, physically it is actually not the path $g(\tau)$ itself that is relevant for the Berry phase, but its projection on the coadjoint orbit $G/H$, where $H$ is a subgroup of $G$ corresponding to the stabilizer of $|\psi\rangle$. For the Berry phase, this implies that only the path on the coadjoint orbit must be closed, $g^{-1}(0)g(\tau_f) \in H$. To ensure gauge invariance of the Berry phase in this setup under transformations from the stabilizer $H$, a boundary term is introduced in (4.67) [275],

$$\theta_g = i \int d\tau \, \langle \psi | U^\dagger_{g(\tau)} \partial_\tau U_{g(\tau)} | \psi \rangle - i \log \langle \psi | U_{g^{-1}(0) g(\tau_f)} | \psi \rangle. \tag{4.69}$$

This boundary term ensures that the Berry phase vanishes for transformations $f(\tau, \sigma)$ belonging solely to the stabilizer $H$ of $|\psi\rangle$. Therefore, this is exactly the boundary term needed to make the complexity functional (4.37) gauge invariant. For the Virasoro group, the above arguments lead to the Berry phase [275]

$$\theta_f = -\frac{1}{2\pi} \int_0^{\tau_f} d\tau \int_0^{2\pi} d\sigma \, \frac{\dot{f}}{f'} \left[ h - \frac{c}{24} + \frac{c}{24} \left( \frac{f''}{f'} \right)' \right] + \left( h - \frac{c}{24} \right) F(0, f(\tau_f, 0)), \tag{4.70}$$

where $|\psi\rangle = |h\rangle$ was chosen to be a primary state with weight $h > 0$. Apart from the boundary term $(h - c/24)F(0, f(\tau_f, 0))$, this is exactly equal to the complexity functional (4.37). This equivalence also holds for $h = 0$ although the boundary term is different in this case.

Note that all solutions to the equations of motion (4.42) define closed paths on coadjoint orbits. Recall that the general solution to (4.42) is given by $f(\tau, \sigma) = g(f_0(\tau, \sigma))$, where $g$ is an arbitrary diffeomorphism and $f_0$ is given by (4.46) for $h > 0$ and by (4.48) for $h = 0$. The inverse of such a solution is given by $F(\tau, \sigma) = F_0(\tau, G(\sigma))$, where $G, F_0$ are the inverses of $g, f_0$ respectively. Then

[15] The operator $U^\dagger_{g(\tau)} \partial_\tau U_{g(\tau)}$ whose expectation value determines the Berry phase is actually related to the Maurer-Cartan form introduced in section 2.4 [275]. The unitary transformation $U_g$ of the Lie group $G$ defines a unitary representation $\mathfrak{u}[X]$ of the corresponding Lie algebra $\mathfrak{g}$ by $U_{\exp(\alpha X)} = \exp(\alpha \mathfrak{u}[X])$ for all $X \in \mathfrak{g}$ and $\alpha \in \mathbb{R}$. The Berry phase is then given as the imaginary unit times the integral over $A = \langle \psi | \mathfrak{u}[\theta_{g(\tau)}] | \psi \rangle$ where $\theta_{g(\tau)}$ is the Maurer-Cartan form (2.142) and $A$ the Berry connection.

it follows that

$$F(0, f(\tau_f, \sigma)) = F_0(0, f_0(\tau_f, \sigma)) = \begin{cases} \sigma + \theta \ , & h > 0 \\ 2\arctan\left(\dfrac{A\tan(\sigma/2) + B}{C\tan(\sigma/2) + D}\right), & h = 0, \end{cases} \tag{4.71}$$

for some numbers $\theta$ and $A, B, C, D$ with $AD - BC = 1$. The quantity on the right hand side is the identity $f(\sigma) = \sigma$ transformed by some element of the stabilizer subgroup $H$ of the orbit ($U(1)$ for $h > 0$ and $PSL(2, \mathbb{R})$ for $h = 0$). Equation (4.71) is the explicit form of the condition $g^{-1}(0)g(\tau_f) \in H$ encoding the requirement that the path $f(\tau, \sigma)$ is closed on the orbit.

Therefore, the conclusion is that the complexity functional (4.37) upon adding the boundary term necessary for gauge invariance is equivalent to a Berry phase. Note that the converse is not true, there exist Berry phases that are not equivalent to a complexity. These are generated by closed paths $f(\tau, \sigma)$ which are non-optimal from the computational complexity viewpoint, i.e. paths which do not solve the equations of motion of the geometric action (4.37). The computational complexity is obtained by minimizing the complexity functional given as the sum of the geometric action together with the boundary term. It is then obvious that the complexity must vanish since the minimal Berry phase is no Berry phase at all[16]: $\theta_f = \mathscr{C} = 0$.

A major motivation for studying the complexity functional introduced in [266] which lead to the geometric action in section 4.3.2, was that the geometric actions also turn up on the gravity side and therefore a "complexity=action" type proposal could be realized. Although it is clear by now that the geometric action does not provide a sensible computational complexity functional, the relation to the gravity side as well as to Liouville theory is still interesting and is presented in the following section 4.3.5.

### 4.3.5. Relation to gravitational actions and Liouville theory

Apart from its origins in group theory, the geometric action on coadjoint orbits of the Virasoro group also arises as an action for the asymptotic degrees of freedom of gravity with asymptotically $AdS_3$ boundary conditions [185, 186, 279] (see [280–283] for earlier work in this direction). In the same vein, Liouville theory has been derived as the combined action arising from the left and right moving Virasoro symmetries of the asymptotic degrees of freedom of $AdS_3$ spaces [284]. Moreover, a direct connection between Liouville theory and the sum of coadjoint orbit actions for two copies of the Virasoro group has been derived in [285]. Liouville theory has also appeared in connection with the complexity proposal from path integral optimization of [286]. I will now review the derivation of the above equivalence statements and provide details how the path integral optimization approach of [286] is related to the complexity proposal of [266] that motivated the investigations in this section.

The starting point of the derivation of actions for the asymptotic degrees of freedom of three-dimensional gravity theories is the Chern-Simons formulation in which the gravity action takes the form

$$S = \frac{1}{64\pi G_N} \int (I_{CS}[A] - I_{CS}[\bar{A}]) \tag{4.72}$$

with

$$I_{CS}[A] = \mathrm{Tr}\left(A \wedge dA + \frac{2}{3} A \wedge A \wedge A\right). \tag{4.73}$$

[16] Of course, the Berry phase can have either sign. In this argument I am implicitly restricting to positive values of $\theta_f$ or putting in the absolute value again which was neglected after section 4.3.2.

For asymptotically $AdS_3$ spaces, $A$ is an $SL(2,\mathbb{R})$ valued connection. The conventions for the $SL(2,\mathbb{R})$ generators used here are

$$\begin{aligned} J_0 &= \bar{J}_0 = \frac{1}{2}\begin{pmatrix} 0 & -1 \\ 1 & 0 \end{pmatrix}, \\ J_1 &= -\bar{J}_1 = \frac{1}{2}\begin{pmatrix} 0 & 1 \\ 1 & 0 \end{pmatrix}, \\ J_2 &= \bar{J}_2 = \frac{1}{2}\begin{pmatrix} 1 & 0 \\ 0 & -1 \end{pmatrix}. \end{aligned} \tag{4.74}$$

To derive the action of the asymptotic dynamics from (4.72), one imposes the asymptotically AdS boundary conditions of [64] which read in terms of the $SL(2,\mathbb{R})$ connections [185, 284]

$$\begin{aligned} A &= \begin{pmatrix} \frac{dr}{2r} + O\left(\frac{1}{r^2}\right) & O\left(\frac{1}{r}\right) \\ r d\sigma^+ + O\left(\frac{1}{r}\right) & -\frac{dr}{2r} + O\left(\frac{1}{r^2}\right) \end{pmatrix}, \\ \bar{A} &= \begin{pmatrix} -\frac{dr}{2r} + O\left(\frac{1}{r^2}\right) & -r d\sigma^- + O\left(\frac{1}{r}\right) \\ O\left(\frac{1}{r}\right) & \frac{dr}{2r} + O\left(\frac{1}{r^2}\right) \end{pmatrix}, \end{aligned} \tag{4.75}$$

where $r$ is the radial direction of the bulk and $\sigma^\pm = \sigma \pm t$ with $\sigma$ being the angular and $t$ the time direction. Moreover, the $SL(2,\mathbb{R})$ connections decompose as $A = g^{-1}dg$ and $\bar{A} = \bar{g}^{-1}d\bar{g}$.

The first step of the derivation of both the Liouville and coadjoint orbit actions from the Chern-Simons theory on $AdS_3$ consists of showing that the Chern-Simons theory reduces to two copies of the chiral Wess-Zumino-Witten model. This follows from a straightforward calculation subject to imposing the boundary conditions $A_- \sim \bar{A}_+ \sim O(1/r)$ from (4.75), which gives [185, 284]

$$S = S_+[g] + S_-[\bar{g}] \tag{4.76}$$

with

$$S_\pm[g] = \frac{k}{2\pi}\int_{\partial M} d\sigma dt \, \mathrm{Tr}((\partial_\sigma g^{-1})(\partial_\pm g)) \mp \Gamma[g]. \tag{4.77}$$

Here, $M$ is the bulk manifold in question and $\Gamma[g] = \frac{k}{2\pi}\int_M \mathrm{Tr}[g^{-1}dg \wedge g^{-1}dg \wedge g^{-1}dg]$ the topological term of the WZW model. Note that in order to obtain a variational principle consistent with the $AdS_3$ boundary conditions, a boundary term

$$S \to S - \frac{k}{4\pi}\int_{\partial M} d\sigma dt (\mathrm{Tr}(A_\sigma^2) + \mathrm{Tr}(\bar{A}_\sigma^2)) \tag{4.78}$$

has to be added to the action (4.72) [185, 284].

To obtain the Liouville action, in the second step the two chiral WZW models are combined into a single non-chiral WZW model [284] with action

$$S = -\frac{k}{\pi}\int_{\partial M} d\sigma dt \, \mathrm{Tr}((\partial_+ h^{-1})(\partial_- h)) - \Gamma[h], \tag{4.79}$$

where $h = g^{-1}\bar{g}$. Then, $h$ is parametrized in a Gauss decomposition,

$$h = \begin{pmatrix} 1 & X \\ 0 & 1 \end{pmatrix}\begin{pmatrix} e^{\omega/2} & 0 \\ 0 & e^{-\omega/2} \end{pmatrix}\begin{pmatrix} 1 & 0 \\ Y & 1 \end{pmatrix}. \tag{4.80}$$

Imposing the remaining boundary conditions (4.75) gives rise to the Liouville action[17]

$$S = S_L = \frac{c}{24\pi}\int_{\partial M} d\sigma dt \left(\frac{1}{2}\partial_+\omega\partial_-\omega + 2e^{\omega}\right), \tag{4.81}$$

where $c = 6k = 3/2G_N$.

The authors of [185], on the other hand, proceed differently by expressing $g$ and $\bar{g}$ separately in a Gauss decomposition,

$$\begin{aligned} g &= \begin{pmatrix} 1 & 0 \\ G & 1 \end{pmatrix}\begin{pmatrix} \lambda & 0 \\ 0 & 1/\lambda \end{pmatrix}\begin{pmatrix} 1 & \psi \\ 0 & 1 \end{pmatrix}, \\ \bar{g} &= \begin{pmatrix} 1 & -\bar{G} \\ 0 & 1 \end{pmatrix}\begin{pmatrix} 1/\bar{\lambda} & 0 \\ 0 & \bar{\lambda} \end{pmatrix}\begin{pmatrix} 1 & 0 \\ \bar{\psi} & 1 \end{pmatrix}. \end{aligned} \tag{4.82}$$

Imposing the remaining AdS boundary conditions of (4.75) gives [185]

$$S_+[F] = -\frac{c}{24\pi}\int_{\partial M} d\sigma dt \left(\frac{(\partial_\sigma^2 F)(\partial_+\partial_\sigma F)}{(\partial_\sigma F)^2} - (\partial_\sigma F)(\partial_+ F)\right), \tag{4.83}$$

where $G|_{\partial M} = \tan(F/2)$. $S_-[\bar{g}]$ gives the same contribution up to interchanging $F \to \bar{F}$ and $\partial_+ \to \partial_-$. If $F, \bar{F}$ depend only on $\sigma^+, \sigma^-$ respectively, then partial derivatives $\partial_+, \partial_-$ w.r.t. $\sigma^+, \sigma^-$ can be expressed through partial derivatives $\partial_t$ w.r.t. $t$. In doing so, (4.83) is identified with the coadjoint action of the Virasoro group for the vacuum orbit $h = 0$ (2.147).

The condition that $G, \bar{G}$ are functions of $\sigma^+, \sigma^-$ respectively represents an additional constraint that cannot be derived from the equation of motion of $G, \bar{G}$. Only for diffeomorphisms $F, \bar{F}$ that satisfy this constraint, the coadjoint orbit actions from the gravity theory and the coadjoint orbit actions as a complexity functional match.[18] The constraint is also necessary to derive the equivalence to the Liouville action, as will become clear below.

To derive the relation between $F, \bar{F}$ of the coadjoint orbit action and $\omega$ from the Liouville action, simply insert the Gauss decompositions (4.80) and (4.82) into $h = g^{-1}\bar{g}$ to obtain

$$e^{-\omega/2} = \lambda\bar{\lambda}(1 + G\bar{G}). \tag{4.84}$$

The fact that the AdS boundary conditions fix $\lambda \sim 1/\sqrt{\partial_\sigma G}$ asymptotically yields

$$\omega \sim \log\left(\frac{(\partial_\sigma G)(\partial_\sigma \bar{G})}{2(1 + G\bar{G})^2}\right) \tag{4.85}$$

up to a constant that can be absorbed by a redefinition of $\omega$. Following [286], this constant is set to zero.[19] If $G, \bar{G}$ depend only on $\sigma^+, \sigma^-$, then this is precisely the general form of the solution of the Liouville equation of motion.

[17] Strictly speaking, the addition of a further boundary term is required to ensure a well-defined variational principle [284]. However, upon imposing the $AdS_3$ boundary conditions, this boundary term gives a vanishing contribution to the on-shell value of the action, hence this boundary can be neglected for the purpose of the following discussion.

[18] Note that this can be circumvented by neglecting the boundary term (4.78), in which case one directly obtains (2.147) [185]. However, then the variational principle is no longer well-defined.

[19] A non-zero value of this constant is equivalent to considering a non-trivial prefactor $\mu \neq 1$ of the $e^{\omega}$ term in the Liouville action.

The Liouville action also appears in connection with the complexity definition of [286] [20], therefore let me summarize this approach here. The computation task considered in [286] is the calculation of the ground state wave functional $\Psi(\phi_1(x)) = \langle \phi_1(x)|0\rangle$ by a Euclidean path integral,

$$\Psi(\phi_1(x)) = \int_{y=-\infty}^{y=0;\phi(y=0,x)=\phi_1(x)} \mathscr{D}\phi \, e^{-S[\phi]}, \tag{4.86}$$

where $\phi$ is a short hand for the fields of the boundary conformal field theory with action $S[\phi]$ while $y$ is the time coordinate in Euclidean signature. The idea is now to evaluate this path integral in a curved background geometry with the constraint that the wave functional $\Psi(\phi_1(x))$ remains invariant up to a prefactor. For any metric in two-dimensions, there exists a coordinate system in which the metric can be written in the form $ds^2 = e^{2\omega}(dy^2 + dx^2)$. Rescaling the metric $\delta_{ij} \to e^{2\omega}\delta_{ij}$ changes the wave functional by the Liouville action (4.81) (or to be precise its Euclidean form) [291],

$$\Psi(\phi_1(x))|_{g_{ij}=e^{2\omega}\delta_{ij}} = e^{S_L[\omega]-S_L[0]}\, \Psi(\phi_1(x))|_{g_{ij}=\delta_{ij}} \,. \tag{4.87}$$

This factor $S_L[\omega]$ is identified in [286] with the cost which is to be minimized. It is argued in [286] that in a computation of the ground state wave functional performed by discretizing the background spacetime in a number of cells, the factor $e^{S_L[\omega]}$ measures the number of repeated computations of the path integral over the same cell. The smaller this number, the more efficiently the wave functional $\Psi(\phi_1(x))$ is calculated according the argument put forward in [286]. Therefore, the optimal calculation procedure is obtained by minimizing the Liouville action, leading to the solution (4.85) to the equations of motion of (4.81). The functions $G, \bar{G}$ in (4.85) determine the background metric for the path integration and thus are the degrees of freedom which are minimized to obtain the complexity.

The relation (4.85) yields a direct mapping between the degrees of freedom that parametrize the complexity functionals of [286] and [266]. There is a small subtlety in this mapping in that the authors of [286] use coordinates $(y, x)$ on the plane where $x \in (-\infty, \infty)$, while [185, 266] work in cylindrical coordinates $(t, \sigma)$ with a periodic coordinate $\sigma \in [0, 2\pi)$. The transformation between these coordinate systems is the same as the transformation between Poincaré patch coordinates and global AdS coordinates near the AdS boundary[21],

$$y = \frac{\sin t}{\cos t - \cos\sigma} \quad , \quad x = \frac{\sin\sigma}{\cos t - \cos\sigma}. \tag{4.88}$$

Using this transformations, explicit expressions for the diffeomorphisms $F, \bar{F}$ for the solutions of the Liouville equation considered in [286] may be found. The first such solution is given by $\bar{G} = -(x+y)$, $G = 1/(x-y)$. In [286], the corresponding background metric of the path integral is a time slice of pure $AdS_3$ and the complexity is obtained as the volume of this time slice. Using (4.88) and the definition $G = \tan(F/2)$, $\bar{G} = \tan(\bar{F}/2)$ yields

$$F(t,\sigma) = \sigma + t \quad , \quad \bar{F}(t,\sigma) = \sigma - t + \pi. \tag{4.89}$$

As needed for a consistent diffeomorphism, $F(t, \sigma + 2\pi) = F(t,\sigma) + 2\pi$ and the same for $\bar{F}$. Furthermore, these diffeomorphisms are solutions of the equations of motion (4.42) thus they indeed induce optimal transformations leading from the target to the reference state.[22]

[20] See also [287–290] for further developments in this direction.

[21] Implicitly, $y$ is analytically continued to Lorentzian signature in this expression.

[22] Note that the diffeomorphisms (4.89) are not only solutions to the equations of motion of the complexity functional

Inserting (4.89) into (4.83), only the second part $-(\partial_\sigma F)(\partial_+ F)$ contributes. Together with the contribution from $\bar{F}$, the complexity is obtained as

$$\mathscr{C} = S_+[F] + S_-[\bar{F}] = -\frac{c}{24\pi}\int_0^{t_f} dt \int_0^{2\pi} d\sigma(-2) = \frac{c}{6}t_f. \tag{4.90}$$

The complexity increases linearly in the time $t_f$ for which the conformal transformation arising from the diffeomorphism acts on the vacuum state. Identifying $t_f$ with the inverse UV cutoff (i.e. letting the conformal transformation act for an infinitely long time), the complexity is proportional to the volume of a time slice of pure $AdS_3$, reproducing the result of [286]. Such an example for which the Schwarzian term in the coadjoint action vanishes, was also considered in [266]. Here we arrived at it from a different angle by mapping the optimal transformation from the path integral complexity proposal of [286] into an optimal transformation for the complexity functional of [266].

Note, however, that the conformal transformation acting on the reference state is trivial in the sense that it involves only the $L_0$ generator of which the vacuum is an eigenstate. Hence, the gate acts only by changing the phase of the vacuum state, i.e. it transforms

$$|0\rangle \to e^{ict_f/6}|0\rangle. \tag{4.91}$$

Since this phase change is a gauge symmetry of the problem, the complexity (4.90) derived above is not a measurable quantity.[23]

The same applies to a primary state with arbitrary weight $h = \bar{h} < c/24$ dual to a conical defect in the bulk. In this case, the action on the corresponding Virasoro orbit takes the form [185]

$$S_+[F] = -\frac{c}{24\pi}\int_{\partial M} d\sigma dt \left(\frac{(\partial_\sigma^2 F)(\partial_+\partial_\sigma F)}{(\partial_\sigma F)^2} - a^2(\partial_\sigma F)(\partial_+ F)\right), \tag{4.92}$$

where $a^2 = 1 - 24h/c$. Again, for this example the diffeomorphisms $F$, $\bar{F}$ which follow from the solution of the Liouville equation considered in [286] are given by (4.89). Inserting this into (4.92), a complexity of $\mathscr{C} = ca^2 t_f/6$ is obtained. As before, the complexity only counts the change of phase in the transformation $|h,\bar{h}\rangle \to e^{ica^2 t_f/6}|h,\bar{h}\rangle$.

## 4.4. Computational complexity, the Fubini-Study metric and "complexity=volume"

The upshot of the last section is that geometric actions do not provide good complexity measures. The issue ultimately stems from a unsuitable choice of cost function (4.35). How should a better cost function be chosen for the circuits built up from consecutive conformal transformations considered here? For this, let me refer back to the original idea discussed in section 2.3.4 where the cost function was given by a metric on the group of unitary operators implementing the circuit. In the circuits considered here the unitaries are associated with Virasoro group elements. Therefore,

(4.37) including the central extension contribution, but are also solutions to the equations of motion of the functional (4.25) without this contribution. In fact, the on-shell value of both complexity functionals is the same for these diffeomorphisms. Thus, in this case, these two complexity measures agree.

[23] Note that while this result shows that interpreting the path integral complexity proposal of [286] in the language of the complexity functional from geometric actions on coadjoint orbits of the Virasoro group is not sensible, it does not exclude that a physically meaningful interpretation of the path integral complexity proposal in terms of unitaries acting on states exists.

choosing a metric on the Virasoro group automatically defines a cost function whose associated complexity is given as the length of the minimal geodesic between two points on the group. This section contains a limited study of cost functions from metrics on the Virasoro group. This idea was briefly mentioned already in [266] although not explored in detail. Geodesic distances on other Lie groups have been applied to computational complexity measures for free quantum field theories in [166, 167].

### 4.4.1. Motivation: geodesics in Lie groups and the Euler-Arnold method

An advantage of choosing the cost function from a metric on the Virasoro group is that well-known techniques from mathematics called Euler-Arnold methods can be used to derive the geodesic equations. These methods are introduced in this subsection and some choices of metric on the Virasoro group considered before in the mathematics literature are investigated w.r.t. their utility as a cost function for computational complexity. The Euler-Arnold method was developed by Arnold in [292, 293] who in particular used this method to rephrase Euler's equations from fluid dynamics as geodesic equations on diffeomorphism groups. The application of the Euler-Arnold method to the Virasoro group was worked out in [294–296].

The Euler-Arnold method provides a simple way of deriving the geodesic equations on a Lie group by replacing the minimization of the length between two points on the group manifold by minimization of an energy functional via the associated Hamilton equations. In general, a positive definite quadratic form $\langle\cdot,\cdot\rangle_g$ [24] on a Lie algebra defines an associated metric on the corresponding Lie group [292]. The length of a curve $X(\tau)$ on the Lie algebra with respect to this metric is given by

$$\ell = \int_0^{\tau_f} d\tau \sqrt{\langle X, X\rangle_g}. \tag{4.93}$$

Geodesics are the curves with minimal length. The main simplification of the Euler-Arnold method is due to replacing minimization of $\ell$ by minimization of the "energy"

$$E = \frac{1}{2}\int_0^{\tau_f} d\tau \langle X, X\rangle_g. \tag{4.94}$$

The two minimal curves obtained in this way coincide provided that the curve is traversed at constant speed, i.e. $\langle X, X\rangle_g$ is constant in $\tau$. Due to the reparametrization invariance in $\tau$ enjoyed by the problem this is always a valid choice to make.

To derive the geodesic equation, it is useful to relate the metric $\langle\cdot,\cdot\rangle_g$ to the pairing $\langle\cdot,\cdot\rangle$ between elements of the Lie algebra $\mathfrak{g}$ and its dual space $\mathfrak{g}^*$. This is achieved by defining the *inertia operator* $A$ mapping the velocity $X \in \mathfrak{g}$ to a corresponding element of $v \in \mathfrak{g}^*$ known as the *intrinsic momentum*. The inertia operator is defined by

$$\langle X, Y\rangle_g = \langle AX, Y\rangle. \tag{4.95}$$

It is common to write the Hamiltonian associated to the energy (4.94) in terms of the intrinsic momentum,

$$H = \frac{1}{2}\langle AX, X\rangle = \frac{1}{2}\langle v, A^{-1}v\rangle. \tag{4.96}$$

Then one can show that the geodesic equation for (4.93) is equivalent to the Euler-Arnold

[24] The $g$ subscript is not an index, but a reminder that the linear functional is associated to a metric.

equation on $\mathfrak{g}^*$ [292, 293][25]

$$\dot{\nu} = -\mathrm{ad}^*_{A^{-1}\nu}\nu, \tag{4.97}$$

where the coadjoint operator $\mathrm{ad}^*_X$ defined in (2.101). The proof of this statement works as follows. To simplify the notation, let me specialize to matrix groups for the moment. In this case, $X$ is related to the group elements $g$ specifying the geodesic path as $X = \dot{g}g^{-1}$. Perturbing the path $g \to g + \delta g$ gives a perturbation $\delta X = \delta\dot{g}g^{-1} + \dot{g}\delta g^{-1}$ and

$$\delta H = \langle AX, \delta X\rangle = \langle \nu, \delta\dot{g}g^{-1} - \dot{g}g^{-1}\delta g g^{-1}\rangle. \tag{4.98}$$

Partially integrating the first term in $t$ and applying the definition (2.101) of the coadjoint operator gives

$$\delta H = -\langle \dot{\nu}, \delta g g^{-1}\rangle + \langle \nu, [\delta g g^{-1}, X]\rangle = -\langle \dot{\nu} + \mathrm{ad}^*_{A^{-1}\nu}\nu, \delta g g^{-1}\rangle. \tag{4.99}$$

Demanding that $\delta H = 0$ vanishes for arbitrary perturbations leads to (4.97).

Now specialize to the Virasoro group. In this case, algebra elements are given by $X \equiv (X(\sigma)\partial_\sigma, r)$ and elements of the dual space $\mathfrak{g}^*$ by $\nu \equiv (\nu(\sigma)d\sigma^2, c)$. From the group theory perspective, the simplest metric to take is given by the inner product

$$\langle (X(\sigma)\partial_\sigma, r), (Y(\sigma)\partial_\sigma, s)\rangle_g = \frac{1}{2\pi}\int d\sigma\, X(\sigma)Y(\sigma) + rs \tag{4.100}$$

which defines a right-invariant $L^2$ metric on the Virasoro group.[26] [27] The length of $(X\partial_\sigma, r)$ is given by $\sqrt{\langle (X\partial_\sigma, r), (X\partial_\sigma, r)\rangle_g}$. Because the natural pairing between elements of $\mathfrak{g}$ and $\mathfrak{g}^*$ is given by (2.125), for the choice of metric (4.100), $A$ simply maps $(X\partial_\sigma, r) \in \mathfrak{g} \to (X d\sigma^2, r) \in \mathfrak{g}^*$. Inserting the coadjoint operator for the Virasoro algebra, equation (2.132), into (4.97) and using the definition of $A$ for the metric (4.100) yields the Korteweg-de Vries (KdV) equation as the geodesic equation together with $\dot{c} = 0$ [296],

$$\dot{\nu} + 3\nu\nu' - \frac{c}{24\pi}\nu''' = 0\,, \quad \dot{c} = 0. \tag{4.101}$$

The KdV equation describes shallow water waves and is well-known for being an exactly solvable non-linear partial differential equation. Note that because the inertia operator $A$ for the metric (4.100) equates $X$ and $\nu$ as well as $r$ and $c$ this can be equivalently written as

$$\dot{X} + 3XX' - \frac{r}{24\pi}X''' = 0\,, \quad \dot{r} = 0. \tag{4.102}$$

However, there are of course other possible choices of inertia operator leading to different metrics. For example, in [296] $A : (X\partial_\sigma, r) \to ((\alpha X - \beta X'')d\sigma^2, r)$ has been considered. For $\alpha = \beta = 1$ the resulting geodesic equation is the Camassa-Holm equation,

$$\dot{\nu} - \dot{\nu}'' + 3\nu\nu' - 2\nu'\nu'' - \nu\nu''' - \frac{c}{24\pi}\nu''' = 0, \tag{4.103}$$

[25] The form of the Euler-Arnold equation (4.97) shown here is also known as Lax pair form or the Lie-Poisson equation. The Euler-Arnold equation formulated on $\mathfrak{g}$ instead of $\mathfrak{g}^*$ is also called the Euler-Poincaré equation.

[26] The metric is called $L^2$ since the length of a vector as measured by this metric defines an $L^2$ norm, $\langle (X\partial_\sigma, r), (X\partial_\sigma, r)\rangle_g = \sum_n X_n^2 + r^2$.

[27] Technically speaking, the quadratic form on the Lie algebra $\mathfrak{g} = T_eM$ defines a metric only at the identity element $e$ of the group. But of course, elements of a generic tangent spaces $T_gM$ can be transported to the identity tangent space by left/right translation. In this way, the inner product on the Lie algebra extends to a metric on the full group manifold.

another equation describing shallow water waves.

Further insight into the Euler-Arnold equation can be obtained by considering the evolution of an arbitrary $v$ under (4.97). One can show that orbits of the coadjoint representation are *invariant manifolds* under this evolution, i.e. starting from a $v(0)$ in some coadjoint orbit, we will evolve to a $v(\tau)$ in the same coadjoint orbit [292]. For the Virasoro case, this is just the familiar statement that acting with conformal transformations on a state in some Verma module gives another state in the same Verma module. Thus, the coadjoint orbit, which tells us which reference state we are considering, is implicitly contained in the choice of boundary condition $v(0)$ for the Euler-Arnold equation. Furthermore, the energy $H = 1/2\langle v, A^{-1}v\rangle$ is a Hamiltonian function defined on a coadjoint orbit [292]. The Euler-Arnold equations (4.97) are then nothing but the Hamilton equations for this function.

For the application to complexity, $X(\tau,\sigma)$ is identified with the infinitesimal Virasoro algebra element $X(\tau,\sigma) = \epsilon(\tau,\sigma) = -\dot{F}/F'$ (see equation (4.20)). Then (4.100) determines how expensive the infinitesimal conformal transformation induced by $\epsilon$ is, i.e. it defines the cost function. In contrast to the cost function (4.17) used in section 4.3, this cost function is state independent. It is obtained by mapping the question 'How expensive is the infinitesimal transformation induced by $\epsilon$?' to the question 'How long is the representation vector of the transformation in the Virasoro algebra?'. Note also that (4.100) assigns a cost to the central extension part $r(\tau)$ of the Virasoro algebra and therefore the computational complexity is no longer solely defined by the conformal transformations $f(\tau,\sigma)$ and their inverses $F(\tau,\sigma)$.

To see whether (4.100) defines a good complexity functional, we would like to know whether it admits optimal paths which not just give a phase change as the geometric action. For this, the KdV equations of motion (4.102) of the complexity functional must be solved. The simplest solutions of (4.102) are given by $\epsilon(\tau,\sigma) = \text{const}$. Correspondingly, $F(\tau,\sigma) = G(\sigma - \epsilon\tau)$. We note that this is the same kind of solutions as already encountered in section 4.3.3 for the equations of motion (4.42) of the geometric action. In particular, since $\epsilon(\tau,\sigma) = \text{const}$ only the $L_0$ generator acts on the reference state, yielding nothing but a phase change.

However, unlike for the equations of motion (4.42) of the geometric action, there also exist non-trivial solutions of (4.102), which in the context of complexity lead to non-trivial unitary transformations $U_f$. These are termed cnoidal waves [297] and are of the form

$$X(\tau,\sigma) = \epsilon(\tau,\sigma) = \tilde{\epsilon} + A\,\mathrm{cn}^2\left(k\frac{\sigma - C\tau}{2\pi}2K(m); m\right), \tag{4.104}$$

where $\tilde{\epsilon}, A, C, k, m$ are parameters of the solution, $\mathrm{cn}(x;m)$ is a Jacobi elliptic function and $K(m)$ is the complete elliptic integral of the first kind. In terms of physical parameters of the wave $\tilde{\epsilon}$ is the trough elevation, $A$ the amplitude and $C$ the phase speed, while $m$ controls the shape of the wave. For $m \to 0$, the solution reduces to a sine wave and for $m \to 1$ it becomes solitonic in nature. The parameters are all dependent on each other, thus together with the wavelength $2\pi/k$ the solution has only two free parameters in total.

Now the main question of interest at this point is: Does the cnoidal wave solutions of the KdV equation suffer from the same problem as the ones for the geometric action, i.e. does only a phase contribute to the complexity? To answer that question, it is necessary to determine which $L_n$ modes act at each time step $\tau$, i.e. the Fourier coefficients of $\epsilon(\tau,\sigma)$ need to be evaluated. For a wave length $\lambda = 2\pi$ ($k = 1$), these are straightforwardly determined from the Lambert series of the Jacobi elliptic function [298],

$$\mathrm{cn}\left((x - C\tau)\frac{K(m)}{\pi}; m\right) = \frac{2\pi}{K(m)\sqrt{m}}\sum_{n=0}^{\infty}\frac{\cos((n+1/2)(x - C\tau))}{2\cosh(\pi(n+1/2)K(1-m)/K(m))}, \tag{4.105}$$

to be

$$\epsilon_n = \tilde{\epsilon}\delta_{n,0} + A\frac{\pi^2 e^{-inC\tau}}{4K^2(m)m}\sum_{r=-\infty}^{\infty}\left[\cosh\left(\pi\left(r+\frac{1}{2}\right)\frac{K(1-m)}{K(m)}\right)\cosh\left(\pi\left(n-r-\frac{1}{2}\right)\frac{K(1-m)}{K(m)}\right)\right]^{-1}. \tag{4.106}$$

For other wavelengths $\lambda = 2\pi/k$ with $k \neq 1$, $\epsilon_{n\notin k\mathbb{Z}} = 0$ while $\epsilon_{n\in k\mathbb{Z}}$ is the same as for $k = 1$. The coefficients quickly converge to zero for $|n| \to \infty$. The speed of the convergence is controlled by $m$; for $m = 0$ only $\epsilon_{0,\pm k}$ are non-zero, while higher and higher $L_n$ modes contribute as $m \to 1$. Thus, clearly more Virasoro generators than just $L_0$ contribute to $U_f$ and the resulting non-trivial time dependent conformal transformation $U_f$ does not just generate a phase. Furthermore, it is possible to control which $L_n$ generators act on the reference state by varying the $m$ parameter of the solution.

Note that the two solutions ($\epsilon$ = const. and $\epsilon$ given by a cnoidal wave) of the KdV equation (4.102) do not exhaust all possibilities. In particular, there exist solutions that are superpositions of (interacting) cnoidal waves which form a kind of generalization of the Fourier expansion in the solution space of the KdV equation [299]. These solutions can have an arbitrary number of parameters, instead of essentially just one (the $m$ parameter) for a single cnoidal wave.

In conclusion, the possible unitary transformations $U_f$ obtainable from solutions of the KdV equation are much less constrained than for the equations of motion of the geometric action. While for the geometric action we only had $\dot{f}/f' = \text{const}$ for $h > 0$, here for any reference state an infinite set of solutions is found with different coefficients of the $L_n$ generators. To precisely determine which $U_f$ are possible and thus to find the complexity between given reference and target states, one needs to solve for the group element $F$ in the equation $\epsilon = -\dot{F}/F'$ for $\epsilon$ given by (4.104). Finding solutions to this non-linear partial differential equation is in general a difficult problem, which is not tackled at this point. Nevertheless, it is clear from the above results that the complexity definition from the metric (4.100) on the Virasoro group has a set of known optimal paths over which one has good control and that – more importantly – are non-trivial in the sense that they do not instantaneously jump to the target state.[28]

### 4.4.2. Complexity from the Fubini-Study metric

The metrics considered in the previous subsection, while simple from the viewpoint of Lie group theory, do not fulfill one of the conditions set up in [270] discussed at the beginning of section 4.3.1: the metrics assign cost to operators that do not change the state $|\psi(\tau)\rangle$. It is clear that this must happen because the metrics depend only on the operators applied at time $\tau$ in the circuit via the Lie algebra elements $X(\tau)$, but not on the state at time $\tau$. Is it possible to choose a metric on the Lie group motivated by the Euler-Arnold method such that the corresponding complexity measure is a more direct implementation of the ideas of [270]? The answer to this question is yes: as shown in [268, 269] the Fubini-Study metric provides a natural candidate.

In fact, computational complexity from the Fubini-Study metric shows interesting connections to the "complexity=volume" proposal. The complexity functional of [268, 269] for perturbative conformal transformations of the vacuum state is equal to the change in the volume of a maximal codimension-one slice in the bulk under the same perturbative conformal transformations as was noticed already in [272] based on the results of [265]. This section starts with a short review of the ideas of [268, 269]. Afterwards, the perturbative calculations of the complexity functional of [268, 269] as well as the "complexity=volume" proposal for perturbative conformal

[28] Note also that unitary transformations $U_f$ giving only a phase change can still lead to a non-vanishing complexity. Therefore, the addition of a boundary term to cancel the phase contribution is necessary to get a well-defined complexity functional from the metric (4.100).

transformations are extended to higher order, showing that the agreement observed at low orders in perturbation theory does not extend to higher orders.

### Definition of the Fubini-Study complexity measure

The complexity measure defined in [268, 269] is based on a cost function given by the square of the Fubini-Study distance (4.3),

$$\mathscr{F}_{\text{FS}} = |\langle\psi(\tau)|Q(\tau)^2|\psi(\tau)\rangle| - |\langle\psi(\tau)|Q(\tau)|\psi(\tau)\rangle|^2, \tag{4.107}$$

where the circuit generator $Q(\tau)$ is defined by (4.5) and (4.10), i.e. the circuit considered in [268, 269] is of type (a) in the classification of section 4.2. The cost function (4.107) can be rewritten by defining $\tilde{Q}(\tau) = U^{\dagger}_{f(\tau)}Q(\tau)U_{f(\tau)}$ where $U_{f(\tau)}$ is the unitary giving the state at time $\tau$, $|\psi(\tau)\rangle = U_{f(\tau)}|\psi_R\rangle$,

$$\mathscr{F}_{\text{FS}} = |\langle\psi_R|\tilde{Q}(\tau)^2|\psi_R\rangle| - |\langle\psi_R|\tilde{Q}(\tau)|\psi_R\rangle|^2. \tag{4.108}$$

The transformation law (4.22) of the energy-momentum tensor under conformal transformations allows for writing $\tilde{Q}(\tau)$ as[29]

$$\tilde{Q}(\tau) = \int_0^{2\pi} \frac{d\sigma}{2\pi}\frac{\dot{f}(\tau,\sigma)}{f'(\tau,\sigma)}\left(T(\sigma) - \frac{c}{12}\{f,\sigma\}\right). \tag{4.109}$$

Using a primary state $|h\rangle = |\psi_R\rangle$ as the reference state, the Fubini-Study cost function (4.107) becomes

$$\mathscr{F}_{\text{FS}} = \int_0^{2\pi} d\sigma d\kappa \frac{\dot{f}(\tau,\sigma)}{f'(\tau,\sigma)}\frac{\dot{f}(\tau,\kappa)}{f'(\tau,\kappa)}\Pi(\sigma-\kappa) \tag{4.110}$$

where

$$\Pi(\sigma-\kappa) = \langle h|T(\sigma)T(\kappa)|h\rangle - \langle h|T(\sigma)|h\rangle\langle h|T(\kappa)|h\rangle \tag{4.111}$$

is the connected two-point function of the stress-energy tensor.

The relation to the Euler-Arnold method emerges as follows [268, 269]. Consider a special class of metrics on the Virasoro group of the following form

$$\langle(X\partial_\sigma, r),(Y\partial_\sigma, s)\rangle_{\text{Diff}^+(S^1)\times\mathbb{R}} = \langle X\partial_\sigma, Y\partial_\sigma\rangle_{\text{Diff}^+(S^1)} + \langle r,s\rangle_{\mathbb{R}} \tag{4.112}$$

where the inner product on the diffeomorphisms is given as

$$\langle X\partial_\sigma, Y\partial_\sigma\rangle_{\text{Diff}^+(S^1)} = \int d\sigma d\kappa X(\sigma)Y(\kappa)\Pi(\sigma-\kappa) \tag{4.113}$$

for some function $\Pi(\sigma-\kappa)$. For instance, the metric (4.100) leading to the KdV equation in the Euler-Arnold method is of this form for $\Pi(\sigma-\kappa) = \delta(\sigma-\kappa)$ where $\delta(\sigma)$ denotes the delta distribution. Now take a closer look at equation (4.110): if $\dot{f}/f'$ is a Virasoro algebra element, this is of the general form (4.112) where $\langle r,s\rangle_{\mathbb{R}} = 0$ and $\Pi(\sigma-\kappa)$ is the connected two-point function (4.111). Thus, equation (4.110) almost but not quite defines a proper metric on the Virasoro group for the following two reasons: first, Virasoro algebra elements in the circuit are

[29] Note again that as in section 4.3, the conventions used for the conformal transformation of the energy-momentum tensor in this section (see equation (4.22)) differ from those of section 4.2 (see equation (4.12)) in order to keep the notation consistent with [268, 269].

given by

$$X(\tau,\sigma) = \epsilon(\tau,\sigma) = -\frac{\dot{F}(\tau,\sigma)}{F'(\tau,\sigma)} \tag{4.114}$$

which is equivalent to the form encountered in (4.110) only with the replacement of the diffeomorphism $f$ by its inverse $F$. Of course, one could construct a cost function that is equivalent to (4.110) with the replacement $f \to F$ simply by evaluating the variance of $Q(\tau)$ in the reference state $|\psi_R\rangle = |h\rangle$ instead of the state $|\psi(\tau)\rangle$ at time $\tau$, although this cost function is then no longer equal to the Fubini-Study distance.[30] Second, note that (4.110) defines a degenerate metric on the Virasoro group. Because the central extension piece $\langle r,s\rangle_{\mathbb{R}}$ is set to zero, the length of group elements in all of the central extension directions is zero. This degeneracy is, however, a welcome feature of the construction since the central extension piece only counts phase changes. By construction the Fubini-Study cost function assigns zero cost to phase changes, avoiding the problems encountered in section 4.3. To see this explicitly, note that the norm of a Virasoro algebra element $X(\sigma) = \sin(n\sigma)$ is given by

$$||X||^2 = \int d\sigma d\kappa\, X(\sigma)X(\kappa)\Pi(\sigma-\kappa) = \pi^2\left(\frac{c}{12}n(n^2-1)+2nh\right). \tag{4.115}$$

If $h > 0$, the norm vanishes for $n = 0$ corresponding to $U(1)$ transformations generated by $L_0$ while for $h = 0$ it vanishes for $n = 0, \pm 1$ corresponding to $PSL(2,\mathbb{R})$ transformations generated by $L_0, L_{\pm 1}$. These are exactly the transformations from the stabilizer subgroup leaving the reference state invariant. Therefore, in summary the Fubini-Study metric on the space of states in the quantum circuit considered here defines a degenerate inner product on the Virasoro group group which is similar to the metrics considered in section 4.4.1.

### Evaluation of the Fubini-Study complexity measure

Let me now proceed to the explicit evaluation of the Fubini-Study complexity measure of [268, 269]. The connected two-point function (4.111) can be obtained explicitly by mapping the well-known result

$$\langle T(z)T(w)\rangle = \frac{c/2}{(z-w)^4} + \frac{2\langle T(w)\rangle}{(z-w)^2} + \frac{\partial_w\langle T(w)\rangle}{z-w} \tag{4.116}$$

from conformal field theory on the plane onto the cylinder and using $\langle h|T(\sigma)|h\rangle = h - c/24$, giving

$$\Pi(\sigma-\kappa) = \frac{c/32}{\sin((\sigma-\kappa)/2)^4} - \frac{h/2}{\sin((\sigma-\kappa)/2)^2} \tag{4.117}$$

Therefore, the complexity functional of [268, 269] is given by

$$\mathscr{C}_{\text{FS}} = \int d\tau\, \mathscr{F}_{\text{FS}} = \int d\tau \int d\sigma d\kappa \frac{\dot{f}(\tau,\sigma)}{f'(\tau,\sigma)}\frac{\dot{f}(\tau,\kappa)}{f'(\tau,\kappa)}\left(\frac{c/32}{\sin((\sigma-\kappa)/2)^4} - \frac{h/2}{\sin((\sigma-\kappa)/2)^2}\right) \tag{4.118}$$

[30] In terms of group theory, the metrics discussed in section 4.4.1 formulated in terms of $\epsilon(\tau,\sigma) = -\dot{F}/F'$ lead to right-invariant computational complexity measures, that is complexity functionals which are invariant under $f(\sigma) \to (f\circ g)(\sigma) = f(g(\sigma))$ for arbitrary diffeomorphisms $g$ independent of $\tau$. In contrast, the Fubini-Study metric formulated in terms of $\hat{\epsilon}(\tau,\sigma) = -\dot{f}/f'$ leads to a left-invariant computational complexity measure, that is a complexity functional which is invariant under $f(\sigma) \to (g\circ f)(\sigma) = g(f(\sigma))$.

The complexity is determined by minimizing (4.118) which involves solving the equations of motion

$$\int d\sigma\Big[\Big(-\frac{\ddot{f}(\tau,\sigma)}{f'(\tau,\sigma)f'(\tau,\kappa)}+\frac{\dot{f}(\tau,\sigma)\dot{f}'(\tau,\sigma)}{f'(\tau,\sigma)^2f'(\tau,\kappa)}+2\frac{\dot{f}(\tau,\sigma)\dot{f}'(\tau,\kappa)}{f'(\tau,\sigma)f'(\tau,\kappa)^2} \\ -2\frac{\dot{f}(\tau,\kappa)\dot{f}(\tau,\sigma)f''(\tau,\kappa)}{f'(\tau,\sigma)f'(\tau,\kappa)^3}\Big)\Pi(\sigma-\kappa)+\frac{\dot{f}(\tau,\sigma)\dot{f}(\tau,\kappa)}{f'(\tau,\kappa)^2f'(\tau,\sigma)}\partial_\kappa\Pi(\sigma-\kappa)\Big]=0. \tag{4.119}$$

Since a general solution is not possible, this is achieved perturbatively. The conformal transformation $f(\tau,\sigma)$ is expanded around the identity,

$$f(\tau,\sigma)=\sigma+\varepsilon f_1(\tau,\sigma)+\varepsilon^2 f_2(\tau,\sigma)+O(\varepsilon^3), \tag{4.120}$$

and the solution of (4.119) is determined order by order in $\varepsilon$. Without loss of generality $\tau$ ranges from 0 to $\tau_f=1$ where the boundary conditions

$$f(0,\sigma)=\sigma\ ,\quad f(1,\sigma)=f(\sigma), \tag{4.121}$$

are imposed. Finally, the singularities of the two-point function $\Pi(\sigma-\kappa)$ at coincident insertion points $\sigma=\kappa$ have to be taken into account when inserting the solution of (4.119) back into (4.118). Strictly speaking, the $\sigma$ or $\kappa$ integral in (4.118) is divergent and therefore a regularization procedure is necessary. As in [268, 269], differential regularization is employed for this purpose whereby the divergent $1/\sin((\sigma-\kappa)/2)$ terms in $\Pi(\sigma-\kappa)$ are expressed as derivatives of $\log[\sin((\sigma-\kappa)/2)^2]$ terms with milder singularities,

$$\Pi(\sigma-\kappa)=\Big[-\frac{c}{24}\partial_\sigma^2\partial_\kappa^2-\Big(h-\frac{c}{24}\Big)\partial_\sigma\partial_\kappa\Big]\log[\sin((\sigma-\kappa)/2)^2]. \tag{4.122}$$

The derivatives are shifted onto the prefactors of these terms by partial integration, neglecting the divergent boundary terms. Finally, only integrals of periodic functions times $\log[\sin((\sigma-\kappa)/2)^2]$ remain which are convergent and equal to

$$\int d\sigma\log[\sin(\sigma/2)^2]\sin(n\sigma)=0,\qquad \int d\sigma\log[\sin(\sigma/2)^2]\cos(n\sigma)=-2\pi/n, \tag{4.123}$$

for $n\in\mathbb{N}$.

The value of the complexity to second order in perturbation theory is determined by the solution of the equations of motion to first order, given by a linearly increasing function in the circuit time parameter $\tau$,

$$\int d\sigma\ddot{f}_1(\tau,\sigma)\Pi(\sigma-\kappa)=0\qquad\Rightarrow f_1(\tau,\sigma)=\tau f_1(\sigma). \tag{4.124}$$

Therefore, the following complexity is obtained,

$$\mathscr{C}_{(2)}=\mathscr{C}_{\mathrm{FS}}|_{O(\varepsilon^2)}=\int d\tau\int d\sigma d\kappa\Pi(\sigma-\kappa)\dot{f}^1(\tau,\sigma)\dot{f}^1(\tau,\kappa) \\ =2\pi^2\sum_n\Big(\frac{c}{12}(|n|^3-|n|)+2h|n|\Big)f_1^nf_1^{-n} \tag{4.125}$$

where $f_1^n$ is the $n$-th Fourier mode of $f_1(\sigma)=f_1(\tau=1,\sigma)$.

To second order, the solution to the equations of motion is quadratic in $\tau$,

$$\begin{aligned}\int d\sigma \ddot{f}_2(\tau,\sigma)\Pi(\sigma-\kappa) &= \int d\sigma \left[\dot{f}_1(\tau,\sigma)(\dot{f}_1'(\tau,\sigma)+2f_1'(\tau,\kappa))+\dot{f}_1(\tau,\sigma)\dot{f}_1(\tau,\kappa)\partial_\kappa\right]\Pi(\sigma-\kappa)\\ &= \int d\sigma \left[f_1(\sigma)(f_1'(\sigma)+2f_1'(\kappa))+f_1(\sigma)f_1(\kappa)\partial_\kappa\right]\Pi(\sigma-\kappa)\\ &\Rightarrow f_2(\tau,\sigma) = \frac{1}{2}A_2(\sigma)\tau^2+B_2(\sigma)\tau+C_2(\sigma)\end{aligned} \tag{4.126}$$

The boundary conditions $f_2(0,\sigma)=0$, $f_2(1,\sigma)=f_2(\sigma)$ fix $C_2(\sigma)=0$, $\frac{1}{2}A_2(\sigma)+B_2(\sigma)=f_2(\sigma)$. Therefore, the complexity to third order in perturbation theory is equal to

$$\begin{aligned}\mathscr{C}_{(3)} = \mathscr{C}_{\text{FS}}|_{O(\varepsilon^3)} &= \int d\tau \int d\sigma d\kappa \Pi(\sigma-\kappa)[2\dot{f}_1(\tau,\sigma)\dot{f}_2(\tau,\kappa)-\dot{f}_1(\tau,\sigma)\dot{f}_1(\tau,\kappa)(f_1'(\tau,\sigma)+f_1'(\tau,\kappa))]\\ &= 2\pi^2\sum_n\left(\frac{c}{12}(|n|^3-|n|)+2h|n|\right)f_1^n\left[2f_2^{-n}-i\sum_m m f_1^m f_1^{-n-m}\right].\end{aligned} \tag{4.127}$$

The expressions for the computational complexity to fourth order in perturbation theory are quite lengthy and relegated to appendix D. The results obtained here are in agreement with calculations of [268, 269] for the Fubini-Study complexity for perturbative conformal transformations with a single Fourier mode.

### Circuit (b)

The calculations above were all performed in the circuit (a) from section 4.2. It turns out that for circuit (b) from section 4.2, the Fubini-Study complexity is the same as that for circuit (a) up to third order in perturbation theory. The Fubini-Study complexity in the circuit (b) is defined analogous to the circuit (a) by simply replacing the circuit generator $Q = Q_{(a)}$ in (4.107) by $Q = Q_{(b)}$, giving

$$\mathscr{F}_{\text{FS,(b)}} = \int_0^{2\pi i} dz dw \frac{1-\dot{f}(t,z)}{f'(t,z)}\frac{1-\dot{f}(t,w)}{f'(t,w)}\Pi(z-w). \tag{4.128}$$

The solution to the equations of motion for the corresponding complexity functional, which determine the optimal path, to the $n$-th order in perturbation theory are given by $n$-th order polynomials with prefactors dependent on $z-t$. Thus, as expected the optimal path in the circuit (b) is different than that of circuit (a). However, an analogous calculation to the one for the circuit (a) shows that up to third order in perturbation theory the final result (4.125), (4.127) for the complexity is the same in both circuits.

## 4.4.3. Complexity=volume for conformal transformations of the vacuum

This section contains a computation of the holographic dual to computational complexity proposed in [52] in bulk geometries dual to perturbative conformal transformations of the vacuum state in order to have a comparison point with the results of section 4.4.2.

The proposal of [52], often referred to as "complexity=volume", equates the computational complexity with the maximal volume of a codimension-one spacelike hypersurface in the bulk. The hypersurface asymptotes to a constant time slice on the boundary in $z,\bar{z}$ coordinates from

section 4.2. In these coordinates the bulk spacetime is a Bañados geometry. However, one can make use of the fact that all asymptotically $AdS_3$ spacetimes have constant curvature to describe the hypersurface as a codimension-one surface in pure $AdS_3$. In this setup in the $w, \bar{w}$ coordinates from section 4.2 the bulk metric is the standard pure $AdS_3$ metric while the hypersurface asymptotes to a diffeomorphism of the constant time slice in $z, \bar{z}$ coordinates. The starting point in the latter approach, will I will use in the following, is the global $AdS_3$ metric in coordinates

$$ds^2 = -\cosh^2\rho dt^2 + d\rho^2 + \sinh^2\rho d\phi^2, \tag{4.129}$$

where I have set the AdS radius $L$ to one without loss of generality (the $L$ dependence can be easily restored by multiplying the final result with $L$). The embedding of the codimension-one hypersurface is determined by $t(\phi, \rho)$. The induced metric on the hypersurface is given by

$$\gamma_{ij}dx^i dx^j = \left(1 - \dot{t}^2\cosh^2\rho\right)d\rho^2 - 2\dot{t}t'\cosh^2\rho d\rho d\phi + \left(\sinh^2\rho - t'^2\cosh^2\rho\right)d\phi^2, \tag{4.130}$$

where $\dot{t} = \frac{\partial}{\partial\rho}t(\rho,\phi)$ and $t' = \frac{\partial}{\partial\phi}t(\rho,\phi)$. For the zeroth order in perturbation theory the boundary conditions are $t(\phi, \rho \to \infty) = t_0 = \text{const}$ and the maximal volume slice is a constant time slice $t(\phi,\rho) = t_0$. The volume is given as the square of the determinant $\gamma$ of the induced metric, giving a UV divergent result

$$V_{(0)} = \int_0^{1/\epsilon_{\text{UV}}} d\rho \int_0^{2\pi} d\phi\sqrt{\gamma} = \int_0^{1/\epsilon_{\text{UV}}} d\rho \int_0^{2\pi} d\phi \sinh\rho = 2\pi\left(\frac{1}{\epsilon_{\text{UV}}} - 1\right). \tag{4.131}$$

Now, expand in a perturbation series around the zeroth order solution with expansion parameter $\varepsilon$,

$$t(\phi,\rho) = t_0 + \varepsilon t_1(\phi,\rho) + \varepsilon^2 t_2(\phi,\rho) + \ldots \tag{4.132}$$

Up to second order the square root of the determinant of the induced metric is given by

$$\sqrt{\gamma} = -\frac{\left(\cosh^2\rho\sinh^2\rho\,\dot{t}_1^2 + \cosh^2\rho\, t_1'^2\right)\varepsilon^2}{2\sinh\rho} + \sinh\rho. \tag{4.133}$$

Note that the first order term $O(\varepsilon)$ in $\sqrt{\gamma}$ vanishes and hence the volume of the maximal slice to first order is equal to the zeroth order result. The location of the maximal volume slice to first order is determined by perform a variation of $\sqrt{\gamma}$ with respect to $t_1$, giving

$$-\left(3\cosh^3\rho - 2\cosh\rho\right)\sinh\rho\,\dot{t}_1 - \cosh^2\rho\, t_1'' - \cosh^2\rho\sinh^2\rho\,\ddot{t}_1 = 0. \tag{4.134}$$

Decomposing $t_1$ in a Fourier series, $t_1 = \sum_n t_1^n(\rho)e^{in\phi}$, yields

$$n^2\cosh^2\rho\, t_1^n(\rho) - \left(3\cosh^3\rho - 2\cosh\rho\right)\sinh\rho\frac{\partial}{\partial\rho}t_1^n(\rho) - \cosh^2\rho\sinh^2\rho\frac{\partial^2}{(\partial\rho)^2}t_1^n(\rho) = 0. \tag{4.135}$$

The general solution is given as a sum of two linearly independent solutions

$$t_1^n(\rho) = C_{n,+}t_{1,+}^n(\rho) + C_{n,-}t_{1,-}^n(\rho) \tag{4.136}$$

where

$$t_{1,\pm}^n(\rho) = \left(\frac{\cosh(\rho) - 1}{\cosh(\rho) + 1}\right)^{\pm|n|/2}\frac{\cosh(\rho) \pm |n|}{\cosh(\rho)}. \tag{4.137}$$

However, $\lim_{\rho\to 0} t_{1,-}^n = \infty$ which is not consistent with the perturbative expansion. Therefore,

the solution is restricted to

$$t_1^n(\rho) = C_1^n \left(\frac{\cosh(\rho)-1}{\cosh(\rho)+1}\right)^{|n|/2} \frac{\cosh(\rho)+|n|}{\cosh(\rho)}. \tag{4.138}$$

The constant $C_1^n$ is determined from the boundary conditions. Inserting this into (4.133) yields the following volume of the maximal slice to second order in the perturbation expansion,

$$\begin{aligned} V &= \int_0^{1/\epsilon_{\text{UV}}} d\rho \int_0^{2\pi} d\phi \sqrt{\gamma} \\ &= V_{(0)} - \varepsilon^2 \pi \int_0^{1/\epsilon_{\text{UV}}} d\rho \frac{\cosh^2\rho}{\sinh\rho} \sum_n \left( n^2 t_1^n t_1^{-n} + \sinh^2\rho \frac{\partial t_1^n}{\partial \rho} \frac{\partial t_1^{-n}}{\partial \rho} \right) \\ &= V_{(0)} + \varepsilon^2 \pi \sum_n \left( -\frac{n^2}{\epsilon_{\text{UV}}} + |n|^3 - |n| \right) C_1^n C_1^{-n}. \end{aligned} \tag{4.139}$$

Taking into account that the cutoff surface $\rho = 1/\epsilon_{\text{UV}}$ also changes under the diffeomorphism $w(z,\bar{z})$, the non-universal UV cutoff dependent terms in second order in the perturbation parameter $\varepsilon$ cancel. Therefore, the final result for the change in volume of the extremal slice compared to pure $\text{AdS}_3$ is finite,

$$V_{(2)} = V|_{O(\varepsilon^2)} = \pi \sum_n \left(|n|^3 - |n|\right) C_1^n C_1^{-n}. \tag{4.140}$$

The third order term $V_{(3)}$ is derived in the same way as the second order one. To third order in $\varepsilon$, the determinant of the induced metric reads

$$\sqrt{\gamma}|_{O(\varepsilon^3)} = -\frac{\cosh^2\rho \sinh^2\rho\, \dot{t}_1 \dot{t}_2 + \cosh^2\rho\, t_1' t_2'}{\sinh\rho} \tag{4.141}$$

The equation of motion for $t_2$ is the same as the one for $t_1$. Thus, the (UV cutoff independent) change in volume to third order is given by

$$V_{(3)} = 2\pi \sum_n \left(|n|^3 - |n|\right) C_1^n C_2^{-n}. \tag{4.142}$$

See appendix D for the "complexity=volume" result to fourth order in perturbation theory.

### 4.4.4. Comparison between the Fubini-Study complexity and complexity=volume

Let me now compare the results for the Fubini-Study complexity measure (4.118) and "complexity=volume" in the bulk geometry corresponding to the target state of the circuit.

The first step for this is to fix the Fourier coefficients $C_i^n$ in (4.139) and (4.142) in terms of the conformal transformation $f(\tau = 1, \sigma) \equiv f(\sigma)$. These coefficients specify the location of the boundary time slice in pure $\text{AdS}_3$ where the maximal volume slice ends. This time slice is the conformal transformation of a constant time slice $t = \text{const}$, specified by

$$t \pm \phi = x^\pm \to \tilde{x}^\pm = f_\pm(x^\pm) = x^\pm + \varepsilon f_{1,\pm}(x^\pm) + \varepsilon^2 f_{2,\pm}(x^\pm) + O(\varepsilon^3), \tag{4.143}$$

where $x^\pm$ are the lightcone coordinates on the boundary of the pure $\text{AdS}_3$ space while $\tilde{x}^\pm$ are the lightcone coordinates on the boundary of the Bañados geometry. The inverse transformation $F_\pm$

defined by $F_\pm(f_\pm(x^\pm)) = x^\pm$ can be expanded as

$$F_\pm(\tilde{x}^\pm) = \tilde{x}^\pm - \varepsilon f_{1,\pm}(\tilde{x}^\pm) + (f'_{1,\pm}(\tilde{x}^\pm) f_{1,\pm}(\tilde{x}^\pm) - f_{2,\pm}(\tilde{x}^\pm))\varepsilon^2 + O(\varepsilon^3). \tag{4.144}$$

Then, the constant time slice $\tilde{t} = t_0$ on the boundary of the Bañados geometry is mapped to the time slice

$$\begin{aligned} t(\tilde{t} = t_0) = t_0 &- \frac{\varepsilon}{2}(f_{1,+}(t_0+\phi) + f_{1,-}(t_0-\phi)) \\ &+ \frac{\varepsilon^2}{4}(f'_{1,+}(t_0+\phi) + f'_{1,-}(t_0-\phi))(f_{1,+}(t_0+\phi) + f_{1,-}(t_0-\phi)) \\ &- \frac{\varepsilon^2}{2}\left(f_{2,+}(t_0+\phi) + f_{2,-}(t_0-\phi)\right) + O(\varepsilon^3) \end{aligned} \tag{4.145}$$

in pure $\mathrm{AdS}_3$. For the circuit considered here, only one of the two lightcone coordinates is transformed such that either $f_+(x^+) = x^+$ or $f_-(x^-) = x^-$. Therefore either the $f_{k,+}$ or $f_{k,-}$ functions vanish. Then, the boundary conditions can be read off from

$$t(\tilde{t} = t_0) \stackrel{!}{=} t_0 + \varepsilon \sum_n C_1^n e^{inx^\pm} + \varepsilon^2 \sum_n C_2^n e^{inx^\pm} + O(\varepsilon^3), \tag{4.146}$$

giving $C_1^n = -f_1^n/2$, $C_2^n = (-f_2^n + \frac{i}{2}\sum_m m f_1^m f_1^{n-m})/2$. Inserting this into (4.139) and (4.142) shows that the volume change is proportional to the Fubini-Study complexity (4.125) and (4.127) respectively where the reference state $|\psi_R\rangle = |0\rangle$ is the vacuum state, i.e. $h = 0$. Therefore up to third order in perturbation theory[31],

$$V - V_{(0)} \propto \mathscr{C}. \tag{4.147}$$

The proportionality constant $3/2\pi c$ has no real physical meaning since the computational complexity is only defined up to an undetermined prefactor. Note, however, that the agreement between the Fubini-Study complexity measure and the volume change does not hold for the fourth order terms derived in appendix D, see equations (D.3) and (D.19). While the terms involving $f_2(\sigma)$ and $f_3(\sigma)$ match in the Fubini-Study complexity and "complexity=volume", those that only involve $f_1(\sigma)$ do not. This shows that the Fubini-Study distance is not directly related to the "complexity=volume" proposal, ruling out this possibility put forward in [272].

Finally, let me note that the Fubini-Study complexity functional (4.118) is not unique in the sense that any complexity functional defined as a time-integral of a function of the Fubini-Study metric,

$$\mathscr{C}_{\mathrm{FS,generalized}} = \int d\tau\, \alpha(\mathscr{F}_{\mathrm{FS}}(\tau)). \tag{4.148}$$

has the same optimal path as (4.118) if $\partial_\tau \mathscr{F}_{\mathrm{FS}}(\tau) = 0$. Here $\alpha$ is a positive function. In the language of the Euler-Arnold method, the requirement $\partial_\tau \mathscr{F}_{\mathrm{FS}}(\tau) = 0$ ensures that the geodesic path in the Virasoro group is traversed with constant speed. Equation (4.118) is therefore only one particular member of a more general family obtained by choosing $\alpha(\mathscr{F}_{\mathrm{FS}}) = \mathscr{F}_{\mathrm{FS}}$. The analysis in this section can also exclude that other members of this family match with the volume change in the "complexity=volume" prescription. To see this, expand the function $\alpha(\mathscr{F}_{\mathrm{FS}})$ in a power series in $\mathscr{F}_{\mathrm{FS}}$. The only term in this expansion that gives an $O(\varepsilon^4)$ contribution to the complexity

[31] Note that both the field theory complexity functional and the gravity result are invariant under replacing the transformation $f(\sigma)$ by its inverse $F(\sigma)$, at least up to the fourth order in perturbation theory. Due to this symmetry, the results for the complexity with the conventions used in section 4.2 and those used in this section are the same since the different conventions amount to replacing $f$ by the inverse $F$ (compare (4.12) and (4.22)).

but no $O(\varepsilon^3)$ and $O(\varepsilon^2)$ contributions is the $\mathscr{F}_{\text{FS}}^2$ term. However by explicit calculation it is easy to see that this term together with the $O(\varepsilon^4)$ contributions from $\mathscr{F}_{\text{FS}}$ terms cannot give a result equal to the fourth order term (D.19) in the perturbation series in $\varepsilon$ of the volume change. Due to the optimal path being linear in $\tau$ to first order in $\varepsilon$ and the time-derivatives acting on $f(\tau,\sigma)$ in the cost function (4.107), a contribution to the cost function of the form $\mathscr{F}_{\text{FS}}^2$ yields a contribution to the complexity proportional to

$$\begin{aligned}\int d\tau\, \mathscr{F}_{\text{FS}}^2 &= \varepsilon^4 \left( \int d\sigma d\kappa f_1(\sigma) f_1(\kappa) \Pi(\sigma-\kappa) \right)^2 + O(\varepsilon^5) \\ &= \varepsilon^4 \left( 2\pi^2 \sum_n \left( \frac{c}{12}(|n|^3 - |n|) + 2h|n| \right) f_1^n f_1^{-n} \right)^2 + O(\varepsilon^5),\end{aligned} \tag{4.149}$$

which clearly cannot match with (D.19). Therefore, a simple relation between the Fubini-Study complexity and the "complexity=volume" proposal does not seem to exist.

## 4.5. Bulk duals to Virasoro circuits

In previous sections, computational complexity measures on circuits composed out of Virasoro group transformations were studied from the field theory perspective. In this section, I will construct a gravitational dual to these complexity measures. The construction is based on using the basic rules of the AdS/CFT correspondence established in section 2.1 to map the quantum circuit to a dual bulk geometry. Recall from section 2.1.2 that the expectation values of CFT operators and their dual sources uniquely define a solution of the bulk equations of motion.

In this section, I will focus on the universal gravitational sector, i.e. the bulk metric, and will not consider other bulk fields. The operator defining the bulk metric is the energy-momentum tensor with its source being the boundary metric $g_{ij}^{(0)}$. Therefore, the task at hand is to find a source configuration $g_{ij}^{(0)}$ such that at each step of the physical time $t$, the boundary state $|\psi(t)\rangle$ is given by the state of the circuit at time $t$. The source $g_{ij}^{(0)}$ together with the expectation value $\langle T_{ij}\rangle$ of the energy-momentum tensor then defines a bulk geometry dual to the circuit. This geometry interpolates between the bulk dual to the reference state at $t<0$ and the bulk dual to the target state at $t>t_f$.[32]

### 4.5.1. Deriving the boundary metric

The quantum circuits defined in section 4.2 are specified by a choice of time evolution operator $Q(\tau)$ from (4.5). The idea now is to equate this time evolution operator with the physical Hamiltonian of a conformal field theory living in a background metric $g_{ij}^{(0)}$,

$$H(t) \stackrel{!}{=} Q(t). \tag{4.150}$$

[32] See also [272] for previous work on computational complexity in AdS/CFT using boundary sources.

The physical Hamiltonian of a CFT in the background $g_{ij}^{(0)}$ is given by[33]

$$H(t) = \int_0^{2\pi} \frac{d\phi}{2\pi} \sqrt{g^{(0)}}\, T^t{}_t. \tag{4.151}$$

The identification (4.150) allows us to derive the correct background metric $g_{ij}^{(0)}$ which triggers the conformal transformations applied at each time step of the circuit from 4.2. This construction yields a single bulk geometry for the entire circuit. Because the Hamiltonian (4.151) is the generator of time translations in the physical time $t$, this construction is the natural method for deriving a bulk dual to the circuit (b) constructed in the previous section in which the circuit parameter $\tau$ is identified with $t$.

However, this method nevertheless allows us to write down a bulk dual to the circuit (a) consisting of a sequence of states living on different time slices of the same spacetime manifold. The two constructions in the implementation of these circuits derived in this section then differ only in the source configuration $g_{ij}^{(0)}$ as will become clear below.

For the particular circuits from section 4.2, it turns out to be sufficient to choose a *flat* boundary metric as source. A general flat metric is parametrized by diffeomorphisms $(w(z,\bar{z}),\ \bar{w}(z,\bar{z}))$ dependent on both $z$ and $\bar{z}$,

$$ds^2_{(0)} = dw d\bar{w} = \frac{\partial w}{\partial z}\frac{\partial \bar{w}}{\partial z} dz^2 + \left(\frac{\partial w}{\partial z}\frac{\partial \bar{w}}{\partial \bar{z}} + \frac{\partial w}{\partial \bar{z}}\frac{\partial \bar{w}}{\partial z}\right) dz d\bar{z} + \frac{\partial w}{\partial \bar{z}}\frac{\partial \bar{w}}{\partial \bar{z}} d\bar{z}^2. \tag{4.152}$$

The constant time slices with respect to which the Hamiltonian $H(t)$ generates time evolution are defined by $z + \bar{z} = \text{const}$. By varying the diffeomorphisms $w, \bar{w}$, the location of these constant time-slices changes and with it the states on them.

Based on this definition for the metric, I will now derive expressions for the diffeomorphisms $w(z,\bar{z})$ and $\bar{w}(z,\bar{z})$ in terms of the conformal transformations $f(t,z)$. For this purpose, the Hamiltonian $H(t)$ is expressed in terms of Virasoro generators and equality with the circuit generator $Q(t)$ is imposed. First, apply the standard tensor transformation rules to obtain

$$\begin{aligned}
T_{zz} &= T(w(z,\bar{z}))\left(\frac{\partial w}{\partial z}\right)^2 + \bar{T}(\bar{w}(z,\bar{z}))\left(\frac{\partial \bar{w}}{\partial z}\right)^2, \\
T_{\bar{z}\bar{z}} &= T(w(z,\bar{z}))\left(\frac{\partial w}{\partial \bar{z}}\right)^2 + \bar{T}(\bar{w}(z,\bar{z}))\left(\frac{\partial \bar{w}}{\partial \bar{z}}\right)^2, \\
T_{z\bar{z}} &= T(w(z,\bar{z}))\frac{\partial w}{\partial z}\frac{\partial w}{\partial \bar{z}} + \bar{T}(\bar{w}(z,\bar{z}))\frac{\partial \bar{w}}{\partial z}\frac{\partial \bar{w}}{\partial \bar{z}},
\end{aligned} \tag{4.153}$$

with $T(z)$ and $\bar{T}(\bar{z})$ defined in (4.7).

Note that in (4.153) – which is a statement about operators – no contributions from the $T_{w\bar{w}}$ component were included. Let me briefly comment on why this is justified. It is well-known that classically, the trace of the energy-momentum tensor in a two-dimensional conformal field theory vanishes. In the quantum theory, $T_{w\bar{w}}$ no longer vanishes identically. However, since the CFT lives in flat space, $T_{w\bar{w}}$ produces only contact terms when inserted in correlation functions. These contact terms do not contribute to the correlation functions containing time-evolved operators.

[33] To see that the Hamiltonian density is given by the time-time-component of the energy-momentum tensor with mixed indices (one covariant and one contravariant index), note that the Legendre transformation of some Lagrangian $\mathscr{L}$ dependent on fields $\Phi_a$ is defined by $\mathscr{H} = (\delta\mathscr{L})/(\delta(\partial_t\Phi_a))\partial_t\Phi_a - \mathscr{L}$ while the energy-momentum tensor from Noether's theorem is given by $T^\mu{}_\nu = (\delta\mathscr{L})/(\delta(\partial_\mu\Phi_a))\partial_\nu\Phi_a - g^\mu{}_\nu\mathscr{L}$.

This can be seen directly from the definition of the time evolution of an operator $\mathcal{O}$,

$$\mathcal{O}(t) = e^{\int_0^t d\tilde{t} H(\tilde{t})} \mathcal{O}(0) e^{-\int_0^t d\tilde{t} H(\tilde{t})}. \tag{4.154}$$

In correlation functions involving both $\mathcal{O}(0)$ and $H(\tilde{t})$, contact terms proportional to $\delta(\tilde{t})$ arise. Since $\tilde{t} = 0$ lies just outside of the integration range for $\tilde{t}$, these delta function terms drop out after performing the integral in (4.154). In fact, these contact term issues arise even in the ordinary treatment of conformal field theory on flat space using the time-slicing defined by the $w, \bar{w}$ coordinates. The textbook definition of the Hamiltonian in these coordinates is given by [95, 96]

$$H = L_0 + \bar{L}_0 = \int \frac{d\phi_w}{2\pi} (T(w) + \bar{T}(\bar{w})). \tag{4.155}$$

However, from the general expression (4.151), it is clear that even in these coordinates $T_{w\bar{w}}$ is in principle present in the Hamiltonian,

$$H = \int \frac{d\phi_w}{2\pi} (T(w) + \bar{T}(\bar{w}) + 2T_{w\bar{w}}(w, \bar{w})). \tag{4.156}$$

The arguments given above show that the trace part $T_{w\bar{w}}$ produces contact terms inside correlation functions that, however, do not contribute to time evolution of operators. This explains why the textbook definition (4.155) is correct even though it differs from the expression obtained from (4.151).

Coming back to the derivation of the bulk dual to the circuit from section 4.2, combining (4.151) with (4.153) leads to the following expression for the Hamiltonian

$$H(t) = \int \frac{d\phi}{2\pi} \left[ \left( \left( \frac{\partial w}{\partial z} \right)^2 - \left( \frac{\partial w}{\partial \bar{z}} \right)^2 \right) T(w(z, \bar{z})) + \left( \left( \frac{\partial \bar{w}}{\partial \bar{z}} \right)^2 - \left( \frac{\partial \bar{w}}{\partial z} \right)^2 \right) \bar{T}(\bar{w}(z, \bar{z})) \right]. \tag{4.157}$$

Then, using a change of integration variable to rewrite the circuit generator as

$$Q(t) = \int \frac{d\phi}{2\pi} T(z) \epsilon(t, z) = -i \int \frac{d\phi}{2\pi} \partial_\phi w(z, \bar{z}) T(w(z, \bar{z})) \epsilon(t, w(z, \bar{z})), \tag{4.158}$$

one can read off $w(z, \bar{z})$ from (4.150). In the remaining part of the section, I will come back to the two circuits from section 4.2 starting from the circuit (b).

### Realizing circuit (b)

For the circuit (b) from section 4.2, the $w$ diffeomorphism is simply given by $f(t, z)$,

$$w(z, \bar{z}) = f(t, z), \tag{4.159}$$

where $t = (z + \bar{z})/2$. On the other hand, the $\bar{w}$ diffeomorphism trivializes,

$$\bar{w}(z, \bar{z}) = \bar{z}. \tag{4.160}$$

No antiholomorphic conformal transformations are performed, therefore the circuit only implements the trivial transformation $\bar{z} \to \bar{z}$. The diffeomorphisms (4.159) and (4.160) lead to the

following energy-momentum tensor expectation values

$$\begin{aligned}
\langle T_{zz}\rangle &= -\frac{c}{24}\left(\frac{\partial w}{\partial z}\right)^2 = -\frac{c}{24}\frac{1}{4}(\dot{f}(t,z)+2f'(t,z))^2 \\
\langle T_{z\bar{z}}\rangle &= -\frac{c}{24}\left(\frac{\partial w}{\partial z}\right)\left(\frac{\partial w}{\partial \bar{z}}\right) = -\frac{c}{24}\frac{1}{4}(\dot{f}(t,z)+2f'(t,z))\dot{f}(t,z) \\
\langle T_{\bar{z}\bar{z}}\rangle &= -\frac{c}{24}\left(1+\left(\frac{\partial w}{\partial \bar{z}}\right)^2\right) = -\frac{c}{24}\left(1+\frac{1}{4}\dot{f}(t,z)^2\right)
\end{aligned} \tag{4.161}$$

in the background

$$ds^2_{(0)} = \left(\frac{1}{2}(\dot{f}(t,z)+2f'(t,z))dz + \frac{1}{2}\dot{f}(t,z)d\bar{z}\right)d\bar{z}. \tag{4.162}$$

Note that this background metric is not of the form $dzd\bar{z}$, even after the circuit has reached the target state. In this region $t > t_{\text{final}}$, $\dot{f}(t,z) = 0$ and $ds^2_{(0)} = f'_{\text{final}}(z)dzd\bar{z}$. Applying a Weyl transformation

$$ds^2_{(0)} \to e^{2\omega(z,\bar{z})}ds^2_{(0)} = \frac{1}{f'_{\text{final}}(F_{\text{final}}(f(t,z)))}ds^2_{(0)} \tag{4.163}$$

on top of this background brings the metric to the form $dzd\bar{z}$ when $t > t_{\text{final}}$. Here $f_{\text{final}}$ is the total conformal transformation we produce after the circuit has finished evolving and the inverse $F_{\text{final}}(z)$ is defined by $f_{\text{final}}(F_{\text{final}}(z)) = z$. At earlier times the metric has a more complicated form as one can see by comparing to (4.162), but it remains flat. To see this note that general Weyl transformations change the Ricci scalar as

$$R \to e^{-2\omega}(R - 2\nabla_i\nabla^i\omega) \tag{4.164}$$

and thus lead to curved background metric. However, the Weyl transformation (4.163) preserves $R = 0$ as can be seen from writing (4.164) in $w, \bar{w}$ coordinates,

$$R \to e^{-2\omega}\partial_w\partial_{\bar{w}}\omega \tag{4.165}$$

which vanishes for $\omega = \omega(w) + \bar{\omega}(\bar{w}) = \omega(f(t,z)) + \bar{\omega}(\bar{z})$. The energy-momentum tensor transforms under Weyl transformations as[34]

$$T_{ij} \to T_{ij} + \frac{c}{6}(\partial_i\omega\partial_j\omega - \frac{1}{2}g_{ij}\partial^k\omega\partial_k\omega - \nabla_i\nabla_j\omega + g_{ij}\nabla^k\nabla_k\omega). \tag{4.166}$$

Therefore, as expected for $t > t_{\text{final}}$ the boundary metric and energy-momentum tensor expectation value becomes

$$ds^2 = dzd\bar{z} \quad \text{and} \quad \langle T_{zz}\rangle = -\frac{c}{24}f'_{\text{final}}(z)^2 + \frac{c}{12}\{f_{\text{final}}(z), z\}, \quad \langle T_{z\bar{z}}\rangle = 0, \ \langle T_{\bar{z}\bar{z}}\rangle = -\frac{c}{24}. \tag{4.167}$$

The intermediate form of the energy-momentum tensor for $t_{\text{initial}} < t < t_{\text{final}}$ is obtained by inserting the Weyl-rescaling (4.163) into the transformation rule (4.166).

Note that the Hamiltonian is not invariant under Weyl transformations due to the energy-

[34] For the expectation value of the energy-momentum tensor, this equation follows from the Weyl anomaly equation (2.17). One can check that this equation also holds as an operator statement by comparing correlation functions obtained from (4.166) with the correlation functions of the energy-momentum tensor in a general background. The latter correlators are easily obtainable for instance from the Polyakov action, the generating functional of connected energy-momentum tensor correlation functions in two-dimensional conformal field theories [300] (see also [301] for an overview over other methods to obtain these correlation functions). I have done this check perturbatively up to second order in perturbation theory around flat space.

momentum tensor transformation (4.166). However, the additional term in the Hamiltonian is proportional to the identity operator. Therefore it only leads to a phase change in the state and has no observable effect.

Let me briefly discuss uniqueness of the circuit constructed above. The circuit and its bulk dual is specified by the boundary metric and energy-momentum tensor expectation value. Therefore, one might ask what is the correct choice of these quantities to implement the same sequence of states as in section 4.2 – equations (4.161) and (4.162) on their own, or supplemented with the Weyl rescaling (4.163)? The answer is that these two choices are equivalent implementations of the same circuit. Because the Hamiltonian changes trivially under the Weyl transformation (4.163), this transformation does not affect the sequence of states in the circuit. What changes, however, are the expectation values of the energy-momentum tensor components. This feature is special to $T_{ij}$. General tensor fields are invariant under Weyl transformations. However, since the energy-momentum tensor depends directly on the background metric through Weyl anomaly and conservation equations (2.17), its expectation values are comparable only if they are evaluated in the same background. In other words, the Hilbert space operator defined by $T_{ij}$ in the background $ds^2_{(0)}$ differs from the Hilbert space operator defined by $T_{ij}$ in the background $e^{2\omega}ds^2_{(0)}$. The Weyl transformation (4.163) I have chosen merely puts the metric at $t > t_{\text{final}}$ in the same form as that used in section 4.2 so that one can compare the expectation values $\langle T_{ij}\rangle$ in the circuit from section 4.2 and its reformulation in this section. As expected, once the transformation to the background $ds^2_{(0)} = dzd\bar{z}$ is performed, agreement with the expectation values from section 4.2 is found.

### A further look at circuit (a)

As was discussed earlier, the natural interpretation of the circuit in case (a) is that of a sequence of states in living in different spacetimes. However, the methods developed above allow also for realizing case (a) as a single quantum circuit similar to case (b) above. As before, a bulk dual to the circuit is found by demanding equality between the circuit generator $Q(\tau)$ and the physical Hamiltonian $H(t)$, i.e. identifying the circuit parameter $\tau$ with the physical time $t$.

An additional issue to take into account is that in case (a) it is necessary to perform a slight reformulation of the circuit in order to be able to demand equality of $H(t)$ given by (4.157) and $Q(t)$ specified in (4.158). The reason for this is that for a trivial conformal transformation $f(t,z) = z$ the circuit generator $Q_{(a)}(\tau = t)$ from section 4.2 vanishes while the Hamiltonian $H(t)$ should reduce to the standard time evolution in a conformal field theory governed by $H(t) = H_0 = L_0 + \bar{L}_0$. Therefore, $H(t)$ is identified not with $Q_{(a)}(t)$ but with $Q_{(a)}(t) + H_0$. The modification $Q_{(a)}(t) \to Q_{(a)}(t) + H_0$ does not change the energy-momentum tensor expectation value[35] and only leads to an additional unobservable phase if the reference state is a primary state such as the vacuum state $|0\rangle$ that is used as reference state here. Therefore, this modification does not change the physics of the problem at hand.

Then, using (4.157) and (4.158) one finds that the $\bar{w}$ diffeomorphism trivializes again, $\bar{w}(z,\bar{z}) = \bar{z}$, while the $w$ diffeomorphism satisfies

$$\dot{w}(t,\phi) = 1 + \epsilon(t, w(t,\phi)). \tag{4.168}$$

It is possible to rewrite (4.168) by using the definition of $\epsilon$ in (4.9) and introducing inverse

[35] The modification is equivalent to the replacement $f \to f + \text{const.}$ in (4.13). If $\langle T(z)\rangle$ is constant, this does not change the energy-momentum expectation value.

functions $W$ and $F$ defined by

$$w(t,W(t,\phi))=\phi\ ,\quad f(t,F(t,z))=z, \tag{4.169}$$

giving[36]

$$-\frac{\dot{W}(t,\phi)}{W'(t,\phi)}=1-\frac{\dot{F}(t,t+i\phi)}{F'(t,t+i\phi)}. \tag{4.170}$$

It is then easy to see that case (a) and (b) are implemented by sources $g_{ij}^{(0)}$ described by closely related diffeomorphisms $w(z,\bar{z})$ differing only in a total vs. partial derivative with respect to the physical time $t$ in their defining equations.

Applying again the Weyl transformation (4.163), the following energy-momentum tensor expectation values are obtained for $t>t_{\text{final}}$,

$$\langle T_{zz}\rangle=-\frac{c}{24}+\frac{c}{12}\{f_{\text{final}}(z),z\},\ \ \langle T_{z\bar{z}}\rangle=0,\ \langle T_{\bar{z}\bar{z}}\rangle=-\frac{c}{24}. \tag{4.171}$$

Compared to the well-known transformation law of the energy-momentum tensor under conformal transformations,

$$T(z)\to f'(z)^2T(z)+\frac{c}{12}\{f(z),z\}, \tag{4.172}$$

in this circuit the $f'(z)^2$ prefactor is absent in the final value of the energy-momentum tensor expectation value. Hence, the circuit (b) more faithfully implements gradual conformal transformations in the sense that the final state yields the well-known energy-momentum tensor transformation rule. Nevertheless, the circuit (a) possesses some interesting features with regard to holographic complexity proposals, as is explained in section 4.5.3 and thus deserves to be studied in detail.

### 4.5.2. Mapping to gravity

The previous two sections showed how to choose the boundary quantities defining the circuits of interest – the expectation value of the stress-energy tensor and the boundary metric – in such a way as to implement the circuits of section 4.2 in terms of Hamiltonian time evolution in a curved background. In this construction, there is a unique bulk geometry associated to this circuit: the holographic dictionary associates the metric underlying the path-integral formulation with the metric on the asymptotic boundary and the corresponding energy-momentum tensor with the subleading fall-off of the bulk metric [73]. As reviewed in section 2.1.2, these two ingredients uniquely specify the bulk metric.

To be more specific, if $g_{ij}^{(0)}$ denotes the boundary metric and $\langle T_{ij}\rangle$ the corresponding expectation value of the energy-momentum tensor, the exact gravity dual to the corresponding time evolution of a state in a holographic conformal field theory takes the form [73]

$$ds^2=\frac{dr^2}{r^2}+\left(\frac{1}{r^2}g_{ij}^{(0)}+g_{ij}^{(2)}+r^2g_{ij}^{(4)}\right)dx^idx^j, \tag{4.173}$$

where $r$ is the radial direction with the asymptotic boundary at $r=0$ and the coefficients $g_{ij}^{(2)}$ and $g_{ij}^{(4)}$ are defined by (2.15) and (2.18). The gravity dual to the circuits of interest is obtained by inserting into the above expression the form of the boundary metric and the associated expectation

[36] Note that $\dot{F}(t,z)$ denotes a derivative of $F$ w.r.t. its first argument and not a total derivative w.r.t. $t$. Likewise, $F'(t,z)$ is a derivative w.r.t. the second argument of the function.

value of the energy-momentum tensor discussed in the previous section. Concretely, for the circuit (b) the boundary metric is given by (4.163) and the energy-momentum tensor expectation value is determined from (4.161) and (4.166) and analogously for the circuit (a). Because the boundary metric is flat, the results then basically tell us which time-slicing of pure $AdS_3$ one has to choose in order to implement the circuit of interest.

The derived bulk metric forms a possible basis for first-principle derivations of bulk duals to various field theory cost functions which have been proposed previously [266, 268, 269, 272]. It can also provide conformal field theory insights on conjectured bulk complexity measures such as "complexity=volume" [52], "complexity=action" [53], "complexity=volume 2.0" [302], or the infinite class of complexity measures recently proposed in [135].

### 4.5.3. Lessons for holographic complexity

Having derived the bulk dual to our circuit, let me now turn to the study of bulk duals of boundary cost functions and – vice versa – boundary duals to bulk complexity measures. I will concentrate on two simple examples: the "complexity=volume" proposal [52] and the Fubini-Study complexity functional already studied in section 4.4.

#### Relation between Fubini-Study complexity and "complexity=volume"

As explained in section 4.4, when the conformal transformation is expressed as a perturbative series around the identity,

$$f(t,z) = z + \varepsilon f_1(t,z) + \varepsilon^2 f_2(t,z) + O(\varepsilon^3), \tag{4.174}$$

the Fubini-Study complexity and the result of the "complexity=volume" calculation in the Bañados geometry dual to the target state are related in the first few orders in perturbation theory. In the circuit construction in this section, there is a bulk dual not only to the target state but to the state at every time step $t$. Therefore, it is interesting to consider the Fubini-Study complexity and the "complexity=volume" proposal at all time steps in the circuit. For the case (b), the following change in volume compared to the vacuum state is obtained (see section 4.4.3)[37],

$$\begin{aligned} V_{(b)} - V_{\text{pure AdS}_3} &= \varepsilon^2 \frac{\pi}{4} \sum_n (|n|^3 - |n|) f_1^n(t) f_1^{-n}(t) \\ &+ \varepsilon^3 \frac{\pi}{4} \sum_n (|n|^3 - |n|) \left( 2 f_1^n(t) f_2^{-n}(t) - i \sum_m m f_1^n(t) f_1^m(t) f_1^{-n-m}(t) \right) + O(\varepsilon^4). \end{aligned} \tag{4.175}$$

On the other hand, for case (a) a general answer for the volume of extremal slices cannot be given because (4.168) cannot be solved for arbitrary time dependence. The most interesting special case is the one in which the time-dependence equals that of the optimal path in the Fubini-Study complexity functional of [268, 269]. In this case, the volume change is given by[38]

$$V_{(a)} - V_{\text{pure AdS}_3} = \varepsilon^2 \frac{\pi}{4} \sum_n (|n|^3 - |n|) \frac{f_1^n(t) f_1^{-n}(t)}{n^2} + O(\varepsilon^3), \tag{4.176}$$

[37] The results in section 4.4.3 are given in terms of parameters $C_1^n$, $C_2^n$, etc. which are the $n$-th Fourier modes parametrizing the location of the time slice on the boundary in $w$, $\bar{w}$ coordinates expanded in perturbation theory. Thus, these parameters are obtained directly from (4.168), taking into account that the $C_1^n$, $C_2^n$ parameters are Fourier modes w.r.t. $\phi_w = (w - \bar{w})/(2i)$. Note also that the calculation in section 4.4.3 is performed in Lorentzian signature.

[38] See section 4.4.2 for the derivation of the optimal path.

See section 4.4.3 and appendix D for details.

It is instructive to compare the above results to the Fubini-Study complexity of [268, 269] which was calculated in section 4.4.2. Evaluating the Fubini-Study complexity between the reference state and the state $|\psi(t)\rangle$ at time $t$ as the target state shows that the volume change (4.175) in the circuit (b) matches as far as the third order in $\varepsilon$,

$$\begin{aligned}\mathscr{C}_{\text{FS}} &= \varepsilon^2 4\pi^2 \sum_n \frac{c}{12}(|n|^3-|n|) f_1^n(t) f_1^{-n}(t) \\ &+ \varepsilon^3 4\pi^2 \sum_n \frac{c}{12}(|n|^3-|n|)\left[2 f_1^n(t) f_2^{-n}(t) - i\sum_m m f_1^n(t) f_1^m(t) f_1^{-n-m}(t)\right] + O(\varepsilon^4).\end{aligned} \tag{4.177}$$

but disagrees in the fourth order (see equation (D.19) and (D.3)). The Fubini-Study complexity in the circuit (a) is equal to that of circuit (b) up to the third order in perturbation theory, therefore (4.177) holds for both circuits. However, the volume change in circuit (a) does not match with any Fubini-Study complexity. This is not surprising since as we have seen above, the circuit (b) is a better implementation of gradual conformal transformations of the vacuum state, in particular giving the correct energy-momentum tensor transformation law (4.12) unlike the circuit (a).

### Bulk dual to the Fubini-Study distance

Going beyond the simple comparisons above, the bulk dual to the circuits derived in this section allows at least in principle a derivation of bulk duals to cost functions from first principles. To see how this works, consider the Fubini-Study metric as an example. In the quantum circuits considered here, the Fubini-Study metric is related to a connected two-point function of the Hamiltonian. In general, connected two-point functions of the energy-momentum tensor are obtained from the boundary perspective by applying variations w.r.t. the boundary metric onto the one-point function,

$$\langle T_{ij} T_{kl}\rangle = \frac{2}{\sqrt{g_{(0)}}} \frac{\delta}{\delta g_{(0)}^{ij}} \langle T_{kl}\rangle. \tag{4.178}$$

The important point is now that using the basic AdS/CFT rules described in section 2.1.2, this can be translated into a bulk calculation giving the same two-point function. This allows in principle writing down the gravity dual to the Fubini-Study cost function used in [268, 269]. Of course, similar derivations work for other cost functions. This method allows for deriving bulk duals to any cost function defined from energy-momentum tensor correlators or vice versa boundary duals to bulk cost functions defined as functionals of the bulk metric.[39] It may of course be the case that the bulk dual for such cost functions does not reduce to a simple geometric quantity. Indeed, in general energy-momentum tensor correlators are derived by applying variations which necessarily change the bulk metric (although of course only slightly) and lead us to different bulk geometry. Therefore, simple geometric duals are expected to exist only for certain special cases in which the effect of the variation of the background drops out in the end.

More concretely, a geometric dual to the Fubini-Study cost function in the circuit (b) can be derived as follows. Recall that the Fubini-Study metric in the circuit is given as the square root of the connected two-point function of the Hamiltonian. This two-point function is in turn given as

[39] For more general cost functions it is necessary to go beyond Virasoro group transformations and also allow elementary gates built out of for instance scalar fields in the circuit.

a double integral over the connected two-point of the Hamiltonian density,

$$\langle H^2(t)\rangle_{\text{conn.}} = \int \frac{d\phi_1}{2\pi}\frac{d\phi_2}{2\pi}\sqrt{\det g(t,\phi_1)}\sqrt{\det g(t,\phi_2)}\langle \mathscr{H}(t,\phi_1)\mathscr{H}(t,\phi_2)\rangle_{\text{conn.}}, \tag{4.179}$$

where $\langle \mathcal{O}_1\mathcal{O}_2\rangle_{\text{conn.}} = \langle \mathcal{O}_1\mathcal{O}_2\rangle - \langle \mathcal{O}_1\rangle\langle \mathcal{O}_2\rangle$. What bulk object could be dual to the two-point function of $\mathscr{H}$? Since the two-point function is an object dependent on two boundary points $(t,\phi_1)$ and $(t,\phi_2)$ which should be defined in a coordinate-invariant way, a simple guess is that it should be related to the length of a geodesic in the bulk between the two boundary points. This in fact turns out to be the case, as I will explain below.

The first step in the derivation is to derive the length of the geodesic. For this, let me compute the length of a geodesic between two arbitrary boundary points. This is particularly simple in Poincare patch coordinates,

$$ds^2 = \frac{1}{r^2}(dr^2 - dy^2 + dx^2), \tag{4.180}$$

in which the geodesic is given by

$$x(r) = \alpha \pm \frac{1}{2}(\chi + 1/\chi)\sqrt{\psi^2 - r^2}, \quad y(r) = \beta \pm \frac{1}{2}(\chi - 1/\chi)\sqrt{\psi^2 - r^2}, \tag{4.181}$$

obtained from minimizing the length

$$\ell = \int dr \frac{\sqrt{1 - y'(r)^2 + x'(r)^2}}{r} \tag{4.182}$$

of a bulk curve with fixed endpoints. The geodesic endpoints lie at $x = \alpha \pm \psi\frac{1}{2}(\chi + 1/\chi)$ and $y = \beta \pm \psi\frac{1}{2}(\chi - 1/\chi)$ in the parametrization chosen. In order to compare the geodesic length with energy-momentum tensor correlators, it is useful to define the geodesic length w.r.t. a cutoff in the radial coordinate $\rho$ of global AdS coordinates,

$$ds^2 = d\rho^2 - \cosh^2\rho\, dt_w^2 + \sinh^2\rho\, d\phi_w^2, \tag{4.183}$$

where $w = t_w + \phi_w$ and $\bar{w} = t_w - \phi_w$.[40] The coordinate transformation between (4.180) and (4.183) is given by

$$\sin(t_w) = \frac{y}{r\cosh\rho}, \quad \cos(\phi_w) = \frac{x}{r\sinh\rho}, \quad \cosh^2\rho = \left(\frac{r}{2} + \frac{1}{2r}(x^2 - y^2 + 1)\right)^2 + \frac{y^2}{r^2} \tag{4.184}$$

and the inverse transformation by

$$r = \frac{1}{\cosh\rho\cos t_w - \sinh\rho\sin\phi_w}, \quad y = r\cosh\rho\sin t_w, \quad x = r\sinh\rho\cos\phi_w. \tag{4.185}$$

The length of half of the geodesic stretching from one endpoint to the midpoint of the geodesic at $r = \psi, x = \alpha, y = \beta$ in the bulk is given by

$$\ell_{\text{half}} = \int_{\tilde{\epsilon}_{\text{UV}}}^{\psi} dr \frac{\sqrt{1 - y'(r)^2 + x'(r)^2}}{r} = \log\left[\frac{\psi + \sqrt{\psi^2 - \tilde{\epsilon}_{\text{UV}}^2}}{\tilde{\epsilon}_{\text{UV}}}\right]. \tag{4.186}$$

Choosing a cutoff $\rho = \text{arcosh}(1/(2\epsilon_{\text{UV}}))$ and rewriting this cutoff as a cutoff in $r$ (i.e. solving

[40] Note that I am working in Lorentzian signature again for the bulk calculations.

$\rho = \text{arcosh}(1/(2\epsilon_{\text{UV}}))$ for $r = \tilde{\epsilon}_{\text{UV}}$ in (4.184)), the geodesic length becomes the sum of the two half-lengths (4.186)

$$\ell = \log\left[\frac{\sin((\phi_{w,2}-\phi_{w,1})/2)^2 - \sin((t_{w,2}-t_{w,1})/2)^2}{\epsilon_{\text{UV}}^2}\right] \tag{4.187}$$

after using (4.185) to rewrite the $\alpha, \beta, \psi, \chi$ parameters in terms of the endpoint coordinates $\phi_{w,1}, \phi_{w,2}, t_{w,1}, t_{w,2}$. In $z, \bar{z}$ coordinates, the length is given by

$$\ell = \log\left[\frac{\sin((w(z_2,\bar{z}_2)-w(z_1,\bar{z}_1))/2)\sin((\bar{w}(z_2,\bar{z}_2)-\bar{w}(z_1,\bar{z}_1))/2)}{\epsilon_{\text{UV}}^2}\right], \tag{4.188}$$

where $z_{1,2} = t + \phi_{1,2}$ and $\bar{z}_{1,2} = t - \phi_{1,2}$.

It is then straightforward to derive an expression for the connected two-point function of the Hamiltonian density in a generic background metric (4.152)

$$\langle \mathscr{H}(t_1,\phi_1)\mathscr{H}(t_2,\phi_2)\rangle_{\text{conn.}} = \frac{c}{32}\left[\frac{\partial_{t_1}w_1\partial_{\phi_1}w_1\partial_{t_2}w_2\partial_{\phi_2}w_2}{\sin^4\left(\frac{w_1-w_2}{2}\right)} + \frac{\partial_{t_1}\bar{w}_1\partial_{\phi_1}\bar{w}_1\partial_{t_2}\bar{w}_2\partial_{\phi_2}\bar{w}_2}{\sin^4\left(\frac{\bar{w}_1-\bar{w}_2}{2}\right)}\right] \tag{4.189}$$

in terms of geodesic lengths $\ell$,

$$\begin{aligned}\langle \mathscr{H}(t_1,\phi_1)\mathscr{H}(t_2,\phi_2)\rangle_{\text{conn.}} = \frac{c}{4}\Big[&(\partial_{\phi_1}\partial_{\phi_2}\ell)(\partial_{t_1}\partial_{t_2}\ell) + (\partial_{\phi_1}\partial_{t_2}\ell)(\partial_{t_1}\partial_{\phi_2}\ell) \\ &- \frac{1}{2}g^{(0)}_{t_1\phi_1}g^{(0)}_{t_2\phi_2}g^{ij}_{(0)}(t_1,\phi_1)g^{kl}_{(0)}(t_2,\phi_2)(\partial_i\partial_k\ell)(\partial_j\partial_l\ell)\Big].\end{aligned} \tag{4.190}$$

After integrating over $\phi_1$ and $\phi_2$, equation (4.190) gives an expression for the Fubini-Study distance defined entirely through the bulk metric. It therefore maps the cost function $\mathscr{F}_{\text{FS}}$ to a purely geometric object in the gravity theory. That such a simple mapping exists is not too surprising due to the universality of two-point functions in conformal field theories. For conformal field theories on the plane with metric $ds^2 = dzd\bar{z}$, a generic two-point function $\langle \mathscr{O}(z_1,\bar{z}_1)\mathscr{O}(z_2,\bar{z}_2)\rangle = |z_1 - z_2|^{-2\Delta}$ is related to the geodesic length $\ell = \log[|z_1 - z_2|^2/\epsilon_{\text{UV}}]$ in a multitude of ways (for instance by taking derivatives or exponentiating).

However, interestingly the expression (4.190) also correctly reproduces the connected two-point function of the Hamiltonian in a thermal state dual to a BTZ black hole. In this case, there are multiple geodesics to consider. The length of a geodesic stretching between two-points on the same asymptotic boundary is given by

$$\ell = \log\left[\frac{\cosh(4\pi^2(\phi_1-\phi_2)/\beta) - \cosh(4\pi^2(t_1-t_2)/\beta)}{\epsilon_{\text{UV}}}\right] \tag{4.191}$$

while geodesics between two different asymptotic boundaries in the maximally extended two-sided BTZ geometry have length

$$\ell = \log\left[\frac{\cosh(4\pi^2(\phi_1-\phi_2)/\beta) + \cosh(4\pi^2(t_1+t_2)/\beta)}{\epsilon_{\text{UV}}}\right]. \tag{4.192}$$

Applying (4.190), integrating over $\phi_1$ and $\phi_2$ as well as summing over all possible winding num-

bers leads to a result proportional to the thermal two-point function[41]

$$\langle H^2\rangle_\beta - \langle H\rangle_\beta^2 = \frac{\partial_\beta^2 Z(\beta)}{Z(\beta)} - \left(\frac{\partial_\beta Z(\beta)}{Z(\beta)}\right)^2 = \frac{2c\pi^2}{3\beta^3} \tag{4.193}$$

where $Z(\beta) = \exp\left(\frac{c}{12}\frac{4\pi^2}{\beta}\right)$ is the thermal partition function of the state dual to the BTZ black hole. That equation (4.190) also applies to the BTZ geometry which is quite far removed from the conformal transformations of pure $AdS_3$ that motivated this equation indicates that this formula might apply more generally to arbitrary asymptotically $AdS_3$ geometries.

Finally, let me stress that the above derivation gives a geometric dual to the Fubini-Study cost function $\mathscr{F}_{\text{FS}}$, but not a dual to the Fubini-Study complexity $\mathscr{C}_{\text{FS}}$. In principle, the circuit construction above also allows for deriving the Fubini-Study complexity in terms of bulk quantities by mapping the cost minimization procedure to the bulk using the bulk dual to the circuit derived in this section. The bulk dual to the computational complexity obtained in this way is a somewhat different object than those of the computational complexity proposals in [51–54]. The "complexity=volume" or "complexity=action" proposals conjecture the computational complexity between an unentangled reference state and the boundary state at time $t$ to be given by a geometric object defined entirely in the bulk subregion dual to the boundary time-slice at time $t$ (the WdW patch). On the other hand, the computational complexity between the vacuum state at time $t = 0$ and a state at time $t > 0$ derived using the methods of this section is a geometric object naturally defined in a codimension-zero region between $t = 0$ and $t > 0$.[42]

Nevertheless, the geometric object dual to the Fubini-Study cost function fulfills some of the properties expected from computational complexity. In particular, because the Fubini-Study distance between two infinitesimally close thermofield double states is constant in time, the time-integral of the gravity dual to the Fubini-Study cost function $\langle H^2\rangle_\beta - \langle H\rangle_\beta^2$ in the BTZ black hole geometry grows linearly in time for arbitrarily long time scales.[43] This growth for an infinite time scale as long as no bulk quantum corrections (i.e. corrections to higher order in $G_N$) are taken into account[44] is one of the hallmark properties of computational complexity in AdS/CFT as originally proposed in [51–54]. From the viewpoint of the Euler-Arnold method, bulk quantum corrections should appear when the geodesic defining the path in the Virasoro group reaches a conjugate point on the Virasoro group manifold. Conjugate points are points on the manifold reachable by multiple geodesics from the origin (for instance, on the sphere with the origin at the south pole there is a conjugate point at the north pole). At a conjugate point, the complexity defined from the Euler-Arnold method as the length of the smallest geodesic changes from the length of one

[41] Note that in the case where the integral runs over geodesic lengths on the same asymptotic boundary, the result is divergent and a regularization procedure is necessary, like for the Fubini-Study complexity functional where differential regularization was used for this purpose. Regularizing by simply restricting the geodesic lengths to be greater than some value $\epsilon_{\text{UV}}$ gives a result where the two-point function of the Hamiltonian emerges at order $O(\epsilon_{\text{UV}}^0)$.

[42] In the context of holographic complexity proposals, a so-called complexity of formation has been defined as the difference between the computational complexity for some state $|\psi\rangle$ and the vacuum state $|0\rangle$ [303]. For instance, in the "complexity=volume" approach, the volume change $V_{(a,b)} - V_{\text{pure AdS}_3}$ is the bulk dual to such a complexity of formation. The Fubini-Study complexity measure as a measure of the computational complexity between a primary state and a descendant in the same Verma module is somewhat analogous to this notion of complexity of formation.

[43] Note that because this calculation considers only the ordinary time-evolution of the thermofield double or thermal state it corresponds to a kind of degenerate version of a quantum circuit where the only gate which one can apply is the time-translation generator $e^{iHt}$ with $H$ being the ordinary CFT Hamiltonian independent of $t$.

[44] This is the case in our construction since the bulk dual to the Fubini-Study distance is defined in the classical gravity theory.

geodesic to that of another one. Since the system returns to the reference state (or at least a state very close to it) at the recurrence time of the system, it is clear that the linear growth in the Fubini-Study complexity cannot continue for more than half of the recurrence time.

Let me also point out that the construction of a geometric quantity determined in terms of geodesic lengths is familiar from the mathematical field of integral geometry [304]. This allows for a reformulation of various geometric objects in the bulk AdS space in terms of geometric objects in the space of boundary anchored geodesics, the so-called kinematic space [305–312]. In particular, the volume of constant time-slices in pure $AdS_3$ and in the one-sided BTZ black hole can be formulated in this way [313, 314],

$$V \propto \sum_w \int d\phi_1 d\phi_2 \, \ell \partial_{\phi_1} \partial_{\phi_2} \ell, \tag{4.194}$$

where $\sum_w$ schematically denotes a sum over winding numbers $w$. This gives a realization of the "complexity=volume" proposal in terms of geodesic lengths. Interestingly, the volume (4.194) formulated in this way has a very similar form to the Fubini-Study distance expression (4.179) which for constant time slices of pure $AdS_3$ and the one-sided BTZ black hole with boundary metric $ds^2_{(0)} = dz d\bar{z}$ reduces to

$$\langle H^2(t) \rangle_{\text{conn.}} \propto \sum_w \int d\phi_1 d\phi_2 \, (\partial_{t_1} \partial_{t_2} \ell)(\partial_{\phi_1} \partial_{\phi_2} \ell)\big|_{t_1 = t_2 = t}, \tag{4.195}$$

although this of course vanishes for pure $AdS_3$. These similarities might be a good starting point to further explore connections between the "complexity=volume" proposal and the Fubini-Study complexity.

Moreover, the formulation of the Fubini-Study distance in terms of geodesic lengths also allows for expressing this quantity in terms of entanglement entropies via the Ryu-Takayanagi formula and its generalization studied in chapter 3. In particular, it is clear that this includes geodesics with all possible values of the winding number $w$ and therefore generalized entanglement entropies for all values of $w$ as well. This might provide a natural way to incorporate bulk quantum corrections into the Fubini-Study distance, since as we have seen in chapter 3 the winding number for the generalized entanglement entropy is bounded by the central charge of the boundary CFT which is proportional to $1/G_N$. Integrating only over geodesics in the BTZ geometry with winding numbers $w \leq w_{\max}$ in (4.179) leads to an expression

$$\langle H(t)^2 \rangle = \frac{2c\pi^2}{3\beta^3} \frac{\sinh\left(\frac{8\pi^3 w_{\max}}{\beta}\right)\left(2 + \cosh\left(\frac{8\pi^3 w_{\max}}{\beta}\right)^2 + 3\cosh\left(\frac{8\pi^3 w_{\max}}{\beta}\right)\cosh\left(\frac{8\pi^2 t}{\beta}\right)\right)}{\left(\cosh\left(\frac{8\pi^3 w_{\max}}{\beta}\right) + \cosh\left(\frac{8\pi^2 t}{\beta}\right)\right)^3} \tag{4.196}$$

which is to very good approximation constant in $t$ for $t < \pi w_{\max}$ followed by a falloff exponential in $t$ for $t > \pi w_{\max}$. Integrating this putative dual to a modification of the Fubini-Study distance which incorporates bulk quantum corrections over $t$ then leads to a time-dependence as expected from figure 2.8, i.e. a linear increase followed by a plateau. Together with the falloff expected due to conjugate points on the Virasoro group manifold, this qualitatively reproduces the entire diagram 2.8. Note however, that there is still some work to be done to elevate the above arguments into a precise correspondence between field theory and gravity observables. In particular, it is unclear at the moment what effects the restriction to geodesics with maximum winding number has on the cost function on the field theory side. Moreover, to precisely reproduce the expectation of [51–54] shown in figure 2.8, the maximum winding number $w_{\max}$ has to scale exponential

with the entropy of the black hole in the bulk. In terms of the generalized entanglement entropy, however, this regime of geodesics with extremely large winding number is not under good control on the field theory side and no universal answers could be obtained in chapter 3. Therefore, the question whether the above construction can provide a concrete realization of the computational complexity conjectures of [51–54] still remains open at the moment.

# 5. Conclusions and Outlook

Let me close with a brief summary of the results obtained in this thesis, as well as an outlook on future directions.

In chapter 3, I investigated a generalized entanglement measure quantifying correlations not only between spatial degrees of freedom but also between different fields. In particular, I gave a gauge-invariant definition of the generalized entanglement entropy taking into account the permutation gauge symmetries underlying its construction. This definition puts the previous work of [46, 189, 190] on generalized entanglement entropy in states dual to conical defects on a firmer footing. Moreover, the definition applies not only to the special class of pure states studied in [46, 189, 190] but also to general mixed states, in particular those involving mixtures of states from multiple twisted sectors. This was used to propose that for a specific choice of bipartition, the generalized entanglement entropy is dual to the length of a geodesic winding around the event horizon of the BTZ black hole. I checked this proposal by explicit calculation of the generalized entanglement entropy for thermal states of the $S_N$ orbifold theory of the D1/D5 system and small perturbations away from the orbifold point to leading order in conformal perturbation theory. To facilitate the computation of the generalized entanglement entropy, I developed monodromy methods for the calculation of conformal blocks on the torus. Taken together, the results of chapter 3 give strong evidence for a duality between the generalized entanglement entropy and the length of a geodesic winding around a black hole horizon or naked singularity. This shows that entanglement data is enough to reconstruct the entire bulk geometry for conical defects and BTZ black holes, strengthening the "entanglement builds geometry" proposal.[1]

In chapter 4, I studied computational complexity measures in a particular class of quantum circuits built up from Virasoro group transformations. Motivated by previous work [266] showing close relations between a computational complexity measure in these circuits and geometric actions on coadjoint orbits of the Virasoro group, the viability of these geometric actions as complexity measures was investigated. While some interesting connections to topics such as Berry phases, the path integral optimization approach to complexity proposed in [286] or geometric actions from the gravity theory emerged from this, the results of this part also showed that geometric actions do not form good computational complexity measures. In particular, in most cases the computational complexity determined by the geometric action simply vanishes.[2] Moreover, I perturbatively determined explicit expressions for another computational complexity functional based on the Fubini-Study distance proposed in [268, 269], motivated by an equivalence between this functional and the "complexity=volume" proposal [51, 52] to leading order in perturbation theory. This calculation showed that the equivalence between the two quantities does not extend to higher orders in perturbation theory. Finally, I presented the construction of a bulk dual to the circuits considered in chapter 4. This involved putting the boundary CFT on a non-trivial background metric such that the time-evolution generated by the Hamiltonian in this background produces the same sequence of states as the quantum circuit in question. The corresponding asymptotically $AdS_3$ geometry followed from well-known standard features of the AdS/CFT cor-

[1] The description of geometric objects in the bulk in terms of geodesics dual to entanglement entropies can be done explicitly for instance using techniques from the mathematical field of integral geometry [305–312]. These techniques necessarily involve winding geodesics when applied to conical defects and black holes [311, 314].

[2] Upon adding a suitable boundary term to ensure gauge invariance.

respondence reviewed in section 2.1.2. This construction allowed the derivation of a bulk dual to the Fubini-Study distance in the circuit, given as an expression in terms of geodesic lengths. Although the detailed characterization of this expression is still work in progress, it fulfills many of the properties expected of it due to the conjectures of [51–54]. In particular, the bulk dual to the Fubini-Study distance even gives correct results outside of the circuit in which it was derived, as was found by considering the time-evolution in the two-sided BTZ black hole geometry which is in accord with the expectations. This gives hope that a realization of a computational complexity functional with the properties expected from [51–54] in the scenarios investigated in chapter 4 (which in particular employ a fully-interacting theory in contrast to many previous works on computational complexity in quantum field theories) is feasible.

Finally, let me give an outlook on possible future directions. The generalized entanglement entropy results of chapter 3 raise a large number of interesting questions:

- How generic are the results for the generalized entanglement entropy? The definition of this entanglement entropy depends on the existence of twisted sectors in the CFT and, moreover, for thermal states only the $S_N$ orbifold theory of the D1/D5 system was considered. Do the generalized entanglement entropy results also hold for other AdS/CFT models and can a generic bottom-up model be found which allows for defining a generalized entanglement entropy? The answer to this question largely depends on whether generic $\mathrm{AdS}_3/\mathrm{CFT}_2$ models include twisted sectors and on the number of these sectors. In many known $\mathrm{AdS}_3/\mathrm{CFT}_2$ constructions, there are indeed a large number of twisted sectors often in the structure of an $S_N$ orbifold theory. These $S_N$ orbifolds of course have a different seed theory than the one for the D1/D5 system. For instance minimal models with $\mathcal{N} = (2,2)$ supersymmetry [315], linear dilaton theories [316–320] and many more such seed theories have been found (see e.g. [321–327]). In fact, for bosonic string theory on $\mathrm{AdS}_3$ times a compact manifold $X$, it has been argued in [324] that the boundary CFT is an $S_N$ orbifold theory with large $N$ for any choice of $X$. The results of chapter 3 remain valid in these models since they depend only on the $S_N$ orbifold structure but not on the seed theory chosen.[3] It would be interesting to determine whether there are counterexamples of $\mathrm{AdS}_3/\mathrm{CFT}_2$ constructions with no twisted sectors or only a small number of them independent of the central charge. If such models exist, then the generalized entanglement entropy from chapter 3 can not be defined in them.

- Can a proof for the generalized Ryu-Takayanagi formula be given similar to the proof by Lewkowycz and Maldacena [113] for the ordinary Ryu-Takayanagi formula? For conical defects, this is essentially trivial since the generalized entanglement entropy is equal to the ordinary entanglement entropy of an interval of length $w+L$ in the pure AdS covering space of the conical defect. However, the situation for the thermal state is less clear.

  Recall that the first step in calculating the generalized entanglement entropy for thermal states was a projection onto a subset $\{C_i\}$ of the twisted sectors, $\rho(\beta) \to \rho_{\{C_i\}}(\beta)$. Does the state $\rho_{\{C_i\}}(\beta)$ have a dual interpretation as a classical spacetime? Of course, at the orbifold point where the calculations in chapter 3 were performed the typical string is of the same size as the AdS radius and a classical geometric description (which also underlies the proof of [113]) of the bulk spacetime is not applicable. However, in the supergravity limit there are some indications that $\rho_{\{C_i\}}(\beta)$ is dual to a classical geometry given by a conical defect of thermal $\mathrm{AdS}_3$ or the BTZ black hole respectively, depending on the temperature. For

[3] The results of section 3.6.6 only apply to these models if they also include a two-cycle twist operator implementing a deformation as in the $S_N$ orbifold theory of the D1/D5 system, which is known to be true for many of the models mentioned above.

the subset $\{C_i\}$ considered in chapter 3 consisting of twisted sectors containing only cycles of length $km$ for $k \in \mathbb{N}$ and a fixed integer $m$, the conical defect is of order $m$ (i.e. a $\mathbb{Z}_m$ identification of thermal $AdS_3$ or the BTZ black hole).

This indication comes from considering the partition function corresponding to this (Euclidean) bulk geometry, $Z = \exp(-S_{\text{grav}})$. Using the holographic renormalization procedure explained in section 2.1.2, the renormalized on-shell action for the conical defects of thermal $AdS_3$ can be easily shown to be $1/m^2$ smaller than that of thermal $AdS_3$ while the renormalized on-shell action for the BTZ black hole is invariant under the $\mathbb{Z}_m$ identification. This is in accord with the thermal partition function for the $\{C_i\}$ subset in the $S_N$ orbifold theory, see equation (C.28). Assuming that this partition function is invariant under the deformation from the orbifold point to the supergravity point (which seems likely given the results of section 3.6.6), this indicates that $\rho_{\{C_i\}}$ is indeed dual to the conical defects of thermal $AdS_3$ or the BTZ black hole.

If this holds true, the proof of [113] is again immediately applicable to the situation at hand since the generalized entanglement entropy in this case again reduces to an ordinary entanglement entropy of an interval of length $w + L$ on a covering space (which in this case is thermal $AdS_3$ or the BTZ black hole instead of pure $AdS_3$). To establish whether this covering space picture is correct, it would be interesting to better understand how the twisted sectors manifest themselves on the gravity side.

- Do generalized Ryu-Takayanagi formulas exist in higher dimensions? There is a limited amount of previous work [328–330] on generalized entanglement entropy in higher dimensions focusing on bipartitions of global symmetry orbits, that is for a global symmetry corresponding to a Lie group the bipartition splits the Lie group manifold in two. In these works, a ten-dimensional space is considered in the bulk consisting of an AdS geometry together with a compact manifold whose isometries correspond to the global symmetry group. The corresponding generalized Ryu-Takayanagi surfaces are given by codimension-two surfaces in the ten-dimensional space which asymptote to a surface bipartitioning the compact part on the AdS boundary. This notion of generalized entanglement is distinct to the generalized entanglement measures considered in this thesis. In particular, unlike in [328–330] the generalized Ryu-Takayanagi surfaces considered in this thesis are extremal but not minimal. Therefore, it would be interesting to understand if extremal but non-minimal codimension-two surfaces exist in higher dimensions which wind around e.g. black hole horizons and probe entanglement shadows. Another important question is if there is an analog of the twisted sectors in higher dimensions, for example in the $\mathcal{N} = 4$ Super-Yang-Mills theory.

- Are there entanglement wedges associated to the subset considered for the generalized entanglement entropy? The code subspace of bulk excitations encoded in the subset might differ from that of a spatial subregion and hence these generalized entanglement wedges might not be spatial subregions. If such generalized entanglement wedges exist, the expectation is that they encode more information about excitations deep in the bulk (i.e. in entanglement shadows) than their counterparts for spatial subregions.

- Is there a simple extension of the generalized Ryu-Takayanagi formula that incorporates bulk quantum corrections? For the ordinary Ryu-Takayanagi formula, it has been argued in [35] that the entanglement entropy of a boundary subregion $A$ is given to all orders in $G_N$ by

$$S_A = \min_{\gamma_A} \left[ \frac{\text{Area}(\gamma_A)}{4G_N} + S_{\text{bulk}} \right], \tag{5.1}$$

where $S_{\text{bulk}}$ is the von Neumann entropy of the quantum state of the matter fields in the entanglement wedge subregion in the bulk. $\gamma_A$, the so-called quantum extremal surface, is the codimension-two surface asymptoting to $\partial A$ on the boundary that minimizes the sum of the area term and the $S_{\text{bulk}}$ term. Can $1/G_N$ corrections corresponding to $1/c$ corrections be included in the generalized entanglement entropy in the same way? This question is especially relevant for studying the generalized entanglement entropy for black holes evaporating into a non-gravitational bath system. In this case it is known that for the ordinary entanglement entropy the quantum extremal surface and the Ryu-Takayanagi surface differ substantially which has implications for the black hole information paradox [31–33].

For the computational complexity studies of chapter 4, the most interesting future directions arise from the bulk dual to the Virasoro group transformation circuit derived in section 4.5.

- The bulk dual to the Virasoro group transformation circuit opens up the possibility of studying aspects of computational complexity measures (such as cost functions, optimal circuits, etc.) from first principles in a simple, well under control model of a quantum circuit. While in this thesis only the Fubini-Study distance was considered as a cost function, a number of other choices have been proposed before in the literature which can be mapped to bulk quantities using the results of section 4.5. Vice versa, holographic computational complexity measures like "complexity=volume" or "complexity=action" can be mapped to boundary quantities in the Virasoro group circuits. For an example of the former computation, consider the $k$ norm cost function (2.96). In the circuits of section 4.5, this cost function takes the form
$$\mathscr{F}_{k,\{p\}}(t) = \left(\sum_n p_n |\epsilon_n(t)|^k\right)^{1/k}, \tag{5.2}$$
for some choice of penalty factors $p_n$. The $\epsilon_n(t)$ Fourier coefficients of $\epsilon(t,z)$ coefficients parametrizing the computation step at time $t$ can be extracted from metric components. For example, for the bulk dual circuit defined by equation (4.161) and (4.162) the function $\epsilon(t,z)$ is encoded in the Fefferman-Graham coefficients $g_{ij}^{(0)}, g_{ij}^{(2)}$ and $g_{ij}^{(4)}$ of the metric as $\epsilon(t, f(t,z)) = g_{tt}^{(0)} = \sqrt{-4g_{tt}^{(2)} - 1} = 16 g_{tt}^{(4)}$. In this way, (5.2) can be related to some (in general quite complicated) expression written in terms of the bulk metric.

- One of the most interesting results of chapter 4 is that the Fubini-Study distance between two states related by infinitesimal time-evolution can be expressed in terms of the length of geodesics in the bulk via (4.190). Therefore, a striking implication is that the Fubini-Study distance is related to the (generalized) entanglement entropy. This relation deserves to be studied further. Especially interesting in this regard is the fact that the restriction on the winding numbers of the geodesics employed in the expression (4.190) in the BTZ black hole case (which is necessary to reproduce the expected saturation behavior of the computational complexity) naturally emerges from the entanglement entropy. Note, however, that the computational complexity for the state dual to the two-sided BTZ black hole geometry was proposed in [59] to grow for a time exponential in the black hole entropy $S$ while for finite $c \sim N$ the generalized entanglement entropy does not seem to allow for an exponentially long growth. The generalized entanglement entropy calculated in chapter 3 increases for a time scale proportional to the winding number which is bounded by $N$. Although the generalized entanglement entropy results from chapter 3 capture only the leading order in $N$, it is unlikely that $1/N$ corrections substantially change this picture. Thus, the growth of the generalized entanglement entropy with time in the thermofield double state seems to be limited by a number linear in $S \sim N$.

- A further question which should be investigated is whether the bulk dual to the Fubini-Study complexity defined by (4.190) can also reproduce the switchback effect [52, 158] in geometries related to the BTZ black hole by the insertion of high-energy shockwaves behind the horizon. The insertion of a shockwave due to the application of a precursor operator leads to a characteristic time delay for the increase in computational complexity [52]. This time delay is reproduced for example by the "complexity=volume" proposal in the BTZ geometry with a shockwave insertion at the location determined by the precursor operator [52]. The fact that the computational complexity in a qubit model agrees with its conjectured holographic description in this quite non-trivial case is a key feature of the holographic complexity proposals of [51–54]. Therefore, the Fubini-Study complexity should reproduce the time delay as well.

These future directions will help in better understanding the remarkable connections between quantum information and gravity that have emerged recently. In particular, they will contribute towards the goal of deciphering the encoding of the bulk geometry in terms of boundary quantities in the AdS/CFT correspondence, a task where already in this thesis significant progress has been made. Thus, there is much to look forward to in this direction in the coming years.

# A. Conventions for elliptic functions

This appendix contains an overview over conventions and useful identities for the Weierstraß elliptic functions used in section 3.4. More information on these functions can be found for example in [298]. All elliptic functions are defined for a lattice $\Lambda$ generated by the identifications $z \sim z+1$ and $z \sim z+\tau$. The Weierstraß elliptic functions $\wp(z), \zeta(z)$ and $\sigma(z)$ are defined by

$$\begin{aligned}
\wp(z) &= -\zeta'(z) = \frac{1}{z^2} + \sum_{(m,n)\neq(0,0)} \left( \frac{1}{(z+n+m\tau)^2} - \frac{1}{(n+m\tau)^2} \right), \\
\zeta(z) &= \frac{\sigma'(z)}{\sigma(z)} = \frac{1}{z} + \sum_{(m,n)\neq(0,0)} \left( \frac{1}{(z+n+m\tau)} - \frac{1}{(n+m\tau)} + \frac{z}{(n+m\tau)^2} \right), \\
\sigma(z) &= z \prod_{(m,n)\neq(0,0)} \left(1 - \frac{z}{n+m\tau}\right) \exp\left( \frac{z}{n+m\tau} + \frac{1}{2}\frac{z^2}{(n+m\tau)^2} \right).
\end{aligned} \tag{A.1}$$

$\wp(z)$ is a true elliptic (i.e. doubly periodic) function while $\zeta(z)$ and $\sigma(z)$ are quasiperiodic:

$$\begin{aligned}
&\wp(z+1) = \wp(z+\tau) = \wp(z) \\
&\zeta(z+1) = \zeta(z) + 2\eta_1, \qquad\qquad \zeta(z+\tau) = \zeta(z) + 2\eta_3 \\
&\sigma(z+1) = -\exp(2\eta_1(z+1/2))\sigma(z), \quad \sigma(z+\tau) = -\exp(2\eta_3(z+\tau/2))\sigma(z),
\end{aligned} \tag{A.2}$$

where $\eta_1 = \zeta(1/2)$ and $\eta_3 = \zeta(\tau/2) = \tau\eta_1 - \pi i$. Another useful definition of $\wp(z)$ and $\zeta(z)$ is given by

$$\begin{aligned}
\wp(z) + 2\eta_1 &= (2\pi i)^2 \sum_{m=-\infty}^{\infty} \frac{Q^m u}{(u-Q^m)^2} = \left(\frac{2\pi i}{\tau}\right)^2 \sum_{m=-\infty}^{\infty} \frac{\tilde{Q}^m \tilde{u}}{(\tilde{u}-\tilde{Q}^m)^2} \\
\zeta(z) - 2\eta_1 z &= i\pi \sum_{m=-\infty}^{\infty} \frac{Q^m+u}{Q^m-u} = -\frac{i\pi}{\tau} \sum_{m=-\infty}^{\infty} \frac{\tilde{Q}^m+\tilde{u}}{\tilde{Q}^m-\tilde{u}},
\end{aligned} \tag{A.3}$$

where $u = e^{-2\pi i z}, Q = e^{2\pi i \tau}$ and $\tilde{u} = e^{2\pi i z/\tau}$, $\tilde{Q} = e^{-2\pi i/\tau}$.

# B. Recursion relations for torus conformal blocks

For completeness, this appendix shows the recursion formulas for the two-point conformal blocks on the torus following as a special case from the general method derived in [213]. For details of the derivation, see [213] and also [212] for the one-point torus block. For the OPE block, the conformal block is given by the following recursion scheme

$$\begin{aligned}
\mathscr{F}^{\mathrm{OPE}}_{21,pq}(h_p,h_q,c) &= U^{\mathrm{OPE}}(h_p,h_q,c) \\
&- \sum_{r\geq 2,s\geq 1} \frac{\partial c_{rs}(h_q)}{\partial h_q} Q^{rs} \frac{A^{c_{rs}(h_q)}_{rs} P^{rs}_{c_{rs}(h_q)}\begin{bmatrix} h_p \\ h_q+rs \end{bmatrix} P^{rs}_{c_{rs}(h_q)}\begin{bmatrix} h_p \\ h_q \end{bmatrix}}{c-c_{rs}(h_q)} \mathscr{F}^{\mathrm{OPE}}_{21,pq}(h_q,h_q+rs,c_{rs}(h_q)) \\
&- \sum_{r\geq 2,s\geq 1} \frac{\partial c_{rs}(h_p)}{\partial h_p} y^{rs} \frac{A^{c_{rs}(h_p)}_{rs} P^{rs}_{c_{rs}(h_p)}\begin{bmatrix} h_q \\ h_q \end{bmatrix} P^{rs}_{c_{rs}(h_p)}\begin{bmatrix} h_2 \\ h_1 \end{bmatrix}}{c-c_{rs}(h_p)} \mathscr{F}^{\mathrm{OPE}}_{21,pq}(h_p+rs,h_q,c_{rs}(h_p))
\end{aligned} \tag{B.1}$$

where the fusion polynomials are given by

$$P^{rs}_{c}\begin{bmatrix} h_1 \\ h_2 \end{bmatrix} = \prod_{m=1-r,m\in 1-r+2\mathbb{N}}^{r-1} \prod_{n=1-s,n\in 1-s+2\mathbb{N}}^{s-1} \frac{\lambda_1+\lambda_2+mb+nb^{-1}}{2} \frac{\lambda_1-\lambda_2+mb+nb^{-1}}{2} \tag{B.2}$$

with $\lambda_i = \sqrt{(b+b^{-1})^2-4h_i}$ while the prefactor is

$$A^{c}_{rs} = \frac{1}{2} \prod_{(m,n)}{}' (mb+nb^{-1})^{-1}, \tag{B.3}$$

where the product $\prod'$ runs over $1-r \leq m \leq r$ and $1-s \leq n \leq s$ excluding the values $(m,n)=(0,0)$ and $(m,n)=(r,s)$. $c_{rs}$ denotes the value of the central charge where degenerate representations of the Virasoro algebra appear,

$$\begin{aligned}
c_{rs}(h) &= 1+6(b_{rs}(h)+b^{-1}_{rs}(h))^2, \\
b_{rs}(h)^2 &= \frac{rs-1+2h+\sqrt{(r-s)^2+4(rs-1)h+4h^2}}{1-r^2}.
\end{aligned} \tag{B.4}$$

The $c$-regular part $U$ is given by

$$U^{\mathrm{OPE}}(h_p,h_q,c) = \left[\prod_{n=2}^{\infty} \frac{1}{1-Q^n}\right] \sum_{i,j\geq 0} Q^i y^j \frac{s_{ij}(h_q,h_p,h_q)(1-h_p-j)_j(h_p+h_1-h_2)_j}{i!(2h_q)_i j!(2h_p)_j}, \tag{B.5}$$

where the rising and falling Pochhammer symbols are defined by by

$$(a)_n = \prod_{k=0}^{n-1}(a+k), \quad (a)^{(n)} = \prod_{k=0}^{n-1}(a-k) \tag{B.6}$$

and

$$\begin{aligned} s_{ij}(h_1,h_2,h_3) &= \langle h_1|(L_{-1}^i)^\dagger \mathcal{O}_{h_2}(1)L_{-1}^j|h_3\rangle \\ &= \begin{cases} \displaystyle\sum_{p=0}^{i}\binom{i}{p}(j)^{(p)}(2h_3+j-1)^{(p)}(h_1+h_2-h_3-(j-p))_{i-p}(h_3+h_2-h_1)_{j-p}\ , \ j\geq i \\ \displaystyle\sum_{p=0}^{j}\binom{j}{p}(i)^{(p)}(2h_1+i-1)^{(p)}(h_3+h_2-h_1-(i-p))_{j-p}(h_1+h_2-h_3)_{i-p}\ , \ i\geq j \end{cases} \end{aligned} \tag{B.7}$$

The recursion formula for the projection block is given by [1]

$$\begin{aligned} \mathcal{F}_{2p,1q}^{\text{projection}}(h_p,h_q,c) =& U^{\text{projection}}(h_p,h_q,c) \\ &- \sum_{r\geq 2,s\geq 1}\frac{\partial c_{rs}(h_q)}{\partial h_q}q_1^{rs}\frac{A_{rs}^{c_{rs}(h_q)}P_{c_{rs}(h_q)}^{rs}\begin{bmatrix}h_p\\h_1\end{bmatrix}P_{c_{rs}(h_q)}^{rs}\begin{bmatrix}h_p\\h_2\end{bmatrix}}{c-c_{rs}(h_q)}\mathcal{F}_{2p,1q}^{\text{projection}}(h_p,h_q+rs,c_{rs}(h_q)) \\ &- \sum_{r\geq 2,s\geq 1}\frac{\partial c_{rs}(h_p)}{\partial h_p}q_2^{rs}\frac{A_{rs}^{c_{rs}(h_p)}P_{c_{rs}(h_p)}^{rs}\begin{bmatrix}h_q\\h_1\end{bmatrix}P_{c_{rs}(h_p)}^{rs}\begin{bmatrix}h_q\\h_2\end{bmatrix}}{c-c_{rs}(h_p)}\mathcal{F}_{2p,1q}^{\text{projection}}(h_p+rs,h_q,c_{rs}(h_p)), \end{aligned} \tag{B.8}$$

where the $c$-regular part is given by

$$U^{\text{projection}}(h_p,h_q,c) = \left[\prod_{n=2}^{\infty}\frac{1}{1-Q^n}\right]\sum_{i,j\geq 0}q_1^i q_2^j\frac{s_{ij}(h_q,h_2,h_q)s_{ji}(h_p,h_1,h_q)}{i!(2h_q)_i j!(2h_p)_j}. \tag{B.9}$$

By explicit calculation, it is easy to check in the first few orders of the series expansion that for $h_1 = h_2$ and $h_{p,q} = \gamma c$, the limits $\lim_{\gamma\to 0}$ and $\lim_{c\to\infty}$ of the OPE block commute. I have checked this up to fourth order in $y, Q$. A more convenient proof is possible with a recursion relation in the conformal weights of the exchanged operators $h_{p,q}$, as derived for the conformal block on the plane in [211]. In fact, the singular parts proportional to $\sim 1/(h_{p,q}-h_{rs})$ of such a recursion relation are proportional to the singular parts $\sim 1/(c-c_{rs}(h_{p,q}))$ of the above recursion relations in $c$ [213]. Using these known singular parts, one can show that the limits $\gamma\to 0$ and $c\to\infty$ commute for the singular parts of this recursion relation to all orders, assuming the above conditions on $h_{1,2,p,q}$. Together, these calculations provide some evidence that the semiclassical limit is well-defined for the vacuum block on the torus derived in section 3.5. Since the vacuum block on the torus in most limits is equivalent to a zero-point block on the replica surface $\mathcal{R}_n$, this also provides evidence that the semiclassical limit for the zero-point vacuum block on $\mathcal{R}_n$ is well-defined.

[1] Note that in [213], two different recursion formulas are presented – the one shown here which is applicable for general conformal blocks and another formula that applies only to a class of conformal blocks termed "necklace blocks" in [213]. Both of these formulas are applicable for the projection block, but they disagree with each other. I have checked that the recursion relation presented here is the correct one by comparing with an explicit calculation in the first few orders of the series expansion in $q_1, q_2$.

# C. The $S_N$ orbifold partition function

This appendix contains an overview over some aspects of the thermal partition function of the $S_N$ orbifold theory, in particular concerning its large $N$ behavior.

## C.1. Recursion formula

The partition function is determined from the following recursion formula,

$$Z_N(\tau) = \frac{1}{N}\sum_{k=1}^{N}\sum_{l=1}^{\lfloor N/k\rfloor}\sum_{j=0}^{k-1}\tilde{Z}\left(\frac{\tau l + j}{k}\right)Z_{N-kl}(\tau), \tag{C.1}$$

where $\tilde{Z}(\tau)$ is the partition function of the seed theory. This can be derived from the generating function $\mathscr{Z}[p]$ [331–334],

$$\mathscr{Z}[p] = \sum_{N\geq 0} p^N Z_N(\tau) = \prod_{n>0}\prod_{m,\bar{m}}(1-p^n q^{m/n}\bar{q}^{\bar{m}/n})^{-d(m,\bar{m})\delta^{(n)}_{m-\bar{m}}}. \tag{C.2}$$

Here,

$$\delta^{(n)}_{m-\bar{m}} = \begin{cases} 1, & m-\bar{m} \text{ divides } n \\ 0, & \text{otherwise.} \end{cases} \tag{C.3}$$

The partition function is obtained by differentiating

$$Z_N(\tau) = \frac{1}{N!}\frac{\partial^N}{\partial p^N}\mathscr{Z}[p]\bigg|_{p=0}. \tag{C.4}$$

The first derivative w.r.t. $p$ is given by

$$\frac{\partial}{\partial p}\mathscr{Z}[p] = \sum_n\sum_{m,\bar{m}}\frac{nd(m,\bar{m})\delta^{(n)}_{m-\bar{m}}}{p(p^{-n}q^{-m/n}\bar{q}^{-\bar{m}/n}-1)}\mathscr{Z}[p]. \tag{C.5}$$

Using that for any $\alpha$,

$$\frac{\partial^{l-1}}{\partial p^{l-1}}\frac{1}{p(p^{-n}\alpha-1)}\bigg|_{p=0} = (l-1)!\sum_{k|l}\frac{\delta_{n,k}}{\alpha^{l/k}}, \tag{C.6}$$

the following recursion formula for the partition function is found,

$$Z_N(\tau) = \frac{1}{N}\sum_{l=1}^{N}\sum_{k|l}\sum_{j=0}^{k-1}\tilde{Z}\left(\tau\frac{l}{k^2}+\frac{j}{k}\right)Z_{N-l}(\tau). \tag{C.7}$$

The second sum in this formula is performed over all divisors $k$ of $l$. Finally, performing a resummation in $k$ such that all terms with the same $k$ are grouped together yields (C.1).

## C.2. Large $N$ behavior

At large $N$, the partition function (C.1) is equal to the universal form valid for general two-dimensional holographic CFTs [209] [1],

$$\log Z_N(\tau) = \begin{cases} \dfrac{\tilde{c}N}{12}\beta + O(N^0), & \beta > 2\pi, \\ \dfrac{\tilde{c}N}{12}\dfrac{4\pi^2}{\beta} + O(N^0), & \beta < 2\pi, \end{cases} \tag{C.8}$$

where $\tilde{c}$ is the central charge of the seed theory. Note that in this formula, I have restricted to purely imaginary $\tau = \frac{i\beta}{2\pi}$. Equation (C.8) is derived in [209] by noting that $\tilde{Z}(\tau)$ can be bounded by

$$\tilde{Z}(\tau) \leq p(\beta)\exp\left(\frac{\tilde{c}}{12}\beta\right)\exp\left(\frac{\tilde{c}}{6}\frac{4\pi^2}{\beta}\right), \tag{C.9}$$

for any seed theory, where $p(\beta)$ is some polynomial in $\beta$. Inserting this into (C.1), at large $N$ the leading terms come from the $k = 1, j = 0$ terms if $\beta > 2\pi$ and the $l = 1, j = 0$ terms if $\beta < 2\pi$. Other terms in $Z_N$ are exponentially suppressed with $e^{-N}$.

In section 3.6, also the decomposition of (C.1) into twisted sectors is needed. The contribution of a single cycle of length $m$ is given by

$$Z_{(m)} = \frac{1}{m}\sum_{j=0}^{m-1}\tilde{Z}\left(\frac{\tau + j}{m}\right). \tag{C.10}$$

In general, a twisted sector contains multiple cycles which in total give a contribution to the partition function of

$$Z_{(1)^{n_1}\ldots(N)^{n_N}} = \prod_{m=1}^{N}\frac{1}{n_m}\sum_{k=1}^{n_m} Z_{(m)}(k\tau)Z_{(m)^{n_m-k}}(\tau), \tag{C.11}$$

where $Z_{(m)^{n_m-k}}(\tau)$ is the contribution of the $(m)^{n_m-k}$ twisted sector recursively determined from (C.11). The total partition function (C.1) is given by summing over all sectors. The dominant contribution to $Z_N$ comes from the untwisted $(1)^N$ sector for $\beta > 2\pi$, while for $\beta < 2\pi$ all sectors contribute. This can be seen explicitly by comparing (C.11) with the dominant contributions to (C.1). Another argument can be given as follows. From [209], it is known that the identity character $\chi_{\mathbb{1}}(\tau)$ belonging to the untwisted sector dominates the partition function for $\beta > 2\pi$, while for $\beta < 2\pi$, the modular transformed identity character $\chi_{\mathbb{1}}(-1/\tau)$ dominates. The modular transformation exchanges the time and space directions of the torus on which the CFT lives. The identity character includes a sum over spin structures with all possible $S_N$ boundary conditions along the time direction. Hence, the modular transformed identity character includes a sum over spin structures with untwisted boundary conditions in the time direction and all possible $S_N$ boundary conditions along the space direction.

The contribution of a single twisted sector to the thermal partition function is non-universal. However, combinations of a large number of twisted sectors can become universal again in the large $N$ limit, as I will show below. In particular, the contribution of a large number $n_m = O(N)$ of short cycles with length $m = O(N^0)$ is universal. Similarly, the contribution of a small number of long cycles with length $m = O(N)$ is also universal in the large $N$ limit.

[1] In this context "universal" means dependent only on the central charge of the CFT and not on details of the spectrum or OPE coefficients.

### Short cycles

First consider the untwisted sector which includes $N$ cycles of length 1. The corresponding contribution to the partition function is given by

$$Z_{(1)^N}(\tau) = \frac{1}{N}\sum_{k=1}^{N}\tilde{Z}(k\tau)Z_{(1)^{N-k}}(\tau). \tag{C.12}$$

I will show that in the large $N$ limit, this contribution is proportional to

$$Z_{(1)^N}(\tau) = e^{\frac{N\tilde{c}}{12}\beta}. \tag{C.13}$$

up to subleading terms in $N$. Note that this holds for all temperatures in contrast to the total partition function (C.1) where the contribution of the untwisted sector is dominant only for $\beta > 2\pi$. The same techniques that were used in [209] to show the universality of the total partition function can be employed to show (C.13). For this, let me define the generating function of (C.12),

$$\mathscr{Z}_{(1)^N}(\tau) = \sum_{N=0}^{\infty} p^N Z_{(1)^N}(\tau) = \prod_{h,\bar{h}}(1-pq^{h-\tilde{c}/24}\bar{q}^{\bar{h}-\tilde{c}/24})^{-\tilde{d}(h,\bar{h})}. \tag{C.14}$$

Here $\tilde{d}(h,\bar{h})$ is the density of states of the seed theory,

$$\tilde{Z}(\tau) = \sum_{h,\bar{h}}\tilde{d}(h,\bar{h})q^{h-\tilde{c}/24}\bar{q}^{\bar{h}-\tilde{c}/24}. \tag{C.15}$$

The right hand side of (C.14) can easily be verified by differentiating w.r.t. $p$. Employing a trick of [334, 335] by rewriting $\mathscr{Z}_{(1)^N}(\tau)$ in terms of $\hat{p} = pq^{-\tilde{c}/24}\bar{q}^{-\tilde{c}/24}$ and factoring out the contribution of the vacuum $h = \bar{h} = 0$, which is assumed to be unique, gives

$$\mathscr{Z}_{(1)^N}(\tau) = \frac{1}{1-\hat{p}}\prod_{h,\bar{h}>0}(1-pq^h\bar{q}^{\bar{h}})^{-\tilde{d}(h,\bar{h})} = \frac{1}{1-\hat{p}}R(\hat{p}). \tag{C.16}$$

Series expanding $R(\hat{p}) = \sum_{k=0}^{\infty} a_k\hat{p}^k$, we see that $Z_{(1)^N}(\tau)e^{-\frac{N\tilde{c}}{12}\beta} = \sum_{k=0}^{N} a_k$ and thus

$$\hat{Z}_{(1)^\infty}(\tau) = \lim_{N\to\infty} Z_{(1)^N}(\tau)e^{-\frac{N\tilde{c}}{12}\beta} = \sum_{k=0}^{\infty} a_k = R(1). \tag{C.17}$$

To prove (C.13), it remains to show that $\log\hat{Z}_{(1)^\infty}$ converges. This is readily achieved by series expanding the $\log(1-q^h\bar{q}^{\bar{h}})$ terms in $\log\hat{Z}_{(1)^\infty}$, giving

$$\log\hat{Z}_{(1)^\infty}(\tau) = \sum_{k=1}^{\infty}\frac{1}{k}((q\bar{q})^{k\tilde{c}/24}\tilde{Z}(k\tau)-1). \tag{C.18}$$

Due to the vacuum contribution having been factored out in (C.16), $(q\bar{q})^{\tilde{c}/24}\tilde{Z}(\tau)-1$ can be bounded by (see [209])

$$(q\bar{q})^{\tilde{c}/24}\tilde{Z}(\tau)-1 \leq \tilde{p}(\tau)q^{h_1}\bar{q}^{\bar{h}_1}e^{\frac{\tilde{c}}{6}\frac{4\pi^2}{\beta}}, \tag{C.19}$$

where $\tilde{p}(\tau)$ is some polynomial in $\tau$ and $h_1, \bar{h}_1$ the conformal weight of the lowest non-vacuum primary of the seed theory. Inserting this back in (C.17) shows that the sum over $k$ converges and

thus $\log \hat{Z}_{(1)^\infty}(\tau) < \infty$. This derivation easily generalizes to the contribution of $n_m$ short cycles of length $m = O(N^0)$ since $Z_{(m)}(\tau)$ from (C.10) can be bounded by $Z_{(m)}(\tau) \leq p(\tau)\tilde{Z}(\tau/m)$ (the sum in (C.10) can be bounded by a factor times its largest term), which implies

$$Z_{(m)^{n_m}}(\tau) = e^{\frac{\tilde{c}}{12}\beta n_m/m}, \tag{C.20}$$

up to terms subleading in $n_m \propto O(N)$.

### Long cycles

To show the universality of long cycle contributions, let me start with the maximally twisted sector. The corresponding contribution to the partition function is given by

$$Z_{(N)}(\tau) = \frac{1}{N}\sum_{j=0}^{N-1}\tilde{Z}\left(\frac{\tau+j}{N}\right). \tag{C.21}$$

In the large $N$ limit, this scales as

$$Z_{(N)}(\tau) = \frac{1}{N}e^{\frac{\tilde{c}}{12}N\frac{4\pi^2}{\beta}}, \tag{C.22}$$

up to $e^{-N}$ corrections. Note that unlike for the untwisted sector, (C.22) includes a prefactor scaling polynomially in $N$. Eq. (C.22) is a straightforward consequence of the Cardy formula. For small $j$, the argument $(\tau+j)/N$ of the seed partition function $\tilde{Z}$ in (C.21) goes to zero as $N \to \infty$, therefore $\tilde{Z}\left(\frac{\tau+j}{N}\right)$ is well-approximated by

$$\tilde{Z}\left(\frac{\tau+j}{N}\right) \propto e^{\frac{\tilde{c}}{12}\frac{\beta N}{j^2+(\beta/2\pi)^2}}. \tag{C.23}$$

For large $j$ (i.e. $j$ scaling proportional to $N$), applying a modular transformation gives

$$\tilde{Z}\left(\frac{\tau+j}{N}\right) = \tilde{Z}\left(-\frac{1}{N\tau}+\frac{\hat{j}}{N}\right). \tag{C.24}$$

If $j$ scales proportional to $N$, then $\hat{j}$ scales proportional to $N^0$, thus the Cardy formula can be applied again to obtain

$$\tilde{Z}\left(\frac{\tau+j}{N}\right) \propto e^{\frac{\tilde{c}}{12}\frac{\beta N}{1+(\hat{j}\beta/2\pi)^2}}. \tag{C.25}$$

Now $\frac{\beta}{j^2+(\beta/2\pi)^2} \leq \frac{4\pi^2}{\beta}$ and $\frac{\beta}{1+(\hat{j}\beta/2\pi)^2} \leq \frac{4\pi^2}{\beta}$, thus the leading contribution to (C.21) in the large $N$ limit is given by the $j=0$ term (C.22). More generally, for multiple long cycles the contribution of $n_m$ cycles of length $m \propto O(N)$ is obtained using (C.11), giving

$$Z_{(m)^{n_m}}(\tau) = \frac{1}{m^{n_m}n_m!}e^{\frac{\tilde{c}}{12}mn_m\frac{4\pi^2}{\beta}} \tag{C.26}$$

up to terms subleading in $N$.

### $S_{N/m}$ subsets

Finally, let me consider the contribution to the thermal partition function of twisted sectors of the form $(m)^{n_m}(2m)^{n_{2m}}(3m)^{n_{3m}}\ldots$ forming an $S_{N/m}$ subset, as considered in chapter 3 for the generalized entanglement entropy. This contribution may of course be obtained simply by applying the

results for the contribution of single twisted sectors given above, however I will also give a more general argument.

The partition function of any large $c$ holographic CFT is obtained from the identity character $\chi_{\mathbb{1}}(\tau)$ at low temperature and its modular transformation $\chi_{\mathbb{1}}(-1/\tau)$ at high temperature [209]. That is, only descendants of the identity operator contribute to the sum over states in the partition function at low temperature. As explained in section 3.6, the identity operator is projected out of the partition function for the $S_{N/m}$ subset and thus the leading contribution comes from the character of the operator $\Sigma$ with weight (3.133). Thus, at low temperatures the partition function is dominated by the character

$$\chi_{\Sigma}(\tau) \propto q^{h_{\Sigma}-c/24} = q^{-\frac{\tilde{c}}{24}\frac{N}{m^2}}, \tag{C.27}$$

where $q = e^{2\pi i\tau} = e^{-\beta}$ and the proportionality constant includes only $O(N^0)$ factors. At high temperatures, the partition function is dominated by the modular transformed vacuum character $\chi_{\mathbb{1}}(-1/\tau)$ similar to the partition function for the full $S_N$ group, such that

$$Z^{\{C_i\}}(\tau) \propto \begin{cases} \exp\left(\frac{\tilde{c}}{12}\beta\frac{N}{m^2}\right), & \beta > 2\pi m \\ \exp\left(\frac{\tilde{c}}{12}\frac{4\pi^2}{\beta}N\right), & \beta < 2\pi m, \end{cases} \tag{C.28}$$

where the proportionality constant includes a $m, N$ dependent prefactor for high temperatures. This prefactor can not be derived by the above argument, but it may easily be obtained from the contribution from single twisted sectors from (C.20) and (C.26).

# D. Details of the perturbative calculation of the Fubini-Study complexity and complexity=volume

This appendix contains the fourth order results for the perturbative calculation from section 4.4 of the Fubini-Study complexity and "complexity=volume" for conformal transformations of the vacuum state.

### Fubini-Study complexity

To third order in perturbation theory, the equation of motion (4.119) leads to a solution of $f(\tau,\sigma)$ as a third order polynomial in $\tau$,

$$f_3(\tau,\sigma) = \frac{1}{6}A_3(\sigma)\tau^3 + \frac{1}{2}B_3(\sigma)\tau^2 + C_3(\sigma)\tau + D_3(\sigma). \tag{D.1}$$

The boundary conditions $f_3(0,\sigma) = 0$, $f_3(1,\sigma) = f_3(\sigma)$ determine enough of $f_3(\tau,\sigma)$ to be able to compute $\mathscr{C}_{(4)}$. However, for $\mathscr{C}_{(4)}$ also the second order e.o.m. (4.126) needs to be solved fully. This is readily accomplished by using the Fourier decomposition of $A_2(\sigma)$. Then (4.126) is equivalent to

$$\begin{aligned}
&\int d\kappa d\sigma \Pi(\sigma-\kappa)A_2(\sigma)e^{-in\kappa} = 2\pi^2\left(\frac{c}{12}(|n|^3-|n|)+2h|n|\right)A_2^n \\
&= \int d\kappa d\sigma[inf_1(\sigma)f_1(\kappa)+f_1(\sigma)(f_1'(\sigma)+f_1'(\kappa))]\Pi(\sigma-\kappa)e^{-in\kappa} \\
&\Rightarrow A_2^n = \frac{-i}{\frac{c}{12}(|n|^3-|n|)+2h|n|}\Bigg[\sum_r f_1^r f_1^{n-r}\Big(\frac{c}{12}(|r|(2n-n^3-r+r^3+2nr(n-r))+|n|(1-n^2)(n-r)) \\
&\qquad\qquad -2h(|r|(2n-r)+|n|(n-r))\Big)\Bigg]
\end{aligned} \tag{D.2}$$

The complexity is then given by

$$\mathscr{C}_{(4)} = \mathscr{C}_{\mathrm{FS}}|_{O(\varepsilon^4)} = \mathscr{C}_{(4)}^A + \mathscr{C}_{(4)}^B + \mathscr{C}_{(4)}^C \tag{D.3}$$

where

$$\begin{aligned}
\mathscr{C}_{(4)}^C &= \int d\sigma d\kappa \Pi(\sigma-\kappa)[f_1(\sigma)f_3(\kappa)+f_3(\sigma)f_1(\kappa)] \\
&= 4\pi^2\sum_n\left(\frac{c}{12}(|n|^3-|n|)+2h|n|\right)f_1^n f_3^{-n},
\end{aligned} \tag{D.4}$$

$$
\begin{aligned}
\mathscr{C}^B_{(4)} &= \int d\sigma d\kappa \Pi(\sigma-\kappa)\Big[ f_2(\sigma)f_2(\kappa) - \frac{1}{2} f_1(\sigma)f_1(\kappa)(f_2'(\sigma)+f_2'(\kappa)) \\
&\qquad - \frac{1}{2}(f_1(\sigma)f_2(\kappa)+f_2(\sigma)f_1(\kappa))(f_1'(\sigma)+f_1'(\kappa))\Big] \\
&= 2\pi^2 \sum_n \Big(\frac{c}{12}(|n|^3-|n|)+2h|n|\Big)\Big[ f_2^n f_2^{-n} - i\sum_m m(f_1^n f_2^m f_1^{-n-m} + f_1^n f_1^m f_2^{-n-m} + f_2^n f_1^m f_1^{-n-m})\Big],
\end{aligned}
\tag{D.5}
$$

and

$$
\begin{aligned}
\mathscr{C}^A_{(4)} &= \int d\sigma d\kappa \Pi(\sigma-\kappa)\Big[ \frac{1}{12}A_2(\sigma)A_2(\kappa) - \frac{1}{12}(A_2(\sigma)f_1(\kappa)+f_1(\sigma)A_2(\kappa))(f_1'(\sigma)+f_1'(\kappa)) \\
&\qquad + \frac{1}{12}f_1(\sigma)f_1(\kappa)(A_2'(\sigma)+A_2'(\kappa)) + \frac{1}{3}f_1(\sigma)f_1(\kappa)(f_1'(\sigma)+f_1'(\kappa))^2\Big] \\
&= 2\pi^2 \frac{c}{12}\sum_{m,n,r} f_1^m f_1^n f_1^{m-r} f_1^{-n-r}\Big[ \\
&- \frac{1}{12}\frac{1}{|r|^3-|r|}\big(|n|(n^3-n+r^3+2nr(n+r)-2r)+(n+r)|r|(r^2-1)\big) \\
&\qquad \big(|m|(m^3-m-r^3+2mr(r-m)+2r)+(m-r)|r|(r^2-1)\big) \\
&- \frac{1}{12}\big((m+2n)|m|(m^2-1)+(n+2m)|n|(n^2-1)+(m+n)|m+n|((m+n)^2-1)\big) \\
&\qquad \frac{1}{|m+n|^3-|m+n|}\Big((n+r)|m+n|((m+n)^2-1) \\
&\qquad + |m-r|\big(r((n+r)^2-1)+n((m+n)^2-1) \\
&\qquad - (m+n)+(n^2-mr)(r-m)\big)\Big) \\
&+ \frac{1}{3}(m-r)(n+r)(|m|(m^2-1)+|n|(n^2-1)+|r|(r^2-1))\Big] + \text{terms proportional to } h.
\end{aligned}
\tag{D.6}
$$

### Complexity=volume

The determinant of the induced metric on the bulk slice to fourth order in perturbation theory is given by

$$
\begin{aligned}
\sqrt{\gamma}|_{O(\varepsilon^4)} = -\frac{1}{8\sinh^3\rho}\Big[ &\cosh^4\rho\sinh^4\rho\,\dot{t}_1^4 + 2\cosh^4\rho\sinh^2\rho\,\dot{t}_1^2 t_1'^2 + \cosh^4\rho\, t_1'^4 \\
&+ 4\cosh^2\rho\sinh^4\rho\,\dot{t}_2^2 + 4\cosh^2\rho\sinh^2\rho\, t_2'^2 \\
&+ 8\cosh^2\rho\sinh^4\rho\,\dot{t}_1\dot{t}_3 + 8\cosh^2\rho\sinh^2\rho\, t_1' t_3'\Big].
\end{aligned}
\tag{D.7}
$$

This gives the following equation of motion for $t_3$,

$$
\begin{aligned}
&\cosh^4\rho\sinh^2\rho\,\dot{t}_1^2 t_1'' + 3\cosh^4\rho\, t_1'^2 t_1'' + \big(\cosh^5\rho\sinh^3\rho + 4\cosh^3\rho\sinh^5\rho\big)\dot{t}_1^3 \\
&+ 4\cosh^4\rho\sinh^2\rho\,\dot{t}_1' t_1' \dot{t}_1 - \big(\cosh^5\rho\sinh\rho - 4\cosh^3\rho\sinh^3\rho\big) t_1'^2 \dot{t}_1 \\
&+ 3\cosh^4\rho\sinh^4\rho\,\dot{t}_1^2\ddot{t}_1 + \cosh^4\rho\sinh^2\rho\, t_1'^2\ddot{t}_1 \\
&+ 2\cosh^2\rho\sinh^4\rho\,\ddot{t}_3 + 2\cosh^2\rho\sinh^2\rho\, t_3'' + 2\big(\cosh^3\rho\sinh^3\rho + 2\cosh\rho\sinh^5\rho\big)\dot{t}_3 = 0.
\end{aligned}
\tag{D.8}
$$

This can be slightly simplified by inserting the equation of motion for $t_1$,

$$\cosh^4\rho\, t_1'^2 t_1'' + \cosh^3\rho \sinh^5\rho\, \dot{t}_1^3 + 2\cosh^4\rho \sinh^2\rho\, \dot{t}_1' t_1' \dot{t}_1 - \cosh^3\rho \sinh\rho\, t_1'^2 \dot{t}_1 + \cosh^4\rho \sinh^4\rho\, \dot{t}_1^2 \ddot{t}_1$$
$$+ \sinh^2\rho \left(\cosh^2\rho \sinh^2\rho\, \ddot{t}_3 + \cosh^2\rho\, t_3'' + \sinh\rho \cosh\rho (3\cosh^2\rho - 2)\dot{t}_3\right) = 0. \tag{D.9}$$

Decomposing $t_3$ in a Fourier series gives

$$\cosh^2\rho \sinh^2\rho\, \ddot{t}_3^n + \sinh\rho \cosh\rho (3\cosh^2\rho - 2)\dot{t}_3^n - n^2 \cosh^2\rho\, t_3^n = g_n(\rho), \tag{D.10}$$

where all the $t_1$-dependent parts have been put into the function $g_n(\rho)$. The solution to this inhomogeneous differential equation is given by a sum of a special inhomogeneous solution and the solution of the homogeneous equation with $g_n(\rho) = 0$. Since the homogeneous equation is equivalent to the e.o.m. for $t_1^m$ and $t_2^m$, the solution is already known. The inhomogeneous solution can be obtained by a Greens function ansatz:

$$-n^2 \cosh^2\rho\, G(\rho,\rho_0) + \cosh\rho \sinh\rho (3\cosh^2\rho - 2)\frac{\partial}{\partial\rho} G(\rho,\rho_0) + \cosh^2\rho \sinh^2\rho \frac{\partial^2}{\partial\rho^2} G(\rho,\rho_0)$$
$$= \delta(\rho - \rho_0). \tag{D.11}$$

It is clear that the solution of (D.11) is equal to the solution of (4.135) when $\rho \neq \rho_0$, therefore the ansatz for $G(\rho,\rho_0)$ is given by

$$G(\rho,\rho_0) = \begin{cases} C_+ t_{1,+}^n + C_- t_{1,-}^n\,, & \rho < \rho_0 \\ \hat{C}_+ t_{1,+}^n + \hat{C}_- t_{1,-}^n\,, & \rho > \rho_0 \end{cases} \tag{D.12}$$

Requiring continuity of $G(\rho,\rho_0)$ at $\rho = \rho_0$ and the proper discontinuity of its derivative to reproduce the right hand side of (D.11) fixes the coefficients $C_\pm$ and $\hat{C}_\pm$. Integrating over $\rho_0$ gives

$$\begin{aligned} t_{3,\text{inhom.}}^n(\rho) = \frac{t_{1,+}^n(\rho)}{2|n|(|n|^2-1)}\Bigg[ &-\int_0^\infty d\rho_0 \frac{(\cosh\rho_0 + |n|)\tanh(\rho_0/2)^{|n|}}{\sinh\rho_0 \cosh\rho_0} g_n(\rho_0) \\ &+ \int_\rho^\infty d\rho_0 \frac{(\cosh\rho_0 - |n|)\tanh(\rho_0/2)^{-|n|}}{\sinh\rho_0 \cosh\rho_0} g_n(\rho_0)\Bigg] \\ + \frac{t_{1,-}^n(\rho)}{2|n|(|n|^2-1)} &\int_0^\rho d\rho_0 \frac{(\cosh\rho_0 + |n|)\tanh(\rho_0/2)^{|n|}}{\sinh\rho_0 \cosh\rho_0} g_n(\rho_0). \end{aligned} \tag{D.13}$$

The inhomogeneous part $t_{3,\text{inhom.}}^n$ of the solution vanishes at $\rho = 0, \infty$,

$$\begin{aligned} \lim_{\rho\to\infty} t_{3,\text{inhom.}}^n(\rho) &= \left(\int_0^\infty d\rho_0 \frac{t_{1,+}^n(\rho_0) g_n(\rho_0)}{2|n|(|n|^2-1)\sinh\rho_0}\right)(t_{1,+}^n(\rho\to\infty) - t_{1,-}^n(\rho\to\infty)) = 0, \\ \lim_{\rho\to 0} t_{3,\text{inhom.}}^n(\rho) &= \left(\int_0^\infty d\rho_0 \frac{(t_{1,-}^n(\rho_0) - t_{1,+}^n(\rho_0)) g_n(\rho_0)}{2|n|(|n|^2-1)\sinh\rho_0}\right) t_{1,+}^n(\rho\to 0) = 0. \end{aligned} \tag{D.14}$$

Therefore, to impose the boundary conditions obeyed by $t_3$, as before only the homogeneous part of the solution needs to be considered. Furthermore, it can be shown that the inhomogeneous part $t_{3,\text{inhom.}}^n$ does not contribute to the volume change. The contribution of $t_{3,\text{inhom.}}^n$ to $V_{(4)}$ is

proportional to

$$
\begin{aligned}
&\int d\rho \frac{\cosh^2\rho}{\sinh\rho}(\sinh^2\rho\, \dot{t}^n_{1,+}(\rho)\dot{t}^{-n}_{3,\text{inhom.}}(\rho) + n^2 t^n_{1,+}(\rho) t^{-n}_{3,\text{inhom.}}(\rho)) \\
&= -\int_0^\infty d\rho \frac{\cosh^2\rho}{\sinh\rho}(\sinh^2\rho\, \dot{t}^n_{1,+}(\rho)\dot{t}^{-n}_{1,+}(\rho) + n^2 t^n_{1,+}(\rho) t^{-n}_{1,+}(\rho)) \int_0^\infty d\rho_0 \frac{t^{-n}_{1,+}(\rho_0) g_{-n}(\rho_0)}{\sinh\rho_0} \\
&\quad + \int_0^\infty d\rho \frac{\cosh^2\rho}{\sinh\rho}(\sinh^2\rho\, \dot{t}^n_{1,+}(\rho)\dot{t}^{-n}_{1,+}(\rho) + n^2 t^n_{1,+}(\rho) t^{-n}_{1,+}(\rho)) \int_\rho^\infty d\rho_0 \frac{t^{-n}_{1,-}(\rho_0) g_{-n}(\rho_0)}{\sinh\rho_0} \\
&\quad + \int_0^\infty d\rho \frac{\cosh^2\rho}{\sinh\rho}(\sinh^2\rho\, \dot{t}^n_{1,+}(\rho)\dot{t}^{-n}_{1,-}(\rho) + n^2 t^n_{1,+}(\rho) t^{-n}_{1,-}(\rho)) \int_0^\rho d\rho_0 \frac{t^{-n}_{1,+}(\rho_0) g_{-n}(\rho_0)}{\sinh\rho_0}.
\end{aligned}
\tag{D.15}
$$

Using that

$$
\int d\rho \frac{\cosh^2\rho}{\sinh\rho}(\sinh^2\rho\, \dot{t}^n_{1,+}\dot{t}^{-n}_{1,+} + n^2 t^n_{1,+} t^{-n}_{1,+}) = |n|^2\left(\frac{1}{|n|} - |n| + \cosh\rho + \frac{1}{\cosh\rho}\right)(\tanh(\rho/2))^{2|n|}
\tag{D.16}
$$

and

$$
\int d\rho \frac{\cosh^2\rho}{\sinh\rho}(\sinh^2\rho\, \dot{t}^n_{1,+}\dot{t}^{-n}_{1,-} + n^2 t^n_{1,+} t^{-n}_{1,-}) = |n|^2\left(\cosh\rho - \frac{1}{\cosh\rho}\right),
\tag{D.17}
$$

and applying partial integration in the last two terms of (D.15), it becomes clear that the contribution of $t^n_{3,\text{inhom.}}$ to $V_{(4)}$ vanishes,

$$
\begin{aligned}
&\int d\rho \frac{\cosh^2\rho}{\sinh\rho}(\sinh^2\rho\, \dot{t}^n_{1,+}(\rho)\dot{t}^{-n}_{3,\text{inhom.}}(\rho) + n^2 t^n_{1,+}(\rho) t^{-n}_{3,\text{inhom.}}(\rho)) \\
&= |n|^2 \int_0^\infty d\rho \frac{t^{-n}_{1,+}(\rho) g_{-n}(\rho)}{\sinh\rho}\Bigg(-\frac{1}{|n|} + |n| + \left(\frac{1}{|n|} + |n| + \cosh\rho + \frac{1}{\cosh\rho}\right)\frac{\cosh\rho - |n|}{\cosh\rho + |n|} \\
&\qquad\qquad - \cosh\rho + \frac{1}{\cosh\rho}\Bigg) \\
&= 0.
\end{aligned}
\tag{D.18}
$$

From the remaining contribution of the homogeneous term in the solution of the equation of motion, the volume change to fourth order is obtained in total as

$$
\begin{aligned}
V_{(4)} &= -\int d\rho\, d\phi \Bigg(\frac{\cosh^2\rho}{\sinh\rho}\left[\sinh^2\rho\, \dot{t}_1\dot{t}_3 + t_1' t_3' + \frac{\sinh^2\rho\, \dot{t}_2\dot{t}_2 + t_2' t_2'}{2}\right] \\
&\qquad + \frac{\cosh^4\rho}{8\sinh^3\rho}\left[\sinh^2\rho\, \dot{t}_1\dot{t}_1 + t_1' t_1'\right]^2\Bigg) \\
&= 2\pi \sum_n (|n|^3 - |n|)\left(C_1^n C_3^{-n} + \frac{1}{2} C_2^n C_2^{-n}\right) \\
&\quad + \frac{\pi}{4}\sum_{n,m,r} |n||m||n+r||m-r| C_n^1 C_m^1 C_{r-m}^1 C_{-n-r}^1 \\
&\qquad \times \left[\alpha_1^{n,m,r}\left(\sum_{i=1}^k \frac{(-1)^{k-i}}{i} + (-1)^k \log 2\right) + \alpha_2^{n,m,r}\right]
\end{aligned}
\tag{D.19}
$$

where I have used the shorthand notation $k = |n| + |m| + |r-m| + |-n-r|$ and

$$\begin{aligned}\alpha_1^{n,m,r} &= \frac{1}{3}(|m|^3 - |m| + |n|^3 - |n| + |r-m|^3 - |r-m| + |n+r|^3 - |n+r|) \\ &\quad + 2m|n|(n-1/n) + 2n|m|(m-1/m),\end{aligned} \tag{D.20}$$

$$\begin{aligned}12\alpha_2^{n,m,r} =& 4(1-k^2) - 3(-1)^{k/2}(k-k^3) \\ &+ (9(-1)^{k/2}k - 12)(2mn - |m-r||n+r| - (|n|+|m|)(|n+r|+|m-r|) - |m||n|) \\ &+ \frac{1}{4k-k^3}\Big[-120 + 28k^2 - 4k^4 \\ &+ (72-12k^2)(2mn - |m-r||n+r| - (|n|+|m|)(|n+r|+|m-r|) - |m||n|) \\ &+ 12\frac{|m||n||m-r||n+r|}{mn(m-r)(n+r)}\Big(6 - 7k^2 + k^4 \\ &+ (2-k^2)(|n||m| + (|n|+|m|)(|m-r|+|n+r|) + |m-r||n+r|) \\ &- (4-2k^2)(m-r)(n+r) - k|n||m|(|m-r|+|n+r|)\Big) \\ &+ (9(-1)^{k/2}(4k-4k^3) - 12(4-k^2) - 12k)\Big(-2m|n|/n - 2n|m|/m \\ &+ (|n|+|m|)|m-r||n+r| - (2mn - |m||n|)(|m-r|+|n+r|)\Big) \\ &+ 12\frac{|m||n|}{mn}\Big(2k(|m-r|+|n+r|) + k(|n|+|m|)(2|m-r||n+r| - (m-r)(n+r)) \\ &+ 4 + 2(2|n||m| - mn)|m-r||n+r| + 4(|n|+|m|)(|n+r|+|m-r|) \\ &- 2|m||n|(m-r)(n+r)\Big)\Big].\end{aligned} \tag{D.21}$$

# Bibliography


[1] J. Erdmenger and M. Gerbershagen, *Entwinement as a possible alternative to complexity*, JHEP **03** (2020) 082, arXiv: 1910.05352 [hep-th].

[2] J. Erdmenger, M. Gerbershagen, and A.-L. Weigel, *Complexity measures from geometric actions on Virasoro and Kac-Moody orbits*, JHEP **11** (2020) 003, arXiv: 2004.03619 [hep-th].

[3] M. Gerbershagen, *Monodromy methods for torus conformal blocks and entanglement entropy at large central charge*, JHEP **08** (2021) 143, arXiv: 2101.11642 [hep-th].

[4] M. Gerbershagen, *Illuminating entanglement shadows of BTZ black holes by a generalized entanglement measure*, JHEP **10** (2021) 187, arXiv: 2105.01097 [hep-th].

[5] J. Erdmenger, M. Flory, M. Gerbershagen, M. P. Heller, and A.-L. Weigel, *Exact Gravity Duals for Simple Quantum Circuits*, arXiv: 2112.12158 [hep-th].

[6] B. P. Abbott et al., *Observation of Gravitational Waves from a Binary Black Hole Merger*, Phys. Rev. Lett. **116** (2016) 061102, arXiv: 1602.03837 [gr-qc].

[7] F. Arute et al., *Quantum supremacy using a programmable superconducting processor*, Nature **574** (2019) 505, arXiv: 1910.11333 [quant-ph].

[8] S. W. Hawking, *Gravitational radiation from colliding black holes*, Phys. Rev. Lett. **26** (1971) 1344.

[9] S. W. Hawking, *Black holes in general relativity*, Commun. Math. Phys. **25** (1972) 152.

[10] J. D. Bekenstein, *Black holes and the second law*, Lett. Nuovo Cim. **4** (1972) 737.

[11] J. D. Bekenstein, *Black holes and entropy*, Phys. Rev. D **7** (1973) 2333.

[12] S. W. Hawking, *Black hole explosions*, Nature **248** (1974) 30.

[13] S. W. Hawking, *Particle Creation by Black Holes*, Commun. Math. Phys. **43** (1975) 199 [Erratum: Commun. Math. Phys. **46** (1976) 206].

[14] A. Strominger and C. Vafa, *Microscopic origin of the Bekenstein-Hawking entropy*, Phys. Lett. B **379** (1996) 99, arXiv: hep-th/9601029.

[15] S. W. Hawking, *Breakdown of predictability in gravitational collapse*, Phys. Rev. D **14** (1976) 2460.

[16] J. D. Bekenstein, *A Universal Upper Bound on the Entropy to Energy Ratio for Bounded Systems*, Phys. Rev. D **23** (1981) 287.

[17] R. Bousso, *A Covariant entropy conjecture*, JHEP **07** (1999) 004, arXiv: hep-th/9905177.

[18] R. Bousso, *The Holographic principle*, Rev. Mod. Phys. **74** (2002) 825, arXiv: hep-th/0203101.

[19] G. 't Hooft, *Dimensional reduction in quantum gravity*, Conf. Proc. C **930308** (1993) 284, arXiv: gr-qc/9310026.

[20] L. Susskind, *The World as a hologram*, J. Math. Phys. **36** (1995) 6377, arXiv: hep-th/9409089.

[21] J. M. Maldacena, *The Large N limit of superconformal field theories and supergravity*, Int. J. Theor. Phys. **38** (1999) 1113 [Adv. Theor. Math. Phys. **2** (1998) 231], arXiv: hep-th/9711200.

[22] J. Erdmenger, N. Evans, I. Kirsch, and E. Threlfall, *Mesons in Gauge/Gravity Duals - A Review*, Eur. Phys. J. A **35** (2008) 81, arXiv: 0711.4467 [hep-th].

[23] J. Casalderrey-Solana, H. Liu, D. Mateos, K. Rajagopal, and U. A. Wiedemann, *Gauge/String Duality, Hot QCD and Heavy Ion Collisions*, Cambridge University Press (2014), ISBN: 9781139136747, arXiv: 1101.0618 [hep-th].

[24] R.-G. Cai, L. Li, L.-F. Li, and R.-Q. Yang, *Introduction to Holographic Superconductor Models*, Sci. China Phys. Mech. Astron. **58** (2015) 060401, arXiv: 1502.00437 [hep-th].

[25] S. A. Hartnoll, A. Lucas, and S. Sachdev, *Holographic quantum matter*, arXiv: 1612.07324 [hep-th].

[26] M. Rangamani, *Gravity and Hydrodynamics: Lectures on the fluid-gravity correspondence*, Class. Quant. Grav. **26** (2009) 224003, arXiv: 0905.4352 [hep-th].

[27] S. Ryu and T. Takayanagi, *Holographic derivation of entanglement entropy from AdS/CFT*, Phys. Rev. Lett. **96** (2006) 181602, arXiv: hep-th/0603001.

[28] B. Czech, J. L. Karczmarek, F. Nogueira, and M. Van Raamsdonk, *The Gravity Dual of a Density Matrix*, Class. Quant. Grav. **29** (2012) 155009, arXiv: 1204.1330 [hep-th].

[29] A. C. Wall, *Maximin Surfaces, and the Strong Subadditivity of the Covariant Holographic Entanglement Entropy*, Class. Quant. Grav. **31** (2014) 225007, arXiv: 1211.3494 [hep-th].

[30] M. Headrick, V. E. Hubeny, A. Lawrence, and M. Rangamani, *Causality & holographic entanglement entropy*, JHEP **12** (2014) 162, arXiv: 1408.6300 [hep-th].

[31] G. Penington, *Entanglement Wedge Reconstruction and the Information Paradox*, JHEP **09** (2020) 002, arXiv: 1905.08255 [hep-th].

[32] A. Almheiri, N. Engelhardt, D. Marolf, and H. Maxfield, *The entropy of bulk quantum fields and the entanglement wedge of an evaporating black hole*, JHEP **12** (2019) 063, arXiv: 1905.08762 [hep-th].

[33] A. Almheiri, T. Hartman, J. Maldacena, E. Shaghoulian, and A. Tajdini, *The entropy of Hawking radiation*, Rev. Mod. Phys. **93** (2021) 035002, arXiv: 2006.06872 [hep-th].

[34] T. Faulkner, A. Lewkowycz, and J. Maldacena, *Quantum corrections to holographic entanglement entropy*, JHEP **11** (2013) 074, arXiv: 1307.2892 [hep-th].

[35] N. Engelhardt and A. C. Wall, *Quantum Extremal Surfaces: Holographic Entanglement Entropy beyond the Classical Regime*, JHEP **01** (2015) 073, arXiv: 1408.3203 [hep-th].

[36] H. Geng and A. Karch, *Massive islands*, JHEP **09** (2020) 121, arXiv: 2006.02438 [hep-th].

[37] B. Swingle, *Entanglement Renormalization and Holography*, Phys. Rev. D **86** (2012) 065007, arXiv: 0905.1317 [cond-mat.str-el].

[38] M. Van Raamsdonk, *Building up spacetime with quantum entanglement*, Gen. Rel. Grav. **42** (2010) 2323 [Int. J. Mod. Phys. **D19** (2010) 2429], arXiv: 1005.3035 [hep-th].

[39] J. M. Maldacena, *Eternal black holes in anti-de Sitter*, JHEP **04** (2003) 021, arXiv: hep-th/0106112.

[40] I. R. Klebanov, D. Kutasov, and A. Murugan, *Entanglement as a probe of confinement*, Nucl. Phys. B **796** (2008) 274, arXiv: 0709.2140 [hep-th].

[41] T. Nishioka and T. Takayanagi, *AdS Bubbles, Entropy and Closed String Tachyons*, JHEP **01** (2007) 090, arXiv: hep-th/0611035.

[42] A. Kitaev and J. Preskill, *Topological entanglement entropy*, Phys. Rev. Lett. **96** (2006) 110404, arXiv: hep-th/0510092.

[43] M. Levin and X.-G. Wen, *Detecting Topological Order in a Ground State Wave Function*, Phys. Rev. Lett. **96** (2006) 110405, arXiv: cond-mat/0510613 [cond-mat.str-el].

[44] V. E. Hubeny, H. Maxfield, M. Rangamani, and E. Tonni, *Holographic entanglement plateaux*, JHEP **08** (2013) 092, arXiv: 1306.4004 [hep-th].

[45] F. Nogueira, *Extremal Surfaces in Asymptotically AdS Charged Boson Stars Backgrounds*, Phys. Rev. D **87** (2013) 106006, arXiv: 1301.4316 [hep-th].

[46] V. Balasubramanian, B. D. Chowdhury, B. Czech, and J. de Boer, *Entwinement and the emergence of spacetime*, JHEP **01** (2015) 048, arXiv: 1406.5859 [hep-th].

[47] B. Freivogel, R. Jefferson, L. Kabir, B. Mosk, and I.-S. Yang, *Casting Shadows on Holographic Reconstruction*, Phys. Rev. D **91** (2015) 086013, arXiv: 1412.5175 [hep-th].

[48] A. Almheiri, X. Dong, and D. Harlow, *Bulk Locality and Quantum Error Correction in AdS/CFT*, JHEP **04** (2015) 163, arXiv: 1411.7041 [hep-th].

[49] E. Mintun, J. Polchinski, and V. Rosenhaus, *Bulk-Boundary Duality, Gauge Invariance, and Quantum Error Corrections*, Phys. Rev. Lett. **115** (2015) 151601, arXiv: 1501.06577 [hep-th].

[50] F. Pastawski, B. Yoshida, D. Harlow, and J. Preskill, *Holographic quantum error-correcting codes: Toy models for the bulk/boundary correspondence*, JHEP **06** (2015) 149, arXiv: 1503.06237 [hep-th].

[51] L. Susskind, *Computational Complexity and Black Hole Horizons*, Fortsch. Phys. **64** (2014) 44 [Fortsch. Phys. **64** (2016) 24], arXiv: 1403.5695 [hep-th].

[52] D. Stanford and L. Susskind, *Complexity and Shock Wave Geometries*, Phys. Rev. D **90** (2014) 126007, arXiv: 1406.2678 [hep-th].

[53] A. R. Brown, D. A. Roberts, L. Susskind, B. Swingle, and Y. Zhao, *Holographic Complexity Equals Bulk Action?*, Phys. Rev. Lett. **116** (2016) 191301, arXiv: 1509.07876 [hep-th].

[54] A. R. Brown, D. A. Roberts, L. Susskind, B. Swingle, and Y. Zhao, *Complexity, action, and black holes*, Phys. Rev. D **93** (2016) 086006, arXiv: 1512.04993 [hep-th].

[55] D. N. Page, *Information in black hole radiation*, Phys. Rev. Lett. **71** (1993) 3743, arXiv: hep-th/9306083.

[56] D. N. Page, *Time Dependence of Hawking Radiation Entropy*, JCAP **09** (2013) 028, arXiv: 1301.4995 [hep-th].

[57] P. Hayden and J. Preskill, *Black holes as mirrors: Quantum information in random subsystems*, JHEP **09** (2007) 120, arXiv: 0708.4025 [hep-th].

[58] T. Hartman and J. Maldacena, *Time Evolution of Entanglement Entropy from Black Hole Interiors*, JHEP **05** (2013) 014, arXiv: 1303.1080 [hep-th].

[59] L. Susskind, *Three Lectures on Complexity and Black Holes*, Springer (2018), arXiv: 1810.11563 [hep-th].

[60] O. Aharony, S. S. Gubser, J. M. Maldacena, H. Ooguri, and Y. Oz, *Large N field theories, string theory and gravity*, Phys. Rept. **323** (2000) 183, arXiv: hep-th/9905111.

[61] M. Ammon and J. Erdmenger, *Gauge/gravity duality: Foundations and applications*, Cambridge University Press, Cambridge (2015), ISBN: 9781107010345.

[62] E. Witten, *Anti-de Sitter space and holography*, Adv. Theor. Math. Phys. **2** (1998) 253, arXiv: hep-th/9802150.

[63] S. S. Gubser, I. R. Klebanov, and A. M. Polyakov, *Gauge theory correlators from noncritical string theory*, Phys. Lett. B **428** (1998) 105, arXiv: hep-th/9802109.

[64] J. D. Brown and M. Henneaux, *Central Charges in the Canonical Realization of Asymptotic Symmetries: An Example from Three-Dimensional Gravity*, Commun. Math. Phys. **104** (1986) 207.

[65] L. Susskind and E. Witten, *The Holographic bound in anti-de Sitter space*, arXiv: hep-th/9805114.

[66] J. V. Rocha, *Evaporation of large black holes in AdS: Coupling to the evaporon*, JHEP **08** (2008) 075, arXiv: 0804.0055 [hep-th].

[67] M. Van Raamsdonk, *Evaporating Firewalls*, JHEP **11** (2014) 038, arXiv: 1307.1796 [hep-th].

[68] A. Almheiri, *Holographic Quantum Error Correction and the Projected Black Hole Interior*, arXiv: 1810.02055 [hep-th].

[69] K. Skenderis, *Lecture notes on holographic renormalization*, Class. Quant. Grav. **19** (2002) 5849, arXiv: hep-th/0209067.

[70] C. Fefferman and C. R. Graham, *Conformal invariants*, Élie Cartan et les mathématiques d'aujourd'hui - Lyon, 25-29 juin 1984, Société mathématique de France (1985), http://www.numdam.org/item/AST_1985__S131__95_0/.

[71] M. Henningson and K. Skenderis, *The Holographic Weyl anomaly*, JHEP **07** (1998) 023, arXiv: hep-th/9806087.

[72] M. Henningson and K. Skenderis, *Holography and the Weyl anomaly*, Fortsch. Phys. **48** (2000) 125, arXiv: hep-th/9812032.

[73] S. de Haro, S. N. Solodukhin, and K. Skenderis, *Holographic reconstruction of space-time and renormalization in the AdS / CFT correspondence*, Commun. Math. Phys. **217** (2001) 595, arXiv: hep-th/0002230.

[74] K. Skenderis and S. N. Solodukhin, *Quantum effective action from the AdS / CFT correspondence*, Phys. Lett. B **472** (2000) 316, arXiv: hep-th/9910023.

[75] J. R. David, G. Mandal, and S. R. Wadia, *Microscopic formulation of black holes in string theory*, Phys. Rept. **369** (2002) 549, arXiv: hep-th/0203048.

[76] R. Blumenhagen, D. Lüst, and S. Theisen, *Basic concepts of string theory*, Springer, Berlin (2013), ISBN: 9783642294969.

[77] J. Polchinski, *String theory*, Cambridge Univ. Press, Cambridge (1998), ISBN: 9780521633031.

[78] G. W. Gibbons, G. T. Horowitz, and P. K. Townsend, *Higher dimensional resolution of dilatonic black hole singularities*, Class. Quant. Grav. **12** (1995) 297, arXiv: hep-th/9410073.

[79] C. G. Callan and J. M. Maldacena, *D-brane approach to black hole quantum mechanics*, Nucl. Phys. B **472** (1996) 591, arXiv: hep-th/9602043.

[80] G. Giribet, C. Hull, M. Kleban, M. Porrati, and E. Rabinovici, *Superstrings on $AdS_3$ at $k = 1$*, JHEP **08** (2018) 204, arXiv: 1803.04420 [hep-th].

[81] M. R. Gaberdiel and R. Gopakumar, *Tensionless string spectra on $AdS_3$*, JHEP **05** (2018) 085, arXiv: 1803.04423 [hep-th].

[82] L. Eberhardt, M. R. Gaberdiel, and R. Gopakumar, *The Worldsheet Dual of the Symmetric Product CFT*, JHEP **04** (2019) 103, arXiv: 1812.01007 [hep-th].

[83] L. Eberhardt, M. R. Gaberdiel, and R. Gopakumar, *Deriving the $AdS_3/CFT_2$ correspondence*, JHEP **02** (2020) 136, arXiv: 1911.00378 [hep-th].

[84] A. Dei, M. R. Gaberdiel, R. Gopakumar, and B. Knighton, *Free field world-sheet correlators for* $AdS_3$, JHEP **02** (2021) 081, arXiv: 2009.11306 [hep-th].

[85] H. Bertle, A. Dei, and M. R. Gaberdiel, *Stress-energy tensor correlators from the world-sheet*, JHEP **03** (2021) 036, arXiv: 2012.08486 [hep-th].

[86] L. Eberhardt, *$AdS_3/CFT_2$ at higher genus*, JHEP **05** (2020) 150, arXiv: 2002.11729 [hep-th].

[87] L. Eberhardt, *Partition functions of the tensionless string*, JHEP **03** (2021) 176, arXiv: 2008.07533 [hep-th].

[88] M. R. Gaberdiel and K. Naderi, *The physical states of the Hybrid Formalism*, JHEP **10** (2021) 168, arXiv: 2106.06476 [hep-th].

[89] M. R. Gaberdiel, B. Knighton, and J. Vošmera, *D-branes in $AdS_3 \times S^3 \times \mathbb{T}^4$ at $k = 1$ and their holographic duals*, JHEP **12** (2021) 149, arXiv: 2110.05509 [hep-th].

[90] S. F. Hassan and S. R. Wadia, *Gauge theory description of D-brane black holes: Emergence of the effective SCFT and Hawking radiation*, Nucl. Phys. B **526** (1998) 311, arXiv: hep-th/9712213.

[91] C. Vafa, *Instantons on D-branes*, Nucl. Phys. B **463** (1996) 435, arXiv: hep-th/9512078.

[92] M. R. Douglas, *Branes within branes*, NATO Sci. Ser. C **520** (1999) 267, arXiv: hep-th/9512077.

[93] M. R. Douglas, J. Polchinski, and A. Strominger, *Probing five-dimensional black holes with D-branes*, JHEP **12** (1997) 003, arXiv: hep-th/9703031.

[94] E. Witten, *On the conformal field theory of the Higgs branch*, JHEP **07** (1997) 003, arXiv: hep-th/9707093.

[95] P. H. Ginsparg, *Applied Conformal Field Theory*, Les Houches Summer School in Theoretical Physics: Fields, Strings, Critical Phenomena, (1988) 1, arXiv: hep-th/9108028.

[96] P. Di Francesco, P. Mathieu, and D. Sénéchal, *Conformal field theory*, Springer, New York (2011), ISBN: 9780387947853.

[97] P. Calabrese and J. L. Cardy, *Entanglement entropy and quantum field theory*, J. Stat. Mech. **0406** (2004) P06002, arXiv: hep-th/0405152.

[98] S. G. Avery, *Using the D1D5 CFT to Understand Black Holes*, PhD thesis, Ohio State University (2010), arXiv: 1012.0072 [hep-th].

[99] M. R. Gaberdiel, C. Peng, and I. G. Zadeh, *Higgsing the stringy higher spin symmetry*, JHEP **10** (2015) 101, arXiv: 1506.02045 [hep-th].

[100] M. A. Nielsen and I. L. Chuang, *Quantum computation and quantum information*, Cambridge Univ. Press, Cambridge (2007), ISBN: 9780521635035.

[101] A. Rényi, *On measures of information and entropy*, Proceedings of the fourth Berkeley Symposium on Mathematics, Statistics and Probability, (1961) 547.

[102] C. Holzhey, F. Larsen, and F. Wilczek, *Geometric and renormalized entropy in conformal field theory*, Nucl. Phys. B **424** (1994) 443, arXiv: hep-th/9403108.

[103] T. Hartman, *Entanglement Entropy at Large Central Charge*, arXiv: 1303.6955 [hep-th].

[104] M. Headrick and T. Takayanagi, *A Holographic proof of the strong subadditivity of entanglement entropy*, Phys. Rev. D **76** (2007) 106013, arXiv: 0704.3719 [hep-th].

[105] M. Rangamani and T. Takayanagi, *Holographic Entanglement Entropy*, Springer (2017), ISBN: 9783319525716, arXiv: 1609.01287 [hep-th].

[106] V. E. Hubeny, M. Rangamani, and T. Takayanagi, *A Covariant holographic entanglement entropy proposal*, JHEP **07** (2007) 062, arXiv: 0705.0016 [hep-th].

[107] R. Bousso, S. Leichenauer, and V. Rosenhaus, *Light-sheets and AdS/CFT*, Phys. Rev. D **86** (2012) 046009, arXiv: 1203.6619 [hep-th].

[108] R. Bousso, B. Freivogel, S. Leichenauer, V. Rosenhaus, and C. Zukowski, *Null Geodesics, Local CFT Operators and AdS/CFT for Subregions*, Phys. Rev. D **88** (2013) 064057, arXiv: 1209.4641 [hep-th].

[109] V. E. Hubeny and M. Rangamani, *Causal Holographic Information*, JHEP **06** (2012) 114, arXiv: 1204.1698 [hep-th].

[110] D. L. Jafferis and S. J. Suh, *The Gravity Duals of Modular Hamiltonians*, JHEP **09** (2016) 068, arXiv: 1412.8465 [hep-th].

[111] D. L. Jafferis, A. Lewkowycz, J. Maldacena, and S. J. Suh, *Relative entropy equals bulk relative entropy*, JHEP **06** (2016) 004, arXiv: 1512.06431 [hep-th].

[112] X. Dong, D. Harlow, and A. C. Wall, *Reconstruction of Bulk Operators within the Entanglement Wedge in Gauge-Gravity Duality*, Phys. Rev. Lett. **117** (2016) 021601, arXiv: 1601.05416 [hep-th].

[113] A. Lewkowycz and J. Maldacena, *Generalized gravitational entropy*, JHEP **08** (2013) 090, arXiv: 1304.4926 [hep-th].

[114] X. Dong, A. Lewkowycz, and M. Rangamani, *Deriving covariant holographic entanglement*, JHEP **11** (2016) 028, arXiv: 1607.07506 [hep-th].

[115] F. M. Haehl, T. Hartman, D. Marolf, H. Maxfield, and M. Rangamani, *Topological aspects of generalized gravitational entropy*, JHEP **05** (2015) 023, arXiv: 1412.7561 [hep-th].

[116] C. Akers, S. Leichenauer, and A. Levine, *Large Breakdowns of Entanglement Wedge Reconstruction*, Phys. Rev. D **100** (2019) 126006, arXiv: 1908.03975 [hep-th].

[117] C. Akers and G. Penington, *Leading order corrections to the quantum extremal surface prescription*, JHEP **04** (2021) 062, arXiv: 2008.03319 [hep-th].

[118] A. Almheiri, D. Marolf, J. Polchinski, and J. Sully, *Black Holes: Complementarity or Firewalls?*, JHEP **02** (2013) 062, arXiv: 1207.3123 [hep-th].

[119] A. Almheiri, D. Marolf, J. Polchinski, D. Stanford, and J. Sully, *An Apologia for Firewalls*, JHEP **09** (2013) 018, arXiv: 1304.6483 [hep-th].

[120] D. Harlow and P. Hayden, *Quantum Computation vs. Firewalls*, JHEP **06** (2013) 085, arXiv: 1301.4504 [hep-th].

[121] D. Harlow, *Jerusalem Lectures on Black Holes and Quantum Information*, Rev. Mod. Phys. **88** (2016) 015002, arXiv: 1409.1231 [hep-th].

[122] E. Lubkin, *Entropy of an n-system from its correlation with a k-reservoir*, J. Math. Phys. **19** (1978) 1028.

[123] D. N. Page, *Average entropy of a subsystem*, Phys. Rev. Lett. **71** (1993) 1291, arXiv: gr-qc/9305007.

[124] S. L. Braunstein, S. Pirandola, and K. Życzkowski, *Better Late than Never: Information Retrieval from Black Holes*, Phys. Rev. Lett. **110** (2013) 101301, arXiv: 0907.1190 [quant-ph].

[125] S. Aaronson, *The Complexity of Quantum States and Transformations: From Quantum Money to Black Holes*, (2016), arXiv: 1607.05256 [quant-ph].

[126] V. Coffman, J. Kundu, and W. K. Wootters, *Distributed entanglement*, Phys. Rev. A **61** (2000) 052306, arXiv: quant-ph/9907047.

[127] T. J. Osborne and F. Verstraete, *General Monogamy Inequality for Bipartite Qubit Entanglement*, Phys. Rev. Lett. **96** (2006) 220503, arXiv: quant-ph/0502176.

[128] S. D. Mathur, *The Information paradox: A Pedagogical introduction*, Class. Quant. Grav. **26** (2009) 224001, arXiv: 0909.1038 [hep-th].

[129] J. Maldacena and L. Susskind, *Cool horizons for entangled black holes*, Fortsch. Phys. **61** (2013) 781, arXiv: 1306.0533 [hep-th].

[130] D. Marolf and J. Polchinski, *Gauge/Gravity Duality and the Black Hole Interior*, Phys. Rev. Lett. **111** (2013) 171301, arXiv: 1307.4706 [hep-th].

[131] B. de Wit, J. Hoppe, and H. Nicolai, *On the Quantum Mechanics of Supermembranes*, Nucl. Phys. B **305** (1988) 545.

[132] T. Banks, W. Fischler, S. H. Shenker, and L. Susskind, *M theory as a matrix model: A Conjecture*, Phys. Rev. D **55** (1997) 5112, arXiv: hep-th/9610043.

[133] L. Susskind, *Entanglement is not enough*, Fortsch. Phys. **64** (2016) 49, arXiv: 1411.0690 [hep-th].

[134] G. T. Horowitz and V. E. Hubeny, *Quasinormal modes of AdS black holes and the approach to thermal equilibrium*, Phys. Rev. D **62** (2000) 024027, arXiv: hep-th/9909056.

[135] A. Belin, R. C. Myers, S.-M. Ruan, G. Sárosi, and A. J. Speranza, *Does Complexity Equal Anything?*, Phys. Rev. Lett. **128** (2022) 081602, arXiv: 2111.02429 [hep-th].

[136] P. Bocchieri and A. Loinger, *Quantum Recurrence Theorem*, Phys. Rev. **107** (1957) 337.

[137] A. Peres, *Recurrence Phenomena in Quantum Dynamics*, Phys. Rev. Lett. **49** (1982) 1118.

[138] K. Bhattacharyya and D. Mukherjee, *On estimates of the quantum recurrence time*, The Journal of Chemical Physics **84** (1986) 3212.

[139] L. C. Venuti, *The recurrence time in quantum mechanics*, arXiv: 1509.04352 [quant-ph].

[140] J. Anandan and Y. Aharonov, *Geometry of Quantum Evolution*, Phys. Rev. Lett. **65** (1990) 1697.

[141] C. H. Papadimitriou, *Computational complexity*, Addison-Wesley, Reading, Mass. (1994), ISBN: 9780201530827.

[142] S. Chapman and G. Policastro, *Quantum computational complexity from quantum information to black holes and back*, Eur. Phys. J. C **82** (2022) 128, arXiv: 2110.14672 [hep-th].

[143] M. A. Nielsen, *A geometric approach to quantum circuit lower bounds*, Quantum Info. Comput. **6** (2006) 213, arXiv: quant-ph/0502070.

[144] E. Knill, *Approximation by quantum circuits*, arXiv: quant-ph/9508006.

[145] D. Poulin, A. Qarry, R. Somma, and F. Verstraete, *Quantum Simulation of Time-Dependent Hamiltonians and the Convenient Illusion of Hilbert Space*, Phys. Rev. Lett. **106** (2011) 170501, arXiv: 1102.1360 [quant-ph].

[146] A. R. Brown and L. Susskind, *Second law of quantum complexity*, Phys. Rev. D **97** (2018) 086015, arXiv: 1701.01107 [hep-th].

[147] L. Susskind, *Black Holes and Complexity Classes*, arXiv: 1802.02175 [hep-th].

[148] F. G. S. L. Brandão, A. W. Harrow, and M. Horodecki, *Local Random Quantum Circuits are Approximate Polynomial-Designs*, Commun. Math. Phys. **346** (2016) 397, arXiv: 1208.0692 [quant-ph].

[149] F. G. S. L. Brandão, W. Chemissany, N. Hunter-Jones, R. Kueng, and J. Preskill, *Models of Quantum Complexity Growth*, PRX Quantum **2** (2021) 030316, arXiv: 1912.04297 [hep-th].

[150] J. Haferkamp, P. Faist, N. B. T. Kothakonda, J. Eisert, and N. Y. Halpern, *Linear growth of quantum circuit complexity*, Nat. Phys. (2022) 1745, arXiv: 2106.05305 [quant-ph].

[151] J. Polchinski, L. Susskind, and N. Toumbas, *Negative energy, superluminosity and holography*, Phys. Rev. D **60** (1999) 084006, arXiv: hep-th/9903228.

[152] S. H. Shenker and D. Stanford, *Black holes and the butterfly effect*, JHEP **03** (2014) 067, arXiv: 1306.0622 [hep-th].

[153] D. A. Roberts, D. Stanford, and L. Susskind, *Localized shocks*, JHEP **03** (2015) 051, arXiv: 1409.8180 [hep-th].

[154] S. H. Shenker and D. Stanford, *Multiple Shocks*, JHEP **12** (2014) 046, arXiv: 1312.3296 [hep-th].

[155] S. Leichenauer, *Disrupting Entanglement of Black Holes*, Phys. Rev. D **90** (2014) 046009, arXiv: 1405.7365 [hep-th].

[156] D. A. Roberts and D. Stanford, *Two-dimensional conformal field theory and the butterfly effect*, Phys. Rev. Lett. **115** (2015) 131603, arXiv: 1412.5123 [hep-th].

[157] S. H. Shenker and D. Stanford, *Stringy effects in scrambling*, JHEP **05** (2015) 132, arXiv: 1412.6087 [hep-th].

[158] L. Susskind and Y. Zhao, *Switchbacks and the Bridge to Nowhere*, arXiv: 1408.2823 [hep-th].

[159] S. Lloyd, *Ultimate physical limits to computation*, Nature **406** (2000) 1047, arXiv: quant-ph/9908043.

[160] W. Cottrell and M. Montero, *Complexity is simple!*, JHEP **02** (2018) 039, arXiv: 1710.01175 [hep-th].

[161] M. A. Nielsen, M. R. Dowling, M. Gu, and A. C. Doherty, *Quantum Computation as Geometry*, Science **311** (2006) 1133, arXiv: quant-ph/0603161.

[162] M. R. Dowling and M. A. Nielsen, *The geometry of quantum computation*, arXiv e-prints (2006) quant, arXiv: quant-ph/0701004.

[163] D. Bao, S. Chern, and Z. Shen, *An Introduction to Riemann-Finsler Geometry*, Springer, New York (2012), ISBN: 9781461212683.

[164] R. Jefferson and R. C. Myers, *Circuit complexity in quantum field theory*, JHEP **10** (2017) 107, arXiv: 1707.08570 [hep-th].

[165] S. Chapman, M. P. Heller, H. Marrochio, and F. Pastawski, *Toward a Definition of Complexity for Quantum Field Theory States*, Phys. Rev. Lett. **120** (2018) 121602, arXiv: 1707.08582 [hep-th].

[166] L. Hackl and R. C. Myers, *Circuit complexity for free fermions*, JHEP **07** (2018) 139, arXiv: 1803.10638 [hep-th].

[167] S. Chapman, J. Eisert, L. Hackl, M. P. Heller, R. Jefferson, H. Marrochio, and R. C. Myers, *Complexity and entanglement for thermofield double states*, SciPost Phys. **6** (2019) 034, arXiv: 1810.05151 [hep-th].

[168] R.-Q. Yang, *Complexity for quantum field theory states and applications to thermofield double states*, Phys. Rev. D **97** (2018) 066004, arXiv: 1709.00921 [hep-th].

[169] R. Khan, C. Krishnan, and S. Sharma, *Circuit Complexity in Fermionic Field Theory*, Phys. Rev. D **98** (2018) 126001, arXiv: 1801.07620 [hep-th].

[170] M. Guo, J. Hernandez, R. C. Myers, and S.-M. Ruan, *Circuit Complexity for Coherent States*, JHEP **10** (2018) 011, arXiv: 1807.07677 [hep-th].

[171] D. Ge and G. Policastro, *Circuit Complexity and 2D Bosonisation*, JHEP **10** (2019) 276, arXiv: 1904.03003 [hep-th].

[172] D. Carmi, R. C. Myers, and P. Rath, *Comments on Holographic Complexity*, JHEP **03** (2017) 118, arXiv: 1612.00433 [hep-th].

[173] B. A. Khesin and R. Wendt, *The geometry of infinite-dimensional groups*, Springer, Berlin (2009), ISBN: 9783540772620.

[174] B. Oblak, *BMS Particles in Three Dimensions*, PhD thesis, Brussels U. (2016), arXiv: 1610.08526 [hep-th].

[175] L. Guieu and C. Roger, *L'Algèbre et le Groupe de Virasoro: aspects géométriques et algébriques, généralisations*, Les Publications CRM (Centre de Recherches Mathématiques de Montréal) (2007), ISBN: 9782921120449.

[176] R. Bott, *ON THE CHARACTERISTIC CLASSES OF GROUPS OF DIFFEOMORPHISMS*, L'Enseignement Mathématique **33** (1978) 209.

[177] V. F. Lazutkin and T. F. Pankratova, *Normal forms and versal deformations for Hill's equation*, Functional Analysis and Its Applications **9** (1975) 306.

[178] A. A. Kirillov, *Orbits of the group of diffeomorphisms of a circle and local Lie superalgebras*, Functional Analysis and Its Applications **15** (1981) 135.

[179] E. Witten, *Coadjoint Orbits of the Virasoro Group*, Commun. Math. Phys. **114** (1988) 1.

[180] A. A. Kirillov, *Lectures on the orbit method*, American Mathematical Society, Providence, R.I. (2004), ISBN: 9780821835302.

[181] M. Nakahara, *Geometry, topology and physics*, Taylor & Francis, New York (2003), ISBN: 9780750306065.

[182] A. Alekseev and S. L. Shatashvili, *Path Integral Quantization of the Coadjoint Orbits of the Virasoro Group and 2D Gravity*, Nucl. Phys. B **323** (1989) 719.

[183] N. Woodhouse, *Geometric Quantization*, Clarendon Press (1997), ISBN: 9780198502708.

[184] A. Maloney and E. Witten, *Quantum Gravity Partition Functions in Three Dimensions*, JHEP **02** (2010) 029, arXiv: 0712.0155 [hep-th].

[185] J. Cotler and K. Jensen, *A theory of reparameterizations for $AdS_3$ gravity*, JHEP **02** (2019) 079, arXiv: 1808.03263 [hep-th].

[186] G. Barnich, H. A. Gonzalez, and P. Salgado-Rebolledo, *Geometric actions for three-dimensional gravity*, Class. Quant. Grav. **35** (2018) 014003, arXiv: 1707.08887 [hep-th].

[187] S. Carlip, *Lectures on (2+1) dimensional gravity*, J. Korean Phys. Soc. **28** (1995) S447, arXiv: gr-qc/9503024.

[188] J. Lin, *A Toy Model of Entwinement*, arXiv: 1608.02040 [hep-th].

[189] V. Balasubramanian, A. Bernamonti, B. Craps, T. De Jonckheere, and F. Galli, *Entwinement in discretely gauged theories*, JHEP **12** (2016) 094, arXiv: 1609.03991 [hep-th].

[190] V. Balasubramanian, B. Craps, T. De Jonckheere, and G. Sárosi, *Entanglement versus entwinement in symmetric product orbifolds*, JHEP **01** (2019) 190, arXiv: 1806.02871 [hep-th].

[191] O. Lunin and S. D. Mathur, *Metric of the multiply wound rotating string*, Nucl. Phys. B **610** (2001) 49, arXiv: hep-th/0105136.

[192] O. Lunin, J. M. Maldacena, and L. Maoz, *Gravity solutions for the D1-D5 system with angular momentum*, arXiv: hep-th/0212210.

[193] M. Taylor, *General 2 charge geometries*, JHEP **03** (2006) 009, arXiv: hep-th/0507223.

[194] M. Ohya and D. Petz, *Quantum entropy and its use*, Springer, Berlin (1993), ISBN: 9780387548814.

[195] H. Barnum, G. Ortiz, R. Somma, and L. Viola, *A Generalization of Entanglement to Convex Operational Theories: Entanglement Relative to a Subspace of Observables*, International Journal of Theoretical Physics **44** (2005) 2127, arXiv: quant-ph/0506099.

[196] H. Barnum, E. Knill, G. Ortiz, and L. Viola, *Generalizations of entanglement based on coherent states and convex sets*, Phys. Rev. A **68** (2003) 032308, arXiv: quant-ph/0207149.

[197] R. Haag, *Local quantum physics: fields, particles, algebras*, Springer, Berlin (1993), ISBN: 9780387536101.

[198] D. Harlow, *The Ryu–Takayanagi Formula from Quantum Error Correction*, Commun. Math. Phys. **354** (2017) 865, arXiv: 1607.03901 [hep-th].

[199] P. V. Buividovich and M. I. Polikarpov, *Entanglement entropy in gauge theories and the holographic principle for electric strings*, Phys. Lett. B **670** (2008) 141, arXiv: 0806.3376 [hep-th].

[200] W. Donnelly, *Decomposition of entanglement entropy in lattice gauge theory*, Phys. Rev. D **85** (2012) 085004, arXiv: 1109.0036 [hep-th].

[201] H. Casini, M. Huerta, and J. A. Rosabal, *Remarks on entanglement entropy for gauge fields*, Phys. Rev. D **89** (2014) 085012, arXiv: 1312.1183 [hep-th].

[202] D. Radicevic, *Notes on Entanglement in Abelian Gauge Theories*, arXiv: 1404.1391 [hep-th].

[203] S. Aoki, T. Iritani, M. Nozaki, T. Numasawa, N. Shiba, and H. Tasaki, *On the definition of entanglement entropy in lattice gauge theories*, JHEP **06** (2015) 187, arXiv: 1502.04267 [hep-th].

[204] S. Ghosh, R. M. Soni, and S. P. Trivedi, *On The Entanglement Entropy For Gauge Theories*, JHEP **09** (2015) 069, arXiv: 1501.02593 [hep-th].

[205] R. M. Soni and S. P. Trivedi, *Aspects of Entanglement Entropy for Gauge Theories*, JHEP **01** (2016) 136, arXiv: 1510.07455 [hep-th].

[206] K. Van Acoleyen, N. Bultinck, J. Haegeman, M. Marien, V. B. Scholz, and F. Verstraete, *The entanglement of distillation for gauge theories*, Phys. Rev. Lett. **117** (2016) 131602, arXiv: 1511.04369 [quant-ph].

[207] A. Zamolodchikov, *Two-dimensional Conformal Symmetry and Critical Four-spin Correlation Functions in the Ashkin-Teller Model*, Zh. Eksp. Teor. Fiz. **90** (1986) 1808, http://jetp.ras.ru/cgi-bin/dn/e_063_05_1061.pdf.

[208] M. Beşken, S. Datta, and P. Kraus, *Semi-classical Virasoro blocks: proof of exponentiation*, JHEP **01** (2020) 109, arXiv: 1910.04169 [hep-th].

[209] T. Hartman, C. A. Keller, and B. Stoica, *Universal Spectrum of 2d Conformal Field Theory in the Large c Limit*, JHEP **09** (2014) 118, arXiv: 1405.5137 [hep-th].

[210] A. B. Zamolodchikov, *Conformal Symmetry in Two-Dimensions: An Explicit Recurrence Formula for the Conformal Partial Wave Amplitude*, Commun. Math. Phys. **96** (1984) 419.

[211] A. B. Zamolodchikov, *Conformal symmetry in two-dimensional space: recursion representation of conformal block*, Teoreticheskaya i Matematicheskaya Fizika **73** (1987) 103 [Theor. Math. Phys. **73** (1987) 1088].

[212] L. Hadasz, Z. Jaskolski, and P. Suchanek, *Recursive representation of the torus 1-point conformal block*, JHEP **01** (2010) 063, arXiv: 0911.2353 [hep-th].

[213] M. Cho, S. Collier, and X. Yin, *Recursive Representations of Arbitrary Virasoro Conformal Blocks*, JHEP **04** (2019) 018, arXiv: 1703.09805 [hep-th].

[214] D. Harlow, J. Maltz, and E. Witten, *Analytic Continuation of Liouville Theory*, JHEP **12** (2011) 071, arXiv: 1108.4417 [hep-th].

[215] T. Eguchi and H. Ooguri, *Conformal and Current Algebras on General Riemann Surface*, Nucl. Phys. B **282** (1987) 308.

[216] T. Azeyanagi, T. Nishioka, and T. Takayanagi, *Near Extremal Black Hole Entropy as Entanglement Entropy via AdS(2)/CFT(1)*, Phys. Rev. D **77** (2008) 064005, arXiv: 0710.2956 [hep-th].

[217] P. Calabrese and J. Cardy, *Entanglement entropy and conformal field theory*, J. Phys. A **42** (2009) 504005, arXiv: 0905.4013 [cond-mat.stat-mech].

[218] J. Cardy and C. P. Herzog, *Universal Thermal Corrections to Single Interval Entanglement Entropy for Two Dimensional Conformal Field Theories*, Phys. Rev. Lett. **112** (2014) 171603, arXiv: 1403.0578 [hep-th].

[219] B. Chen, J.-B. Wu, and J.-j. Zhang, *Short interval expansion of Rényi entropy on torus*, JHEP **08** (2016) 130, arXiv: 1606.05444 [hep-th].

[220] B. Chen and J.-q. Wu, *Large interval limit of Rényi entropy at high temperature*, Phys. Rev. D **92** (2015) 126002, arXiv: 1412.0763 [hep-th].

[221] T. Faulkner, *The Entanglement Renyi Entropies of Disjoint Intervals in AdS/CFT*, arXiv: 1303.7221 [hep-th].

[222] B. Chen and J.-q. Wu, *Holographic calculation for large interval Rényi entropy at high temperature*, Phys. Rev. D **92** (2015) 106001, arXiv: 1506.03206 [hep-th].

[223] S. F. Lokhande and S. Mukhi, *Modular invariance and entanglement entropy*, JHEP **06** (2015) 106, arXiv: 1504.01921 [hep-th].

[224] M. Headrick, A. Lawrence, and M. Roberts, *Bose-Fermi duality and entanglement entropies*, J. Stat. Mech. **1302** (2013) P02022, arXiv: 1209.2428 [hep-th].

[225] S. Datta and J. R. David, *Rényi entropies of free bosons on the torus and holography*, JHEP **04** (2014) 081, arXiv: 1311.1218 [hep-th].

[226] B. Chen and J.-q. Wu, *Rényi entropy of a free compact boson on a torus*, Phys. Rev. D **91** (2015) 105013, arXiv: 1501.00373 [hep-th].

[227] S. Mukhi, S. Murthy, and J.-Q. Wu, *Entanglement, Replicas, and Thetas*, JHEP **01** (2018) 005, arXiv: 1706.09426 [hep-th].

[228] B. Chen and J.-q. Wu, *Universal relation between thermal entropy and entanglement entropy in conformal field theories*, Phys. Rev. D **91** (2015) 086012, arXiv: 1412.0761 [hep-th].

[229] T. Barrella, X. Dong, S. A. Hartnoll, and V. L. Martin, *Holographic entanglement beyond classical gravity*, JHEP **09** (2013) 109, arXiv: 1306.4682 [hep-th].

[230] A. Belin, C. A. Keller, and I. G. Zadeh, *Genus two partition functions and Rényi entropies of large c conformal field theories*, J. Phys. A **50** (2017) 435401, arXiv: 1704.08250 [hep-th].

[231] G. A. Baker and P. R. Graves-Morris, *Padé approximants*, Addison-Wesley, Reading, Mass. (1981), ISBN: 9780201135121.

[232] N. Engelhardt and A. C. Wall, *Extremal Surface Barriers*, JHEP **03** (2014) 068, arXiv: 1312.3699 [hep-th].

[233] J. M. Maldacena and A. Strominger, *AdS(3) black holes and a stringy exclusion principle*, JHEP **12** (1998) 005, arXiv: hep-th/9804085.

[234] R. Balian, *Gain of information in a quantum measurement*, Eur. J. Phys. **10** (1989) 208.

[235] H. M. Wiseman and J. A. Vaccaro, *Entanglement of Indistinguishable Particles Shared between Two Parties*, Phys. Rev. Lett. **91** (2003) 097902, arXiv: quant-ph/0210002 [quant-ph].

[236] I. Klich and L. S. Levitov, *Scaling of entanglement entropy and superselection rules*, arXiv e-prints (2008) arXiv:0812.0006, arXiv: 0812.0006 [quant-ph].

[237] A. Lukin, M. Rispoli, R. Schittko, M. E. Tai, A. M. Kaufman, S. Choi, V. Khemani, J. Léonard, and M. Greiner, *Probing entanglement in a many-body–localized system*, Science **364** (2019) 256, arXiv: 1805.09819.

[238] M. Goldstein and E. Sela, *Symmetry-resolved entanglement in many-body systems*, Phys. Rev. Lett. **120** (2018) 200602, arXiv: 1711.09418 [cond-mat.stat-mech].

[239] S. G. Avery, B. D. Chowdhury, and S. D. Mathur, *Deforming the D1D5 CFT away from the orbifold point*, JHEP **06** (2010) 031, arXiv: 1002.3132 [hep-th].

[240] S. G. Avery, B. D. Chowdhury, and S. D. Mathur, *Excitations in the deformed D1D5 CFT*, JHEP **06** (2010) 032, arXiv: 1003.2746 [hep-th].

[241] A. Pakman, L. Rastelli, and S. S. Razamat, *A Spin Chain for the Symmetric Product CFT(2)*, JHEP **05** (2010) 099, arXiv: 0912.0959 [hep-th].

[242] C. T. Asplund and S. G. Avery, *Evolution of Entanglement Entropy in the D1-D5 Brane System*, Phys. Rev. D **84** (2011) 124053, arXiv: 1108.2510 [hep-th].

[243] B. A. Burrington, A. W. Peet, and I. G. Zadeh, *Operator mixing for string states in the D1-D5 CFT near the orbifold point*, Phys. Rev. D **87** (2013) 106001, arXiv: 1211.6699 [hep-th].

[244] Z. Carson, S. Hampton, S. D. Mathur, and D. Turton, *Effect of the deformation operator in the D1D5 CFT*, JHEP **01** (2015) 071, arXiv: 1410.4543 [hep-th].

[245] Z. Carson, S. Hampton, S. D. Mathur, and D. Turton, *Effect of the twist operator in the D1D5 CFT*, JHEP **08** (2014) 064, arXiv: 1405.0259 [hep-th].

[246] Z. Carson, S. D. Mathur, and D. Turton, *Bogoliubov coefficients for the twist operator in the D1D5 CFT*, Nucl. Phys. B **889** (2014) 443, arXiv: 1406.6977 [hep-th].

[247] Z. Carson, S. Hampton, and S. D. Mathur, *Second order effect of twist deformations in the D1D5 CFT*, JHEP **04** (2016) 115, arXiv: 1511.04046 [hep-th].

[248] Z. Carson, S. Hampton, and S. D. Mathur, *One-Loop Transition Amplitudes in the D1D5 CFT*, JHEP **01** (2017) 006, arXiv: 1606.06212 [hep-th].

[249] Z. Carson, S. Hampton, and S. D. Mathur, *Full action of two deformation operators in the D1D5 CFT*, JHEP **11** (2017) 096, arXiv: 1612.03886 [hep-th].

[250] B. A. Burrington, I. T. Jardine, and A. W. Peet, *Operator mixing in deformed D1D5 CFT and the OPE on the cover*, JHEP **06** (2017) 149, arXiv: 1703.04744 [hep-th].

[251] S. Hampton, S. D. Mathur, and I. G. Zadeh, *Lifting of D1-D5-P states*, JHEP **01** (2019) 075, arXiv: 1804.10097 [hep-th].

[252] B. Guo and S. D. Mathur, *Lifting of states in 2-dimensional $N = 4$ supersymmetric CFTs*, JHEP **10** (2019) 155, arXiv: 1905.11923 [hep-th].

[253] B. Guo and S. D. Mathur, *Lifting of level-1 states in the D1D5 CFT*, JHEP **03** (2020) 028, arXiv: 1912.05567 [hep-th].

[254] B. Guo and S. D. Mathur, *Lifting at higher levels in the D1D5 CFT*, JHEP **11** (2020) 145, arXiv: 2008.01274 [hep-th].

[255] A. A. Lima, G. M. Sotkov, and M. Stanishkov, *On the dynamics of protected ramond ground states in the D1-D5 CFT*, JHEP **07** (2021) 120, arXiv: 2103.04459 [hep-th].

[256] A. Belin, C. A. Keller, and A. Maloney, *Permutation Orbifolds in the large N Limit*, arXiv: 1509.01256 [hep-th].

[257] A. Bhattacharyya, A. Shekar, and A. Sinha, *Circuit complexity in interacting QFTs and RG flows*, JHEP **10** (2018) 140, arXiv: 1808.03105 [hep-th].

[258] V. Balasubramanian, M. Decross, A. Kar, and O. Parrikar, *Quantum Complexity of Time Evolution with Chaotic Hamiltonians*, JHEP **01** (2020) 134, arXiv: 1905.05765 [hep-th].

[259] T. Ali, A. Bhattacharyya, S. S. Haque, E. H. Kim, N. Moynihan, and J. Murugan, *Chaos and Complexity in Quantum Mechanics*, Phys. Rev. D **101** (2020) 026021, arXiv: 1905.13534 [hep-th].

[260] R.-Q. Yang and K.-Y. Kim, *Time evolution of the complexity in chaotic systems: a concrete example*, JHEP **05** (2020) 045, arXiv: 1906.02052 [hep-th].

[261] A. Kar, L. Lamprou, M. Rozali, and J. Sully, *Random matrix theory for complexity growth and black hole interiors*, JHEP **01** (2022) 016, arXiv: 2106.02046 [hep-th].

[262] V. Balasubramanian, M. DeCross, A. Kar, Y. Li, and O. Parrikar, *Complexity growth in integrable and chaotic models*, JHEP **07** (2021) 011, arXiv: 2101.02209 [hep-th].

[263] V. Balasubramanian, P. Caputa, J. Magan, and Q. Wu, *A new measure of quantum state complexity*, arXiv: 2202.06957 [hep-th].

[264] B. Craps, M. De Clerck, O. Evnin, P. Hacker, and M. Pavlov, *Bounds on quantum evolution complexity via lattice cryptography*, arXiv: 2202.13924 [quant-ph].

[265] M. Flory and N. Miekley, *Complexity change under conformal transformations in $AdS_3/CFT_2$*, JHEP **05** (2019) 003, arXiv: 1806.08376 [hep-th].

[266] P. Caputa and J. M. Magan, *Quantum Computation as Gravity*, Phys. Rev. Lett. **122** (2018) 231302, arXiv: 1807.04422 [hep-th].

[267] I. Akal, *Reflections on Virasoro circuit complexity and Berry phase*, Phys. Rev. D **105** (2022) 025012, arXiv: 1908.08514 [hep-th].

[268] M. Flory and M. P. Heller, *Conformal field theory complexity from Euler-Arnold equations*, JHEP **12** (2020) 091, arXiv: 2007.11555 [hep-th].

[269] M. Flory and M. P. Heller, *Geometry of Complexity in Conformal Field Theory*, Phys. Rev. Res. **2** (2020) 043438, arXiv: 2005.02415 [hep-th].

[270] J. M. Magán, *Black holes, complexity and quantum chaos*, JHEP **09** (2018) 043, arXiv: 1805.05839 [hep-th].

[271] I. Bengtsson and K. Zyczkowski, *Geometry of Quantum States: An Introduction to Quantum Entanglement*, Cambridge University Press (2007), ISBN: 9781139453462.

[272] A. Belin, A. Lewkowycz, and G. Sárosi, *Complexity and the bulk volume, a new York time story*, JHEP **03** (2019) 044, arXiv: 1811.03097 [hep-th].

[273] P. Bueno, J. M. Magan, and C. S. Shahbazi, *Complexity measures in QFT and constrained geometric actions*, JHEP **09** (2021) 200, arXiv: 1908.03577 [hep-th].

[274] N. Chagnet, S. Chapman, J. de Boer, and C. Zukowski, *Complexity for Conformal Field Theories in General Dimensions*, Phys. Rev. Lett. **128** (2022) 051601, arXiv: 2103.06920 [hep-th].

[275] B. Oblak, *Berry Phases on Virasoro Orbits*, JHEP **10** (2017) 114, arXiv: 1703.06142 [hep-th].

[276] E. Aldrovandi and L. A. Takhtajan, *Generating functional in CFT and effective action for two-dimensional quantum gravity on higher genus Riemann surfaces*, Commun. Math. Phys. **188** (1997) 29, arXiv: hep-th/9606163.

[277] J. Mickelsson, *String Quantization on Group Manifolds and the Holomorphic Geometry of Diff S1 / S1*, Commun. Math. Phys. **112** (1987) 653.

[278] B. Bradlyn and N. Read, *Topological central charge from Berry curvature: Gravitational anomalies in trial wave functions for topological phases*, Phys. Rev. B **91** (2015) 165306, arXiv: 1502.04126 [cond-mat.mes-hall].

[279] T. G. Mertens, *The Schwarzian theory — origins*, JHEP **05** (2018) 036, arXiv: 1801.09605 [hep-th].

[280] M. Banados, *Three-dimensional quantum geometry and black holes*, AIP Conf. Proc. **484** (1999) 147, arXiv: hep-th/9901148.

[281] T. Nakatsu, H. Umetsu, and N. Yokoi, *Three-dimensional black holes and Liouville field theory*, Prog. Theor. Phys. **102** (1999) 867, arXiv: hep-th/9903259.

[282] A. Garbarz and M. Leston, *Classification of Boundary Gravitons in $AdS_3$ Gravity*, JHEP **05** (2014) 141, arXiv: 1403.3367 [hep-th].

[283] G. Barnich and B. Oblak, *Holographic positive energy theorems in three-dimensional gravity*, Class. Quant. Grav. **31** (2014) 152001, arXiv: 1403.3835 [hep-th].

[284] O. Coussaert, M. Henneaux, and P. van Driel, *The Asymptotic dynamics of three-dimensional Einstein gravity with a negative cosmological constant*, Class. Quant. Grav. **12** (1995) 2961, arXiv: gr-qc/9506019.

[285] J. Navarro-Salas and P. Navarro, *Virasoro orbits, AdS(3) quantum gravity and entropy*, JHEP **05** (1999) 009, arXiv: hep-th/9903248.

[286] P. Caputa, N. Kundu, M. Miyaji, T. Takayanagi, and K. Watanabe, *Anti-de Sitter Space from Optimization of Path Integrals in Conformal Field Theories*, Phys. Rev. Lett. **119** (2017) 071602, arXiv: 1703.00456 [hep-th].

[287] A. Bhattacharyya, P. Caputa, S. R. Das, N. Kundu, M. Miyaji, and T. Takayanagi, *Path-Integral Complexity for Perturbed CFTs*, JHEP **07** (2018) 086, arXiv: 1804.01999 [hep-th].

[288] T. Takayanagi, *Holographic Spacetimes as Quantum Circuits of Path-Integrations*, JHEP **12** (2018) 048, arXiv: 1808.09072 [hep-th].

[289] J. Boruch, P. Caputa, and T. Takayanagi, *Path-Integral Optimization from Hartle-Hawking Wave Function*, Phys. Rev. D **103** (2021) 046017, arXiv: 2011.08188 [hep-th].

[290] J. Boruch, P. Caputa, D. Ge, and T. Takayanagi, *Holographic path-integral optimization*, JHEP **07** (2021) 016, arXiv: 2104.00010 [hep-th].

[291] P. H. Ginsparg and G. W. Moore, *Lectures on 2-D gravity and 2-D string theory*, Theoretical Advanced Study Institute (TASI 92): From Black Holes and Strings to Particles, (1993) 277, arXiv: hep-th/9304011.

[292] V. Arnold, *Mathematical methods of classical mechanics*, Springer, New York (1989).

[293] V. Arnold, *Sur la géométrie différentielle des groupes de Lie de dimension infinie et ses applications à l'hydrodynamique des fluides parfaits*, Annales de l'Institut Fourier **16** (1966) 319.

[294] V. Y. Ovsienko and B. A. Khesin, *Korteweg-de Vries superequation as an Euler equation*, Functional Analysis and Its Applications **21** (1987) 329.

[295] G. Misiołek, *A shallow water equation as a geodesic flow on the Bott-Virasoro group*, Journal of Geometry and Physics **24** (1998) 203.

[296] B. Khesin and G. Misiołek, *Euler equations on homogeneous spaces and Virasoro orbits*, Advances in Mathematics **176** (2003) 116, arXiv: math/0210397.

[297] D. J. Korteweg and G. de Vries, *On the change of form of long waves advancing in a rectangular canal, and on a new type of long stationary waves*, Philosophical Magazine **39** (1895) 422.

[298] *NIST Digital Library of Mathematical Functions*, F. W. J. Olver, A. B. Olde Daalhuis, D. W. Lozier, B. I. Schneider, R. F. Boisvert, C. W. Clark, B. R. Miller, B. V. Saunders, H. S. Cohl, and M. A. McClain, eds., http://dlmf.nist.gov/.

[299] A. R. Osborne, *Solitons in the periodic Korteweg–de Vries equation, the FTHETA-function representation, and the analysis of nonlinear, stochastic wave trains*, Phys. Rev. E **52** (1995) 1105.

[300] A. M. Polyakov, *Quantum Geometry of Bosonic Strings*, Phys. Lett. B **103** (1981) 207.

[301] K. Nguyen, *Holographic boundary actions in $AdS_3/CFT_2$ revisited*, JHEP **10** (2021) 218, arXiv: 2108.01095 [hep-th].

[302] J. Couch, W. Fischler, and P. H. Nguyen, *Noether charge, black hole volume, and complexity*, JHEP **03** (2017) 119, arXiv: 1610.02038 [hep-th].

[303] S. Chapman, H. Marrochio, and R. C. Myers, *Complexity of Formation in Holography*, JHEP **01** (2017) 062, arXiv: 1610.08063 [hep-th].

[304] L. A. Santaló, *Integral Geometry and Geometric Probability*, Addison-Wesley, Reading, Mass. (1976), ISBN: 9780201135008.

[305] B. Czech, L. Lamprou, S. McCandlish, and J. Sully, *Integral Geometry and Holography*, JHEP **10** (2015) 175, arXiv: 1505.05515 [hep-th].

[306] B. Czech and L. Lamprou, *Holographic definition of points and distances*, Phys. Rev. D **90** (2014) 106005, arXiv: 1409.4473 [hep-th].

[307] B. Czech, L. Lamprou, S. McCandlish, and J. Sully, *Tensor Networks from Kinematic Space*, JHEP **07** (2016) 100, arXiv: 1512.01548 [hep-th].

[308] B. Czech, L. Lamprou, S. McCandlish, and J. Sully, *Modular Berry Connection for Entangled Subregions in AdS/CFT*, Phys. Rev. Lett. **120** (2018) 091601, arXiv: 1712.07123 [hep-th].

[309] B. Czech, L. Lamprou, S. McCandlish, B. Mosk, and J. Sully, *A Stereoscopic Look into the Bulk*, JHEP **07** (2016) 129, arXiv: 1604.03110 [hep-th].

[310] J. de Boer, F. M. Haehl, M. P. Heller, and R. C. Myers, *Entanglement, holography and causal diamonds*, JHEP **08** (2016) 162, arXiv: 1606.03307 [hep-th].

[311] J. C. Cresswell and A. W. Peet, *Kinematic space for conical defects*, JHEP **11** (2017) 155, arXiv: 1708.09838 [hep-th].

[312] J.-d. Zhang and B. Chen, *Kinematic Space and Wormholes*, JHEP **01** (2017) 092, arXiv: 1610.07134 [hep-th].

[313] R. Abt, J. Erdmenger, H. Hinrichsen, C. M. Melby-Thompson, R. Meyer, C. Northe, and I. A. Reyes, *Topological Complexity in $AdS_3/CFT_2$*, Fortsch. Phys. **66** (2018) 1800034, arXiv: 1710.01327 [hep-th].

[314] R. Abt, J. Erdmenger, M. Gerbershagen, C. M. Melby-Thompson, and C. Northe, *Holographic Subregion Complexity from Kinematic Space*, JHEP **01** (2019) 012, arXiv: 1805.10298 [hep-th].

[315] A. Belin, N. Benjamin, A. Castro, S. M. Harrison, and C. A. Keller, *$\mathcal{N} = 2$ Minimal Models: A Holographic Needle in a Symmetric Orbifold Haystack*, SciPost Phys. **8** (2020) 084, arXiv: 2002.07819 [hep-th].

[316] B. Balthazar, A. Giveon, D. Kutasov, and E. J. Martinec, *Asymptotically free $AdS_3/CFT_2$*, JHEP **01** (2022) 008, arXiv: 2109.00065 [hep-th].

[317] E. J. Martinec, *AdS3's with and without BTZ's*, arXiv: 2109.11716 [hep-th].

[318] L. Eberhardt, *A perturbative CFT dual for pure NS–NS $AdS_3$ strings*, J. Phys. A **55** (2022) 064001, arXiv: 2110.07535 [hep-th].

[319] E. J. Martinec, *A Defect in AdS3/CFT2 Duality*, arXiv: 2201.04218 [hep-th].

[320] A. Dei and L. Eberhardt, *String correlators on $AdS_3$: analytic structure and dual CFT*, arXiv: 2203.13264 [hep-th].

[321] S. Gukov, E. Martinec, G. W. Moore, and A. Strominger, *The Search for a holographic dual to AdS(3) x S**3 x S**3 x S**1*, Adv. Theor. Math. Phys. **9** (2005) 435, arXiv: hep-th/0403090.

[322] L. Eberhardt, M. R. Gaberdiel, and W. Li, *A holographic dual for string theory on $AdS_3 \times S^3 \times S^3 \times S^1$*, JHEP **08** (2017) 111, arXiv: 1707.02705 [hep-th].

[323] L. Eberhardt and M. R. Gaberdiel, *Strings on $AdS_3 \times S^3 \times S^3 \times S^1$*, JHEP **06** (2019) 035, arXiv: 1904.01585 [hep-th].

[324] L. Eberhardt and M. R. Gaberdiel, *String theory on $AdS_3$ and the symmetric orbifold of Liouville theory*, Nucl. Phys. B **948** (2019) 114774, arXiv: 1903.00421 [hep-th].

[325] S. Datta, L. Eberhardt, and M. R. Gaberdiel, *Stringy $\mathcal{N} = (2,2)$ holography for $AdS_3$*, JHEP **01** (2018) 146, arXiv: 1709.06393 [hep-th].

[326] L. Eberhardt and I. G. Zadeh, *$\mathcal{N} = (3,3)$ holography on $\mathrm{AdS}_3 \times (\mathrm{S}^3 \times \mathrm{S}^3 \times \mathrm{S}^1)/\mathbb{Z}_2$*, JHEP **07** (2018) 143, arXiv: 1805.09832 [hep-th].

[327] M. R. Gaberdiel and J. A. Mann, *Stringy CFT duals with $\mathcal{N} = (2, 2)$ supersymmetry*, JHEP **01** (2020) 160, arXiv: 1910.10427 [hep-th].

[328] A. Mollabashi, N. Shiba, and T. Takayanagi, *Entanglement between Two Interacting CFTs and Generalized Holographic Entanglement Entropy*, JHEP **04** (2014) 185, arXiv: 1403.1393 [hep-th].

[329] A. Karch and C. F. Uhlemann, *Holographic entanglement entropy and the internal space*, Phys. Rev. D **91** (2015) 086005, arXiv: 1501.00003 [hep-th].

[330] M. Taylor, *Generalized entanglement entropy*, JHEP **07** (2016) 040, arXiv: 1507.06410 [hep-th].

[331] R. Dijkgraaf, G. W. Moore, E. P. Verlinde, and H. L. Verlinde, *Elliptic genera of symmetric products and second quantized strings*, Commun. Math. Phys. **185** (1997) 197, arXiv: hep-th/9608096.

[332] R. Dijkgraaf, *Fields, strings, matrices and symmetric products*, arXiv: hep-th/9912104.

[333] P. Bantay, *Symmetric products, permutation orbifolds and discrete torsion*, Lett. Math. Phys. **63** (2003) 209, arXiv: hep-th/0004025.

[334] C. A. Keller, *Phase transitions in symmetric orbifold CFTs and universality*, JHEP **03** (2011) 114, arXiv: 1101.4937 [hep-th].

[335] J. de Boer, *Large N elliptic genus and AdS / CFT correspondence*, JHEP **05** (1999) 017, arXiv: hep-th/9812240.

# Acknowledgements

First of all, I would like to thank by supervisor Johanna Erdmenger for guiding me through my PhD projects as well as giving advice on preparing talks, writing publications and career advancement. Without her support in these areas, for which I am very grateful, this PhD thesis would not have been written.

I would like to thank as well a number of other people from the TP3 group in Würzburg, especially Anna-Lena Weigel for collaborating on various projects, Christian Northe for always being up to discussing conformal field theory and René Meyer for fruitful cooperation in teaching string theory which has helped me a lot in understanding this topic better. Moreover, I am grateful for getting to know all of the other members of the TP3 group. They have made my time in Würzburg a pleasant experience and their research projects contributed greatly to the diverse range of topics in theoretical physics that I was exposed to during my PhD: I have had interesting conversations on topics such as algebraic quantum field theory with Pascal Fries, Ignacio Reyes and Christian Simon, AdS/CFT applications to hydrodynamics and condensed matter with Ioannis Matthaiakakis and Kevin Grosvenor or connections between AdS/CFT and aperiodic quantum chains (a topic which I worked on for by Bachelor thesis and definitely did not expect to encounter again in my PhD!) with Pablo Basteiro, Rathindra Nath Das and Giuseppe di Giulio.

I also benefited a lot from discussions on computational complexity with my collaborators Mario Flory and Michał Heller from outside of Würzburg who I enjoyed working with. Michał Heller also deserves a mention for helping with my postdoc applications.

Furthermore, I would like to thank the ct.qmat Cluster of Excellence for financial support and in particular the organizers of the cluster retreats for putting together these fun and engaging events.

Finally, I thank the members of the development team for the sagemath computer algebra system for answering questions regarding its use and incorporating the bug fixes and improvements I sent to them.